MODELLING TECTONIC, CLIMATIC AND EUSTATIC EFFECTS ON OROGEN/FORELAND BASIN SYSTEMS

by

David D. Johnson

Submitted in partial fulfillment of the requirements
for the degree of Doctor of Philosophy

at

Dalhousie University
Halifax, Nova Scotia
July, 1995

ISBN 0-612-08773-5

Name DAVID DWIGHT JOHNSON

Dissertation Abstracts International is arranged by broad, general subject categories. Please select the one subject which most nearly describes the content of your dissertation. Enter the corresponding four-digit code in the spaces provided.

OCEANOGRAPHY — SUBJECT TERM

0372 — SUBJECT CODE

U·M·I

Subject Categories

THE HUMANITIES AND SOCIAL SCIENCES

COMMUNICATIONS AND THE ARTS
Architecture 0729
Art History 0377
Cinema 0900
Dance 0378
Fine Arts 0357
Information Science 0723
Journalism 0391
Library Science 0399
Mass Communications 0708
Music 0413
Speech Communication 0459
Theater 0465

EDUCATION
General 0515
Administration 0514
Adult and Continuing 0516
Agricultural 0517
Art 0273
Bilingual and Multicultural 0282
Business 0688
Community College 0275
Curriculum and Instruction 0727
Early Childhood 0518
Elementary 0524
Finance 0277
Guidance and Counseling 0519
Health 0680
Higher 0745
History of 0520
Home Economics 0278
Industrial 0521
Language and Literature 0279
Mathematics 0280
Music 0522
Philosophy of 0998
Physical 0523
Psychology 0525
Reading 0535
Religious 0527
Sciences 0714
Secondary 0533
Social Sciences 0534
Sociology of 0340
Special 0529
Teacher Training 0530
Technology 0710
Tests and Measurements 0288
Vocational 0747

LANGUAGE, LITERATURE AND LINGUISTICS
Language
- General 0679
- Ancient 0289
- Linguistics 0290
- Modern 0291

Literature
- General 0401
- Classical 0294
- Comparative 0295
- Medieval 0297
- Modern 0298
- African 0316
- American 0591
- Asian 0305
- Canadian (English) 0352
- Canadian (French) 0355
- English 0593
- Germanic 0311
- Latin American 0312
- Middle Eastern 0315
- Romance 0313
- Slavic and East European 0314

PHILOSOPHY, RELIGION AND THEOLOGY
Philosophy 0422

Religion
- General 0318
- Biblical Studies 0321
- Clergy 0319
- History of 0320
- Philosophy of 0322

Theology 0469

SOCIAL SCIENCES
American Studies 0323

Anthropology
- Archaeology 0324
- Cultural 0326
- Physical 0327

Business Administration
- General 0310
- Accounting 0272
- Banking 0770
- Management 0454
- Marketing 0338

Canadian Studies 0385

Economics
- General 0501
- Agricultural 0503
- Commerce-Business 0505
- Finance 0508
- History 0509
- Labor 0510
- Theory 0511

Folklore 0358
Geography 0366
Gerontology 0351

History
- General 0578
- Ancient 0579
- Medieval 0581
- Modern 0582
- Black 0328
- African 0331
- Asia, Australia and Oceania 0332
- Canadian 0334
- European 0335
- Latin American 0336
- Middle Eastern 0333
- United States 0337

History of Science 0585
Law 0398

Political Science
- General 0615
- International Law and Relations 0616
- Public Administration 0617

Recreation 0814
Social Work 0452

Sociology
- General 0626
- Criminology and Penology 0627
- Demography 0938
- Ethnic and Racial Studies 0631
- Individual and Family Studies 0628
- Industrial and Labor Relations 0629
- Public and Social Welfare 0630
- Social Structure and Development 0700
- Theory and Methods 0344

Transportation 0709
Urban and Regional Planning 0999
Women's Studies 0453

THE SCIENCES AND ENGINEERING

BIOLOGICAL SCIENCES
Agriculture
- General 0473
- Agronomy 0285
- Animal Culture and Nutrition 0475
- Animal Pathology 0476
- Food Science and Technology 0359
- Forestry and Wildlife 0478
- Plant Culture 0479
- Plant Pathology 0480
- Plant Physiology 0817
- Range Management 0777
- Wood Technology 0746

Biology
- General 0306
- Anatomy 0287
- Biostatistics 0308
- Botany 0309
- Cell 0379
- Ecology 0329
- Entomology 0353
- Genetics 0369
- Limnology 0793
- Microbiology 0410
- Molecular 0307
- Neuroscience 0317
- Oceanography 0416
- Physiology 0433
- Radiation 0821
- Veterinary Science 0778
- Zoology 0472

Biophysics
- General 0786
- Medical 0760

EARTH SCIENCES
Biogeochemistry 0425
Geochemistry 0996
Geodesy 0370
Geology 0372
Geophysics 0373
Hydrology 0388
Mineralogy 0411
Paleobotany 0345
Paleoecology 0426
Paleontology 0418
Paleozoology 0985
Palynology 0427
Physical Geography 0368
Physical Oceanography 0415

HEALTH AND ENVIRONMENTAL SCIENCES
Environmental Sciences 0768

Health Sciences
- General 0566
- Audiology 0300
- Chemotherapy 0992
- Dentistry 0567
- Education 0350
- Hospital Management 0769
- Human Development 0758
- Immunology 0982
- Medicine and Surgery 0564
- Mental Health 0347
- Nursing 0569
- Nutrition 0570
- Obstetrics and Gynecology 0380
- Occupational Health and Therapy 0354
- Ophthalmology 0381
- Pathology 0571
- Pharmacology 0419
- Pharmacy 0572
- Physical Therapy 0382
- Public Health 0573
- Radiology 0574
- Recreation 0575
- Speech Pathology 0460
- Toxicology 0383

Home Economics 0386

PHYSICAL SCIENCES

Pure Sciences
Chemistry
- General 0485
- Agricultural 0749
- Analytical 0486
- Biochemistry 0487
- Inorganic 0488
- Nuclear 0738
- Organic 0490
- Pharmaceutical 0491
- Physical 0494
- Polymer 0495
- Radiation 0754

Mathematics 0405

Physics
- General 0605
- Acoustics 0986
- Astronomy and Astrophysics 0606
- Atmospheric Science 0608
- Atomic 0748
- Electronics and Electricity 0607
- Elementary Particles and High Energy 0798
- Fluid and Plasma 0759
- Molecular 0609
- Nuclear 0610
- Optics 0752
- Radiation 0756
- Solid State 0611

Statistics 0463

Applied Sciences
Applied Mechanics 0346
Computer Science 0984

Engineering
- General 0537
- Aerospace 0538
- Agricultural 0539
- Automotive 0540
- Biomedical 0541
- Chemical 0542
- Civil 0543
- Electronics and Electrical 0544
- Heat and Thermodynamics 0348
- Hydraulic 0545
- Industrial 0546
- Marine 0547
- Materials Science 0794
- Mechanical 0548
- Metallurgy 0743
- Mining 0551
- Nuclear 0552
- Packaging 0549
- Petroleum 0765
- Sanitary and Municipal 0554
- System Science 0790

Geotechnology 0428
Operations Research 0796
Plastics Technology 0795
Textile Technology 0994

PSYCHOLOGY
General 0621
Behavioral 0384
Clinical 0622
Developmental 0620
Experimental 0623
Industrial 0624
Personality 0625
Physiological 0989
Psychobiology 0349
Psychometrics 0632
Social 0451

Dedication

Katherine my soul mate

For sharing the joys and the burdens of this road less travelled (peu à peu),

and making this dream a reality.

and

my Parents

For showing me this place, among many others, and nurturing my dreams

with your abiding love.

Table of Contents

List of Figures

List of Tables

Abstract

In orogen/foreland basin systems, the development of basin stratigraphy is strongly influenced by the rates of several first order processes: orogen tectonics, surface processes, climate, isostasy and eustasy. A composite kinematic planform model has been developed to look for stratigraphic signatures that reflect the dominant influence of one of these basin controlling processes or the interaction among several processes.

The orogen/foreland basin model links component models of orogen tectonics, surface processes, orographically controlled precipitation, lithospheric flexure and eustasy in an internally consistent manner. Critical Coulomb wedge theory is used to create a doubly-vergent wedge-shaped orogen. The surface processes model couples diffusive and advective transports to erode, redistribute and deposit material. Fluvial transport is determined by both surface slope and discharge; the latter is controlled by precipitation and collection. Orographic rainfall is determined by topography, extraction efficiency and vapour flux. The isostasy model uses either an elastic or a thermally activated linear viscoelastic plate rheology to flexurally compensate for changes in orogenic, sedimentary and water loads. Eustasy is uniform change in model sea level.

Model results show, in planform and section, parallel and oblique continent/ continent collision and orogen growth with pro- and retro-foreland basins. The effects of basin setting, along-strike changes in tectonics, prevailing 'wind' direction and feedback among processes on the rates of orogen growth and basin filling are discussed. Stratigraphy is shown as facies bounded by chronostratigraphic and erosional surfaces. Facies are described by characteristics of the model's depositional environments.

Synthetic stratigraphy is presented for orogen/foreland basin systems that have experienced changes in tectonics, climate or eustasy as either step or sinusoid functions. Stratigraphic assemblages show both the transient and steady state system response to these changes. Response times are estimated for tectonic and climatic forcing and used to illustrate how stratal geometry and facies distributions vary when the period of forcing is either approximately the same as or much greater than the response time.

Tectonic and climatic processes are shown to have similar effects on landform evolution and therefore the distribution of alluvial, coastal and marine facies. These similarities allow combinations of tectonic and climatic forcing to enhance or retard their mutual effects on stratigraphic development. Potentially distinctive effects of tectonic and climate processes are discussed. Eustasy is shown to have a subordinate effect to tectonic and climatic processes on alluvial plain development and a dominant effect on landform evolution proximal to the coast. Erosional surfaces associated with eustasy are shown to vary significantly with the rate of sea-level change.

List of Symbols

General

l	- length (metres)
t	- time (years)
m	- metres
km	- kilometres
ky	- 10^3 years
My	- 10^6 years
mm/y	- millimetres per year
x, y, z	- Cartesian coordinates
cl	- cell length
τ	- response time

Tectonic Processes

α	- slope of wedge surface
β	- slope of decollement
CVB	- common vertical boundary
μ	- effective internal coefficient of friction ($\phi = \text{arcTan}(\mu)$)
μ_b	- effective basal coefficient of friction ($\phi_b = \text{arcTan}(\mu)$)
Θ	- wedge taper ($\alpha+\beta$)
Θ_{min}	- minimum critical Coulomb taper
Θ_{max}	- maximum critical Coulomb taper
v_T	- tectonic convergence velocity [l/t]
T_P	- position of pro-wedge deformation front
T_R	- position of retro-wedge deformation front
d_P	- pro-wedge thickness at the deformation front [l]

d_R	- retro-wedge thickness at the deformation front [l]
ν_P	- rate of pro-wedge deformation front advance [l/t]
ν_R	- rate of retro-wedge deformation front advance [l/t]
$Q_T(pro)$	- tectonic flux of material into the pro-wedge caused by ν_T [l^3/t]
$Q_T(CVB)$	- tectonic flux of material across the CVB [l^3/t]
$Q_{TA}(pro)$	- flux of material into the pro-wedge caused by wedge growth [l^3/t]
$Q_{TA}(retro)$	- flux of material into the pro-wedge caused by wedge growth [l^3/t]
l_s	- strike length scale of coherent deformation [l]
Δt_T	- tectonic timestep [t]
θ	- angle between convergent continental margins
τ_T	- tectonic response time [t]

Surface Processes

Δt_S	- surface processes timestep [t]
h	- surface elevation [l]
q_s	- diffusive material transport [l^3/t]
∇h	- surface gradient (slope) [l/l]
u_s	- transport velocity of erodible surface layer [l/t]
h_s	- erodible surface layer thickness [l]
K_s	- diffusivity ($K_s = u_s \times h_s$) [l^2/t]
A	- area [l^2]
q_r	- fluvial discharge [l^3/t]
K_f	- fluvial transport coefficient
q_f^{eqb}	- fluvial equilibrium carrying capacity [l^3/t]
q_f	- fluvial sediment transport [l^3/t]
t_f	- fluvial erosional or depositional time scale [t]

l_f	- fluvial erosional or depositional length scale [l]
Q_S	- sediment flux [l^3/t]
$Q_{S(pro)}$	- pro-foreland orogen-to-basin sediment flux [l^3/t]
$Q_{S(retro)}$	- retro-foreland orogen-to-basin sediment flux [l^3/t]

Climate Process

h_R	- extraction height scale [l]
l_R	- extraction length scale [l]
a_R	- extraction efficiency ($a_R = h_R \times l_R$) [l^2]
h_{min}	- elevation below which precipitation is uniform [l]
ν_R	- precipitation rate [l/t]
Q_V	- vapour flux [l^3/t]
τ_C	- climate response time [t]

Eustasy

ν_E	- rate of eustatically forced relative sea-level change [l/t]

Acknowledgments

*"No man is an island entire of himself.
Each man is a piece of the cc.,tinent, a part of the main."
John Donne - 17th Meditation*

Of the many people I thank for their time and effort on my behalf, first and foremost I thank Chris Beaumont who stretched me to my limits making this research experience both challenging and rewarding.

I thank both the many and the few members of my supervisory committee who provided considerable support and direction: Bernie Boudreau, Ron Boyd, Martin Gibling, Paul Hill, Layer Mayer and Glen Stockmal. In particular I thank Bernie Boudreau and Martin Gibling for reading the thesis and providing many helpful suggestions while on sabbatical. I also extend special thanks to Paul Hill who joined the committee late and provided valuable support and direction.

Bob Courtney is thanked for generating the Green functions used in the isostasy calculations.

Special thanks are extended to Juliet Hamilton for her help with numerous projects and always walking the extra mile. To Susan Ellis, thank you for being a running mate on this long journey.

Thanks are extended to Peter Bugden, Neal Hamilton, David McCurdy, John Osler and Mark Paton who cheerfully provided direction and assistance with computer hardware and software problems. I also thank Dianne Crouse for her help with administrative issues.

Finally, I give thanks for the many fine people of D-Lab and beyond who added the joie de vivre to my life at Dalhousie. Thank you Charles and Jessie McCurdy for your steadfast support.

CHAPTER 1

INTRODUCTION

1.1 Orogen/Foreland Basin Systems

Geoscientists are in a sense historians, individuals who seek to understand the complex interactions of what has occurred by examining what has been preserved. In the study of orogens and their adjacent foreland basins, the stratigraphy of these basins synoptically records information about processes that operate both within and beyond the basin. The challenge lies in unraveling the stratigraphic record. The goal of this research is to identify how tectonics, climate and eustasy, as fundamental earth processes, are individually and jointly expressed in the stratigraphy of orogen/foreland basin systems.

Orogen/foreland basin systems form where one plate or crustal segment impinges upon another. Whether the convergence is between continents as with Iberia/Europe (Muñoz, 1992), micro-continents and a continent as with the North American Cordillera (Monger, 1989) or an oceanic arc and continental plate as with Taiwan (Davis *et al.*, 1983) the result is the formation of an orogenic belt along the interplate suture. These belts are believed to form by detachment and imbrication of the sedimentary and crustal veneer of the convergent plates above a zone of subduction, a relationship first suggested by Ampferer (1906, cit. Bally, 1981). It is now generally accepted that the development of an orogen belt places a load on the plates along the zone of convergence, and that foreland basins are created by flexural isostatic compensation of the orogenic load. This understanding owes its beginning to Hall, who in 1857 suggested that the accumulation of sedimentary rocks may be related to the formation of mountain systems and Dutton, who in 1889 introduced the concept of isostasy as the mechanism for basin formation (Bally, 1989). Aubouin in 1965 noted the asymmetry of foreland basins and the advance of orogenesis from outer deeper-water 'eugeosyncline' toward the inner shallower 'miogeosyncline' (Allen *et al.*, 1986). The concept of flexural isostatic compensation was proposed by Price (1973) to account for the characteristic asymmetric thickening of foreland basin strata toward the orogen.

The term 'foreland basin' was formally introduced by Dickinson (1974) who proposed two genetic classes of foreland basins: 1) peripheral foreland basins - situated against the outer arc of the orogen during continent-continent collision (A-type subduction, Bally and Snelson, 1980) and 2) retro-arc foreland basins - situated behind the magmatic arc and linked with subduction of oceanic lithosphere (B-type subduction, Bally and Snelson, 1980) (Allen *et al.*, 1986). Johnson and Beaumont (1995) propose a broader classification of foreland basins into pro- or retro-foreland basins dependent upon whether the basin is positioned over the subducting or overriding plate respectively. This classification eliminates the reference to an arc, because not all orogenic forelands have an arc (e.g., Pyrenees, Muñoz, 1992); nor is it concerned with the type of plate collision (A- or B-type) because the type of collision may change with time (e.g., 'micro-continent' or exotic terrane accretion, Canadian Cordillera, Monger, 1989).

Foreland basin stratigraphy synoptically records information about the processes that operate both within and beyond the basin. The fundamental processes of any orogen/foreland basin system include orogen tectonics; lithospheric flexural isostatic compensation of the orogenic load; surface processes which erode, transport and deposit sediment in the foreland basin; climatic processes influenced by topography and which influence subaerial surface processes; and eustatic processes which influence both the distribution and behaviour of surface and subsurface processes. The sedimentary record is synoptic because stratigraphic development of foreland basins is controlled by subaerial and submarine surface processes, and these processes both influence and are influenced by tectonics, climate and eustasy among others.

The influence of these fundamental processes on basin stratigraphy has long been identified. The effects of tectonics on landform and sedimentation were recognized as early as 1802 by Playfair (*cit.* Blair and Bilodeau, 1988). Davis in 1899 conceptualized the effects of tectonics on the evolution of landform as a "geographic cycle of landforms" ('Davis Cycle') (*cit.* Blair and Bilodeau, 1988); this view has been widely applied to the interpretation of stratigraphic successions since at least 1917, although Blair and Bilodeau (1988) contend that it may not be valid in all cases. Climate was also recognized to have significant influence on stratigraphy as early as 1895 by Gilbert, who suggested that rhythmic stratigraphic patterns in the Cretaceous of Colorado reflected response in sedimentary facies to changes between wetter and drier climatic conditions and orbital rhythms (Fischer *et al.*, 1990). However, climate change as a mechanism for forcing changes in stratigraphic development has gained acceptance only in recent years, based partly on the strong correlation between periodicity in orbital rhythms and periodic changes in the atmospheric and oceanic environments and partly on an increased understanding of how environmental changes are preserved in the stratigraphic record (Fischer *et al.*, 1988). Finally, sea-level changes have been recognized to affect the sedimentary record since at least 1669 (Steno, *cit.*, Peper, 1993); understanding how eustatic changes affect the distribution of subaerial and submarine processes and thus the sedimentary record remains a subject of debate. The recent development of 'sequence stratigraphy', which began as a systematic approach to identifying sedimentary deposits that are genetically related to sea-level changes, (Vail *et al.*, 1977; Van Wagoner *et al.*, 1988; Posamentier *et al.*, 1988), is a prime example of how understanding the ocean environment and the effects of sea-level change have changed in the last two decades.

While there is no debate that tectonic, climatic and eustatic effects are observed in foreland basin stratigraphy, there is considerable debate about the characteristics of their signatures. Understanding the relationships between these fundamental processes and basin strata is important because of its effect on our interpretation of the sedimentary record and orogen/foreland basin development. The importance of this understanding is not purely scientific, but is also economic and strategic, because foreland basins hold significant quantities of non-metallic base resources, most notably oil, gas, and coal. For example, the Middle Jurassic to Cretaceous strata of the Western Canadian Foreland Basin have reserves of approximately 1.7 trillion barrels of heavy oil, 5.6 billion barrels of conventional oil (BBO) and 67 trillion cubic feet of gas (TCF), while the Zagros Foreland Basin, Iraq, holds ~150 BBO and 650 TCF (Macqueen and Leckie, 1992).

1.2 The Objective and Approach

The fundamental question being addressed in this research is: What are the relative effects of tectonic, climatic and eustatic processes on the stratigraphic development of a foreland basin ?

Numerical modelling is an approach that has been successful in addressing other questions of foreland basins. If models can be created that reasonably replicate to first order the fundamental processes operating in orogen/foreland basin systems, then an integrated orogen/foreland basin model can be used to explore how these processes independently and corporately influence the development of synthetic foreland basin stratigraphy. Comparison of synthetic stratigraphy with observed foreland basin stratigraphy may then provide useful analogues for understanding how natural processes may have interacted to create known orogen/foreland basin systems.

The kinematic planform orogen/foreland basin model presented in this thesis has been developed by creating a model for orogen tectonics, modifying existing surface processes, climate and isostasy models and then integrating all these models into a composite model, as discussed in Chapter 2. The composite model has been designed to show the three-dimensional development of an orogen/foreland system. Model experiments investigate how these fundamental processes interactively control the evolution of orogen/foreland basin systems and how stratigraphic development varies with periodic fluctuations of one process or more, relative to a reference model. Comparisons of results with examples from natural foreland basins are included to illustrate the general applicability of the model. The experiments are not designed to yield results for detailed comparison with any particular orogen/foreland basin system.

1.3 Previous Foreland Basin Models

Quantitative models developed over approximately the last thirteen years have improved our understanding of how orogen/foreland basin systems develop by identifying and quantifying some of the principal controlling processes. A chronological summary of the evolution of these models is provided in Table 1.1.

Initially, foreland basin models focused on the flexural behaviour of the lithosphere and its relationship to orogenic and stratigraphic loads. In these models, orogenic loads are temporally and spatially prescribed as part of the model input. For example, Jordan (1981) uses thrust sheet geometry, Quinlan and Beaumont (1984) use block-load distributions, and Stockmal *et al.* (1986) use a critical wedge geometry. Of these models, those that develop a chronostratigraphic succession assume that the basin fills to either a horizontal datum representing sea level or a pre-defined bathymetric profile (Table 1.1). Flexural isostatic compensation for tectonic and sedimentary loads is commonly calculated assuming that the lithosphere behaves as an elastic or viscoelastic plate overlying an inviscid fluid. Chronostratigraphy in these models therefore reflects changes in the orogenic load and flexural properties of the lithosphere. The model of

Table 1.1 - Orogen/Foreland Basin Models												
Author(s)	year	Format	Tectonics		Surface		Climate		Isostasy		Eustasy	W/L
Beaumont	1981	section	block	S	flat-fill	S	– –		viscoelastic	P	– –	– –
Jordan	1981	section	thrust sheet	S	back-strip	S	– –		elastic	P	– –	– –
Karner & Watts	1983	section	gravity	S	No		– –		elastic	P	✔	✗
Quinlan & Beaumont	1984	planform	block	S	flat-fill	S	– –		viscoelastic	P	✔	✗
Stockmal *et al.*	1986	section	critical wedge geometry	S	profile	S	– –		elastic	P	– –	✔
Beaumont *et al.*	1988	planform	block	S	flat-fill	S	– –		viscoelastic	P	✔	✗
Mitrovica *et al.*	1989	section	subduction dynamics	P	– –		– –		elastic	P	– –	– –
Flemings & Jordan	1989 1990	section	critical wedge geometry + fault-bend-fold	S	diffusion	P	– –		elastic	P	– –	– –
Jordan & Flemings	1991	section	same as above	S	diffusion	P	– –		elastic	P	✔	✗
Sinclair *et al.*	1991	section	critical wedge geometry	S	diffusion	P	– –		elastic	P	– –	– –
Coakley & Watts	1991	section	– –		profile	S	– –		elastic	P	– –	– –
Paola *et al.*	1992	section	– –		diffusion	P	– –		subsidence	S	– –	– –
Gurnis	1992	section	subduction dynamics	P	flat-fill	S	– –		– –		– –	– –
Zoetemeijer *et al.*	1992	section	fault-bend-fold	S	flat-fill	S	– –		– –		– –	– –
Peper	1993	section	critical wedge geometry + in plane stress	S	diffusion	P	– –		elastic	P	✔	✔
Johnson & Beaumont	in press	planform	doubly-vergent kinematic critical wedge	P	advection + diffusion	P	orographic rainfall	P	elastic or viscoelastic	P	✔	✔

Table 1.1. Chronological summary of developments in orogen/foreland basin model evolution. P denotes process. S denotes specified. W/L denotes water load.

Beaumont (1981), Quinlan and Beaumont (1984) and Beaumont *et al.* (1988) differs from other models by illustrating in planform how the time-dependent processes controlling relaxation of stress in the lithosphere may cause a change in shape of the foreland basin without a change in surface load. These models demonstrate how such changes in shape, principally by migration of the peripheral bulge, can create regionally extensive erosional surfaces in foreland basin stratigraphy. Changes in basin shape may also be caused by the sublithospheric effects of mantle convection, as illustrated by the dynamic models of Mitrovica *et al.* (1989) and Gurnis (1992).

Flemings and Jordan (1989) made a fundamental improvement by incorporating diffusive material transport for erosion, sediment transport and deposition. Their sectional model combines diffusive material transport as a surface process with orogen geometry based on critical wedge theory (Dahlen, 1984) and flexural isostatic compensation on an elastic lithosphere. This model shows that basin stratigraphy varies with the orogen-to-basin sediment flux, the sediment transport rate in the basin, the rate of orogen advance, and the flexural properties of the lithosphere. Orogenic overthrusting is simulated by *a priori* advance of the wedge-shaped load. Flemings and Jordan (1990), using a similar model, illustrate how episodic changes in orogen growth rate cause sedimentation rates to increase adjacent to the orogen during times of 'thrusting' and in the distal basin during times of quiescence. Further, peripheral bulge migration with changes in load distribution is shown to create regionally extensive erosional surfaces without relaxation of stress in the lithosphere.

Sinclair *et al.* (1991) use an approach almost identical to Flemings and Jordan (1989) to demonstrate how changes in orogen growth rate can create the first-order stratigraphic characteristics of the North Alpine Foreland Basin, Switzerland. They simulate variations in orogen growth rate by varying the rate of overthrusting and the slope of the orogen. Paola *et al.* (1992), taking a simpler approach, replace basin subsidence caused by orogen growth and isostatic compensation with a linear decrease in basin subsidence across their model, and replace erosion-based orogen-to-basin sediment flux with *a priori* variation in sediment flux into the basin model. They show that the stratigraphic response to periodic variations in sediment flux, subsidence rate and the diffusion transport coefficient (diffusivity) depends largely upon the period of change relative to the time scale of the basin; they define the latter as the basin length squared divided by the diffusivity. Peper (1993) uses an approach similar to Flemings and Jordan (1989), but incorporates in-plane stress and water loading. His results show how mechanisms that cause a change in "accumulation space" (orogen loads, in-plane stress, water load and eustasy) compete with orogen-to-basin sediment flux to control the stratigraphic architecture of foreland basins.

1.4 The Orogen/Foreland Basin Model

A kinematic planform foreland basin model has been constructed which incorporates tectonic, surface, climatic, isostatic and eustatic processes. The details of this model are discussed in Chapter 2. The model uses an approach similar to Flemings and Jordan (1989), and is designed to investigate how the rates of fundamental processes determine stratigraphic development in an orogen/foreland basin system. The model differs from, complements or extends previous models in several important ways.

- The model incorporates planform variations in all processes to show the effects of along-strike changes in fundamental processes on the rates of erosion, rates and directions of sediment transport and rates of deposition. Development of the model in planform is important because, in nature, orogens and their flanking foreland basins typically vary significantly along strike. The planform model enables presentations in 'map view' as well as in cross section.

- The model creates an orogenic belt along the zone of convergence between adjacent continental plates flanked by pro- and retro-foreland basins (Johnson and Beaumont, 1995) as integral components of an orogen/foreland basin system.

- Tectonic processes create a doubly-vergent wedge-shaped orogen whose elevation, surface relief and state (constructive, steady, destructive) (Jamieson and Beaumont, 1988) are determined by the competition among model processes instead of *a priori* development of the orogen to an externally specified shape.

- Surface processes incorporate an advective transport mechanism as a simple fluvial transport model. As a consequence, surface processes, independently or in combination with other model processes, can both create and destroy surface relief over a range of length scales.

- Model fluvial systems erode, transport and deposit material in relation to river discharge, slope and material properties of the riverbed. Surface transport therefore varies spatially and temporally with evolution of the topography and changes in magnitude and distribution of precipitation.

- Orographically controlled rainfall is introduced as a simple 'climate' model. Precipitation varies with surface elevation and depletion of the prevailing water vapour flux, creating spatial variability in precipitation similar to that observed across natural orogenic belts. Climate conditions can vary between wetter and drier with variations in the magnitude of the initial vapour flux at the upwind boundary of the model.

- Eustasy and isostatic compensation for changes in water loads are incorporated.

- Model processes are interconnected so that a change in the rate of any one process causes feedback in the rates of all other processes.

The orogen/foreland basin model has the necessary properties to investigate further how changes in tectonics, precipitation and eustasy interact to affect the development of foreland basin stratigraphy. However, this model, like its precursors (Table 1.1), is unlikely to be sufficiently accurate or complete to allow more than a first order comparison of model results with natural orogen/foreland basin systems.

1.5 Model Experiments

Model experiments are conducted to investigate how tectonically, climatically and eustatically forced changes in model processes affect the development of foreland basin stratigraphy. Two reference models (MT1, MT3) are created that use constant tectonic, climatic and eustatic forcing. The convergent plate margin geometry is parallel in one model and non-parallel in the other in order to show along-strike variability in orogen/foreland basin development. These reference models, and initial conditions for all models, are discussed in Chapter 3.

Periodic variations in the rates of tectonic, climatic or eustatic processes are introduced to examine how processes interact to influence stratal development in a basin. The rate of each process varies as either a step function or a sine function in a series of experiments. The orogen/foreland basin model is an integrated process-response system and has a composite response which characterizes the system's ability to respond to periodic changes in the rates of each process. The integrated nature of the response is explored by evaluating how the character of the system response changes when the rate of one or more processes is altered, while all other model conditions remain constant.

Tectonics

The tectonic models (MT1-MT7) discussed in Chapter 3 illustrate the effects of pro- and retro-foreland basin settings and periodic variation in the rate of orogen growth on stratigraphic development. Models contrasting different foreland basin settings show how the rate of orogen advance affects the development and preservation of stratigraphy. Models using periodic variation in the rate of tectonic convergence between adjacent plates illustrate how changes in orogen growth rate and orogen state are expressed in basin stratigraphy. A step-function in the rate of tectonic convergence is used to estimate the composite response of the system and show the stratigraphic response when the change in orogen state is much faster than the minimum response time of the system. Sinusoidal variations in tectonic processes illustrate how stratigraphic development varies when the periods of fluctuation are either short or long relative to the estimated minimum response time.

Climate

The climate models (MC1-MC5) discussed in Chapter 4 illustrate how asymmetry in precipitation across an orogen and periodic change between wetter and drier climatic conditions influence stratigraphic development. Similar to the tectonic models, models with a step function are used to estimate the composite response time of the system and models with sinusoidal variations are used to illustrate how stratigraphic development varies with short and long periods of fluctuation relative to the response time.

Chapter 4 also presents two experiments (MTC1, MTC2) with periodic variations in both tectonic and climate processes. These combination models are used to show how the effects of tectonic and climatic processes on foreland basin stratigraphy can reinforce and counteract each other.

Eustasy

Model results for eustasy (ME1-ME5), discussed in Chapter 5, are used to illustrate how spatially uniform step and sinusoidal variations in sea level affect stratigraphic development. Step-function models show the maximum extent of transgressive/regressive cycles because the step response is initially independent of sediment flux to or away from the coast. Sinusoidal variations show how competition among sediment flux to the coast, sediment flux away from the coast, topography and the rate of sea-level change affects both the extent of transgressive/regressive cycles, and the lag or lead time between sea-level change and the onset of transgression or regression. In addition, step and sinusoidal variations in sea level are used to illustrate the factors controlling erosion of the coastal plain.

Chapter 5 also contains the results of four experiments using periodic variations in both eustasy and climate (MCE1, MCE2) or both eustasy and tectonics (MTE1, MTE2). These experiments show how the effects of tectonic and climatic processes can be reinforced, countered or masked by the effects of eustasy.

1.6 Discussions and Conclusions

Discussions of the model and its results, as well as comparison with real orogen/foreland basin systems, are included in each chapter. These discussions are expanded in Chapter 6 to examine the strengths and weaknesses of the model and the implications of the results. Conclusions drawn from the model and model results are summarized in each chapter, expanded in Chapter 6 and restated in Chapter 7 to address the fundamental question.

CHAPTER 2

THE OROGEN/FORELAND BASIN MODEL

2.1 Introduction

The goal of this research is to develop a greater understanding of the relative contributions of the processes of orogeny, climate and eustasy to the development of foreland basin stratigraphy. For this purpose, I have developed a kinematic orogen/foreland basin model that links processes and shows the evolution of orogen/foreland basin systems in both planform and cross section (Fig. 2.1).

The orogen/foreland basin model integrates a model which I developed for orogen tectonics with versions of existing models for surface processes (Beaumont *et al.*, 1992; Kooi and Beaumont, 1994), orographically controlled precipitation (Beaumont *et al.*, 1992) and flexural isostatic compensation (Beaumont, 1978; Courtney and Beaumont, 1983; Quinlan and Beaumont; 1984, Beaumont *et al.*, 1988). In addition, I have incorporated isostatic compensation for changes in water load in the integrated model.

The model is structured so that topography and stratigraphy evolve with time, from an initial condition, through the action and interaction of model processes. The rate of each process is determined by the characteristics of the evolving topographic surface (notably surface slope and elevation), time dependent parameter values and constant parameter values. The common dependence of each process on surface topography integrates all model processes. This integration allows, for example, a temporal change in a parameter value controlling the rate of one process to induce responses in the rates of all other processes, which in turn feed back and influence the rate of the process that initially experienced a change. As a consequence, changes in parameter values produce

Orogen and Foreland Basin Model

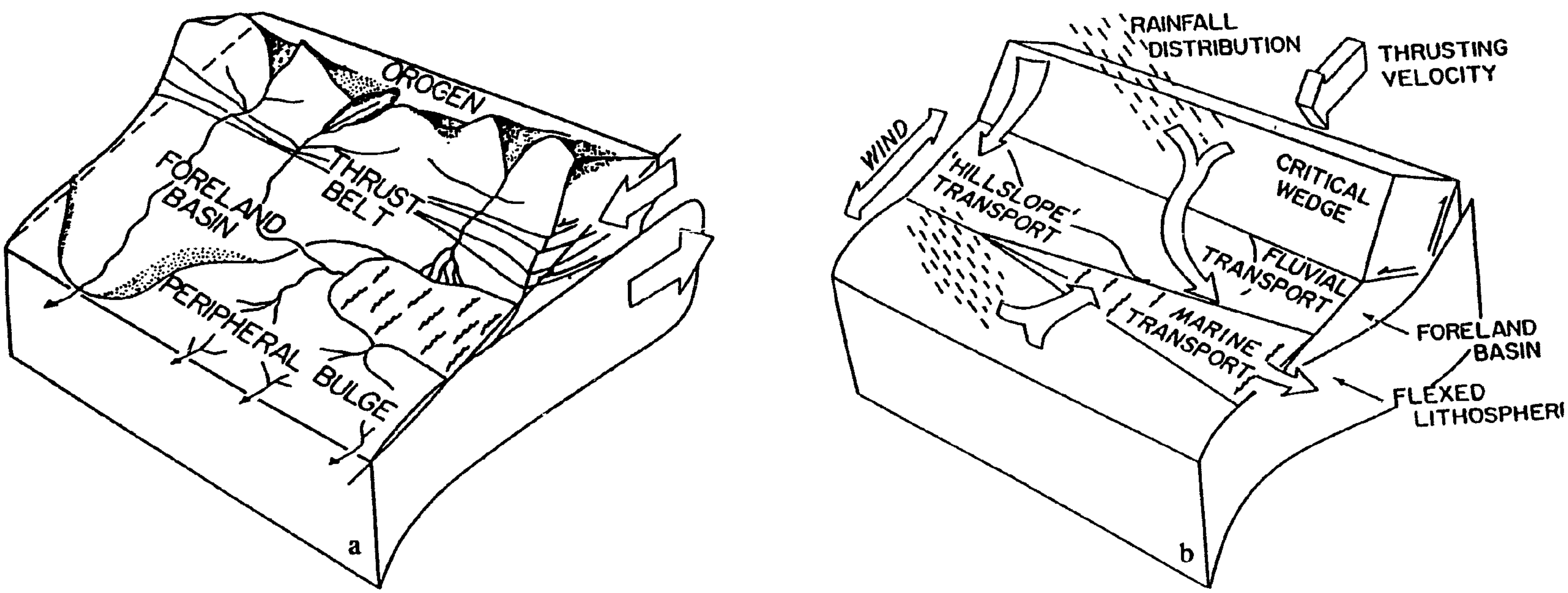

Figure 2.1. Schematic diagrams of: a) Fundamental characteristics of an orogen/foreland basin system; arrows indicate convergence direction. b) Components of the composite planform orogen/foreland basin model; arrows indicate material tranport directions.

time-dependent responses in topography and basin stratigraphy. Topography at any time is therefore a consequence of the historical interactions among all model processes, and basin stratigraphy is a synoptic record of how these interactions control the evolution of the orogen/foreland basin system.

The integrated model is structured to calculate the incremental change in orogen growth, surface topography, and basin stratigraphy given a set of initial conditions and parameter values (Fig. 2.2). Each increment or tectonic time step (Δt_T) represents 50,000 years of geologic time. Within each tectonic time step the tectonic and isostasy models are used to calculate the effects of orogen growth and changes in water load on topography. The surface-processes model then uses changes in topography and sea level in conjunction with precipitation to calculate incrementally the effects of erosion and sedimentation on landform evolution. Orographically controlled precipitation is calculated by the climate model as surface topography evolves with each surface-processes time step (ΔtS). Surface-processes time steps are 1/100th of a tectonic time step (5000 years) to increase temporal resolution. The model results presented in subsequent chapters are those at the end of a tectonic time step and typically after several million years of orogen/foreland basin development.

In this chapter each of the component models and the choice of initial conditions, constant parameter values, and time-dependent parameter values are discussed. In addition a number of geological concepts as applied to the model results are reviewed.

2.2 Tectonic Model

The kinematic tectonic model approximates the planform and sectional two-sided character of the tectonic load distribution in an orogenic belt and the kinematics of

Integrated Orogen/Foreland Basin Model Flow Chart

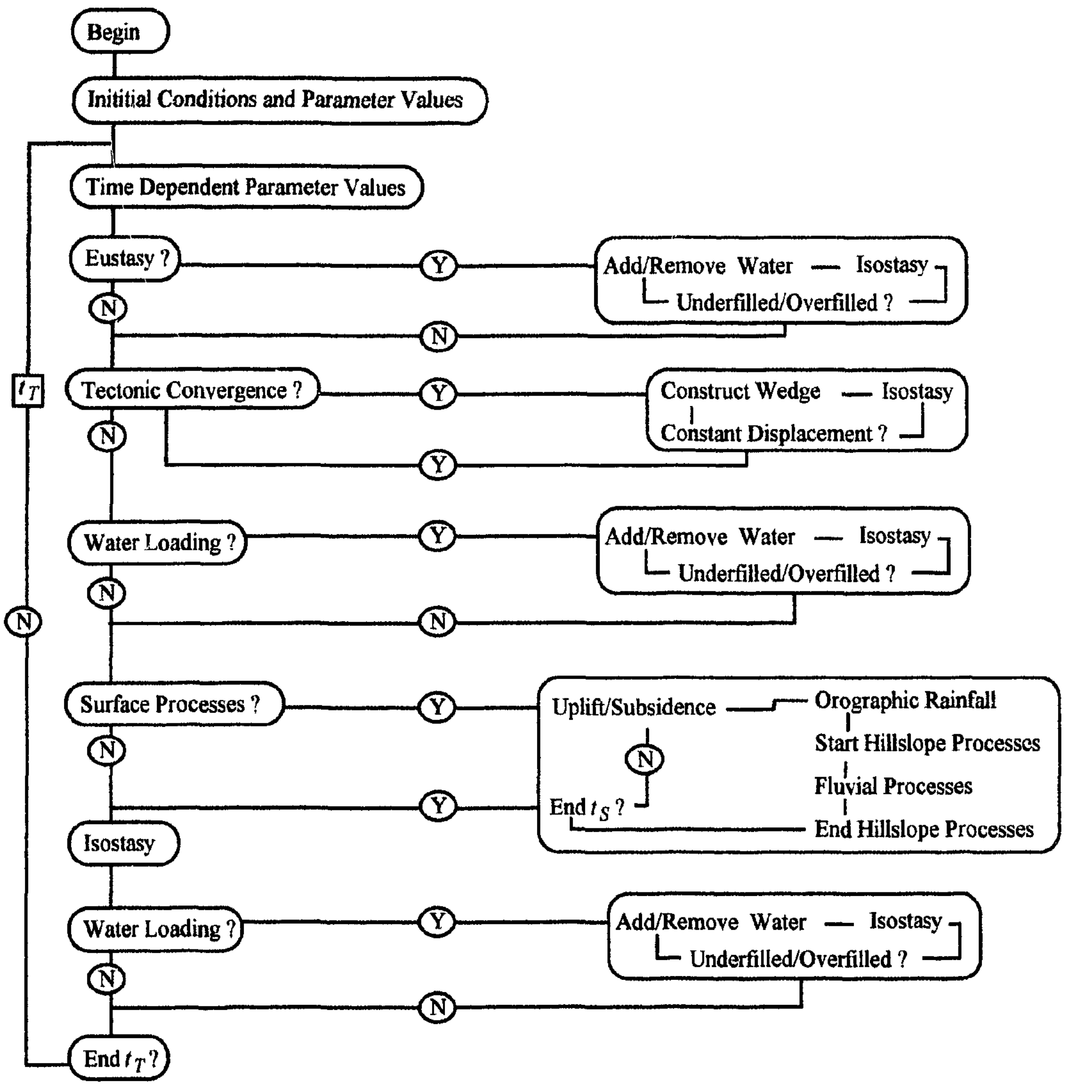

Figure 2.2. The flow chart shows how the component models are interconnected to create the composite orogen/foreland basin model and fundamental decision points in the modelling process. "Y" and "N" represent yes and no respectively. t_T refers to a tectonic timestep and t_S refers to surface processes time step. See text for discussion of component models.

orogen growth. It is more important that the model predict orogen geometry than internal deformation, because of the effects of orogen topography on surface processes and of tectonic load distribution on the flexural isostatic displacement of the lithosphere. While the mechanics of orogen development remain poorly understood, critical-wedge theory provides a basic working model for the geometrical development of a plane-strain orogenic wedge (Chapple, 1978; Davis *et al.*, 1983; Stockmal, 1983; Dahlen, 1984; Dahlen *et al.*, 1984; Dahlen and Suppe, 1988; Willett, 1992).

I have made a tectonic model that creates a doubly-vergent wedge-shaped orogen based on noncohesive critical Coulomb[1] wedge theory (Dahlen, 1984; Dahlen *et al.*, 1984), 'sand-box' experiments (Malavieille, 1984) and dynamical numerical models of doubly-vergent Coulomb wedges (Beaumont *et al.*, 1992; Willett, 1992; Willett *et al.*, 1993). Chapple (1978) was the first to note that the fundamental characteristics of thin-skinned fold and thrust belts are analogous to those of a critically tapering wedge: "a wedge shaped deforming region, a weaker layer at the base of the wedge, and large amounts of shortening and thickening within the wedge." Davis *et al.* (1983) show that, in dip section, the geometry of foreland fold-and-thrust belts is similar to that of the central portion of a critical Coulomb wedge. However, this application of critical Coulomb wedge theory (Dahlen, 1984; Dahlen *et al.*, 1984) limits the comparison of critically tapering wedges to orogenic foreland fold-and-thrust belts, excluding the central and opposing side of each orogen. Malavieille (1984) recognized the two-sided character of orogens and showed with sand-box experiments how doubly-vergent wedge growth may be analogous to orogen growth (Fig. 2.3a). Willett *et al.* (1993) and

---

[1] Coulomb refers to the Coulomb-Navier criterion for failure, $|\eta|=S+\sigma\mu$, where η is shear stress, σ is normal stress, S is cohesion and μ is the internal coefficient of friction (Ranalli, 1987).

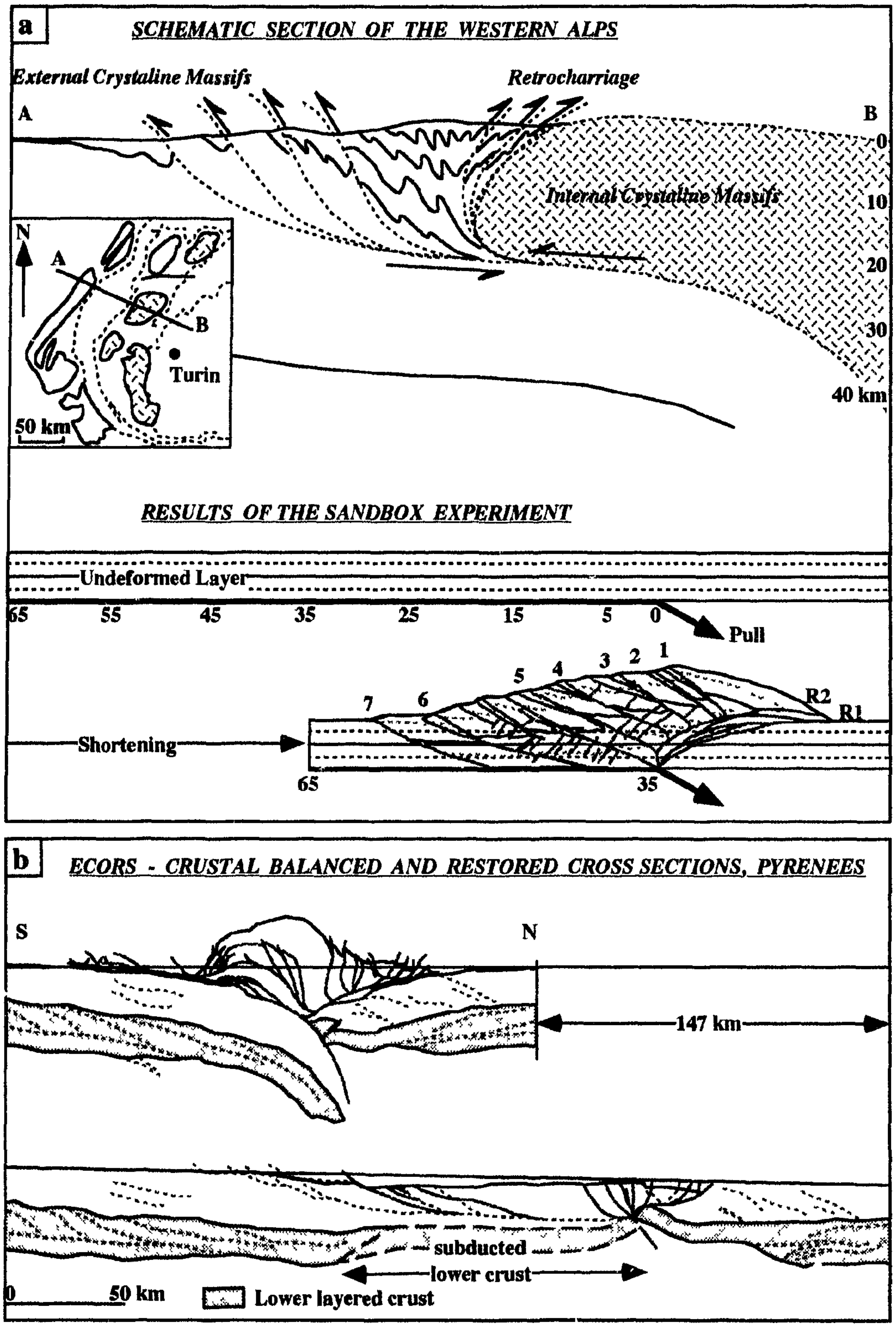

Figure 2.3 a) Malavieille's (1984) comparison of the Western Alps and 'sandbox' model results. b) Balanced crustal and restored sections through the Pyrenees, modified after Munoz (1992)

Beaumont *et al.* (1994) similarly recognized the two-sided character of orogens and used dynamical numerical models of doubly-vergent critical wedge growth to approximate the evolution of complete sections of plane-strain compressional orogens. They assumed that a convergent orogen grows by subduction-like asymmetric detachment and underthrusting of the mantle lithosphere (*e.g.*, Pyrenees, Fig. 2.3b). In their models, the overlying 'crust' undergoes compressional deformation because of shear stress applied to its base by 'subduction'; the result is a central block uplift and two oppositely verging tectonic wedges in the crust (Beaumont *et al.*, 1992; Willett *et al.*, 1993). Willett *et al.* (1993) interpret the mechanics of this critical doubly-vergent Coulomb wedge growth as an extension of uniform-taper critical Coulomb wedge mechanics (Dahlen, 1984). They suggest that orogens, like doubly-vergent wedges, are geometrically asymmetric during the early stages of development but may be more symmetrical during some phases of their evolution.

The tectonic model creates an orogenic load above the zone of convergence between the two plates (Fig. 2.4). Crust and sediment above a prescribed zone of weakness in either plate are accreted to the orogen, with convergence supplying material for orogen growth. In the absence of surface processes, the orogen grows in a geometrically symmetric manner. The model does not include creation of an asymmetric orogen that becomes progressively symmetric like that of Willett *et al.* (1993), because the wedge dynamics controlling the transition from asymmetry to symmetry are not well understood. In the integrated orogen/foreland basin model, orogen geometry and load distribution are asymmetric because the rates of precipitation, erosion, sedimentation, isostatic compensation and tectonic accretion of basin strata are not uniform across the model. These processes introduce asymmetry into the orogenic load distribution, while tectonic processes work to restore symmetry. Orogen elevation, relief, state and load

Orogen and Foreland Basin System

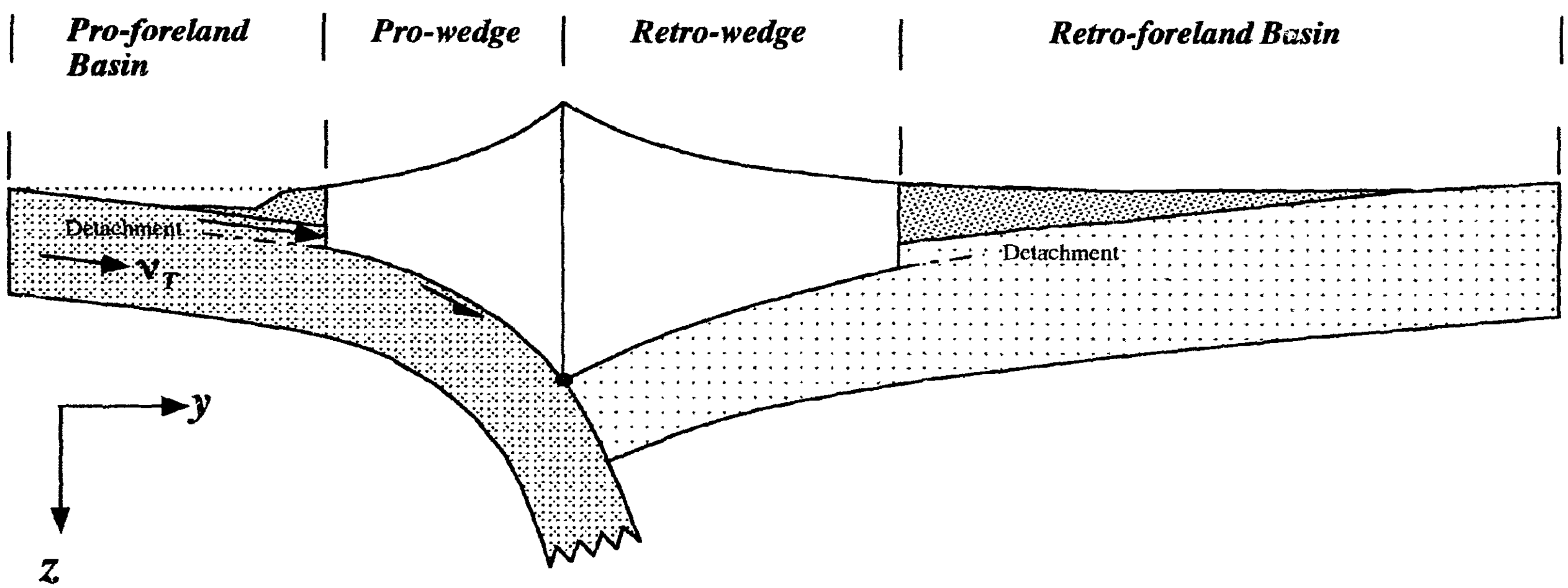

Figure 2.4. Schematic section through an orogen/foreland basin system. The prefix 'pro' is used to identify those elements of the doubly-vergent wedge-shaped orogen and flanking foreland basin that overlie the subducting plate, while 'retro' is used to identify similar elements of the system overlying the overriding plate. In Cartesian coordinates convergence between adjacent plates is parallel to y, z is vertical, and x is parallel to the strike of the orogen.

distribution are influenced by the interaction among all model processes. In this regard the present tectonic processes model differs from the one-sided orogen of Flemings and Jordan (1989), their fault-bend-fold model (Flemings and Jordan, 1990; Jordan and Flemings, 1991) and the one-sided geometric models of Sinclair *et al.* (1991) and Peper (1993). The rates of these processes both influence and are influenced by the evolution of model topography.

Terminology for orogens and foreland basins is problematic when considering both sides of an orogen together with the flanking foreland basins. The terminology recently proposed by Willett *et al.* (1993) and Johnson and Beaumont (1995) is used to distinguish the sides of the orogen and the two foreland basins (Fig. 2.4). In their terms, elements of the orogen and foreland that overlie the subducting plate are identified by the prefix 'pro', while elements of the orogen and foreland that overlie the overriding plate are identified by the prefix 'retro.' This modification of existing terminology conforms partly to Dickinson's (1974) foreland basin terminology in that both retro-arc and retro-foreland basins are located on the overriding plate. However, 'retro-arc foreland basin' refers to those basins in a back-arc setting, while 'retro-foreland basin' refers more generally to all foreland basins (including retro-arc foreland basins) positioned over the overriding plate in a convergent setting. Similarly, both the peripheral and pro-foreland basins are positioned over the subducting plate. However, the term pro-foreland basin avoids confusion with the usage of 'peripheral' to characterize both the basin and the peripheral bulge.

The tectonic model does not include the effects of mantle convection (Mitrovica *et al.*, 1989; Gurnis, 1992) or in-plane stress (Cloetingh, 1988; Peper, 1993) on the orogen/foreland basin system. Mantle convection is not included because there is no simple kinematic approximation of this process to describe how sublithospheric loading changes in planform with growth of the orogen and filling of the basin. The effects of in-plane stress have not been included because vertical deflections of the lithosphere are significantly smaller (on the order of ~10 m) than deflections caused by vertical loads on the lithosphere (basin ~1000 m, bulge ~100 m) (Peper, 1993). If present, therefore, in-plane stress may have a modifying effect on the peripheral bulge and very little effect in the basin.

Discussion of the tectonic model focuses first on how the tectonic processes operate in dip section, then how the planform effects of orogen growth are taken into consideration. The model operates on a uniform grid with cell size (*cl*) and grid dimension, 50 *cl* by 100 *cl*. In Cartesian coordinates, the strike of the model orogen is parallel to x, the direction of tectonic convergence between adjacent plates is parallel to y, and z is vertical (Fig. 2.4).

2.2.1 Wedge Statics

In section, the tectonic model opposes non-cohesive critical Coulomb wedges about a common-vertical-boundary (*CVB*, ①, Fig. 2.5). This boundary is a vertical surface, parallel to x, and fixed to the model grid. The pro- and retro-wedges are both bounded by the *CVB*, a decollement (②, Fig. 2.5), a deformation front (③, Fig. 2.5) and a subaerial or submarine surface. Material within these bounds is on the verge of failure everywhere when the wedges are critical (Dahlen, 1984).

The lower boundary of either wedge is assumed to form along a zone of weakness in the lithosphere (④, Fig. 2.5). This zone, or potential detachment surface, is fixed at a position in the model lithosphere as part of the initial conditions. Failure along this surface creates a frictional sliding surface, *i.e.*, a decollement, which forms the base of either wedge. Sediment, sedimentary rocks and crustal material above the detachment

Components of the Doubly-Vergent Wedge-Shaped Orogen

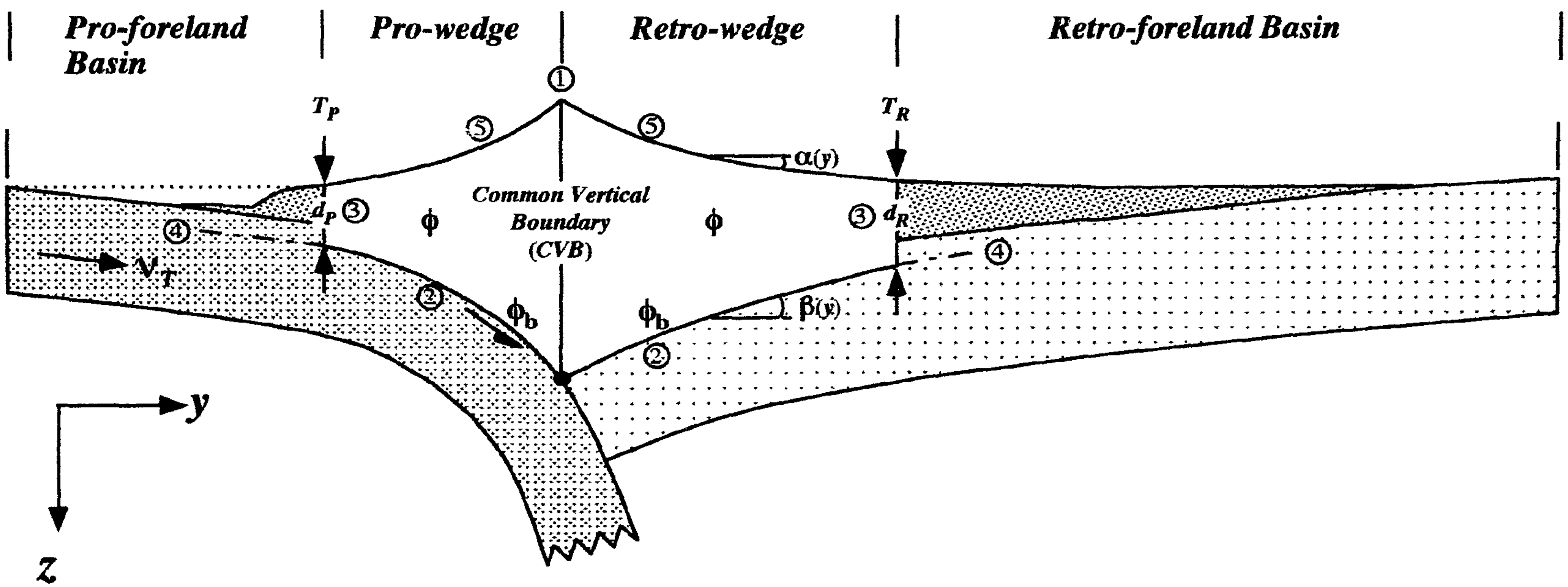

Figure 2.5 Schematic section through an orogen/foreland basin system showing the fundamental components of the doubly-vergent model wedge: 1) pro- and retro-wedge common vertical boundary (*CVB*), 2) decollements, 3) deformation front position (T_P/T_R) and thickness (d_P/d_R), 4) potential detachment surface, 5) wedge surface, internal (ϕ) and basal (ϕ_b) coefficients of friction where ϕ=arctan(μ), and surface slopes of the wedge (α) and decollement (β).

surface are accreted to the wedge, while material below the decollement is not involved with orogen growth. Material accreted to either wedge is assumed to have a bulk density of 2600 kg/m^3. Surface slopes of the decollements ($\beta(y)$, ②, Fig. 2.5) are determined in part by the initial shape of the potential detachment surface and in part by the effects of flexural isostatic compensation on the shape and dip of the decollements and the potential detachment surface. The potential detachment surface forms the base of the model wedge, *i.e.*, the flexural part continues to greater depth.

The *CVB* rises vertically from the intersection of the pro- and retro-decollements. In the dynamical models of Willett *et al.* (1993) and Beaumont *et al.* (1994), this intersection occurs at the 'singularity' where shear stress reverses sign at the intersection of the two convergent plates. The *CVB* replaces the 'block-uplift' that separates pro- and retro-wedges in sandbox experiments (Malavieille, 1984) and in dynamical numerical models (Beaumont *et al.*, 1992; Willett *et al.*, 1993), because the mechanics of block-uplift displacement and deformation are not well understood. In the kinematic model, the pro- and retro-wedges must be the same length along the *CVB*.

For simplicity, the model does not distinguish between subaerial and submarine environments when determining the critical taper and thence the surface slope of the orogenic wedge at any point. The upper surface of the pro- and retro-wedges in both the subaerial and submarine environments is, therefore, considered to be a stress-free boundary. The local subaerial or submarine surface slope ($\alpha(y)$, ⑤, Fig. 2.5) is calculated on the basis of critical Coulomb-wedge theory (Dahlen, 1984; Dahlen *et al.*, 1984) as,

$$\alpha(y) = \left(\left(\beta(y) + \mu_b\right)/\left(1 + 2\mu\right)\right) - \beta(y) \qquad (2.2.1)$$

where μ is the effective internal coefficient of friction (Fig. 2.5) and μ_b the effective coefficient of friction along the basal decollement (Fig. 2.5), such that $\alpha(y)+\beta(y)$ is at minimum critical taper (Θ_{min}) (Dahlen, 1984; Barr and Dahlen, 1990). In this study μ is always much greater than μ_b, and therefore $\Theta_{min}(y)$ obeys the small angle assumption, *i.e.*, $\alpha(y)+\beta(y) << 1$ radian (Dahlen *et al.*, 1984). The effective coefficients of friction are assumed to be the same for both subaerial and submarine environments. It is also assumed that when the change in the decollement slope is small (*i.e.*, $\Delta\beta << 1°$) over discrete intervals (Δy), the calculated change in critical taper over Δy using Eq 2.2.1 provides a reasonable approximation of how the critical taper will vary in a dynamic wedge. As a consequence, pro- and retro-wedge thickness (l) at y_o can be calculated as,

$$l(y_o) = d + \int_{T}^{y_o} \left(Tan\alpha(y) + Tan\beta(y)\right)\partial y \quad (2.2.2)$$

where d is the thickness of the wedge at the pro-wedge (d_P) or retro-wedge (d_R) deformation front and T is the position of the pro-wedge (T_P) or retro-wedge (T_R) deformation front (Fig. 2.5).

Deformation fronts of both the pro- and retro-wedges are assumed to be vertical to simplify calculations of the material flux ($Q_{T(pro)}$ or $Q_{T(retro)}$) into either wedge. While these fronts are neither vertical in nature nor in a critical Coloumb wedge, this simplification is unlikely to cause a significant error.

2.2.2 Wedge Kinematics

In the model, orogenic growth refers to the increase in pro- and retro-wedge size in cross-sectional area. Convergence results in offscraping of material from the subducting plate into the orogen, driving orogen growth. Pro- and retro-wedges develop over weak basal decollements and material is added to the pro- and retro-wedges by frontal accretion. Inside the wedge, material is assumed to deform by pure shear so as to maintain critical taper. This assumption is consistent with the dynamical numerical model results of Willett (1992). Furthermore, while pro-wedge growth is a consequence of convergence and frontal accretion, retro-wedge growth is caused by the transfer of material from the pro-wedge and subsequent entrainment of the retro-autochthon, similar to dynamical numerical models of doubly-vergent wedges (Willett *et al.*, 1993; Beaumont *et al.*, 1994). It is assumed that there is no net material transport along strike in the wedge, because the dynamics of three-dimensional wedge behaviour remain poorly understood and plane-strain critical-wedge theory provides no insight into wedge mechanics when properties of the wedge vary in the strike direction. Therefore, wedge kinematics as discussed below refer to the rates of processes within any grid-row parallel to convergence.

Wedge Growth without Surface Processes

In the absence of surface processes, the pro- and retro-wedges grow in a geometrically symmetrical manner about the *CVB*, at a rate determined by the rate at which material is accreted to the pro-wedge ($Q_T(pro)$, ①, Fig. 2.6) per unit length along strike,

$$Q_T(pro) = v_T \times d_p \qquad (2.2.3)$$

where v_T is the relative velocity of convergence between subducting and overriding plates; v_T is constant along strike. The material accreted to the wedge (M_T) per dip grid-row (j) within a tectonic time step (Δt_T) is the space-time integrated tectonic flux, i.e.,

$$M_{T_j} = v_T \times d_{P_j} \times cl \times \Delta t_T \qquad (2.2.4)$$

where M_{T_j} and d_{P_j} are M_T and d_P respectively for grid row j ; cl is the cell size and thus the width of each grid row. Pro- and retro-wedge growth rates are assumed to be constant throughout Δt_T, because v_T and d_p are constant over Δt_T. d_p is constant

Material Flow Through the Orogen and Foreland Basin System

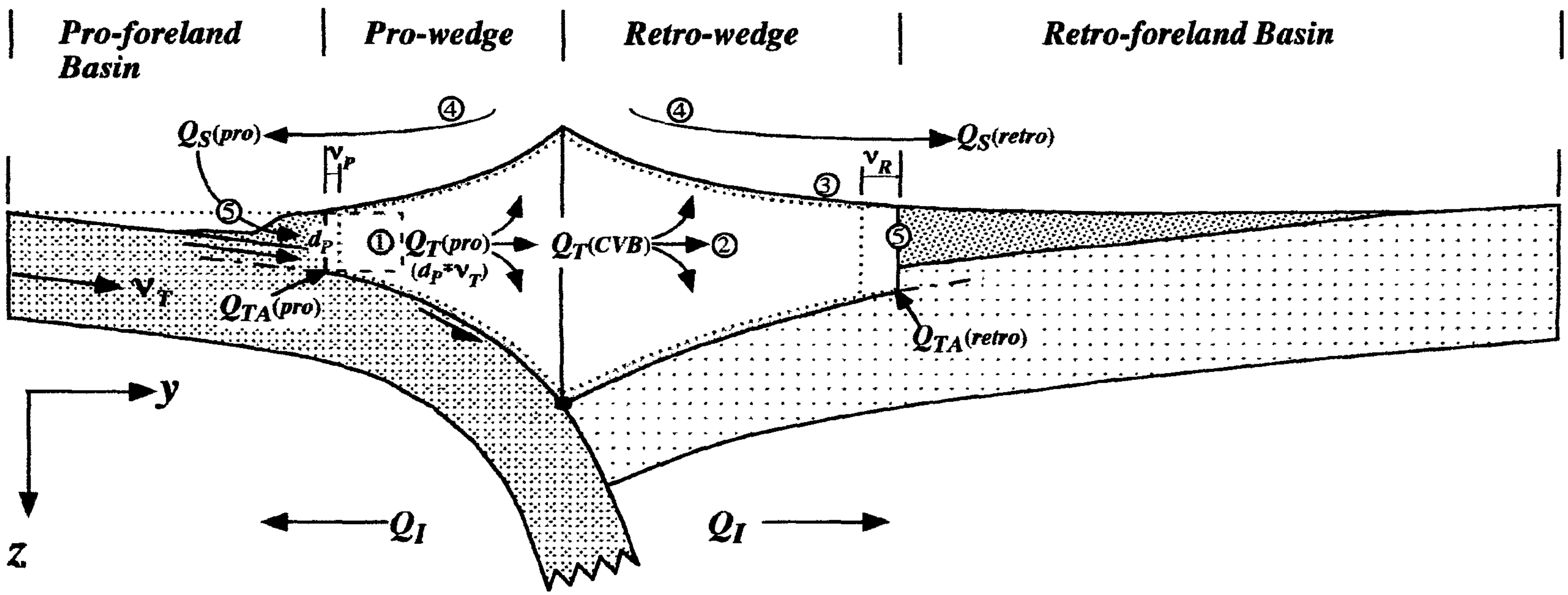

Figure 2.6. Schematic section through an orogen/foreland basin system showing flow of material through the doubly-vergent model wedge 1) Material flux into pro-wedge (Q_T(pro)) caused by convergence (v_T). 2 - 3) Grey perimeter represents wedge growth with distribution of material flux through the pro- and retro-wedge ($Q_T(CVB)$) by internal deformation. Q_{TA}(retro) and Q_{TA}(pro) represents material added to the wedge by virtue of wedge growth. 4) Material flux out of the orogen owing to surface processes (Q_S(pro) and Q_S(retro)). 5) Re-entrainment of material eroded from the orogen back into the orogen. Q_I represents the horizontal flux of material in the asthenosphere caused by flexural compensation of the growing orogenic load.

throughout Δt_T because the tectonic time step is made short enough that the tectonic convergence ($\Delta t_T \times v_T$) is much less than the model cell size.

Internal deformation of the wedges distributes a material volume equivalent to $Q_T(pro)$ between the pro- and retro-wedge (②, Fig. 2.6) such that each wedge maintains minimum critical taper. The local critical taper changes with time as isostatic compensation for the growing orogenic load alters the dip of the basal decollements. Pro- and retro-wedge growth is, therefore, only approximately self-similar (③, Fig. 2.6). Isostatically compensated critical pro- and retro-wedge geometries for each tectonic time step are determined for all grid-rows by iterative wedge constructions.

In the model, $Q_T(pro)$ is used to build the wedges while $Q_{TA}(pro/retro)$ is a consequence of wedge growth and geometry. Critical wedge taper influences $Q_{TA}(pro/retro)$ by determining the ratio of vertical to horizontal wedge growth. Isostasy influences $Q_{TA}(pro/retro)$ indirectly through its affect on critical wedge taper. Material flux into the pro-wedge is the sum of $Q_T(pro)$ and $Q_{TA}(pro)$. The rate of pro-wedge deformation front advance relative to the material above the detachment in the pro-foreland basin is, therefore, the sum of v_T and the horizontal rate of pro-wedge growth (v_P, Fig. 2.6). In contrast, material flux into the retrowedge is the sum of $Q_T(CVB)$ and $Q_{TA}(retro)$ where $Q_T(CVB)$ is material flux across the *CVB*. The rate of retro-wedge deformation front advance is, therefore, equal to the rate of horizontal retro-wedge growth (v_R, Fig. 2.6).

Wedge Response to Surface Processes

The flow of material through the model orogen/foreland basin system is into the orogen by accretion (①, Fig. 2.6), out of the orogen by erosion and fluvial transportation (④, Fig. 2.6), and possibly recycling back into the orogen by accretion (⑤, Fig. 2.6). This cyclic flow of material through the orogen and adjacent basin is a fundamental characteristic of natural orogen/foreland basin systems (Schwab, 1986). In the model, surface processes are linked to tectonic processes such that material volume is conserved between the orogen and the basins. In addition, tectonic flux $Q_T(pro)$ into the orogen is partitioned between the pro- and retro-wedges with consideration for the rate at which material is removed by surface processes. Therefore, the effects of non-uniform erosion of an orogen caused by non-uniform precipitation, for example, enhance the flow of material through the orogen. In nature, spatial variability in erosion rates and the attendant enhanced rate of material flow through an orogen is one factor that can contribute to variation in the metamorphic grade of rocks exposed at the surface (Jamieson and Beaumont, 1988; Beaumont *et al.*, 1992; Willett *et al.*, 1993).

In the orogen/foreland basin model, tectonic processes compete with surface processes. The tectonic processes work to achieve stable pro- and retro-wedges at local minimum critical taper (Θ_{min}), while erosion and sedimentation modify the local surface slope (α) and the decollement slope (β) through isostatic compensation such that wedge taper (Θ, where $\Theta=\alpha+\beta$) may not be critical (*i.e.*, $\Theta \neq \Theta_{min}$). Changes in wedge taper alter the response of the wedge under applied stress. According to critical Coulomb-wedge theory, a compressional wedge is stable provided the taper is between the minimum (Θ_{min}) and maximum (Θ_{max}) critical taper, and deforms internally only when $\Theta < \Theta_{min}$ or $\Theta > \Theta_{max}$ (Dahlen, 1984; Dahlen *et al.*, 1984; Willett, 1992). If local wedge taper becomes less than the minimum critical taper, then that portion of the wedge is no longer on the verge of Coulomb failure; it is incapable of transmitting stress, and it deforms internally until minimum critical taper is restored. Conversely, if local wedge taper is increased to a value between minimum and maximum critical taper, that portion of the wedge becomes stable and behaves as a rigid body that can be displaced along the decollement as part of the wedge. If local wedge taper is increased such that $\Theta > \Theta_{max}$, that portion of the wedge becomes unstable and collapses until $\Theta = \Theta_{max}$ (Willett, 1992).

An example of how an eroded retro-wedge is restored to critical taper is used to illustrate the application of critical-wedge theory. The retro-wedge surface has been locally modified by erosion, increasing the surface slope such that Θ is between Θ_{min} and Θ_{max} in some places, but reducing surface slopes in other places such that $\Theta < \Theta_{min}$, as illustrated in Figure 2.7. The case where $\Theta > \Theta_{max}$ is not discussed because Θ_{max} is much greater than surface slopes created by the interaction of tectonic and surface processes in the model for the parameter values used in this study.

$\Theta < \Theta_{min}$

The retro-wedge deformation front prior to erosion is at $T_R(1)$. After erosion the wedge taper between *CVB* and $T_R(2)$ is greater than or equal to Θ_{min} (①, Fig. 2.7). The wedge toe, $T_R(2)$, is at the point where Θ first becomes less than Θ_{min}. Deformation is localized to the region immediately adjacent to $T_R(2)$. Stress cannot be transmitted significantly past $T_R(2)$ until the critical angle adjacent to $T_R(2)$ is restored to Θ_{min}. The previously deformed region between $T_R(1)$ and $T_R(2)$ is therefore tectonically inactive even if locally Θ exceeds Θ_{min} (②, Fig. 2.7).

$\Theta = \Theta_{min}$

At $T_R(2)$ local wedge taper is equal to Θ_{min}, and therefore the wedge is on the verge of Coulomb failure. Material and stress transmitted into the retro-wedge from the pro-wedge causes local deformation at and basinward of $T_R(2)$, increasing the local basinward taper to Θ_{min}, thereby advancing the deformation

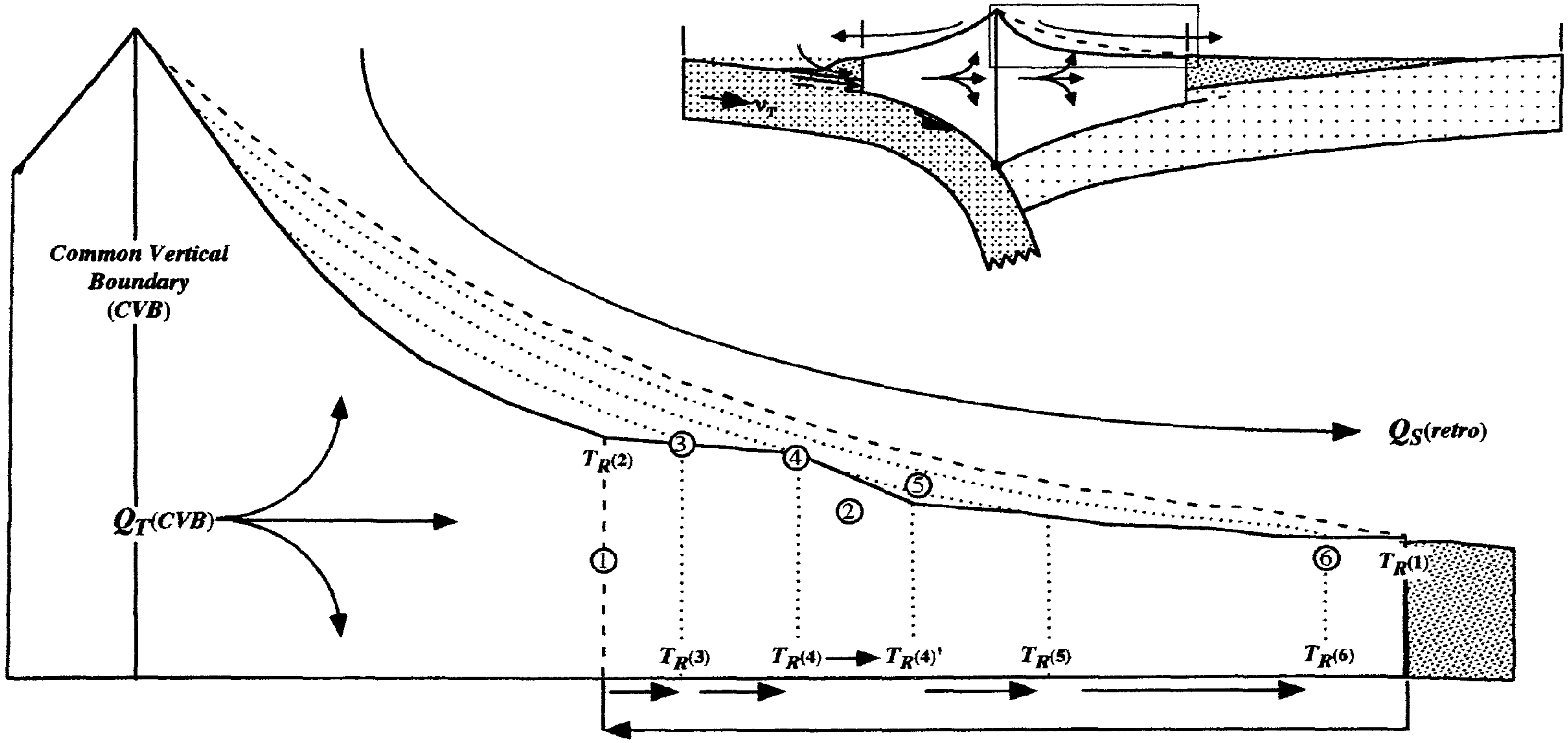

Figure 2.7. Enlarged schematic section of the retro-wedge (see box) showing the effects of erosion (difference between solid and dashed surface lines) and the progressive restoration of the wedge (dotted lines) to critical taper. Changes in the wedge toe position with time are labelled $T_R(1)$ to $T_R(6)$. $T_R(1)$ is prior to erosion. $T_R(2)$ is immediately after erosion. $T_R(2)$ to $T_R(6)$ show advance of wedge toe with wedge restoration.

front. Deformation at $T_R(2)$ locally reduces the wedge taper behind $T_R(2)$ to less than critical. This change results in deformation of the wedge toward the *CVB* to maintain critical taper, thereby increasing the region of the wedge that is at critical taper. Deformation of the wedge continues to increase the region of critical taper, simultaneously forward and backward as the wedge builds itself upward in a self-similar fashion (③, $T_R(3)$, Fig. 2.7).

$\Theta > \Theta_{min}$

At $T_R(4)$ the model encounters a region ($T_R(4)$ and $T_R'(4)$) similar to the region between the *CVB* and $T_R(2)$ where $\Theta_{min} < \Theta < \Theta_{max}$. The model identifies regions such as these where the wedge can transmit stress and requires the deformation front to advance past these regions without causing deformation. In the example, the deformation front advances with wedge growth to $T_R(4)$ and then jumps forward to $T_R'(4)$ over a region $\Theta_{min} < \Theta < \Theta_{max}$ (④, Fig. 2.7). As wedge growth continues, local headward deformation does not extend past $T_R(4)$ until the region between $T_R(4)$ and the wedge toe ($T_R(5)$) is at critical taper (⑤, Fig. 2.7). After critical taper extends to $T_R(4)$ the wedge will continue to grow forward past $T_R(5)$ and backward toward the CVB at critical taper.

In the integrated orogen/foreland basin model, this process of tectonic growth continues while surface processes modify the taper of the orogen and the isostasy model compensates for changes in the orogenic load. If the tectonic processes were unaffected by surface processes, the wedge would grow in a uniform, approximately self-similar manner.

In the model, accreted material is assumed to be distributed by internal deformation through the wedges (Fig. 2.6) and is partitioned between both the pro- and retro-wedges in response to the effects of surface processes. The accreted material is used incrementally and alternately to establish or extend critically tapered segments of the pro- and retro-wedges. In either wedge a critically tapered segment spans the distance between two or more cell centres beginning at either wedge toe. The critically tapered segments grow horizontally when vertical growth allows the segment to extend the critical wedge taper up or down dip. The vertical growth of pro- and retro-wedge segments is determined by either the incremental amount of material available for wedge growth or the material required to advance the wedge toe to the next cell. In the latter case, the unused portion of the material becomes available for restoring the alternate side of the wedge. As a consequence one side of the wedge may receive a greater proportion of $Q_T(pro)$ in any tectonic time step. This fact is important because pro- and retro-wedges are not eroded at equal rates, and therefore they will not be fully restored to critical taper at the same time. Where both sides of the wedge are restored to critical taper and erosion rates were uniform, then material flux would be partitioned equally between pro- and retro-wedges.

2.2.3 Planform Wedge

In nature, thrust sheet displacements show that tectonic deformation in convergent orogenic belts is coherent along strike over length scales from metres to hundreds of kilometres. While plane-strain critical-wedge theory provides some insight into how wedge mechanics may respond to the effects of surface processes in dip section, it provides little insight into how wedge mechanics may respond in strike section. Currently there is little understanding of the mechanics that cause coherence in thrust sheets or of the factors that control their strike length; nor is there an understanding of how along-strike coherence interacts with surface processes to influence the development of surface relief. Nonetheless, orogenic belts do show shorter wavelength (<10 km) and larger amplitude in along-strike surface relief as expressed by the fluvial network development. For example, the major river valleys crossing the front ranges of the Canadian Cordillera. In general, longer wavelength (<100 km) along-strike changes in surface relief of comparable amplitude appear to be less evident in orogenic belts. In the model, therefore, I assume that along-strike coherent deformation causes preferential preservation of surface relief with wavelengths shorter than the length scale of coherent deformation, and conversely causes restoration of surface relief with longer wavelengths.

In the model, the shorter wavelength surface relief is preserved by creating a new low-pass filtered topography from the existing topography. The low-pass filter surface relief is calculated using a moving average of surface relief over l_S along each strike grid-row. The length l_S is chosen to characterize the length scale over which deformation is coherent; l_S is an odd-numbered integral multiple of cl. The difference between the current topography and low-pass filtered topography is calculated and stored. Tectonic processes as previously described operate on the low-pass filtered topography and then the stored short wavelength surface relief is combined with the tectonically altered low-pass filtered topography to create a new surface topography. The result is that along-strike surface relief with length scales shorter than l_S are preferentially preserved relative to surface relief with length scales longer than l_S.

The characteristic length scale (l_S) for coherent deformation is perhaps the most difficult aspect to constrain in this model, because coherent along-strike deformation is not well understood, nor is there a good statistical analysis of thrust-sheet widths in modern orogens. As a consequence, maps showing orogens over length scales comparable to that of the model are used to provide an estimate of average thrust widths of 50-100 km. It is acknowledged that thrusting occurs on a range of scales, and therefore average thrust width measured in this manner will vary with map scale. In addition, experiments show that model results are relatively insensitive to values of l_S greater than 75 km. The length scale of coherent deformation, l_S, has been set at this length as the best compromise between measurements of natural thrust sheets and model sensitivity. Although this component of the orogen/foreland basin model is admittedly the weakest, it does provide a mechanism for coherent deformation without ad hoc assumptions about the mechanics of along-strike material transport in critical wedges or orogenic belts.

2.3 Surface Processes Model

The surface processes model describes surface material flux (Q_S) on geologic time scales caused by a combination of hillslope, fluvial and submarine transport processes. This model, as incorporated into the orogen/foreland basin model, has already been described in detail by Beaumont *et al.* (1992), Kooi and Beaumont (1994) and Kooi and Beaumont (submitted). In the subaerial environment, the model couples short-range diffusive (hillslope) and long-range advective (fluvial) material transport (Fig. 2.8). Long-range transport is influenced by the effects of orographically controlled precipitation. In the submarine environment, only short-range transport is used.

The use of diffusion to model sediment transport by all processes in the marine environment is an obvious oversimplification. I have chosen to use this approach because, 1) it has been used with moderate success by Kenyon and Turcotte (1985), Syvitski *et al.* (1988) and Flemings and Jordan (1989), 2) other marine transport models operate on space and time scales at least an order of magnitude smaller than those used by surface processes herein, 3) development of a model which couples both advective and diffusive 'bulk' transport mechanisms for submarine transport, similar to the

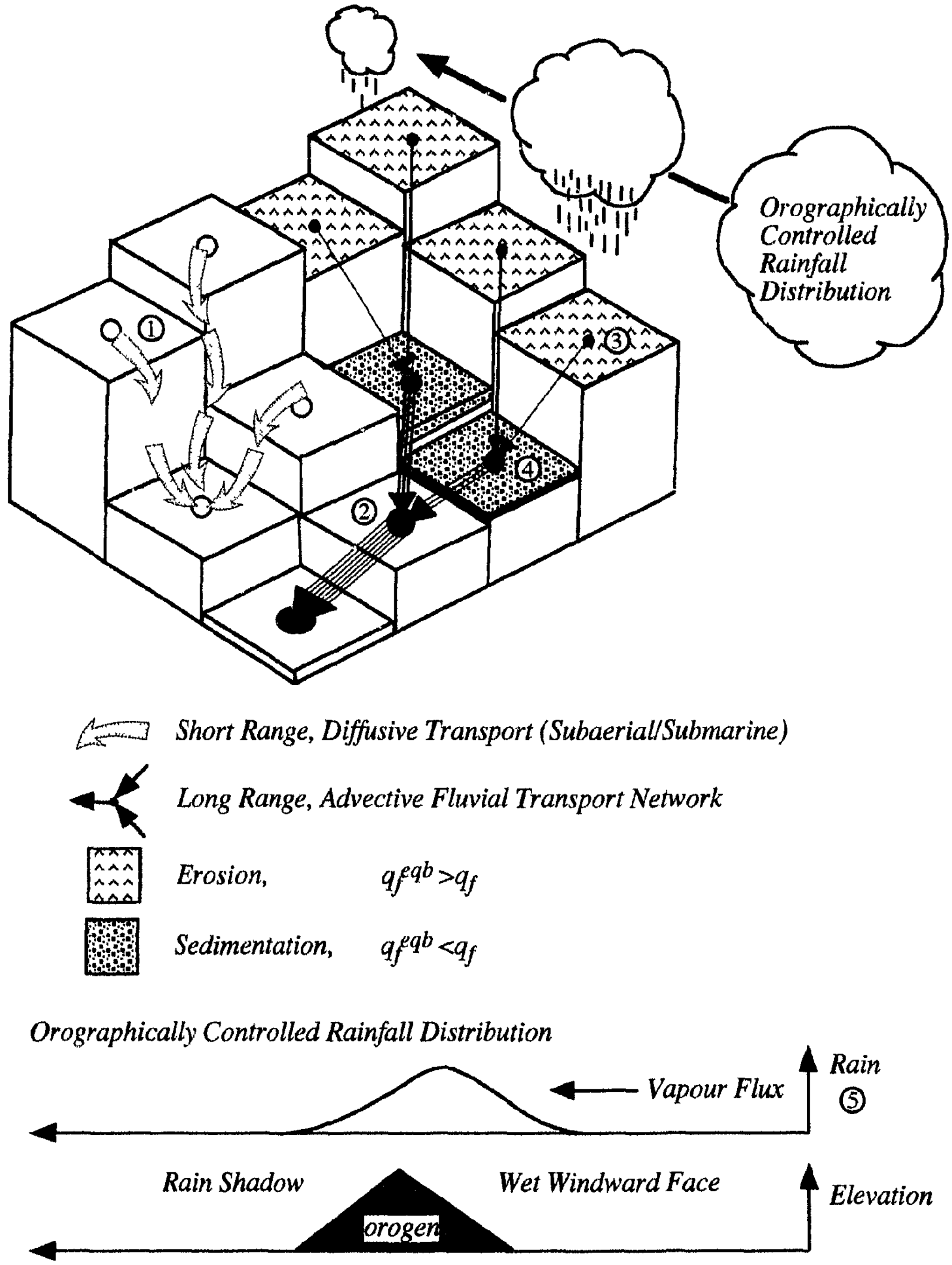

Figure 2.8. Surface processes model includes diffusive transport (grey arrows) in the submarine environment, and diffusive and advective (fluvial) transport (black arrows) in the subaerial environment. Fluvial erosion and sedimentation are determined by the sediment load in the river (q_f), and the river's equilibrium carrying capacity (q_f^{eqb}), which is proportional to river power (slope x discharge). Fluvial discharge at any point is the up-slope sum of orographically distributed rainfall collected within a watershed (black arrows). Rainfall changes with depletion of vapour flux and extraction efficiency, which varies with elevation.

approach used by Beaumont *et al.* (1992) for subaerial transport, is beyond the scope of this study. As a consequence model results show perhaps the simplest view of how submarine transport interacts with subaerial transport in a foreland basin setting.

In nature, material transport by surface processes is highly variable and often 'event dominated', while in the model diffusive and advective processes are continuous. Therefore, parameter values are chosen such that mean transport on time scales greater than the surface process model time step and spatial scales greater than cl is approximately equivalent to that in nature, as discussed in Chapter 3.

The surface processes component of the integrated model uses a time step (Δt_S) that is 100 times shorter than the 'tectonic' time step (Δt_T) in order to increase temporal resolution. The effects of tectonics and isostasy are assumed to occur at uniform rates during the tectonic time step. In the surface processes model, these effects are summed and applied in incremments of Δt_S / Δt_T of the total displacement to each surface processes time step. By this means tectonics and isostasy have a continuous uniform effect on topographic evolution. At the end of each surface process time step, topography is modified by the combined effects of surface processes, tectonics and isostasy and sea level is adjusted for eustasy, so that surface processes always operate on a current model planform.

The numerical implementation of the surface processes model is the same as that described by Beaumont *et al.* (1992); steady-state conditions are assumed during each of the surface processes model time steps (Δt_S) and surface processes model equations are integrated numerically over the uniform grid of square cells.

2.3.1 Short-Range Diffusive Transport

In nature, subaerial hillslope processes such as soil creep, slope wash, rockfall and gravity slides transport material from hillsides to the adjacent valleys (Carson and Kirkby, 1972). In the model, the cumulative effects of these processes are represented as linear diffusion that conserves volume (①, Fig. 2.8), following Culling (1960, 1965), Hanks *et al.* (1984) and Flemings and Jordan (1989). Similarly, the cumulative effects of the submarine processes responsible for net offshore transport, such as creep, gravity slides and density currents are represented as linear diffusion following Bagnold, 1963; Kenyon and Turcotte, 1985; Syvitiski *et al.*, 1988 and Jordan and Flemings, 1991. This representation assumes that the effect of submarine transport processes on shallow surface slopes (~ 1°) is much greater in both length and width than in vertical thickness, and that the frequency of transport increases with steeper surface slopes. As noted by Kooi and Beaumont (1994), while on short time scales the magnitude and frequency of material transport by the various processes of slope wasting are distinctly different, on long time scales these processes distribute material over short distances and are dependent upon surface slope. While Kooi and Beaumont (1994) were referring to hillslopes and not large-scale long-range processes, I expect this observation is likely to be true in the marine environment where the various processes responsible for slope wasting are the dominant mechanism of offshore transport.

In the model, the horizontal material flux (q_S) is related to the local slope (∇h) by

$$q_S = -K_S \nabla h \qquad (2.3.1)$$

where K_S is the diffusivity. It is assumed that material volume is conserved and the effects of dissolution of material are negligible; therefore, the transport equation (Eq. 2.3.1) can be combined with the continuity equation,

$$\frac{dh}{dt} = -\nabla q_s \tag{2.3.2}$$

to give the linear diffusion equation for the rate of change in local height owing to erosion or sedimentation by short-range processes,

$$dh/dt = K_s \nabla^2 h \tag{2.3.3}$$

The diffusivity (K_s) can be interpreted as

$$K_s = u_s h_s, \tag{2.3.4}$$

where u_s is the transport speed of an erodible surface layer of thickness h_s (Beaumont *et al.*, 1992). Surface layer thickness (h_s) is related to the depth of weathering or perhaps regolith thickness, while the transport speed (u_s) is a measure of the ease with which materials are transported. In the model, K_s varies with the type of surface material (consolidated material or alluvium) and the efficiency of transport in the submarine or subaerial environment.

The values of K_s used for short range transport in the subaerial environment are smaller than those used in the submarine environment. This difference in values primarily reflects the fact that surface processes in the subaerial environment are subdivided into diffusive and advective transport, while surface processes in the marine environment are diffusive transport alone. Were diffusive transport used as the only mechanism for subaerial transport, as in the Paola *et al.* (1992) model, then the subaerial values of K_s would be more nearly on par with those used in the marine environment. The choice of both subaerial and submarine K_s is explained in Section 2.8

2.3.2 Long-Range Advective Transport

In nature, fluvial transport is the principal mechanism for long-range subaerial material transport from the orogen to the basin in orogen/foreland basin systems that have not experienced glaciation. In this model, orogen/foreland basin systems are assumed to be unaffected by glaciation. Fluvial transport of suspended sediment and bedload is represented as a network of one-dimensional rivers (Beaumont *et al.*, 1992; Kooi and Beaumont, 1994), each of which is like a corridor draining the surface topography via the paths of steepest descent (②, Fig. 2.8). There is no distinction between hillslopes and river channels in the model because of the large spatial scale of the model (50*cl* x 100*cl*) and low resolution of the model grid (*cl*=15 km).

The ability of any river to transport material (*i.e.*, the local equilibrium 'carrying capacity', q_f^{eqb}) is considered to be proportional to the product of local fluvial discharge and river slope, referred to by Bagnold (1966) as stream or river power (Armstrong, 1980; Begin *et al.*, 1981; Chase, 1992),

$$q_f^{eqb} = -K_f q_r \, dh/dl \qquad (2.3.5)$$

where q_r is river discharge, dh/dl is river slope in the direction of drainage, and K_f is a dimensionless transport coefficient. This relationship is thought (P. L. Heller, pres. comm.) to be basically the same as the semi-empirical relationship for the volume rate of sediment that can be transported per unit width of stream developed by Meyer-Peter and Muller (1948, *cit.* Paola *et al.*, 1992)

$$q_{transported} = K(\eta - \eta_c)^m \qquad (2.3.6)$$

where K is a transport coefficient, η is the shear stress on the stream bed related to stream velocity, ηc is the shear stress required to put sediment in motion, and m is an empirically determined power of 3/2.

The local river discharge (q_r) is determined by the net precipitation rate (v_R) over the upstream watershed area (A) (Fig. 2.8).

$$q_r = \int v_R dA \qquad (2.3.7)$$

The distribution of precipitation rates (ν_R) is determined by the climate model. Precipitation is the effective precipitation used in fluvial transport once allowance is made for evaporation and infiltration. Water is conserved in the model.

The linear dependence of carrying capacity (q_f^{eqb}) on discharge (q_r) is shown by Kooi and Beaumont (1994) to be appropriate for long time scales, provided that Δt_S is greater than the periods between maximum floods and that river slopes are not significantly altered by erosion on time scales less than Δt_S (Kooi and Beaumont, 1994).

The model assumes that a river must work on the landscape in order to transfer material from the substrate into the fluvial sediment flux (Beaumont *et al.*, 1992; Kooi and Beaumont, 1994). The change in sediment flux (q_f) in a river, from the perspective of an observer traveling with the velocity of the sediment in the river (*i.e.*, Lagrangian reference frame), is determined by a first-order kinetic reaction,

$$\frac{dq_f}{dt} = \frac{1}{t_f}\left(q_f^{eqb} - q_f\right) \qquad (2.3.8)$$

where $1/t_f$ is a rate constant and ($q_f^{eqb} - q_f$) is the degree of disequilibrium between carrying capacity and fluvial sediment flux (Beaumont *et al.*, 1992). From the perspective of an observer fixed to the landscape (*i.e.*, Eulerian reference frame), the change in sediment flux with time is,

$$\frac{dq_f}{dt} = \frac{\partial q_f}{\partial t} + \left(\nu_f \times \frac{\partial q_f}{\partial l}\right) \qquad (2.3.9)$$

where ν_f is the velocity of the sediment in the river. In the model, sediment transport is assumed to be in steady state and does not vary within a time step (Δt_S) (Beaumont *et al.*, 1992).

Therefore, $\partial q_f/\partial t$=0 and Eq. 2.3.9 reduces to,

$$\frac{dq_f}{dt} = \nu_f \times \frac{dq_f}{dl}$$

or

$$\frac{dq_f}{dl} = \frac{1}{v_f} \times \frac{dq_f}{dt} \tag{2.3.10}$$

The time dependence of erosion and deposition ($1/t_f$), to the observer in a Lagrangian reference frame (Eq. 2.3.8), therefore takes the form of a spatial dependence to the observer in the Eulerian reference frame,

$$\frac{\partial h}{\partial t} = \frac{dq_f}{dl} = \frac{1}{t_f \times v_f}\left(q_f^{eqb} - q_f\right) \tag{2.3.11}$$

where $t_f \times v_f$ is equivalent to an erosional/depositional length scale l_f, the distance required for the disequilibrium, $q_f^{eqb} - q_f$, to be reduced by a factor of $1/e$, when q_f^{eqb} and q_f^{eqb} are constant. When $t_f \times v_f \rightarrow 0$ erosion and deposition are instantaneous (Eq. 2.3.11), because as $t_f \times v_f \rightarrow 0$, then it follows that $q_f \rightarrow q_f^{eqb}$ (Eq. 2.3.6); therefore, the rivers transport sediment at capacity (Kooi and Beaumont, 1994).

When $q_f^{eqb} > q_f$, a model river erodes material from its underlying substrate (③, Fig. 2.8). The rate of erosion is determined both by the disequilibrium, $q_f^{eqb} - q_f$ and the erosional length scale of the substrate (l_f). The erosional length scale is inversely proportional to the detachability of the substrate; thus lower values of l_f correspond to unconsolidated materials, while higher values correspond to consolidated materials.

A model river deposits material when $q_f^{eqb} < q_f$ (④, Fig. 2.8). This situation occurs when the reduction in the slope of the riverbed is greater than increase in discharge (Eq. 2.3.6). Because there is no apparent mechanical restriction to deposition, the depositional length scale used in the model experiments is set near to the resolution limit of the model ($\sqrt{2} \times cl$). This has the same effect as letting $t_f \times v_f \rightarrow 0$. As a result, rivers in a depositional mode are always carrying at capacity and the rate of deposition approximately equals the down-slope change in carrying capacity,

$$\frac{\partial h}{\partial t}=\frac{dq_f}{dl}\cong\frac{dq_f^{eqb}}{dl}$$

or

$$\frac{\partial h}{\partial t}\cong-K_f\left(\frac{dq_r}{dl}\frac{dh}{dl}+q_r\frac{d^2h}{dl^2}\right) \qquad (2.3.12)$$

Therefore, long-range fluvial transport is 'effectively diffusive' when the down-slope change in discharge is negligible or $\frac{dq_r}{dl}\frac{dh}{dl}\langle\langle q_r\frac{d^2h}{dl^2}$. Under these conditions sediment transport becomes similar, for example, to Flemings and Jordan (1989) and Paola *et al.* (1992). However, sediment transport differs significantly from these and other similar models in that diffusivity is not constant nor specified; instead effective diffusivity varies as the product of the fluvial transport coefficient (K_f) and river discharge (q_r). This dependence on fluvial discharge means that the diffusivity varies spatially and temporally with changes in the drainage network and in precipitation rate. As a consequence, the effective diffusivity evolves with the development of the orogen/foreland basin system. Furthermore, the long-range transport model further differs from the simple diffusion models when the change in down-slope discharge is not negligible or when $\frac{dq_r}{dl}\frac{dh}{dl}$ is significant relative to $q_r\frac{d^2h}{dl^2}$. These conditions arise when discharge increases with collection or local precipitation.

2.4 Climate Model

In this study, 'climate' is limited to the prevailing wind direction and the magnitude and distribution of precipitation. These elements of climate are incorporated into the orogen/foreland basin model because of the effect of orogen topography on the precipitation rate and the effect of the precipitation rate on fluvial transport. In nature, upward deflection and adiabatic decompression of moist air crossing a mountain belt cause an overall increase in precipitation rates on the orogen (Barros and Lettenmaier, 1994). The prevailing wind direction and depletion of moisture in the air create an asymmetry in precipitation across the orogen that results in wetter windward slopes and drier leeward slopes (*i.e.*, a rain shadow); this effect is referred to as orographically controlled precipitation. The climate model is a parametric simplification of the physics of orographic rainfall, because modelling the dynamics of this process is beyond the scope of this study.

Orographic control of precipitation requires that the distribution and magnitude of rainfall evolve along with the topography of the orogen/foreland basin system. I have used the same model as Beaumont *et al.* (1992). In their model, this evolution is accomplished by relating precipitation rate (ν_R) to the residual moisture content of the advected air (*i.e.* vapour flux, Q_V) and local topographic elevation ($h(y)$). The precipitation rate ($\nu_R(y)$) is assumed to have a constant mean value at a given location during each model time step (Δt_S). Rain is extracted from the incident vapour flux ($Q_V(y)$) as it passes from the model boundary over the current model topography, normal to the strike of the orogen according to,

$$\nu_{R(y)} = -\left(\frac{dQ_{V(y)}}{dy}\right) = \frac{h_{(y)}}{a_R} Q_{V(y)} \qquad (2.4.1)$$

where a_R is the extraction efficiency. This parameter is the product of a height scale (h_R) and a length scale (l_R); were $h(y)=h_R$, *then* $1/e$ of $Q_V(y)$ would be converted to precipitation over l_R. Depletion of $Q_V(0)$ by $\nu_R(y)$, per unit area, proceeds according to

$$Q_{V(y)} = Q_{V(0)} - \int_0^y \nu_{R(y)} dy \qquad (2.4.2)$$

where $Q_V(0)$ is the initial incident vapour flux at the model boundary (⑤, Fig. 2.8). Spatial variations in vapour flux ($Q_V(y)$) occur because of the effects of topography ($h(y)$) on precipitation rate ($\nu_R(y)$), where a_R remains constant. However, the precipitation rate also influences the development of topography ($h(y)$) through its effect on fluvial discharge (q_r, Eq. 2.3.2) and consequently on the rates of fluvial erosion, transportation and deposition (Eq. 2.3.11). Therefore, a feedback exists between precipitation and fluvial processes.

The magnitude and distribution of precipitation rate (*i.e.*, the model climate) are fundamentally controlled by the value of the initial incident water vapour flux ($Q_V(0)$), the extraction efficiency (a_R) and surface topography (Fig. 2.8). In the model experiments, $Q_V(0)$ remains constant unless it is varied to cause a change between wetter and drier climatic conditions, a_R always remains constant and topography evolves because of the interaction of tectonic, surface, climatic, isostatic and eustatic processes.

2.5 Isostasy Model

The orogen/foreland basin model uses the flexural isostatic compensation model developed by Courtney and Beaumont (1983). Their model has previously been used to explore the planform behaviour of loading and unloading a thermally activated viscoelastic lithosphere (Courtney and Beaumont, 1983; Quinlan and Beaumont, 1984; Beaumont *et al.*, 1988). The model assumes that the lithosphere behaves as a continuous Maxwell-solid plate overlying an inviscid fluid halfspace. Courtney and Beaumont (1983) use the Green function convolution techniques of Beaumont (1978) to calculate the elastic planform response to loading and unloading, and also the time-dependent viscoelastic response. In the present study, the flexural isostatic calculations are simplified by assuming that the lithosphere behaves as a continuous elastic plate of uniform thickness. This isostatic model is used because of its ability to calculate the planform effects of loading and unloading, as well as to allow future work on the viscoelastic effects of isostatic compensation on foreland basin stratigraphy.

2.6 Eustasy

Eustasy in the model is a spatially uniform change in sea level relative to the model datum. Sea level may vary instantaneously or linearly throughout a tectonic time step and is at steady state within a surface processes time step.

Changes in the distribution of water are isostatically compensated because water, by virtue of density and volume, exerts a significant vertical force on the lithosphere. Water load changes as water is displaced by orogenic and sedimentary material and as bathymetry changes with eustatic and isostatic changes in relative sea level. In addition, changes in orogenic and sedimentary loads are substantially reduced where these loads displace water instead of air.

It is assumed for simplicity that changes in foreland basin volume are sufficiently small that they do not cause a global change in sea level.

2.7 Orogen/Foreland Basin Model Summary

The orogen/foreland basin model links simple component models of tectonic, surface, climatic and isostatic processes together in an internally consistent manner. Each of these processes directly or indirectly influences the others through its individual effect on landform evolution.

The tectonic process creates a doubly-vergent wedge-shaped orogen based on critical Coulomb wedge theory (Dahlen, 1984; Dahlen et al., 1984), sandbox experiments (Malavieille, 1984) and dynamical numerical models of doubly-vergent critical wedges (Willett, 1992; Willett *et al.*, 1993; Beaumont *et al.*, 1994). The model orogen grows in proportion to the rate at which foreland basin material is accreted to the orogen and responds systematically to the effects of isostatic compensation, surface processes and the effects of orographically controlled precipitation. This tectonic model differs from the sectional, one-sided, geometrical (Flemings and Jordan, 1989; Sinclair *et al.*, 1991; Peper, 1993), fault-bend-fold (Flemings and Jordan, 1990; Jordan and Flemings, 1991), and wedge models in that:

- Planform orogenic load distributions are created.
- Dip sections can be used to approximate the evolution of plane-strain compressional orogens.
- Orogen state is determined by competition between the rate at which material is added to the orogen by tectonic processes and removed by surface processes.
- Orogen and foreland basin landform evolution is determined by the competition between tectonic and surface processes.
- Orogen growth has an indirect effect on itself through orographically controlled precipitation.

The surface processes model uses short-range (diffusive) and long-range (advective) transport to modify surface topography in response to surface slope and fluvial discharge. Incorporating fluvial advective transport as a component of subaerial transport makes this model significantly different from previous foreland basin models that contain only diffusion (*e.g.*, Flemings and Jordan, 1989, 1990; Sinclair *et al.*, 1991; Peper, 1993) in that:

- Spatial and temporal variations in surface transport evolve with topography because fluvial transport capacity is linearly dependent on discharge (Eq. 2.3.6). Discharge is determined by topography and precipitation rate (Eq. 2.4.1, 2.4.2) and fluvial sediment flux is determined by a first-order kinematic reaction (Eq. 2.3.11).
- Planform fluvial transport can be used to demonstrate the effects of along-strike transport on the development of foreland basin stratigraphy.

The climate model is a parametric approximation of how elevation, relief, moisture content and prevailing wind direction affect precipitation rates in mountainous regions. The orographic control on precipitation rate in the model results in:

- Increasing denudation rates and, therefore, increasing sediment yield with greater surface relief because of the dependence of fluvial transport on discharge, consistent with observations of natural drainage basins (*e.g.*, Ahnert, 1970)
- Asymmetry in precipitation rates across complete sections of an orogen, analogous to the wet windward and dry leeward faces of modern orogens (*e.g.*, Southern Andes, Prohaska, 1976)

Further variation of the initial incident vapour flux ($Q_V(0)$) provides a mechanism for scaling mean precipitation rates up or down, thereby allowing the effects of climate change on precipitation and hence on foreland basin stratigraphy to be addressed.

The isostasy model approximates how planform changes in surface loads affect orogen and foreland basin topography on an elastic lithosphere. This model differs from other foreland basin models in that it considers the planform effect of changes in load distribution and the effects of changes in water load on the orogen/foreland basin system. It does not consider the effects of mantle convection (Mitrovica *et al.*, 1989, Gurnis, 1992) or in-plane stress (Cloetingh, 1988; Peper, 1993) on the orogen/foreland basin system.

2.8 Model Initial Conditions, Boundary and Parameter Values

Initial conditions, boundary and parameter values for the model are chosen to reproduce average conditions within small, rapidly evolving collisional orogens (*e.g.*, Alpine System, Homewood *et al.*, 1986; Taiwan, Covey, 1986). Parameter values are listed in Table 2.1.

Initial Convergent Continent Geometries and Model Boundaries

Each model involves oceanic subduction leading to closure of an ocean basin and collision between two continents. Model orogens begin their evolution as submarine accretionary wedges that grow above a subduction axis, then become progressively exposed subaerially as tectonism involves continent/continent collision (*e.g.*, Taiwan, Davis *et al.*, 1983; Lundberg and Dorsey, 1988; Outer-Banda Arc, Audley-Charles, 1986). Two simple convergent continental-margin geometries are used, which place convergent margins parallel or at an oblique angle to each other respectively (Fig. 2.9). The convergent margin geometry used determines whether the orogen/foreland basin system develops synchronously or asynchronously along strike.

Tectonic flux into the orogen ($Q_T(pro)$) is an important factor controlling the rate of orogen growth (Fig. 2.6). While oceanic crust is subducted, $Q_T(pro)$ corresponds to the product of v_T and d, where d *(500 m)* is the offscraping of sediment deposited in the pro-foreland basin together with oceanic sediment and crustal material from above the detachment (Fig. 2.9). When continent/continent collision begins, $Q_T(pro)$ increases with d as up to 2500m of additional detached crustal material is entrained into the orogen. The convergence velocity and vapour flux at the model boundaries (Q_V, Fig. 2.6) are perpendicular to the axis of subduction and uniform along strike (Fig. 2.9). All other parameters are either determined by the model or are uniform across the model. Therefore, v_T and d are the principal factors controlling variations in $Q_T(pro)$ and orogen growth along strike. Tectonism proceeds along strike at a rate determined by v_T and the angle θ between the continental margin of the subducting pro-lithosphere and the axis of subduction along the boundary of the retro-lithosphere (Fig. 2.9). $Q_T(pro)$ is not affected by isostatically forced elevation changes in the convergent continent because the

Initial Conditions

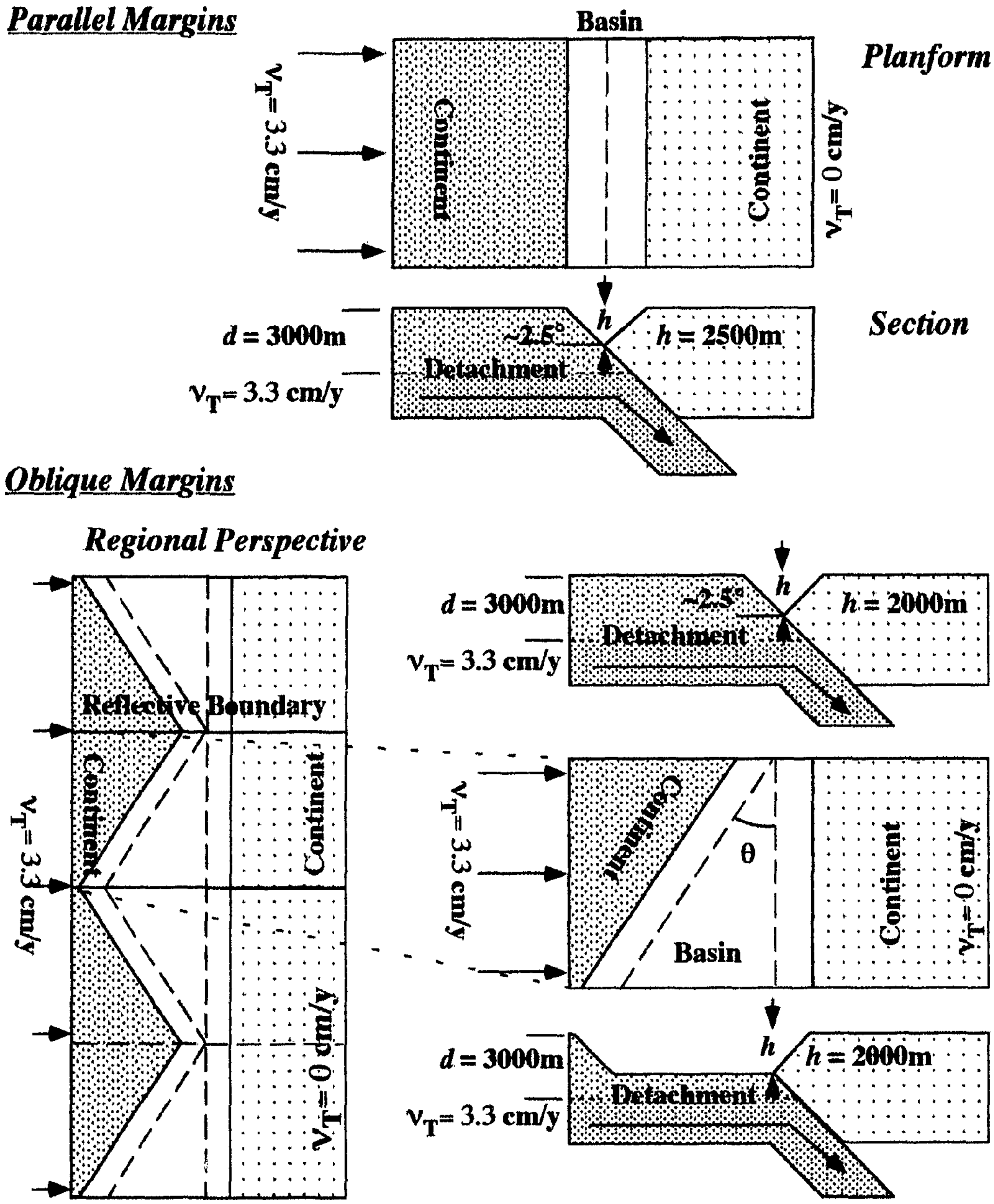

Figure 2.9. The parallel and oblique initial conditions, as termed above, differ only in the obliquity (θ) between continental margins. When continental margins are parallel, the margins meet at depth to form a marine basin of depth h. With tectonic convergence, a surface layer of thickness d is detached from the pro-lithosphere while the lower layer is underthrust and subducted with velocity v_T. When the continental margins are oblique with respect to each other, the continental margins are juxtaposed at one end of the model and separated by a marine basin of depth h at the other. With tectonic convergence, orogen growth and pro-lithospheric convergence begins. Model boundaries perpendicular to the strike of the subduction axis are reflective. At a regional scale, the oblique inital condition represents collision between a straight margin and one with salients and promontories.

detachment is at a fixed horizon in the model lithosphere (Fig. 2.9); therefore, the thickness of crustal material entrained remains constant.

Models that use a parallel convergent-margin geometry create orogen/foreland basin systems that are essentially uniform along strike; those that use an oblique convergent-margin geometry create systems with along-strike variability in tectonics. This variability results in longitudinal sediment transport in both the subaerial and marine environments, similar to the longitudinal transport commonly observed in natural foreland basins (*e.g.*, Taiwan, Covey, 1986; Molasse Foreland Basin, Homewood *et al.*, 1986; Ebro Basin, Marzo *et al.*, 1988; Alberta Basin, Leckie, 1989; Himalayan Foreland Basin, Burbank, 1992). Model basins developed with oblique geometry are used to demonstrate how competition between longitudinal and transverse sediment transport influences the development of foreland basin stratigraphy.

Model boundaries that are parallel to v_T and perpendicular to the strike of the subduction axis (*e.g.*, dip boundaries) are reflective, that is, each model represents only part of an orogen/foreland system, the rest of the system being reflectively continued along strike (Fig. 2.9). On a large scale, an initial condition with oblique convergent margin boundaries represents the collision of a sawtooth margin with a straight one. The model can therefore address the consequences of the collision of promontories and salients (*e.g.*, Paleozoic Appalachian foreland basin, Thomas, 1977), and of diachronous convergence (*e.g.*, Taiwan, Davis *et al.*, 1983) on the evolution of foreland basin stratigraphy.

Parameter Values

Orogen Geometry and Surface Relief

Effective internal (ϕ) and basal coefficients (ϕ_b) of friction influence the geometrical growth of the doubly-vergent wedge-shaped orogen (Fig. 2.5). Values for ϕ and ϕ_b are chosen to create orogens with average surface slopes on the order of 1° to 6°, similar to the range of surface slopes found on present day wedges (Davis *et al.*, 1983).

Surface relief over length scales of less than l_S is preserved with orogen growth because the orogen is expected to deform coherently over l_S (see Sec. 2.2.3). The length scale l_S is perhaps the most difficult aspect of the model to constrain (Table 2.1). The choice of l_S is explained in Section 2.2.3.

Surface Processes

In the surface processes model, short-range (hillslope) transport diffusivities (K_s, Table 2.1) are chosen to be consistent with empirically based estimates of diffusivity. Kooi and Beaumont (1994) show that estimates of effective diffusivities from natural examples depend on the scale at which they are measured. In numerical models this same dependency on scale is related to the resolution of the model grid. Models with advective and diffusive transport cannot faithfully reproduce the effects of fluvial transport when model drainage density should be greater than the model grid. As a consequence, all transport at smaller scales is represented by diffusion, and K_s must be scaled to achieve the appropriate mass flux for surface relief smoothed to the grid scale.

The values of K_s in the subaerial environment are chosen so that for a grid size *cl*, values of K_s, scaled in the same manner as Kooi and Beaumont (1994), are comparable with diffusivities based on escarpment retreat (Nash, 1980; Coleman and Watson, 1983; Hanks *et al.*, 1984). Similarly, the values of K_s in the submarine

Table 2.1 - Orogen/Foreland Basin Model Parameters	
Size of Planform Model	1500 km x 750 km
Cell size (cl)	15 km
Initial Fractal Surface Relief	Maximum Amplitude 100 m Fractal Dimension 2.5
Tectonics	
Coulomb Wedge Coefficients of Friction	Internal $\mu = 0.3249$ ($\phi = 18°$) Basal $\mu_b = 0.0524$ ($\phi_b = 3°$)
Initial Potential Detachment Thickness (d)	Ocean 200 m, Continent 3000 m
Convergence Rate (v_T)	0.0 to 0.033 m/y
Strike Coherence Length (l_s)	75 km
Timestep	50,000 y
Surface Processes	
Hillslope and Marine (diffusive) Transport	
$K_S^{subaerial}$	Bedrock 5 m^2/y, Sediment 20 m^2/y
K_S^{marine}	Bedrock 125 m^2/y, Sediment 500 m^2/y
Fluvial (advective) Transport	
River Transport Coefficient (K_f)	0.02
Erosion Length Scale (l_f^{erode})	Bedrock 100 km, Alluvium 25 km
Depositional Length Scale ($l_f^{deposit}$)	25 km ($\sim\sqrt{2}cl$)
Orographic Incident Vapour Flux	
Initial Incident Vapour Flux ($Q_V(0)$) (uniform precipitation equivalent)	0.5 or 1.0 m/y
Extraction Length Scale (l_R)	50 km
Topographic Height Scale (h_R)	1 km
Eustasy	
Period	0, 400 ky or 3 My
Elevation Range	± 50 m
Isostasy	
Lithospheric Flexure (*Similar to a thin elastic plate*)	Effective Thickness 30 km Young's Modulus 1×10^{11} Pa Poisson's Ratio 0.25
Densities	Mantle 3400 kg/m^3 Crust and Sediment 2600 kg/m^3

environment are comparable to diffusivities based on delta progradation (Begin *et al.*, 1981; Kenyon and Turcotte, 1985).

The values of K_f and l_f used in long range (fluvial) transport (Table 2.1) cannot be easily compared with measurements from natural systems, as stated by Kooi and Beaumont (1994). These values are therefore chosen to produce fluvial erosion and sedimentation rates of ~0 to 5 mm/y, similar to the rates of erosion and sedimentation in natural orogen/foreland basin systems (Schwab, 1986; Dahlen and Suppe, 1988; Kukal, 1990). Similarly, values of K_f and l_f are acceptable based on modelling studies of geomorphic land form evolution (Kooi and Beaumont, submitted), escarpment evolution (Kooi and Beaumont, 1994), and denudation of the Southern Alps, New Zealand (Beaumont *et al.*, 1992). While the results of these studies help establish internal consistency, they do not prove either the correctness of the values of K_f and l_f in specific cases or of the surface process model in general.

In the model, the initial continent surfaces are either horizontal or sloping downward with a gradient of 1/10000 toward their convergent margin. Fluvial systems on continents with a small tilt drain toward the developing foreland basins, thus preventing strike boundaries from becoming fluvial baselevel. A small amount of fractal roughness is added to the continental surfaces to establish an initial drainage network (Table 2.1); the same pattern of surface roughness is introduced in each model experiment.

Orographic Precipitation

The orographic precipitation model is a simple parametric model (Sec. 2.4). Parameter values Q_V, l_R and h_R (Table 2.1) are chosen to give rainfall distributions comparable to those observed in low to moderate latitude orogens (*e.g.*, Taiwan, Watts, 1969; Central North American Cordillera, Barry and Chorley, 1971; Southern Alps, Maunder, 1971; Southern Andes, Prohaska, 1976; Sumatra, Nieuwolt, 1981). Mean annual and multi-year rainfall distributions on the natural orogens are used to estimate how 'wet' and 'dry' might be defined in the context of orogen/foreland basin systems. For example, the west coast of South Island, New Zealand, is considered 'wet' with an annual precipitation of up to 8 m/y (Maunder, 1971). Conversely, the eastern slope of the Argentinean Andes with less than 2 m/y is considered 'dry'; due to its very steep orographic gradient, much of the orogen receives less than 1 m/y (Prohaska, 1976).

Isostasy

Flexural isostatic calculations approximate a continuous, uniformly thick, elastic lithosphere with an effective thickness of 30 km and a half flexural wavelength of ~300 km (Table 2.1), comparable to estimates for the effective elastic thickness of the West European Platform beneath the Alps, the East European Plate beneath the Carpathians, the Adriatic beneath the Apennines, and the Arabian Shield beneath the Zagros Orogen (Allen and Allen, 1990).

Time-Dependent Parameters

In the tectonic, climatic and eustatic models, designated 'MT', 'MC' and 'ME' respectively, only one parameter value changes with time while other values remain constant; convergence velocity (v_T) varies in MT models, vapour flux (Q_V) in MC models and sea level in ME models. Sinusoidal and step function variations in each of these parameter values are used to show how fluctuations in the rate of each process affect foreland basin stratigraphy. In addition, two parameter values are varied simultaneously in several models to show how tectonic and climatic ('MTC'), tectonic and eustatic ('MTE') or climatic and eustatic ('MCE') processes can reinforce, counteract or modify each other.

2.9 Geological Concepts in the Context of the Model

Several concepts as applied to orogen/foreland basin systems and model results are discussed below. These concepts include graded rivers, relative sea level, underfilled and overfilled foreland basins, model sedimentary facies and progradation, aggradation and retrogradation.

Graded Rivers

Explanations of erosion and aggradation by fluvial processes are made easier by using the concept of the 'graded river', an idealization of a state which rivers are considered to evolve toward but never attain. In this state, sediment transported from upstream is delivered downstream without erosion of the riverbed or deposition. As indicated by Kooi and Beaumont (submitted), this definition corresponds to the description by Mackin (1948) and is in accord with some other definitions of graded state (Schumm, 1977; Howard, 1982; Morisawa, 1985). Thus, in the surface process model, the term 'grade' or 'graded' refers to an equilibrium condition where the carrying capacity of the river is equal to its sediment flux. Under these circumstances the disequilibrium in the entrainment-deposition reaction vanishes (Eq. 2.3.9). This disequilibrium controls the rate of the fluvial erosion or deposition and thus the rate at which the river approaches a graded state.

As in nature, model rivers are always adjusting toward grade, whereas changes in the landform or fluvial baselevel caused by other model processes disturb the tendency of the rivers to actually become graded. Rates of erosion or deposition, and therefore the rate of landform evolution, reflect the dynamics of this competition between the rate at which tectonics, isostasy or eustasy create disequilibrium and the rate at which the rivers can adjust toward grade. Kooi and Beaumont (submitted) note that when the response time of the river is much shorter than the time period of extrinsic changes in landform or baselevel, the river will evolve in 'near equilibrium' with these changes. This 'near equilibrium' is referred to as a 'dynamic equilibrium' (Howard, 1982; Kooi and Beaumont, submitted). Under these conditions, portions of a river may almost maintain an equilibrium profile regardless of extrinsic changes. For example, in a model basin that is aggrading along a fluvial profile, subsidence which reduces the river slope is countered by sedimentation such that the river maintains a near equilibrium profile with time. Such a profile represents a dynamic equilibrium between the effects of subsidence and fluvial limitations of aggradation. If the rate of either tectonics or precipitation were to change over a period much longer than the response time of the river, then the river profile would evolve toward a new profile while maintaining dynamic equilibrium. Under these circumstances, landform evolution is dictated by the dynamic equilibrium. Conversely, when the response time of the river is much longer than the time period of extrinsic changes in landform or baselevel, the river profile is in disequilibrium. In this case, landform evolution reflects the transition from disequilibrium toward dynamic equilibrium.

Relative Sea Level

The expression 'relative sea-level change' as used herein refers to a change in sea level relative to a fixed datum at or near the sea floor caused by the cumulative effects of tectonics, isostasy and eustasy; this usage is consistent with that of Posamentier et al. (1988). A change in relative sea level differs from bathymetry in that it excludes the effect of sedimentation. It is therefore possible to have a rise in relative sea level and a decrease in bathymetry. Eustasy creates a uniform change in relative sea level over scales relevant to the development of foreland basin stratigraphy. Conversely, changes in relative sea level caused by tectonics or isostasy are typically non-uniform over these scales. In the model, tectonics may create a change in relative sea level by a tectonic change in submarine orogen topography and by isostatic compensation for changes in orogenic load. Relative sea-level changes caused by isostasy are inherently non-uniform because changes in orogenic, sedimentary and seawater loads are compensated by lithospheric flexure. For example, changes in lithosphere elevation caused by flexural isostatic compensation adjacent to a change in load are on the order of 20 to 40 times greater than, and in the opposite direction to, the related maximum vertical displacement on the peripheral bulge. Eustasy adds a uniform component at basin scales and either enhances or diminishes the non-uniform effects of tectonism and isostasy on the net 'relative change' in sea level.

In each experiment, sea level has an initial uniform elevation relative to datum. The datum is a uniform horizontal surface defined as 0.0 m elevation.

Sequence Stratigraphic Terminology

The following sequence stratigraphic terms are used as defined by Van Wagoner *et al.* (1988, 1990), Posamentier *et al.* (1988).

Parasequence - A parasequence is a relatively conformable succession of genetically related beds or bedsets bounded by marine-flooding surfaces or their correlative surfaces. Depending on their position within a sequence, a parasquence may be bounded above or below by a sequence boundary.

Sequence - A sequence is a relatively conformable succession of genetically related strata bounded by unconformities or their correlative conformities.

Type-1 unconformity - is an unconformity characterized by fluvial incision, sedimentary bypass of the 'shelf' and an abrupt basinward shift in facies.

Type-2 unconformity - is an unconformity characterized by subaerial exposure with minor subaerial truncation, and a basinward shift in facies. A Type-2 unconformity is not characterized by fluvial incision.

Underfilled and Overfilled Foreland Basins

In planform, the portion of a foreland basin within a catchment is considered to be sediment-filled when the crest of the peripheral bulge acts as the fluvial baselevel and all rivers downstream of the deformation front of the orogen have reached grade (Johnson and Beaumont, 1995). When the rivers are at grade, there is no net deposition in the catchment and, by implication, no space for additional sediment accumulation. The distinction between underfilled and overfilled is partly determined by whether any portion of a foreland basin has been filled to the level where drainage crosses the peripheral bulge. The basin is underfilled when drainage has not breached the bulge or when the basin has filled to the level at which catchment drainage crosses the bulge, but the bulge still acts as effective baselevel and there is still net deposition in the basin. Within a catchment, the basin is considered overfilled when the bulge is effectively baselevel and there is net erosion upstream, or if the fluvial system is regrading in response to a baselevel beyond the peripheral bulge. The portion of a foreland basin within a catchment becomes overfilled either because alluvial facies onlap the peripheral bulge or because incision of the peripheral bulge and subsequent regrading of the catchment result in net denudation of the foreland basin fill. These definitions of filled, underfilled and overfilled encompass Flemings and Jordan's (1989) and DeCelles and Burden's (1992) usage of these terms. Further, the definitions imply that 'accommodation' (Jervey, 1988) in a foreland basin does not depend simply on sea level, but instead on how tectonism, climate, isostasy and eustasy influence river grade and the elevation of the peripheral bulge.

Sedimentary Facies

In the context of the model, sedimentary facies characterize the depositional environment as marine, coastal or subaerial. A marine facies designation means that the model environment remained marine during the entire surface-processes time step (t_S). A coastal facies designation is used where marine and subaerial sedimentation has occurred during t_S. Subaerial facies means that alluvial sedimentation has occurred throughout t_S.

Subaerial facies in the model are described by the river power, *i.e.*, the slope-discharge product of the fluvial environment at the time the sediments were deposited. River power provides the best estimate available from the model of the energy of a fluvial depositional environment. Grain size is not considered because there is no simple way to predict the availability of grain sizes for entrainment by a model river at any point. However, it should be noted that in nature grain size is an important control on river slope as illustrated by the Meyer-Peter and Muller (1948, *cit.* Paola *et al.*, 1992) relationship (Eq. 2.3.6) between sediment transport and shear stress. Fluvial architecture is not considered because the model lacks the spatial and temporal resolution to create bedding structures.

Higher river-power facies in the model describe the distribution of higher energy fluvial environments, which may be associated in nature with coarser grain sizes. For example, such facies characterize deposition in a river with a slope of 0.001 draining a 100 km x 100 km catchment with a mean annual rainfall greater than 5 m/yr. Lower river-power facies describe the distribution of lower energy fluvial environments, which may be associated in nature with finer grain sizes. For example, these facies characterize deposition in a river with a slope of 0.001 draining a 100 km x 100 km catchment with a mean annual rainfall less than 0.5 m/yr. A weakness of this approach to assigning river-power facies is the assumption that a complete range of grain sizes is available for deposition and that flow regime can be related to discharge without knowledge of the cross-sectional area of the stream. For the present model formulation, river-power facies are the best measure available to associate properties of the model sediment with those of natural systems. The boundaries between low, moderate and high river-power facies were chosen to illustrate the range and changes in facies that can occur on an alluvial plain.

Progradation, Aggradation, and Retrogradation

Transgression and regression are recorded depositionally as progradation or retrogradation of coastal facies, while aggradation of coastal facies records a stationary coastline position. Retrogradation and aggradation only occur with a relative rise in sea level, while progradation can occur with either a rise or fall. The effects of transgression and regression can also be recorded as an erosional gap (i.e., lacuna) in the sedimentary record.

Progradation, aggradation or retrogradation of coastal facies are fundamentally controlled by fluvial transport to the coast, submarine transport away from the coast, topography of the coastal region, relative sea-level change and littoral drift (Galloway, 1989; Heller *et al.*, 1993; Schumm, 1993; Wescott, 1993). Aggradation of coastal facies accompanies a relative rise in sea level when the net sediment accumulation rate equals

MT1 - Constant v_T, Q_V, and v_E

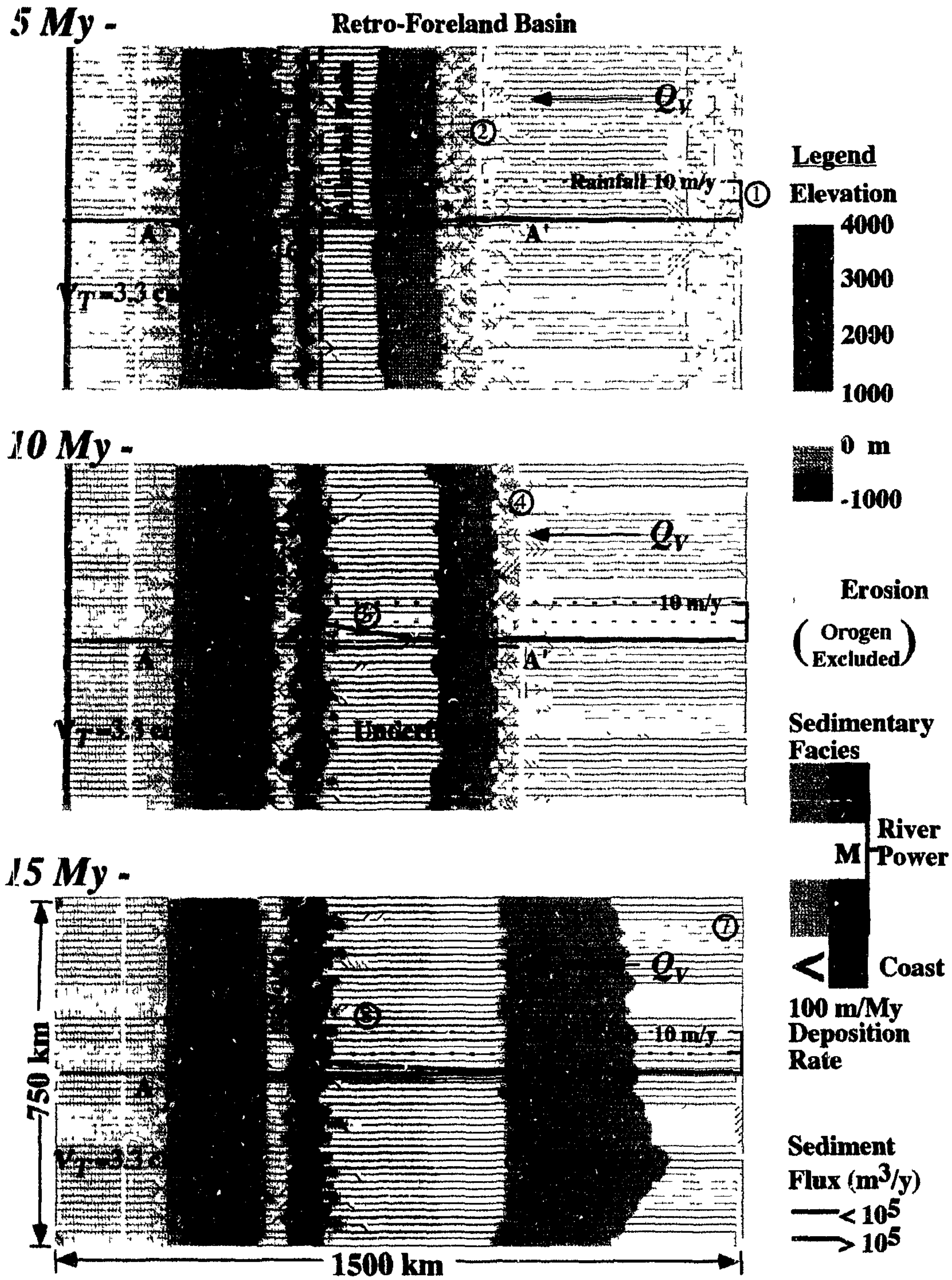

Figure 3.2. Planform surface elevation (grey scale), facies distribution (colour), denudation (pink) and fluvial drainage network (lines) for MT1 at 5, 10, and 15 My MT1 shows the filling of the retro-foreland basin and the transition from underfilled to overfilled between 10 My and 15 My. Rainfall distributions (dark blue lines) are shown along lines of section (A-A').

Factors Controlling Progradation, Aggradation and Retrogradation

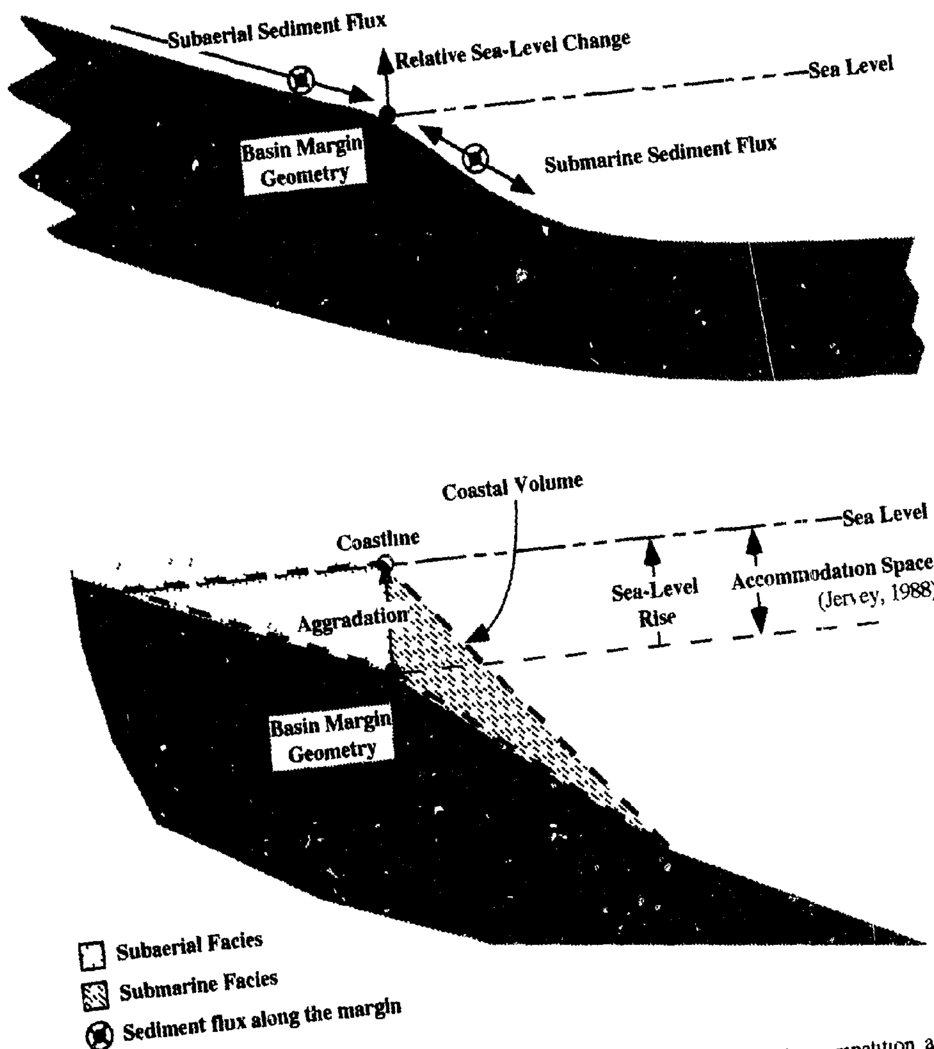

Figure 2.10 Progradation, aggradation and retrogradation are determined by the competition among sediment flux to, along, and away from the coast, and the change in coastal volume. Coastal volume is the minimum volume that must be filled in order that neither transgression nor regression occurs. With a relative sea-level rise, aggradation occurs when net sediment flux to the coast equals the change in coastal volume, progradation occurs when the net sediment flux exceeds the change in coastal volume, retrogradation occurs when the net sediment flux is less than the change in coastal volume.

the rate of increase in 'coastal volume', defined here as the basin volume per unit length along the coast that must be filled in order that neither transgression nor regression occur (Fig. 2.10). The rate of increase in this volume is determined by the geometry of the coastal region, the rate of relative sea-level rise and the depositional submarine surface slope required to sustain aggradation. Retrogradation occurs when the net sediment flux to the coast is less than the rate of change in coastal volume. Progradation occurs when the net sediment flux to the coast is greater than the rate of change in coastal volume.

In the model, the local net sediment flux to the coast is the difference between the local fluvial carrying capacity at the coast, and the submarine sediment flux away from the coast. Surface slopes typically increase at the coast because transport to the coast is greater than transport away from the coast. Net sediment flux varies along the coast with discharge and subaerial surface slope between fluvial systems, and submarine surface slope. Within a single fluvial system where discharge remains constant, net sediment flux is locally dependent upon the change in surface slope at the coast (coastal geometry) and the difference between the fluvial and submarine transport coefficients. The change in surface slope at the coast is determined by coastal geometry, change in coastal volume and net sediment flux to the coast.

Chapter 3

Effects of Tectonics on Orogen/Foreland Basin Systems

3.1 Introduction

Orogen tectonics and flexural isostatic compensation are fundamental processes controlling the development of any orogen/foreland basin system. These processes are significantly affected by surface processes, which modify the rate of orogen growth and distribute sediments throughout the foreland basin and beyond. Since surface processes are principally influenced by topography, climate and sea level, they are the fundamental connection between orogen tectonics and isostasy, climate and eustasy. This chapter focuses on how tectonics affect the development of the orogen/foreland basin system, and in particular foreland basin stratigraphy.

Model results are used to demonstrate the interaction among tectonic and the other fundamental processes. Feedback effects among model processes illustrate the importance of such mechanisms in natural orogen/foreland basin systems.

Comparisons of model results with examples from natural foreland basins have been introduced to demonstrate the general applicability of the model. Model experiments are not designed to create results for detailed comparison with any particular orogen/foreland basin system. It is doubtful that this model, like its precursors (Table 1.1), is sufficiently complete or that the processes are modelled accurately enough to allow for more than a first-order comparison with natural systems. Favourable first-order comparisons between the characteristics of natural and synthetic orogen/foreland basin systems would, however, support the value of this work.

Model results show the development of stratigraphy in the pro- and retro-foreland basins and contrast conditions that either enhance or inhibit asymmetry across orogen/foreland basin systems. Subduction creates asymmetry between pro- and retro-foreland settings through the rates of pro- and retro-foreland basin convergence with the orogen and, therefore, the rate at which strata accrete to the orogen. The rate of basin filling varies inversely with the rate of entrainment of basin strata into the orogen (hereafter referred to as entrainment). Asymmetry in the rates of basin filling is also caused by asymmetry in the rate at which material is eroded from the orogen and returned to the basin; filling rates vary directly with erosion rates. A principal cause of asymmetry in erosion rates across an orogen is asymmetry in rainfall distribution. This asymmetry is caused by orographically controlled depletion of the water vapour in the prevailing wind (vapour flux). Orographically controlled asymmetry in rainfall is characterized by wetter windward and drier leeward sides of an orogen, and therefore higher erosion and sediment transport rates in the windward basin. Johnson and Beaumont (1995) refer to the cycling of material into the orogen by entrainment and back into the basin by erosion and surface transport as 'tectonic recycling'; Schwab (1986) demonstrates that tectonic recycling is a first-order characteristic of foreland basins in nature. The combination of asymmetry in entrainment and erosion rates may either reinforce or counteract the effect of each process on the rates of tectonic recycling and basin filling.

Foreland basin stratigraphy typically records the competition between transverse and longitudinal sediment transport during basin filling (*e.g.*, Ebro Foreland Basin, Marzo *et al.*, 1988; Fig. 3.1). One mechanism that creates competition between longitudinal and transverse sediment transport is along-strike variations in tectonics.

Longitudinal vs. Transverse Transport, Eocene, Ebro Basin

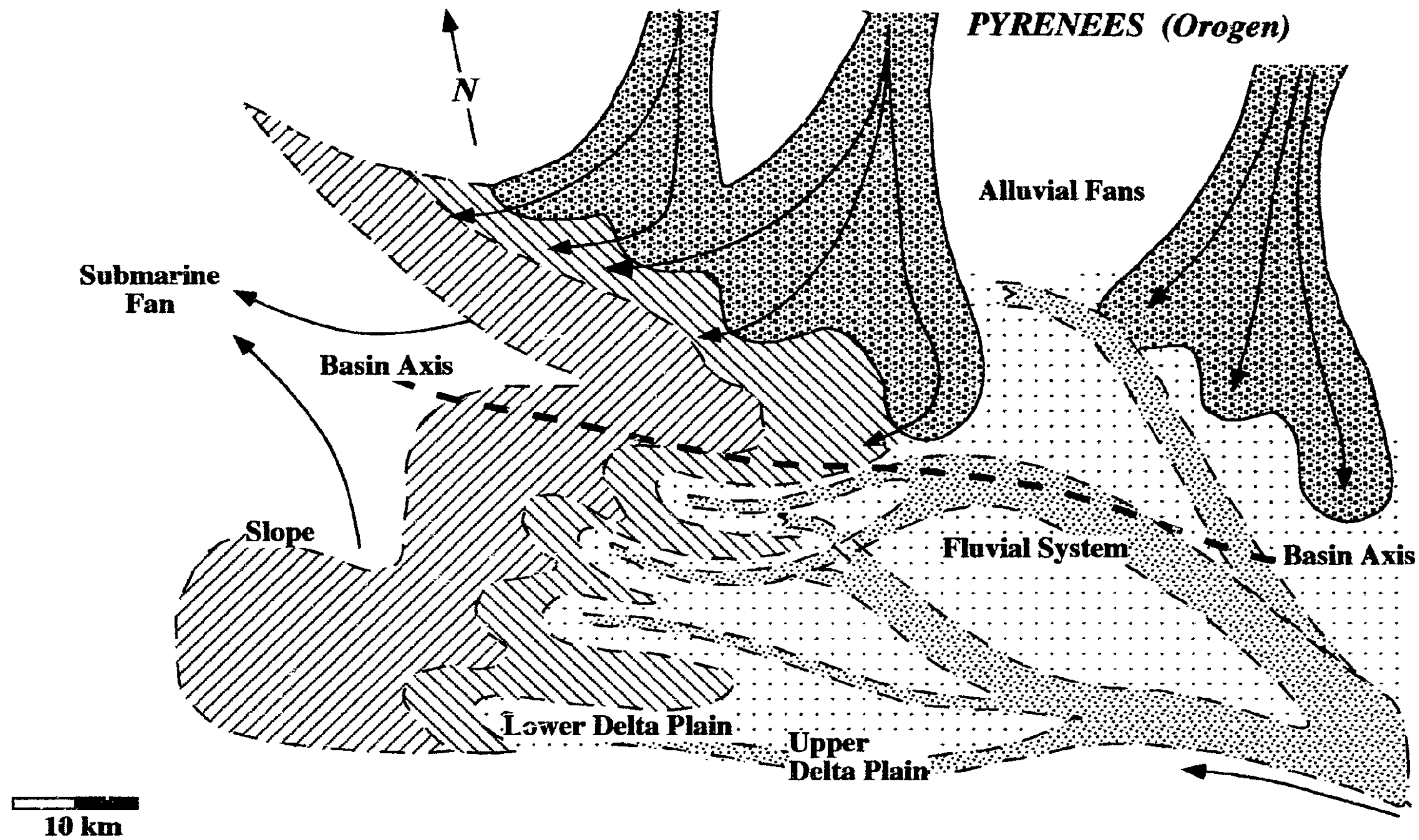

Figure 3.1. Architecture of the Eocene Castissent Formation in the Ebro Foreland Basin, Spain, include a complex of alluvial fan deltas shedding clastics from the adjacent Pyrenean orogen, a fluvial system subparallel to the basin axis feeding the prograding delta complex, and marine processes transporting sediment northwest, away from the delta front (after Marzo *et al*, 1988). Arrows show the direction of sediment transport.

Two of the many possible causes of such along-strike variations are irregular plate margins (*e.g.*, Appalachians, Thomas, 1977) and localized collisions along longer continental margins, as with micro-continent or arc collision (*e.g.*, Taiwan, Lundberg and Dorsey, 1988; Canadian Cordillera, Monger, 1989). Model orogen/foreland basin systems that evolve from continent/continent collision between non-parallel continental margins are presented to show the effect of longitudinal sediment transport on foreland basin stratigraphy; this effect has not been previously modelled.

Foreland basin stratigraphy is also influenced by temporal changes in tectonics. Such changes may result from causes such as micro-continent or arc collision events (*e.g.*, Canadian Cordillera, Monger, 1989) or cessation of tectonism caused by "jamming" of continent/continent collision (*e.g.*, Molasse Foreland Basin, Homewood *et al.*, 1986). In the model, cyclic variation in the rate of tectonic convergence (V_T), and thus in orogen tectonics, causes changes between constructive (net material gain) and destructive (net material loss) orogen states (Jamieson and Beaumont, 1988).

The effect of temporal changes in tectonism on landform and sedimentation has long been recognized and although stratigraphy follows as a natural consequence of landform evolution, earth scientists continue to have difficulty in systematically relating stratigraphic signatures to changes in tectonism (*e.g.*, Blair and Bilodeau, 1988). In the model, development of basin stratigraphy is controlled by the rates and feedbacks among processes controlling landform evolution of both the orogen and basin. Model results illustrate the effects of temporal changes in tectonics by showing how stratigraphic sequences develop in an integrated orogen/foreland basin system that experiences periodic changes in orogen state.

The response of the orogen/foreland basin system to temporal changes in any process is determined by the interaction of all model processes. This response can be observed both in how the orogen-to-basin sediment flux (Q_S) changes with time and in the stratigraphy. Change in Q_S may be characterized in terms of either a composite system response time (τ_S), where τ_S is the lapse time associated with an *e*-folding change in Q_S , or in the individual response times characterizing the response of the system to changes in tectonics (τ_T) or climate (τ_C) alone. The effect of climate is mentioned in this chapter because of the orographic control on precipitation. Where τ_T and τ_C differ the composite response of Q_S with time will initially reflect the dominance of the process with the shorter response time and later reflect the dominance of the process with the longer response time.

The idea of using time to characterize the ability of an earth system to respond to changes in tectonics is not new. For example, Paola *et al.* (1992) suggest that there is a natural time scale for any basin, which they define as the square of the basin length divided by the diffusivity. Most recently, Kooi and Beaumont (submitted), using the same surface processes model but with different parameter values, precipitation and tectonics, demonstrate that landform evolution may have a response time characteristic of the integrated system. The implication for orogen/foreland basin systems is that the degree of influence that a change in tectonics has on the development of basin stratigraphy may depend largely upon the period of the change relative to the tectonic response time and other response times of the system.

Model results are presented showing the difference between composite and tectonic response. Models are also presented which show how the effects of sinusoidal variations in v_T on stratigraphy change when the period of v_T is much longer than the minimum response time and on the order of the minimum response time.

3.2 Foreland Basin Setting

3.2.1 Pro-foreland vs. Retro-foreland Basin Setting

Model results of MT1 and MT2 contrast the development of basin stratigraphy in pro- and retro-foreland basin settings. In both settings, basin strata are accreted to the orogen by thrusting during orogen growth. The settings differ tectonically in that the pro-foreland basin overlies the subducting plate similar to, for example, the Taiwan Foreland Basin (Covey, 1986). The rate at which foreland basin strata are accreted to the growing orogen is determined by the rate of orogen growth and the velocity of convergence between the lithosphere and the orogen. The rate of entrainment is typically much larger in the pro-foreland than in the retro-foreland. Model results are presented for wet windward retro-foreland (MT1) and pro-foreland (MT2) basins that have developed from a parallel convergent continental margin geometry (Fig. 2.9) with constant v_T, Q_V and v_E. Conditions in MT1 favour asymmetry in development of the pro- and retro-foreland basins, while those in MT2 favour symmetry.

MT1 - Asymmetry in Orogen/Foreland Basin Evolution

Model MT1 results show the 15 My evolution of an orogen/foreland basin system at 5, 10 and 15 My in planform (Fig. 3.2) and transverse section (A-A', Fig. 3.3). The retro-foreland basin along A-A' is enlarged to show basin stratigraphy. Rainfall distributions along A-A' (Figs. 3.2, 3.3) change with growth of the orogen and the alluvial plain. These distributions are representative of the rainfall along strike because the

MT1 - Constant v_T, Q_V, and v_E

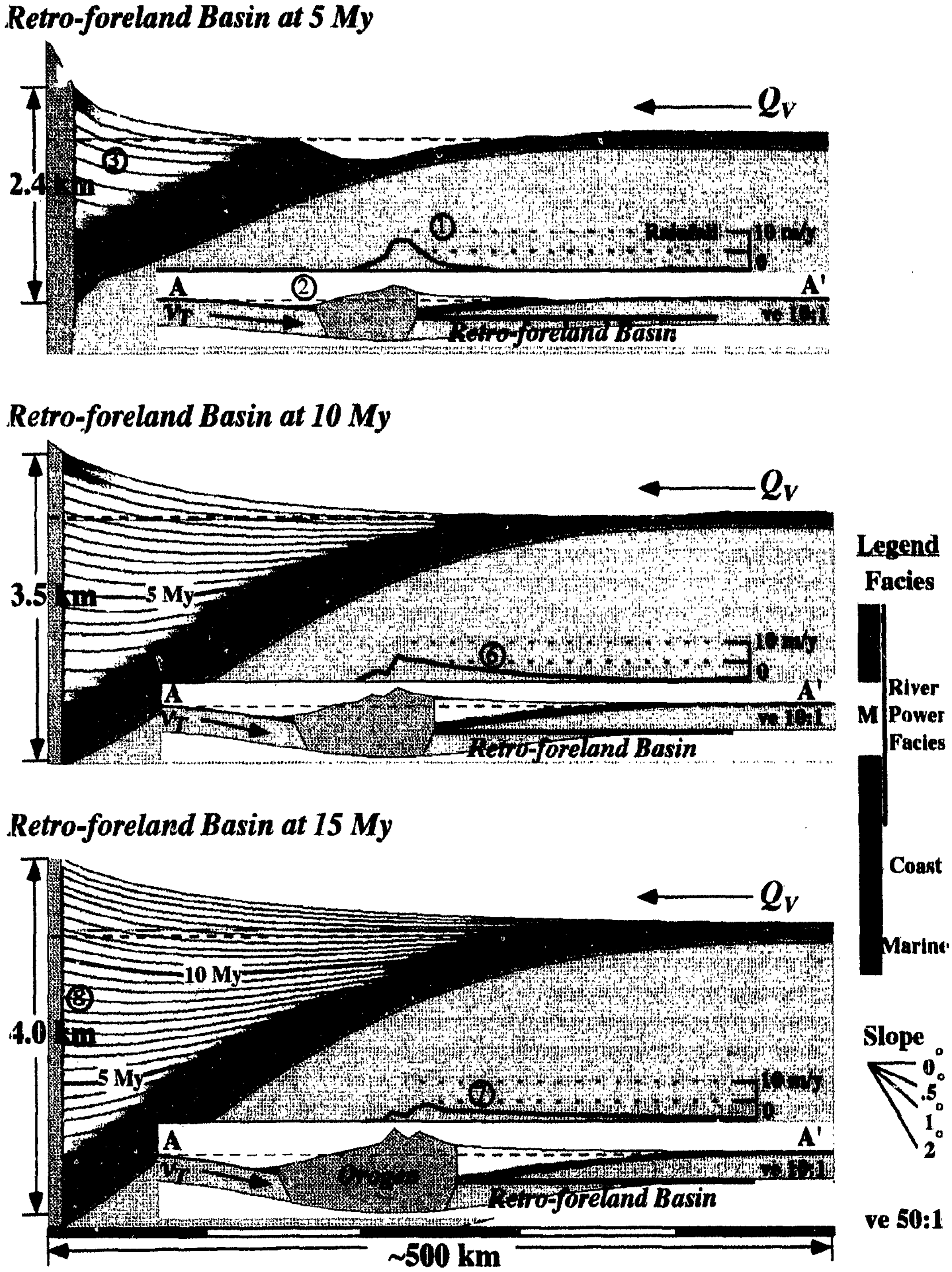

Figure 3.3. Stratigraphic development of the MT1 retro-foreland basin is shown at 5, 10 and 15 My. Insets show the regional section A-A' at each time. The black bar in each inset indicates the portion of the retro-foreland basin along A-A' that has been enlarged. Sedimentary facies are in colour. Time lines (black) are at 500 ky intervals.

convergent continental margins are parallel to each other and v_T and Q_V are uniform along strike.

MT1 - Evolution During the First 5 My

At 5 My, the 165 km of convergence has created an orogen with a maximum height of ~1.4 km and a width of ~120 km (Figs. 3.2, 3.3). Sedimentary filling of the pro- and retro-foreland basins is asymmetric, in part because of the asymmetry in the rate of tectonic convergence across the orogen, and in part because the windward retro-foreland receives the most precipitation (①, Figs. 3.2, 3.3). Both foreland basins have significant marine seaways. Drainage from the peripheral bulges into and away from the basins can be seen from the river network (②, Fig. 3.2). The drainage patterns reflect minor incision and capture by the rivers during gentle flexural warping of the fractally roughened initial surface. Elsewhere, the initial surface roughness has had little influence on the evolution of the drainage network, as evidenced by the self-organized (*i.e.*, path of steepest descent) dip-parallel linear drainage off the rapidly rising orogen (③, Fig. 3.2). At this stage, incision within the orogen is insufficient for the rivers to be captured and a more mature network to develop.

The MT1 pro-foreland basin is sediment starved (②, Fig. 3.3) primarily because sediments are tectonically recycled (Johnson and Beaumont, 1995). As the pro-autochthon converges with respect to the orogen, pro-foreland basin strata are carried toward and accreted to the orogen ($Q_T(pro)$). This process keeps the pro-foreland basin relatively empty unless the orogen-to-basin sediment flux ($Q_S(pro)$) becomes larger than the tectonic flux. In nature, pro-foreland basins with significant tectonic recycling may not be as underfilled as MT1, because either $Q_S(pro)$ or $Q_T(pro)$ may favour more preservation of basin strata, or other processes unrelated to orogen-to-basin sediment flux may contribute significantly to pro-foreland basin filling. Such processes could include continental drainage, carbonate deposition, chemical precipitation and pelagic sedimentation.

The MT1 retro-foreland basin contains a prograding sedimentary wedge which is ~2.4 km thick adjacent to the orogen and ~200 km wide (③, Fig. 3.3). Progradation occurs because the orogen-to-basin sediment flux ($Q_{S(retro)}$) is greater than the competing effect of basin subsidence caused by isostatic compensation for the growing orogenic and sedimentary loads. Surface slopes on the alluvial plain vary from greater than ~1/100 (0.6°) adjacent to the orogen to less than ~1/1000 (0.06°) adjacent to the retro-foreland seaway. Submarine surface slopes of the prograding wedge (~0.5°) are steeper than slopes of the adjacent coastal plain because sediment transport in the seaway basin is less efficient than on the fluvially dominated alluvial plain. The seaway is ~250 m deep and has maintained this depth for at least 3.5 My. The approximately constant seaway depth is indicated by the uniform thickness of marine facies at the base of the prograding wedge (④, Fig. 3.3). The decreasing time-line separation indicates that sedimentation rates decrease slightly with growth of the wedge.

Because the continent was initially entirely subaerially exposed, an erosional surface extends beneath the entire prograding wedge; this erosional surface has been enhanced by uplift and migration of the peripheral bulge. At 5 My, significant erosion is occurring on the seaward side of either bulge (②, Fig. 3.2). Erosion rates are higher here because peripheral bulges are asymmetric about their point of maximum elevation, with the steeper surface slopes facing the orogenic load (Turcotte and Schubert, 1982). Sediment flux to the seaway from the bulge does not contribute significantly to the stratigraphic record because sediment flux from the small drainage catchments is low. In addition, migration of the peripheral bulge and redistribution of sediments by marine processes prevent accumulation of continentally derived sediments.

MT1 - Evolution Between 5 My and 10 My

At 10 My the total tectonic convergence is ~330 km, resulting in growth of the orogen to ~2.2 km elevation and ~170 km width (Figs. 3.2, 3.3). The asymmetry of pro- and retro-foreland basin filling increases with orogen growth and greater development of the retro-foreland basin alluvial plain. Isostatic compensation for these growing loads causes the peripheral bulge to migrate ~60 km from its position at 5 My (④, Fig. 3.2). In addition, growth of the alluvial plain increases the asymmetry of the rainfall distribution.

In the retro-foreland basin, the seaway is filled by 10 My (Figs. 3.2, 3.3). After ~6 My, marine facies begin to taper out and the rate of progradation increases (⑤, Fig. 3.3). Time lines show that sedimentation rates decrease while progradation rates increase with filling of the basin (Fig. 3.3). Time-line evolution is an expression of how model rivers evolve toward a dynamic equilibrium. In the early stages of basin evolution, the disequilibrium in river profiles is large because subsidence rates proximal to the growing orogen and baselevel rise are both large; the result is high sedimentation rates as river profiles evolve toward grade. Later in basin evolution, the subsidence rate proximal to the orogen is approximately unchanged, while subsidence and baselevel changes in the distal basin are smaller, the latter because basin subsidence by flexural isostatic compensation decreases with increasing distance from the change in load. As a consequence, the disequilibrium in river grade, and therefore sedimentation rate, decreases with increasing distance from the change in load.

The reduction in marine facies thickness reflects a decrease in seaway depth with increasing distance from the orogen. Seaway depth decreases with progradation primarily because basin subsidence, caused by flexural isostatic compensation, decreases with increasing distance between the change in orogenic and sedimentary loads and the seaway. This decrease in basin subsidence also causes a decrease in the rate of change of coastal volume as the coastline migrates away from the orogen. Progradation rate increases with basin filling because the rate of change in coastal volume decreases faster than the decrease in sediment flux to the coast. By 10 My, the basin is entirely subaerial but is still underfilled because it has not yet filled to the level at which the drainage direction reverses along the incised valleys in the peripheral bulge (④, Fig. 3.2).

At 10 My, the width of the retro-foreland basin has increased to ~350 km, while the deformation front (retro-wedge toe) surface elevation has remained approximately constant at ~600 m (Figs. 3.2, 3.3). Therefore, both the average river slope and sedimentation rate have decreased as the basin filled. Two positive feedbacks in the model reinforce the decrease in surface slope and sedimentation rate. In the first case, progradation increases the horizontal distance from the deformation front to fluvial baselevel. The result is a reduction in river slope and thus the gradient in fluvial carrying capacity, that is, change in carrying capacity (q_f^{eqb}) along the river course. This reduction brings rivers toward dynamic equilibrium. The reduction in sedimentation rates along the river course increases sediment transport away from the orogen to more distal parts of the basin, promoting progradation. In the second case, the decrease in surface slope is accompanied by a decrease in the gradient of orographically controlled precipitation and $Q_f(y)$ across the windward alluvial plain (⑤, Fig. 3.2; ⑥, Fig. 3.3). This increase in rainfall uniformity across the alluvial plain decreases the gradient in q_f^{eqb} through its dependence on discharge, reinforcing the first feedback effect.

MT1 - Evolution Between 10 My and 15 My

By 15 My the orogen is ~3.0 km in height and ~210 km in width (Fig. 3.2). Continued growth confirms that $Q_T(pro)$ into the orogen exceeds the rate of erosion. Tectonic recycling also continues to dominate over sedimentation in the pro-foreland basin. Filling of the retro-foreland basin has continued, but at a reduced rate (Fig. 3.3) Asymmetry between the pro- and retro-foreland basin has increased with growth of the orogen and preferential filling of the retro-foreland basin. The asymmetry in rainfall distribution has also increased, becoming more uniform over the retro-foreland and drier over the pro-wedge (⑦, Fig. 3.3).

In the orogen, fluvial incision has created drainage networks on the pro- and retro-wedges (⑥, Fig. 3.2). These networks are partly an artifact because there is a somewhat regular pattern in topography along the strike of the orogen. This pattern is related to the length scale (l_s) over which wedge growth is forced to be coherent, and surface relief is preserved.

By 15 My the retro-foreland basin is overfilled. In this basin, drainage from the orogen crosses the peripheral bulge and the model boundary is baselevel for all catchments (⑦, Fig. 3.2). Between 10 My and 15 My progressive deposition in the distal axial depression has steadily filled valleys on the basin side of the peripheral bulge. Eventually, basin filling raised the baselevel of rivers to the point where they breached the peripheral bulge along the antecedent valleys. Subsequently, fluvial sedimentation extended the alluvial plain across the peripheral bulge. On the alluvial plain, fluvial transport is primarily normal to the orogen. This drainage pattern reflects the uniformity in sediment transport out of the orogen ($Q_S(retro)$) along strike, and the tendency for rivers to counter development of irregularities across the plain through avulsion (⑧, Fig. 3.2). The result is a uniform alluvial plain.

The retro-foreland basin stratigraphy indicates that sedimentation rates are highest adjacent to the orogen (⑧, Fig. 3.3). Rivers adjacent to the orogen are most strongly disturbed from a graded state as the orogen grows because the rates of basin subsidence are greatest adjacent to the change in load. The progressive decrease in time-line convergence away from the orogen is a consequence of the strong influence of orographic precipitation on sediment transport and alluvial plain growth. Due to progressive filling of the retro-foreland basin, the net change in the sediment flux across the basin is larger than the corresponding change in isostatic compensation· that is, basin-wide sedimentation outpaces flexural subsidence. The orogen grows rapidly in the first 5 My. In the model, and in nature, surface slopes are steep and spatial gradients in rainfall are large. Surface slopes in the model range from less than 0.1 to more than 4 degrees, while surface slopes of alluvial plains are observed to have slopes of less than 0.1 to more than 10 degrees in nature. Precipitation gradients in the model are as high as 1/3 m/y/km and less than those found, for example, in the southern Argentinean Andes (Prohaska, 1976). The associated high gradients in fluvial carrying capacity allow rivers to deposit a thick, rapidly aggrading, subaerial sedimentary wedge with a high surface slope adjacent to the orogen. Between 5 and 15 My fluvial controls make sedimentation progressively more progradational. The decline of surface slopes makes rainfall more uniform across the fluvial plain, reinforcing progradation and a further decline in surface slopes (①, ⑥ & ⑦, Fig. 3.3). If interpreted as an effectively diffusive process, similar to the models of Flemings and Jordan (1989, 1990) or Paola *et al.* (1992), this evolution would require that the diffusivity vary spatially and evolve with time to emulate the effects of the changes in rainfall distribution with time.

MT1 - Orogen to Retro-foreland Basin Sediment Flux

An along-strike sum of the retro-foreland basin, orogen-to-basin sediment flux ($Q_S(retro)$) is used as an indicator of how the integrated tectonic, surface, climatic and isostatic processes respond to changes in v_T, Q_V and v_E. This flux is useful as an indicator, because orogen denudation rates are affected by tectonically driven change in orogen growth, changes in vapour flux and the effects of isostatic adjustments for changes in orogen, as well as sedimentary and water loads on the lithosphere. An along-strike sum of $Q_S(retro)$ is used to reduce the effects of changes in drainage patterns with orogen growth.

In MT1, the orogen is in a continuously constructive state during its 15 My evolution. The orogen-to-basin sediment flux ($Q_S(retro)$) initially increases rapidly, then continues to increase at a progressively slower rate (Fig. 3.4). During the first 5 My, $Q_S(retro)$ increases as a consequence of orogen growth because denudation increases as precipitation increases with orogen elevation. The initial increase in $Q_S(retro)$ reflects changes in precipitation when the sum of precipitation is much less than the basin-to-orogen vapour flux ($Q_V(y)$). However, after 5 My precipitation rates on the orogen begin to decline as precipitation on the growing alluvial plain depletes $Q_V(y)$ (①, ⑥ and ⑦, Fig. 3.3). $Q_S(retro)$ thus becomes asymptotic as $Q_V(y)$ decreases, reflecting how precipitation and erosion rates on the windward orogen vary as surface topography of the orogen and basin evolves. There is a negative feedback here in that a decrease in erosion rates enhances the orogen growth, thereby counteracting the rate of decrease in $Q_S(retro)$.

Orogen to Retro-Foreland Basin Sediment Flux, $Q_S(retro)$

Material Flow in Orogen/Foreland System

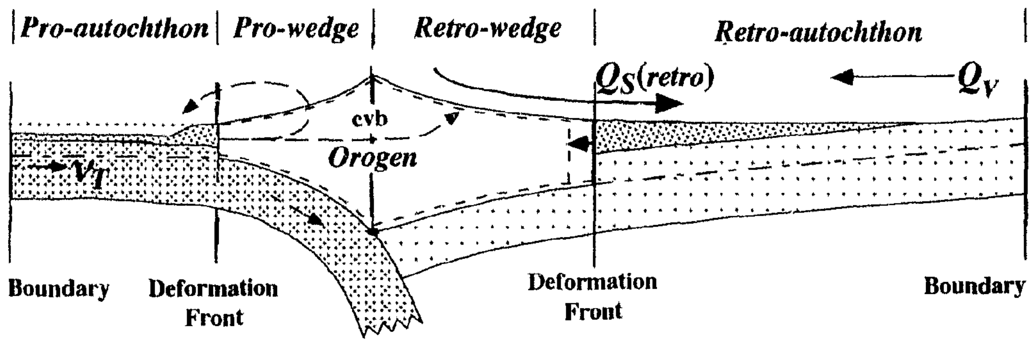

MT1 - $Q_S(retro)$ with Constant V_T, Q_V and V_E

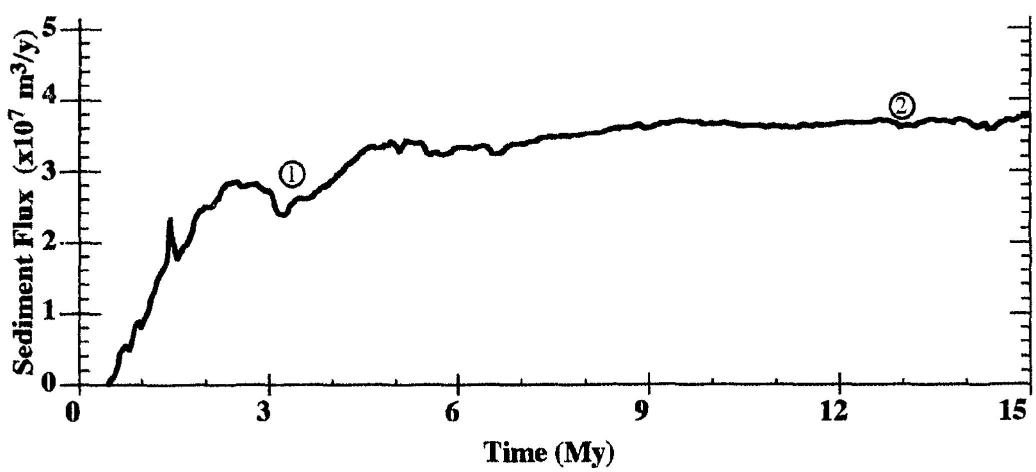

Figure 3.4. Schematic section of an orogen/foreland basin system is shown in the upper panel. Arrows indicate the direction of convergence, prevailing wind direction, and flow of material through the orogen/foreland basin system in MT1. Arrows in pro-wedge and foreland basin indicate the dominance of tectonic recycling, while arrows in the retro-wedge and foreland basin indicate the dominant flow of material through the orogen and into the basin. The lower panel shows how sediment flux across the retro-wedge deformation front into the retro-foreland basin, $Q_S(retro)$, varies with time.

Minor variability in $Q_S(retro)$ is caused in part by river capture along the common vertical boundary (*CVB*) separating the pro- and retro-wedges (①, Fig. 3.4). This variability ceases once drainage networks are established. Other minor variability in $Q_S(retro)$ is caused by temporal variations in $Q_V(retro)$ that result from changes in surface relief and therefore precipitation on the peripheral bulge (②, Fig. 3.4).

MT2 - Symmetry in Orogen/Foreland Basin Evolution

Model MT2 results illustrate the 15 My evolution of an orogen/foreland basin system where model conditions promote symmetry between the pro- and retro-foreland basins. MT2 parameter values are the same as MT1, except that V_T is reduced to 1.0 cm/y (~1/3 of MT1), the prevailing wind direction is reversed, and the position of the *CVB* is shifted so that the MT2 orogen is the same distance from the upwind model boundary as MT1. MT2 results show a slowly developing windward pro-foreland basin at 5, 10 and 15 My in planform (Fig. 3.5) and section (Fig. 3.6).

At 5 My, after 50 km of tectonic convergence, MT2 shows the emergence of an incipient orogen with an elevation of ~600 metres and a width of ~45 km (Figs. 3.5, 3.6). The orogen at this stage is not much larger than a big accretionary prism (*e.g.*, Lesser Antilles, Westbrook, 1988). Rainfall distribution across the incipient orogen is essentially symmetric because the vapour flux is not significantly depleted by precipitation on the windward side of the orogen. Small prograding sedimentary wedges have begun to infill the pro- and retro-foreland basins (①, Fig. 3.6); the sedimentary fill in the pro-foreland basin is 1 km thick. The regional view shows that the pro- and retro-foreland basins are essentially geometrically symmetric about the orogen (A-A', Fig. 3.6).

MT2 - Constant v_T, Q_V, and v_E

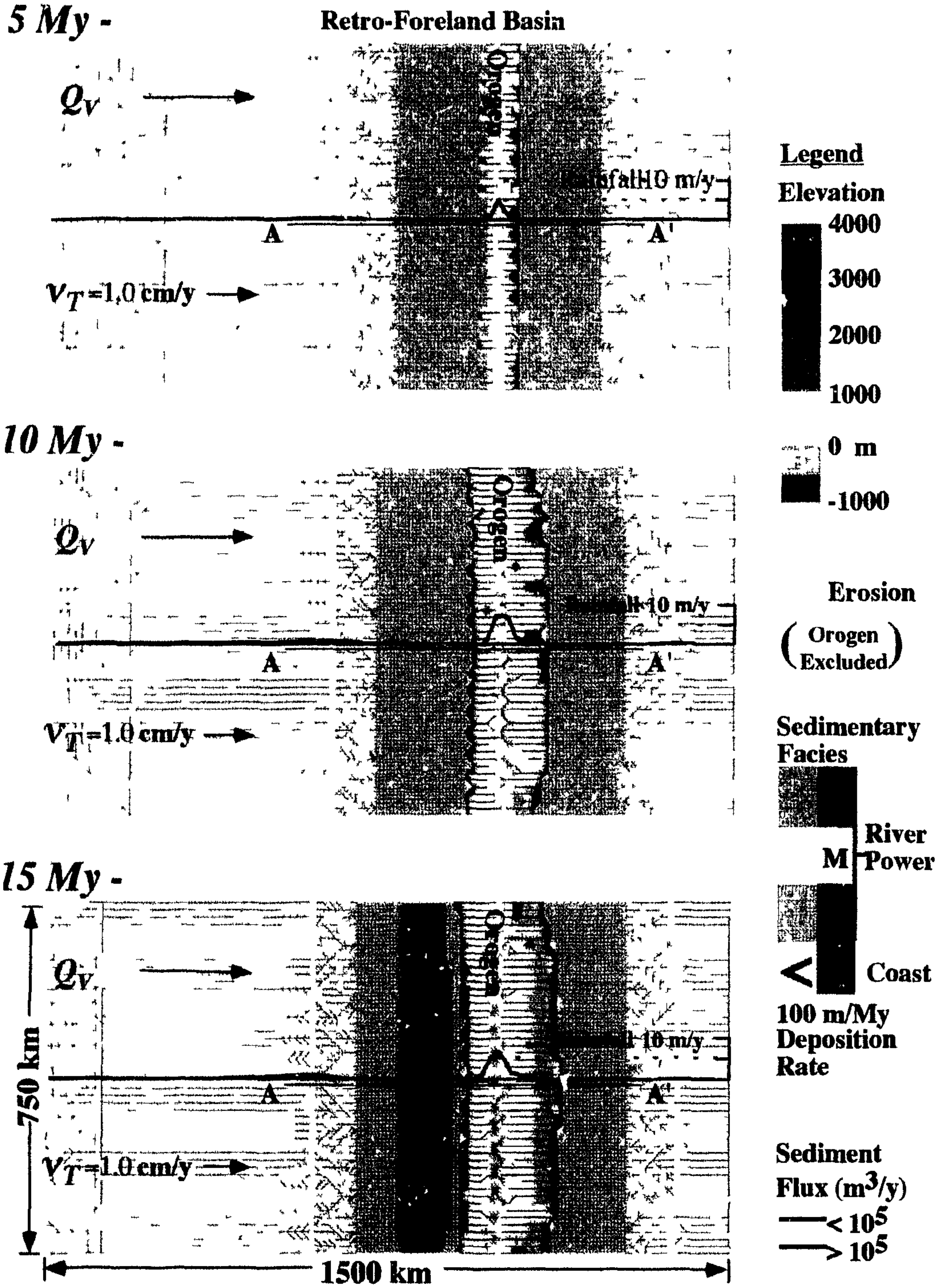

Figure 3.5. MT2 shows development of an orogen/foreland basin system with conditions that favour symmetry across the orogen. Planform surface elevation (grey), facies distribution (colour), denudation (pink) and fluvial drainage network (lines) are shown at 5, 10, and 15 My. Rainfall distributions (dark blue lines) are shown along lines of section A-A'.

MT2 - Constant v_T, Q_V, and v_E

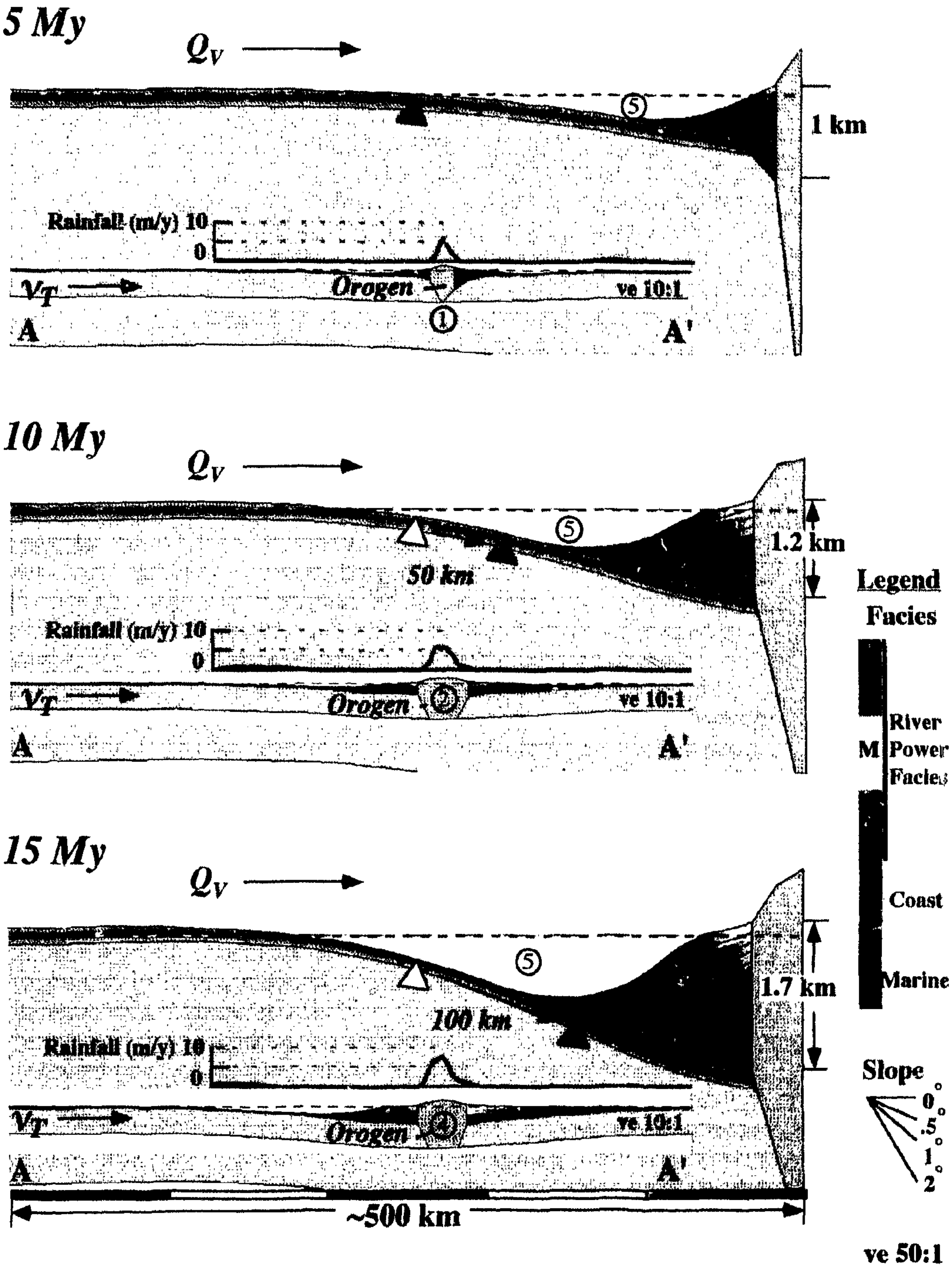

Figure 3.6. Development of the MT2 pro-foreland basin is shown at 5, 10 and 15 My; regional section A-A' inset. Basin facies are in colour and time lines are at 0.5 My intervals. Rainfall distributions are shown above regional sections (A-A', inset).

At 10 My after 100 km of tectonic convergence, the orogen is ~1000 m high and ~60 km wide (Figs. 3.5, 3.6). This slow rate of growth reflects the high rate of tectonic recycling. Most of the crust and pro-foreland basin strata entrained into the orogen are either eroded from the pro-wedge and returned to the pro-foreland basin or pass through the orogen before being eroded from the retro-wedge and deposited in the retro-foreland basin. The orogen is flanked by alluvial plains and prograding sedimentary wedges which partially infill both basins. Growth of these sedimentary wedges indicate that pro- and retro-wedge orogen-to-basin sediment flux (Q_S(pro) and Q_S(pro) respectively) exceed the rate at which sediment is re-entrained into either side the orogen. The increase in asymmetry between the pro- and retro-foreland basins (②, Fig. 3.6) indicates that the ratio of Q_S (orogen-to-basin sediment) to sediment re-entrainment is lower in the pro-foreland basin than the retro-foreland basin. In other words, $Q_{S(pro)}$ is less able to offset the effect of convergence between the pro-wedge and pro-foreland basin, than $Q_{S(retro)}$ is able to offset convergence between the retro-wedge and retro-foreland basin.

At 15 My, after 150 km of tectonic convergence, the orogen is only ~1100 m high and ~60 km wide (Figs. 3.5, 3.6). Continued growth of the orogen is observed in the ~0.5 km increase in depth of the pro- and retro-foreland basins adjacent to the orogen (③, Fig. 3.6). Isostatic compensation for the increased sediment and water loads in the basins lessen the increase in orogen elevation. Asymmetry between the pro- and retro-foreland basins continues to increase, although sedimentary wedges in both basins continue to prograde (④, Fig. 3.6). Growth of these sedimentary wedges indicates that orogen-to- basin flux (Q_S) continues to exceed the rate at which basin strata are entrained into either side of the orogen. However, the progressive increase in seaway depth in the

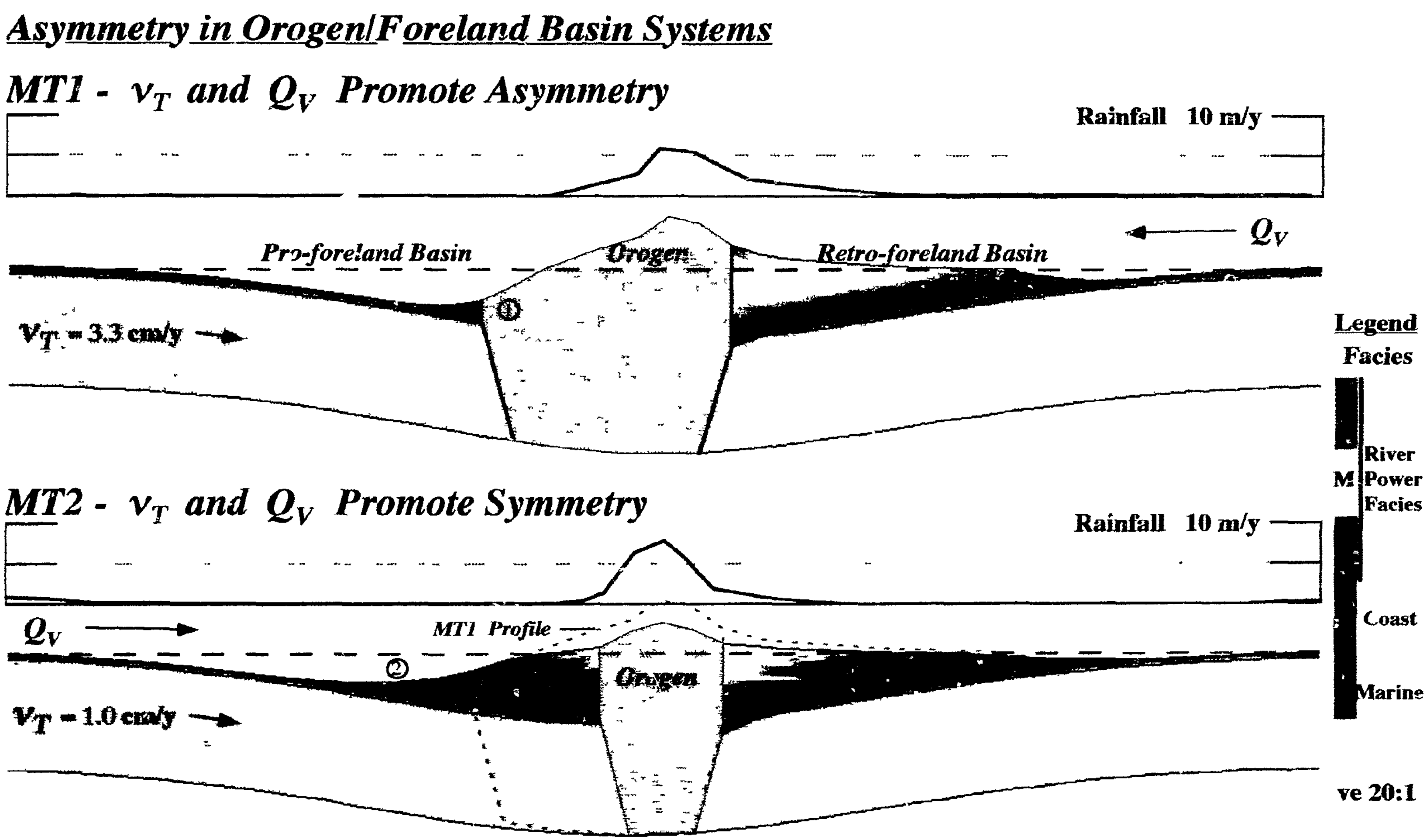

Figure 3 7 Sections show MT1 and MT2 orogens and their flanking foreland basins after approximately equivalent amounts of tectonic convergence. Basin facies are in colour Rainfall distributions are shown above each section. The red dashed line on MT2 is the MT1 orogen and foreland basins profile.

pro-foreland basin between 0 and 15 My indicates that Q_S(pro) has not kept pace with the effects of isostatic compensation (⑤; Fig. 3.6), unlike the retro-foreland basin (④; Fig. 3.6). Therefore the pro-foreland basin is growing faster than it is filling, while the converse is true for the retro-foreland basin. It is interesting to note that, although relative sea level is rising and the shoreline position of the pro-foreland alluvial plain remains approximately constant relative to the orogen, basin stratigraphy shows not only aggradation but also progradation. This progradation reflects the migration of the seaway over the pro-lithosphere with tectonic convergence between the pro-lithosphere and the orogen.

The 150 km of tectonic convergence experienced in MT2 by 15 My is similar to the 165 km of tectonic convergence experienced in MT1 by 5 My. In section, comparison of MT1 at 5 My to MT2 at 15 My contrasts the asymmetry between pro- and retro-foreland basins (Fig. 3.7). MT1 and MT2 orogens differ in that the MT1 orogen is thicker and much wider. The difference in width is a consequence of the pro-wedge deformation front advance (①, Fig. 3.7). The position of the deformation front is determined by the limit of continuous critical taper basinward from the *CVB*. The difference in deformation front positions is a consequence of steeper surface slopes in MT1. These steeper surface slopes are a consequence of lower precipitation rates, and therefore less efficient sediment transport away from the orogen. Much of the difference in thickness between the MT1 and MT2 orogens is accounted for in the difference between MT1 and MT2 pro-foreland basin strata (②, Fig. 3.7). In MT2, the pro-foreland basin strata are considerably thicker than equivalent strata in MT1 (②, Fig. 3.7). This difference is a consequence of both vT and the prevailing direction of Q_V. The slower v_T in MT2 reduces the rate of strata entrainment into the orogen, and the windward setting of the pro-foreland basin in MT2 increases denudation of the pro-wedge and thus $Q_{S(pro)}$. While both v_T and the prevailing direction of $Q_{T'}$ contribute to creating greater symmetry between pro- and retro-foreland basins in MT2 relative to MT1, the windward setting of the pro-foreland basin has a greater effect because of its effect on both the deformation front advance and Q_S(pro).

3.2.2 Planform Variability in Tectonism

Foreland basin stratigraphy is influenced by the competition between transverse and longitudinal sediment transport in both subaerial and submarine environments (Ebro Basin, Marzo *et al.*, 1988; Fig. 3.1). In MT3, the convergent continental margins are oblique to each other rather than parallel as in MT1 and MT2; orogen development is therefore diachronous along strike. MT3 results illustrate the effects of along-strike variation in orogenic tectonism on longitudinal and transverse sediment transport. All parameter values used in MT3 are the same as MT1. Evolution of the MT3 orogen/foreland basin system is shown after 5, 10 and 15 My in planform (Fig. 3.8), section (Figs. 3.9, 3.10) and fence diagram (Fig. 3.11).

MT3 Evolution Prior to 5 My

Development of the MT3 system begins with continent/continent collision near A-A' that proceeds along strike toward C-C' (Fig 3.8). At 5 My, continent/continent collision is just beginning at B-B'. The width of the orogen and the extent of the retro-foreland basin filling therefore decrease between A-A' and B-B' (Fig. 3.8). Between B-B' and C-C', convergence between oceanic and continental lithosphere provides only minor tectonic flux into the incipient orogen relative to the continent/continent collision at A-A'. This difference in flux is because of the lesser thickness of material above the

MT3 - Constant v_T, Q_V, and v_E

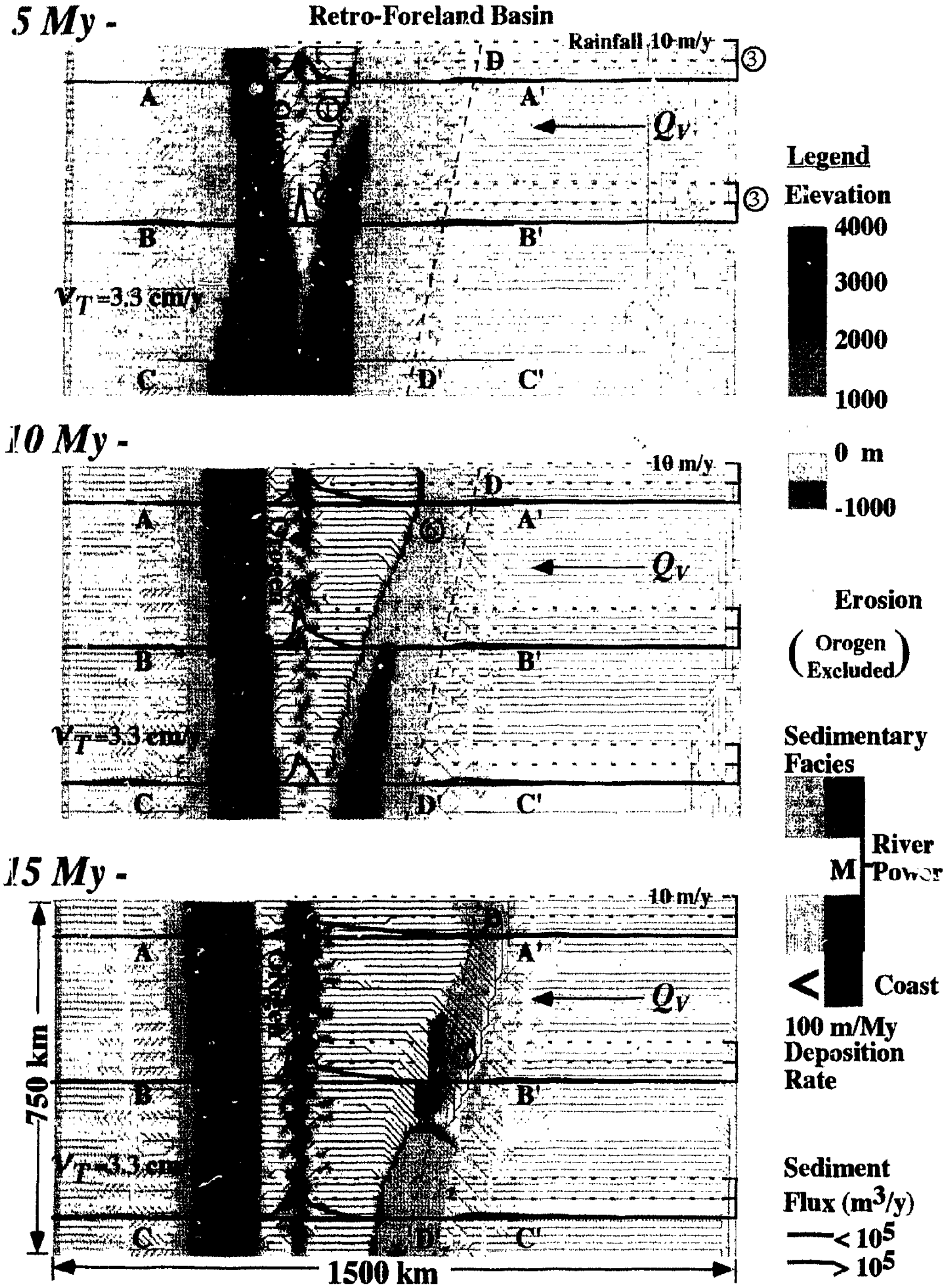

Figure 3.8. Planform surface elevation (grey), facies distribution (colour), erosion (pink) and fluvial drainage network (lines) for MT3 at 5, 10, and 15 My. MT3 shows the effects of collision between oblique continental margins. Rainfall distributions are shown over lines of section A-A', B-B' and C-C'. Peripheral bulge migration is seen relative to Section D-D'. At 5 My the -1500 m bathymetric contour is a dashed line

potential detachment horizon in the oceanic lithosphere relative to the continental lithosphere. The incipient orogen between B-B' and C-C' is most like a doubly-vergent accretionary prism developing over a subduction zone. Two natural examples of accretionary prisms that developed into small orogens are Taiwan (Covey, 1986) and the Outer-Banda Arc (Audley-Charles, 1986).

At 5 My, MT3 and MT1 have similar drainage networks, except for local deflections of rivers along the coast of the MT3 retro-foreland seaway (Figs. 3.2, 3.8). The direction of the rivers in MT3 demonstrates that dip slopes of the upper alluvial plain are larger than strike slopes (①, Fig. 3.8). The direction of alluvial plain progradation in the retro-foreland basin is predominantly perpendicular to the strike of the orogen. However, on the distal alluvial plain rivers are deflected toward the deepest part of the seaway indicating the influence of along-strike submarine transport on surface dip direction, fluvial transport and basin filling. The lack of alluvial plain development in the pro-foreland basin (②, Fig. 3.8; ①, Fig. 3.9) is caused by tectonic recycling as in MT1 (Sec. 3.2.1; Johnson and Beaumont, 1995).

The retro-foreland seaway is deeper adjacent to where continent/continent collision is just beginning at B-B', than where the orogen is the largest, along A-A' (Fig. 3.8) because of the greater ratio of relative sea-level rise to orogen-to-basin sediment flux ($Q_S(retro)$) at B-B'. The uniform thickness of material above the potential detachment surface in the convergent continents (Fig. 2.9) means that the deepest part of the retro-foreland basin is not determined by inherited continental margin topography, although in nature topography may be a critical factor. The rate of relative sea-level rise (basin subsidence) caused by isostatic compensation of tectonic orogen growth is approximately uniform between A-A' and B-B', because the rate of orogen growth is approximately

MT3 - Constant v_T, Q_V, and v_E

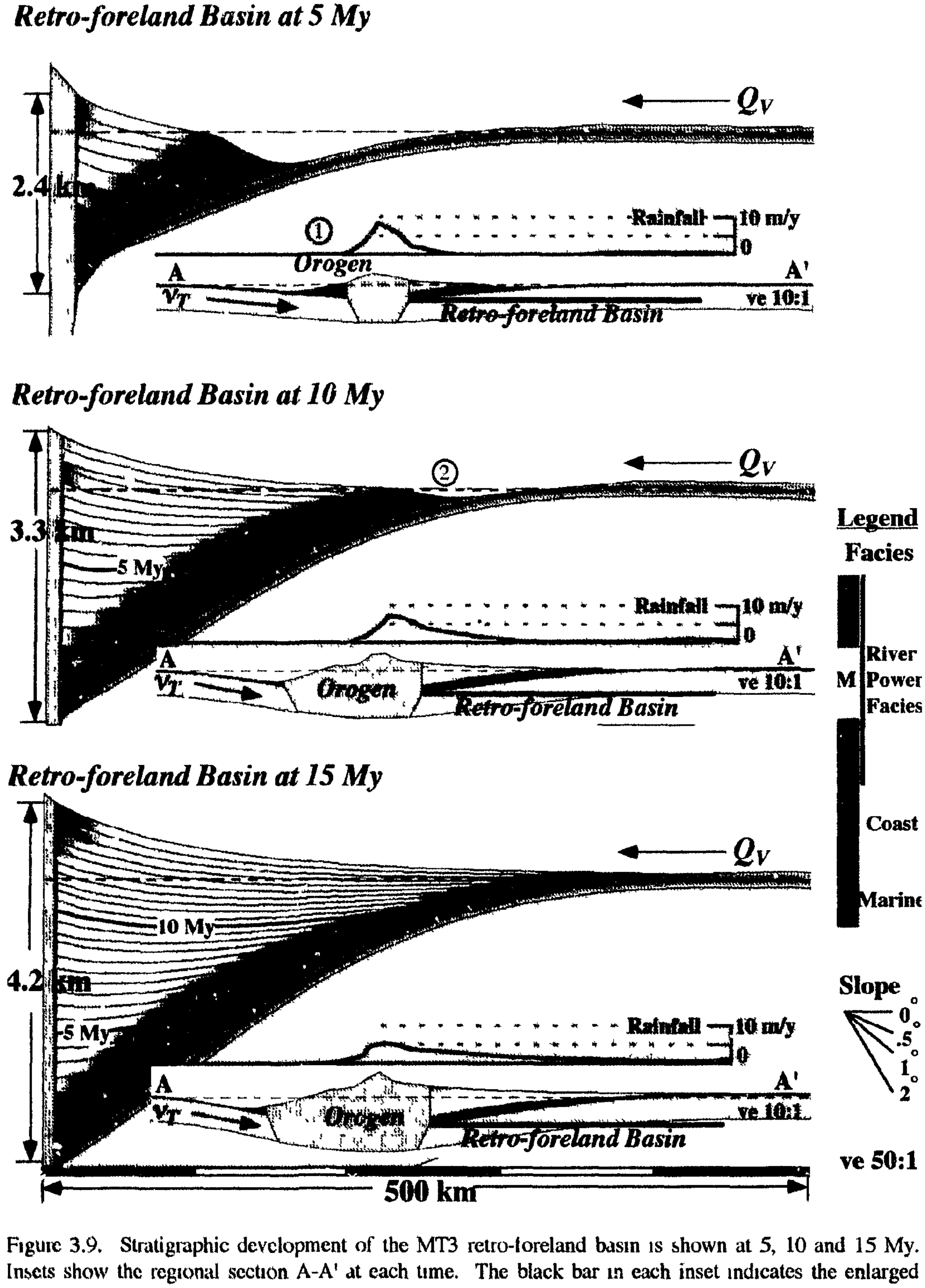

Figure 3.9. Stratigraphic development of the MT3 retro-foreland basin is shown at 5, 10 and 15 My. Insets show the regional section A-A' at each time. The black bar in each inset indicates the enlarged portion of the retro-foreland. Sedimentary facies are in colour and time lines are at 500 ky intervals Rainfall distributions are shown over regional sections (blue lines).

MT3 - Constant v_T, Q_V, and v_E

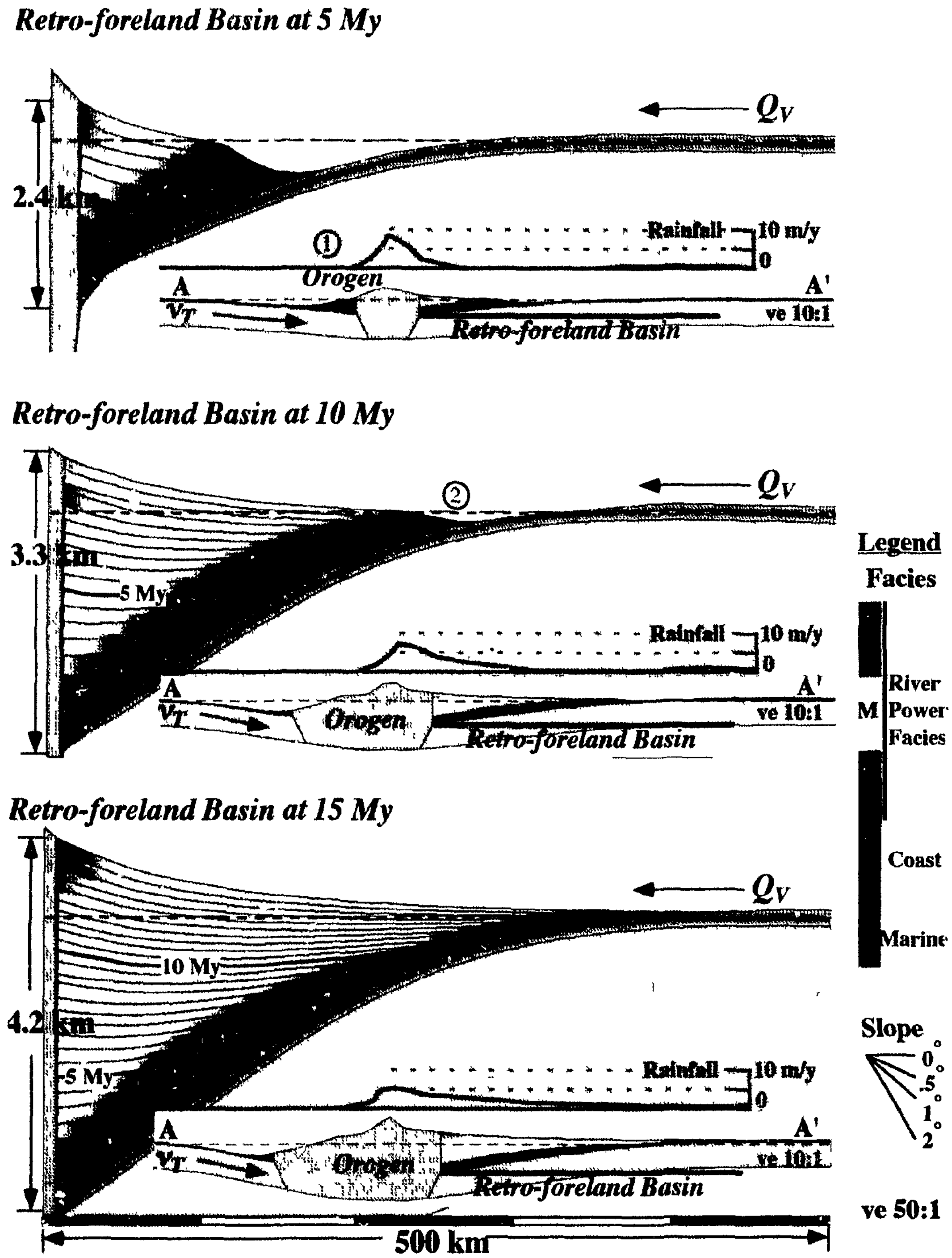

Figure 3.9. Stratigraphic development of the MT3 retro-foreland basin is shown at 5, 10 and 15 My. Insets show the regional section A-A' at each time. The black bar in each inset indicates the enlarged portion of the retro-foreland. Sedimentary facies are in colour and time lines are at 500 ky intervals. Rainfall distributions are shown over regional sections (blue lines).

uniform (Fig. 3.8). The orogen, however, decreases in elevation from A-A' to B-B' because of the shorter duration of continent/continent collision toward B-B'. $Q_S(retro)$ is lower due to the smaller orogen and the attendant decrease in precipitation and erosion toward B-B' (③, Fig. 3.8). The MT3 retro-foreland basin is therefore deeper adjacent to the incipient orogen where the elevation is low and interaction with the climate is minimal (④, Fig. 3.8). The deepest region of the pro- and retro-foreland seaways lies adjacent to the subducting oceanic lithosphere (⑤, Fig. 3.8). The 2800 m difference in surface relief between the subducting continental and oceanic lithospheres is greater than any difference in seaway depth caused by an along-strike variation in the ratio of flexural subsidence to orogen-to-basin sediment flux. Figure 3.8 illustrates that migration of seaway bathymetry in a retro-foreland basin correlates with growth of the orogen.

At 5 My, the MT3 orogen is smaller and the retro-foreland basin is less filled along A-A' (Figs. 3.8, 3.9) than in MT1 (Figs. 3.2, 3.3). These differences are a consequence of longitudinal marine sediment transport toward the deeper portions of both the pro- and retro-foreland seaways. The orogen is smaller in MT3 because longitudinal transport in the pro-foreland basin distributes orogen-to-basin sediment flux along strike, thereby reducing the volume of sediment available to be tectonically recycled. The retro-foreland basin is less filled in MT3 because marine along-strike transport reduces the rate of transverse alluvial-plain progradation.

In natural environments the effects, for example, of littoral drift, along shore currents or density currents may act to either enhance or inhibit sediment transport toward the depocentre. The model does not incorporate advective transport processes for the submarine environment.

MT3 Evolution Between 5 and 10 My

In MT3, as in MT1, 330 km of convergence by 10 My leads to significant growth of the orogen and deepening of the retro-foreland basin while seaway bathymetry decreases.

Rainfall distributions in MT3 along A-A', B-B' and C-C' characterize both the variation in rainfall along strike and the evolution of rainfall distribution as the orogen grows (Fig. 3.8). While the orogen is low and narrow, the rainfall distribution is essentially symmetric as in C-C'. The high rainfall rates and approximately symmetric rainfall distribution indicate that the vapour flux ($Q_V(y)$) is not significantly depleted by rainfall across the retro-foreland. Section A-A', in contrast to C-C', shows an increase in precipitation over the alluvial plain and a decrease over the orogen caused respectively by increasing elevation of the alluvial plain with basin filling and rainfall across the alluvial plain depleting $Q_V(y)$ prior to its arrival at the orogen. The result is increasing asymmetry of rainfall distribution with the growth of the orogen and development of the alluvial plain (Fig. 3.8).

MT3 and MT1 are similar along A-A', except that longitudinal marine sediment transport leaves the seaway open in MT3 (⑥, Fig. 3.8), whereas there is no axial transport in MT1 (Fig. 3.2). In section, marine sediments along A-A' are modestly thicker than the equivalent marine facies in MT1 (②, Fig. 3.9; ⑤, Fig 3.3). The thickness of marine facies in MT3 and MT1 reflects the initial surface elevation of the continent prior to continent/continent collision, the competition between sedimentation flux to and away from the coast, and isostatic compensation for the growing sedimentary and orogenic loads. Sediments are modestly thicker in MT3 because of the longitudinal marine transport of sediment, which increases sediment transport away from the coast by redistributing sediments out into the basin, reducing the rate of progradation and increasing the seaway margin slopes.

MT3 Evolution Between 10 and 15 My

At 15 My and 500 km of convergence, the MT3 drainage network differs significantly from MT1. In MT1, the drainage network extends across the peripheral bulge. In MT3, it has become oblique to orogen strike, with an axial or trunk river system transporting sediment longitudinally along the retro-foreland basin axis (⑦, Fig. 3.8). Instead of depositing sediment in the distal retro-foreland or transporting it across the peripheral bulge as in MT1 (Fig. 3.2), the drainage system in MT3 transports sediment along the basin axis toward the retro-foreland basin seaway. The flow of rivers, either across the alluvial plain or along the basin axis, following the path of steepest descent establishes a competition between transverse and longitudinal fluvial transport. Sedimentation related to transverse rivers builds up the MT3 alluvial plain, which could eventually result in drainage across the peripheral bulge as in MT1 (Figs. 3.8, 3.2). Longitudinal transport in MT3 diverts sediment that may have been used to build up the distal alluvial plain along the basin axis (Fig. 3.8). This diversion promotes longitudinal progradation and filling of the retro-foreland basin (D-D', Fig. 3.11).

Rainfall distributions in MT3 show an increase in asymmetry with the development of the alluvial plain (Fig. 3.8). There is a strong rain shadow over the leeward side of the orogen and fluvial erosion rates are on the order of 0.1 mm/y. By contrast, erosion rates on the windward slope of the orogen are five to tenfold larger and sedimentation rates across the retro-foreland alluvial plain are on the order of 0.2 mm/y adjacent to the orogen and ~0.005 mm/y on the lower alluvial plain. The high precipitation rates on the upper alluvial plain increase the carrying capacity of the rivers across the plain and much of the sediment is transported to the coast where sedimentation rates are on the order of ~0.4 mm/y.

In MT3, the trunk river system that drains the axis of the retro-foreland basin has a gradient of ~1/10000 (⑦, Fig. 3.8), approximately the same gradient found in modern foreland basins. For example, the Himalayan foreland basin has an axial surface slope of the basin of ~0.00012, while anastomosing rivers in the Magdalena foreland basin have gradients on the order of 0.00001 (Magdalena, Smith, 1986). Sedimentation rates are low along the basin axis, but facies continue to aggrade as rivers build toward equilibrium in response to axial progradation and basin subsidence (A-A', Fig. 3.10; D-D', Fig. 3.11). The amount of axial progradation required before sedimentation along the basin axis is sufficient to divert the upper trunk river across the peripheral bulge depends upon the trunk river gradient and the drainage divide elevation of the bulge. In MT3 at 15 My, the peripheral bulge is ~70 m high; therefore, the basin must be filled along strike for at least 700 km before aggradation will cause diversion of the trunk river across the bulge. The situation in MT3 implies that a foreland basin may never become overfilled if the gradient and strike length of the axial drainage system are insufficient to allow aggradation of the fluvial system to the elevation of the drainage divide. Only for long orogens would aggradation of alluvial sediments be sufficient to favour drainage across the peripheral bulge (*cf.* North American Cordillera). Therefore, in situations such as the Himalayan foreland basin where the slope of the basin axis is ~0.00012, axial drainage will persist unless changes in sea level, climate and/or orogen tectonics cause an increase in river gradient and/or a decrease in the elevation of the drainage divide across the Decca Plateau (*e.g.*, upper Chambal, Luni or Naramada catchment boundaries).

MT3 - Constant v_T, Q_V, and v_E

Retro-foreland Basin at 15 My, along A-A'

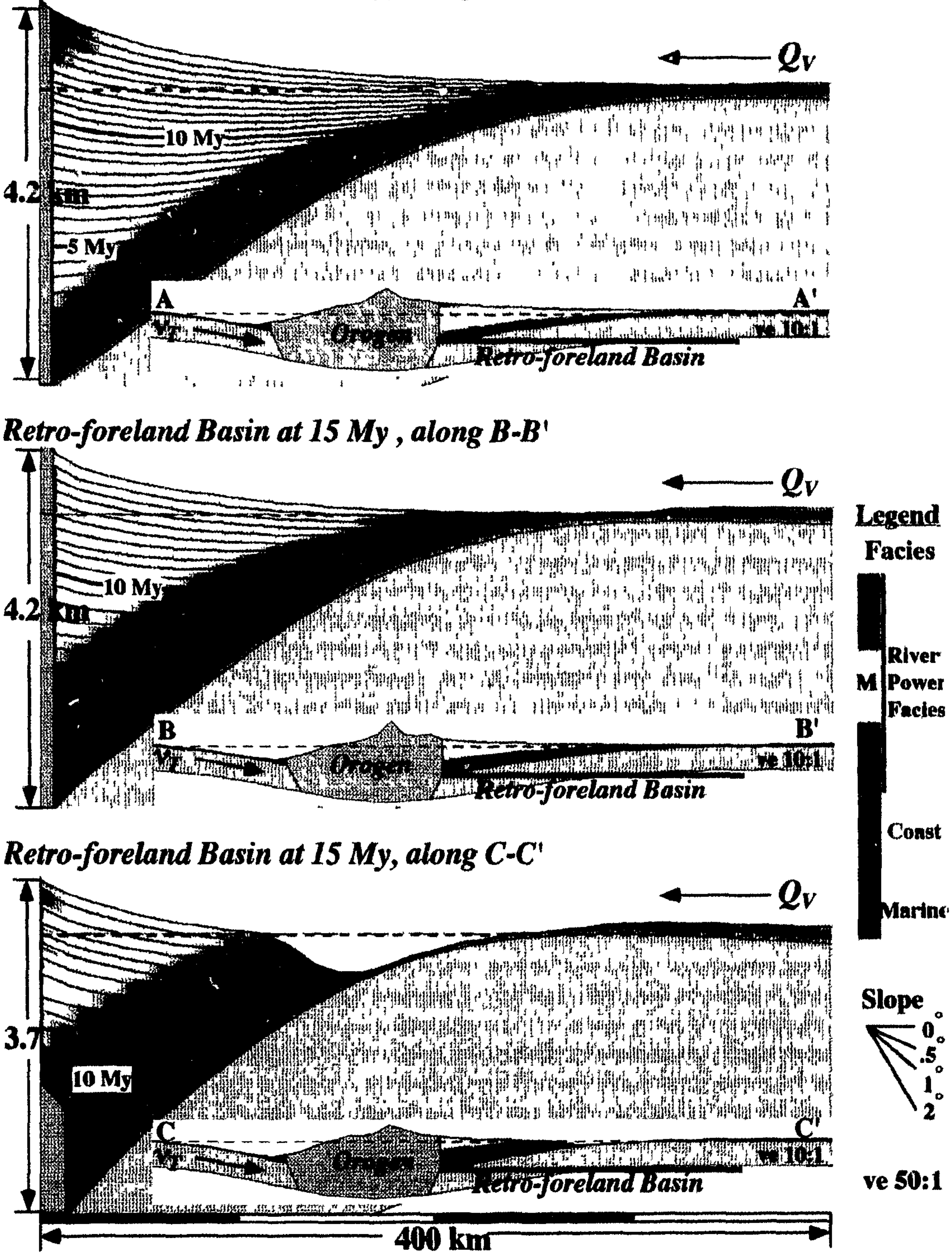

Figure 3.10. Stratigraphic development of the MT3 retro-foreland basin is shown at 15 My, along sections A-A', B-B' and C-C' (regional sections inset). The black bar in inset indicates enlarged portion of the retro-foreland basin. Sedimentary facies are in colour. Time lines (black) are at 500 ky intervals.

MT3 - Constant v_T, Q_V, and v_E

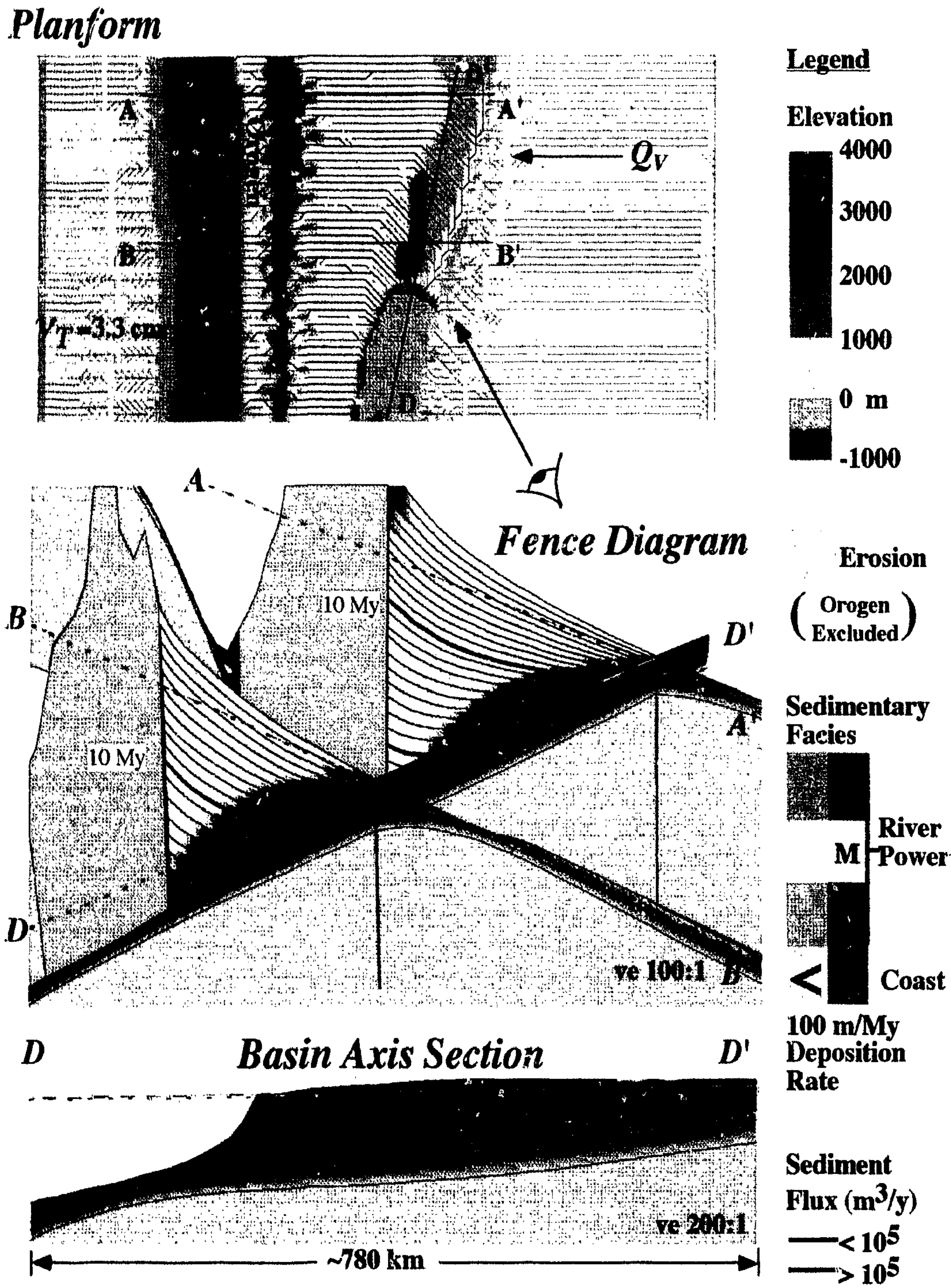

Figure 3.11. The MT3 retro-foreland basin at 15 My is shown in planform, fence diagram and axial section. The fence diagram shows spatially the progradation of sedimentary facies (colour) and the time-line geometry (black) in dip sections A-A' and B-B' and strike section D-D'. (This diagram illustrates how the interconnected sections appear from an elevated position, looking down into the retro-foreland basin; see 'eye', top panel.)

Progradation and aggradation of alluvial facies along the basin axis in MT3 (Fig. 3.11) are somewhat analogous to aggrading river deposits found, for example, in the Molasse Foreland Basins (Homewood *et al.*, 1986), the Alberta Foreland Basin (Leckie, 1989) and the North Slope Foreland Basin, Alaska (Bird and Molenaar, 1992). In the North Slope Foreland Basin, the Nanushuk and Coleville groups provide good examples of axial progradation (Fig. 3.12). The basin lies between the Brooks Range and Barrow Arch, which subparallels the continental margin and acts as the northern boundary of the foreland basin. Figure 3.12 shows paleo-transport directions in the Nanushuk Group and foreset dip directions in the Torok Formation (Bird and Molenaar, 1992). Between the Aptian and the Cenomanian, a thick delta, delta-slope and basinal sequence prograded east-northeastward, subparallel to the orogen and the basin axis. The Nanushuk Group comprises the deltaic part of the sequence, while the Torok Formation comprises the pro-delta shelf, slope and basinal deposits that are coeval with the deltaic part of the sequence (Bird and Molenaar, 1992). Progradation of this sequence was interrupted by a significant Cenomanian transgression followed by renewed northeasterly progradation of the deltaic and prodelta facies of the Coleville Group (Fig. 3.12).

In MT3 at 15 My, the retro-foreland basin at A-A' (Figs. 3.9, 3.10) appears similar to A-A' in MT1 (Fig. 3.3). However, unlike MT1, in MT3 the thickness of marine facies increases significantly along strike in the basin (①, Fig. 3.10). This increase in marine facies is caused by an along-strike increase in basin depth coeval with continent/continent collision and occurring as a consequence of flexural isostatic compensation of the growing orogen and sedimentary loads along strike. Another expression of this flexural deepening is found along the basin axis, where marine facies thicken and surface slopes of the marine margin increase with progradation

Axial Progradation in the North Slope Foreland Basin

Reconstructed Structural/Stratigraphic Axial Section A-A' at End Cretaceous

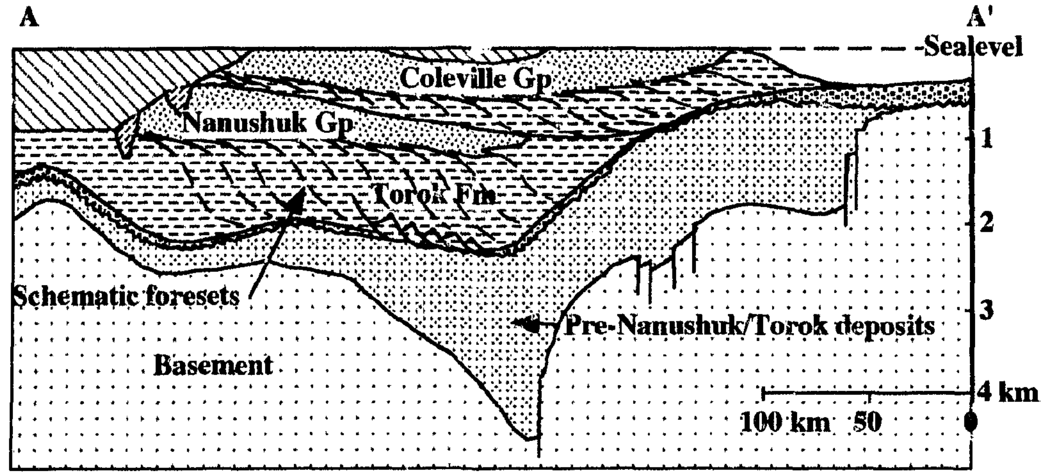

Nanushuk Group Paleotransport and Torok Formation Foreset Dip Directions

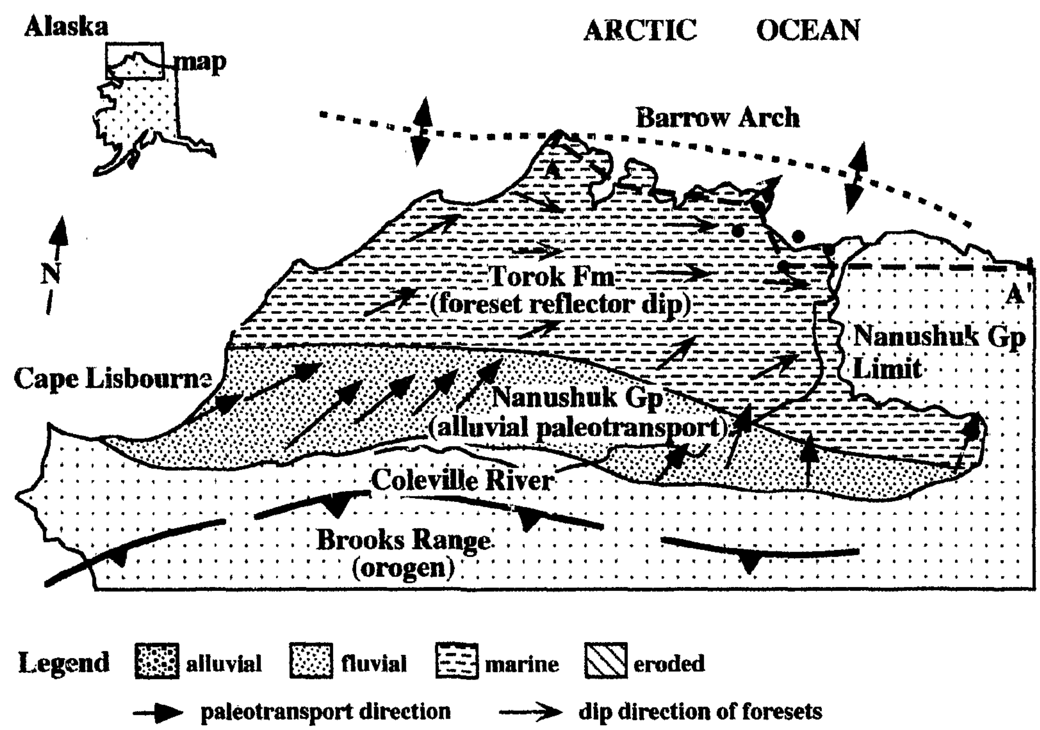

Figure 3.12. Modified after Bird and Molenaar (1992). The alluvial/deltaic Nanushuk Gp. and the lateral, coeval, prodelta slope and basinal mudstones of the Torok Fm show progradation to the east/northeast (A-A') as evidenced by the direction of alluvial paleotransport in the Nanushuk Gp., the dip direction of foreset reflectors in the Torok Fm., and by dipmeter data from the Nanushuk Gp. and Torok Fm. (not shown).

(①, Fig. 3.11). The decreasing rate of progradation indicates that sediment flux to the coast becomes progressively less able to keep pace with basin subsidence. Therefore, either sediment supply or basin subsidence can limit the extent of axial progradation. A natural example of flexural deepening causing an along-strike increase in the proportion of marine facies may occur in the Taiwan foreland basin. Covey (1986) observes that fluvial/shallow marine sedimentation in the older northern Taiwan foreland basin changes to deep marine sedimentation in the younger southern basin. He suggests that this change in facies is a consequence of an oblique collision and the northeast-to-southwest development of the Taiwan orogen and foreland basin (Covey, 1986).

3.3 Tectonic Periodicity

Orogen/foreland basin systems develop over time scales of 10^6 years (*e.g.*, Taiwan) to 108 years (*e.g.*, Alberta Foreland Basin). Systems that develop over periods of 10^8 years are typically interpreted to have cycled between constructive and destructive states with multiple episodes of orogenic tectonism (*e.g.*, Alberta Foreland Basin, Fermor and Moffat, 1992; Stockmal *et al*, 1992). Variations in the rate of orogen growth, and consequently orogen state, strongly influence the stratigraphic development of foreland basin stratigraphy. Essentially, changes in basin stratigraphy are a consequence of the effects of flexural isostatic compensation and changes in orogen elevation on river gradients and precipitation. This discussion examines how the change between constructive and destructive orogen states is recorded stratigraphically, and how this change in state is a probable cause of lower-order sequences in foreland basin stratigraphy (Heller *et al.*, 1988; Flemings and Jordan, 1990).

Changes in the rate of orogenic tectonism occur on time scales of seconds (*e.g.*, earthquakes) to 10^7 years (*e.g.*, Alpine tectonics, Switzerland, Homewood *et al.*, 1986;

Cordilleran tectonics, Canada Monger, 1989; and Fermor and Moffat, 1992). As the time scales between changes in orogen state decrease, the length scales over which these changes are recorded in stratigraphy become limited by interaction among first-order processes that control orogen/basin evolution (*i.e.*, the composite response time of the tectonic, surface and isostatic processes as an integrated system). Therefore, the stratigraphic record of high frequency changes in orogen state, where the period of change is less than the composite response time of the orogen/foreland basin system, may be significantly different than for low frequency changes, where the period of change is much greater than the response time (Paola *et al.*, 1992). In order to investigate the composite response time of an integrated orogen/foreland basin system and the stratigraphic response of the system to an instantaneous change in orogen state, a step function in ν_T is used to 'switch' the tectonic flux into the orogen 'on' and 'off.' The change in orogen-to-basin sediment flux (Q_S) with each change in ν_T is used to estimate the system response time (τ_T) to changes in tectonism. Comparative model results are then produced using sinusoidal fluctuations in ν_T with periods either on the order of or much longer than τ_T.

3.3.1 Step Function Periodicity in Tectonics

Model orogen/foreland basin results are developed using both oblique (MT4) and parallel (MT5) convergent margin settings (Fig. 2.9) and the same parameter values as MT1 and MT3 (Table 2.1), except that ν_T is varied with time either as an 'on/off' step function or as a wave function while all other parameter values remain constant.

MT4 - Change in Orogen State and Retro-foreland Basin Stratigraphy

Model MT4 uses an oblique convergent margin setting with a 3 My on/off step function in v_T to show the effects of changing orogen states on longitudinal and transverse fluvial sediment transport. Although tectonics are not observed to change in a periodic manner in nature, a 3 My period is used to enable comparison of tectonic model results with those of climate and eustasy. In subsequent chapters, climate and eustasy models use a 3 My period because climate fluctuations are observed for similar periods (Crowley and North, 1991; Harrison, 1991), and this period approximates sequence periodicity from Haq *et al.*'s (1988) coastal onlap chart. Step changes in v_T cause the orogen to alternate instantly between constructive and destructive states. The resulting cyclic changes in orogen state cause the formation of stacked lower-order sequences. The sequences created by each tectonic/quiescent cycle are characterized by either rapid retrogradation of river-power facies or transgression above the sequence boundary followed by progradation of alluvial facies away from the orogen. Sequence boundaries are characterized by erosional surfaces and temporally equivalent facies associated with a relative fall in sea level. The boundaries are aerially extensive and typically overlain by a flooding surface. These results are consistent with the conceptual "two-phase stratigraphic model of foreland basin sequences" proposed by Heller *et al.* (1988) and the numerical model results of Flemings and Jordan (1990). In addition, the results of MT4 partially support the proposal by Blair and Bilodeau (1988) that a change from higher-energy alluvial to marine, lacustrine, or lower-energy fluvial environments is an indicator of orogenic tectonism.

MT4 Evolution Prior to 9 My

At 9 My, MT4 has experienced 6 My of tectonic convergence in two 3 My periods separated by an intervening period of quiescence (Fig. 3.13, top right). In planform, MT4 is similar to MT3, except that a fan delta forms where antecedent continental drainage transects and incises the peripheral bulge (①, Fig. 3.13; Fig. 3.8) as a consequence of the 1/10000 continental tilt initial-condition. The fan delta has coastal facies along its marine margin, low river-power facies (green) along its continental edges, and a fan of moderate river-power facies (yellow) across the central region. The geometry of this facies distribution is a product of laterally oscillating migration of the river downstream from a relatively stationary point, similar to natural deltaic systems (*e.g.*, Nile or Niger, Bhattacharya and Walker, 1992). The near stationary position of the delta, as observed from the relative abundance of alluvial sediments adjacent to the delta at A-A' relative to B-B' and C-C' (①, Figs. 3.14, 3.15), indicates that continental drainage has persisted in this location throughout the model's evolution.

In MT4, low order sequences develop due to changes between constructive and destructive orogen states, as conceptually proposed by Heller *et al.* (1988). Figure 3.15 shows two such sequences: a 0-6 My sequence is shown in all three panels, and the development of a 6-12 My sequence in the lower two panels. The sequence developed between 0-6 My comprises a sedimentary wedge associated with orogenic tectonism between 0-3 My and a shallowing upward succession capped by alluvial sediments deposited during the subsequent period of quiescence ('c' and 'd', Fig. 3.14). The sedimentary wedge deposited during the past 3 My phase of orogen growth overlies the 6 My sequence boundary. The onset of orogen tectonics is marked by extensive flooding and retrogradation of alluvial facies proximal to the orogen. The sudden rise in relative

MT4 - Periodic v_T, Constant Q_V and v_E

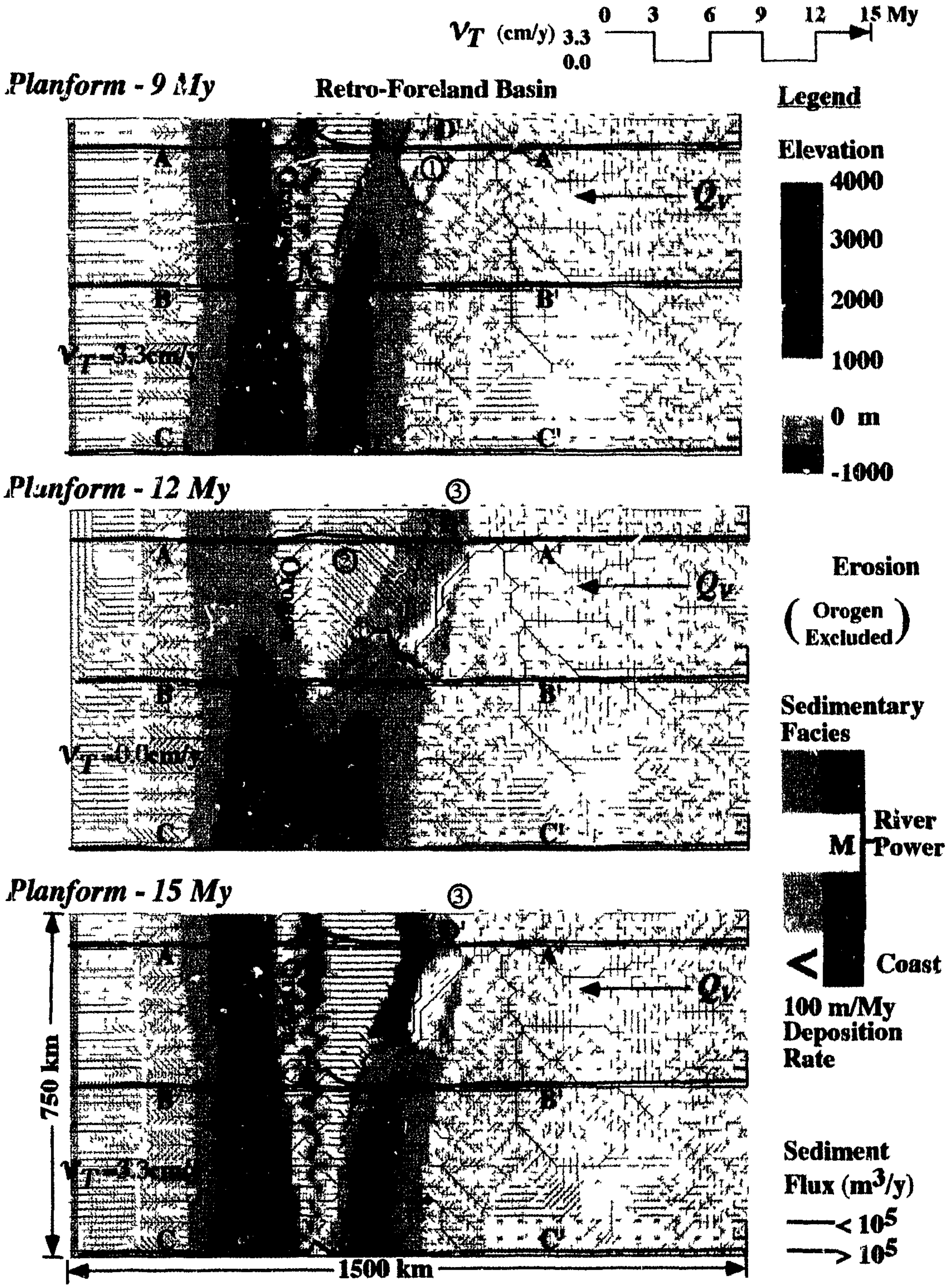

Figure 3.13. MT4 experiences periodic changes in v_T (top). The planform surface elevation (grey), facies distribution (colour), erosion (pink) and fluvial drainage network (lines) are shown for MT4 at 9, 12 and 15 My. In each case, results are shown just prior to the change in v_T. Rainfall distributions are shown over sections A-A', B-B' and C-C'.

MT4 at 15 My - Periodic v_T, Constant Q_V and v_E

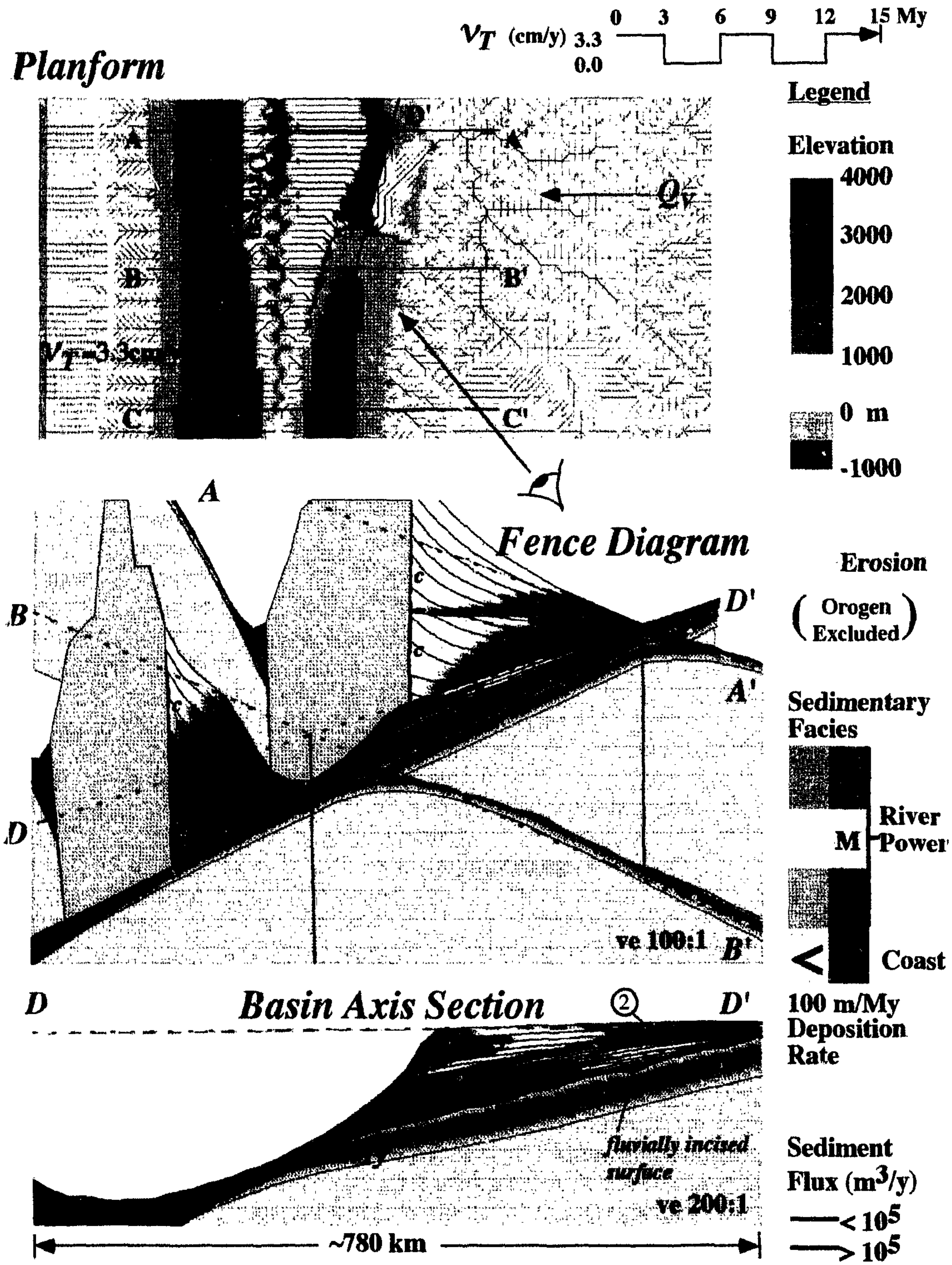

Figure 3.17. MT4 in planform, fence diagram and axial section at 15 My shows the spatial changes in sedimentary facies distribution (colour) and time-line geometries (black) caused by changes between constructive (c) and destructive (d) orogen states.

MT4 - Periodic v_T, Constant Q_V and v_E

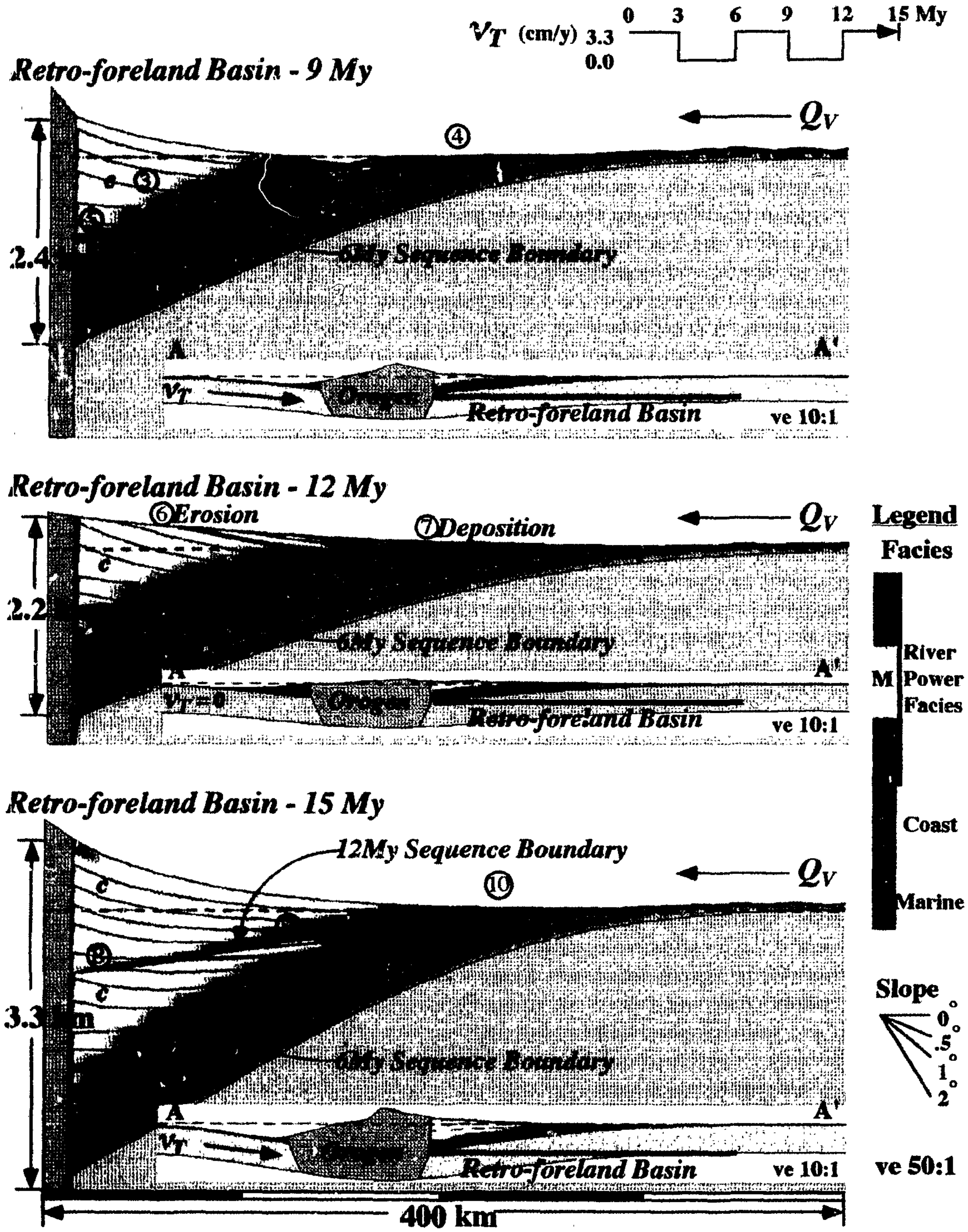

Figure 3.14. Development of the MT4 retro-foreland basin is shown at 9, 12 and 15 My, regional section A-A' inset. Sections show facies (colour) and time-line geometries (black) associated with constructive (c) and destructive (d) orogen states; 'c' to 'd' change is a heavy black line. Time lines are at 500 ky intervals.

MT4 - Periodic v_T, Constant Q_V and v_E

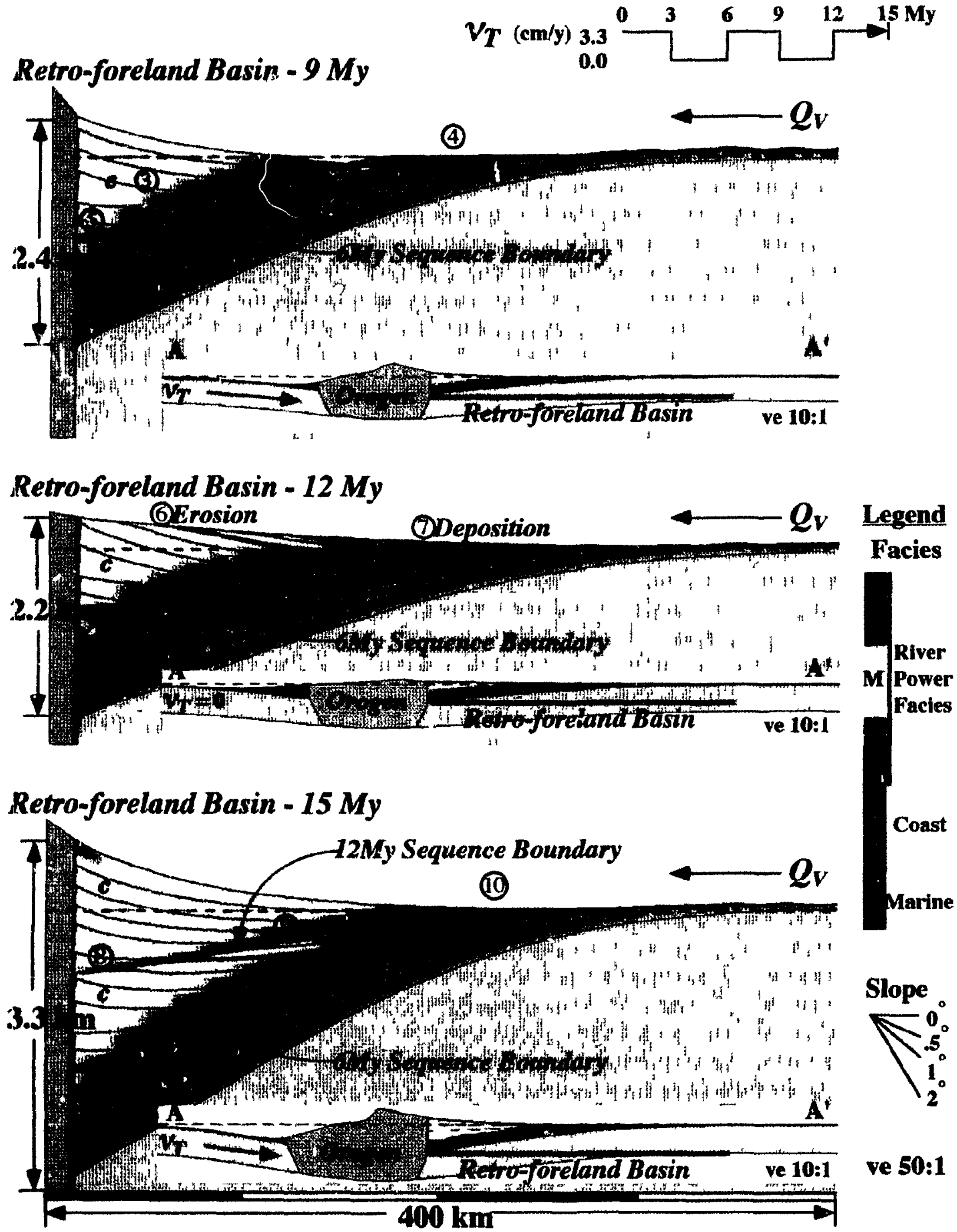

Figure 3.14 Development of the MT4 retro-foreland basin is shown at 9, 12 and 15 My, regional section A-A' inset. Sections show facies (colour) and time-line geometries (black) associated with constructive (c) and destructive (d) orogen states; 'c' to 'd' change is a heavy black line. Time lines are at 500 ky intervals.

MT4 - Periodic v_T, Constant Q_V and v_E

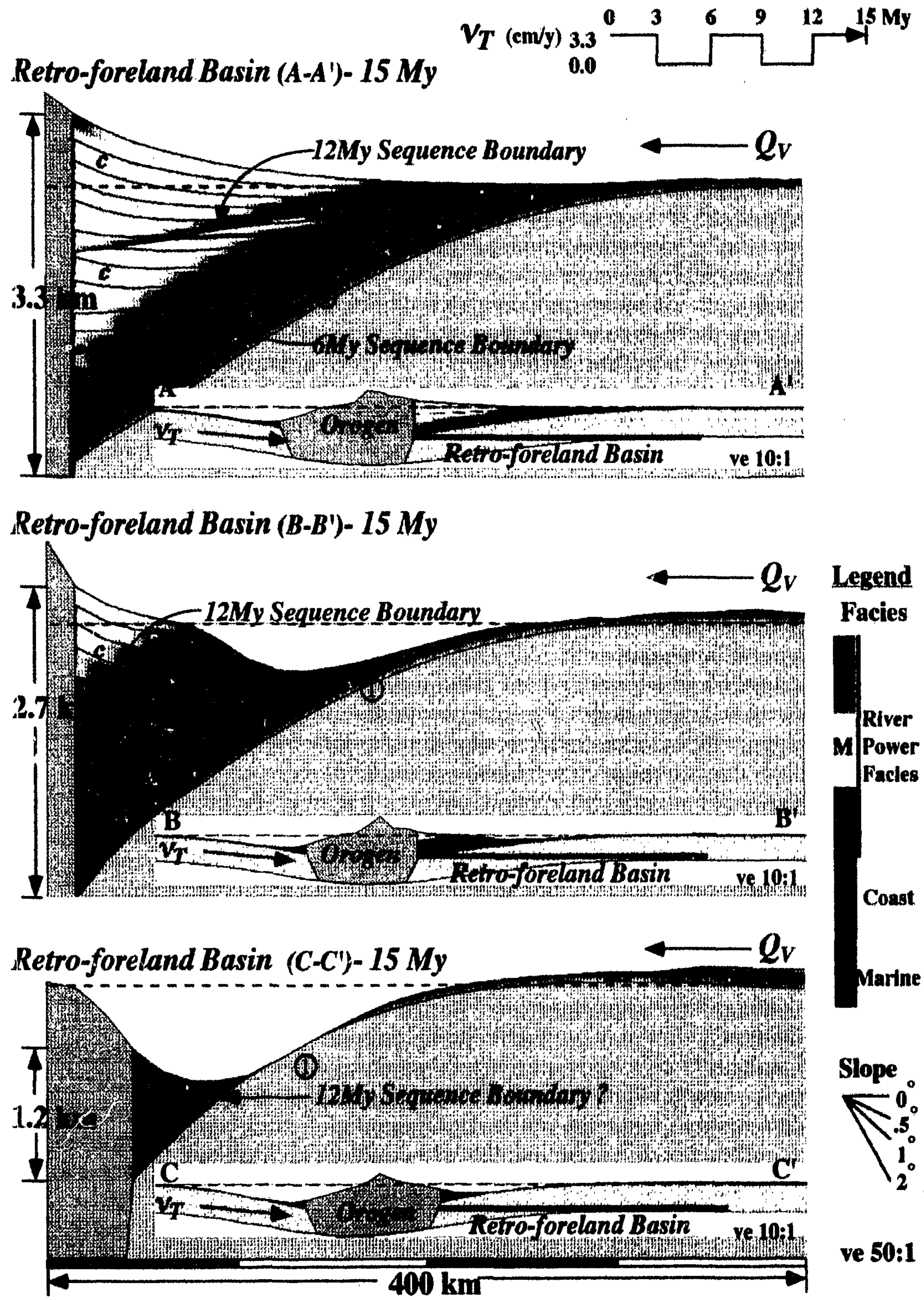

Figure 3.15. MT4 retro-foreland basin at 15 My along sections A-A', B-B' and C-C' (inset). Sections show facies (colour) and time-line (black) changes along strike. Time lines are at 500ky intervals. Sediment deposited during constructive and destructive orogen states are denoted by 'c' and 'd' respectively.

sea level is caused by isostatic compensation for the increased orogenic load. Flexural uplift of the peripheral bulge in response to the change in orogenic load is indicated by the basinward shift (*i.e.*, toward the orogen) of the coastal facies (②, Fig. 3.14). Within 500 ky the alluvial wedge adjacent to the orogen progrades further into the basin (③, Fig. 3.14) because orogen-to-basin sediment flux is greater than the rate of increase in accommodation space. As the orogen and sedimentary wedge grow in width, isostatic compensation for the advancing load causes the peripheral bulge to migrate away from the orogen, resulting in a relative sea-level rise and retrogradation of the fan delta facies onto the continent (④, Fig. 3.14).

The instantaneous onset of orogenic tectonism at 6 My causes transgression and flooding of much of the basin, superimposing marine over alluvial facies. In nature, such a flooding surface would typically place fine-grained marine sediments over coarser alluvial sediments (*e.g.*, Dunvegan Formation, Alberta Basin, Leckie and Smith, 1992; Plint *et al.*, 1993). Blair and Bilodeau (1988) argue that flooding and the shift to fine-grained sedimentation marks the onset of orogenic tectonism. While this point may be valid, it is only consistent with model results for the central region of the basin. On either basin margin, adjacent to the orogen or proximal to the emergent peripheral bulge, there are indicators of a coeval shift to higher-energy depositional environments (⑤ and ②, Fig. 3.14). Isostatic compensation in response to renewed orogenic tectonism causes subsidence of the alluvial plain adjacent to the growing orogen. This change in surface topography causes an increase in the disequilibrium between actual and graded river profiles that results in higher sedimentation rates (⑤, Fig. 3.14). In nature, these changes along the basin margins would likely cause a decrease in the sorting and may result in an increase in grain size, in apparent contradiction to Blair and Bilodeau's (1988) argument.

The decrease in sorting is expected as a consequence of the increase in river power gradient (i.e., a greater decrease in river power over a shorter distance). Grain size may or may not increase depending on the factors controlling erosion and abrasion of clasts from the orogen or peripheral bulge.

MT4 Evolution Between 9 and 12 My

The end of tectonic convergence at 9 My causes a change in orogen state characterized by exhumation of the orogen and isostatic rebound of the lithosphere. The result is uplift of the basin adjacent to the orogen and subsidence of the basin further than one-half flexural wavelength from the orogen. The upper alluvial plain experiences an increase in elevation and surface slope, causing an increase in precipitation and local discharge. The combination of an increase in surface slope and river discharge reverses the disequilibrium in fluvial transport from overcapacity to under capacity, and rivers adjacent to the orogen begin to incise the sedimentary section (②, Fig. 3.13; ⑥, Fig 3.14). Erosion and rebound rates both decrease with time as orogen elevation and precipitation decrease; the decrease in precipitation causes the decrease in erosion rate. Basin strata are exhumed to the greatest extent adjacent to the orogen, where isostatic rebound is greatest (②, Fig. 3.13).

Erosion and redeposition of sediments in the subaerial and submarine portions of the basin are referred to as reworking of basin sediments. Fluvial deposition of sediments from the orogen or redeposition of reworked sediments occurs where river disequilibrium changes from under to overcapacity (⑦, Fig 3.14), due to decreasing surface slopes across the alluvial plain. Heller *et al.* (1988) suggest that the Ogallala Formation and its temporally equivalent erosional surface provide a good natural analog of reworking; in this case, the reworking associated with late Miocene and Pliocene erosion of the North American Cordillera (Fig. 3.16). The reworking of sediments by proximal erosion and distal deposition is also offered as a possible mechanism for the regional distribution of late-Eocene to Pliocene gravels in the Alberta Basin (Leckie and Smith, 1992).

The change in orogen state is accompanied by increases in the rates of transverse and longitudinal progradation and basin filling (Figs. 3.13, 3.14). These rate increases are a consequence of a fall in relative sea level and tilting of the basin accompanying isostatic rebound. Progradation proceeds without erosion of the coastal zone (①, D-D', Fig. 3.17) because sediment flux to the seaway extends the alluvial plain faster than sea level falls. Sediment flux is greater than the minimum required for progradation because denudation is localized to the orogen and upper alluvial plain, while isostatic compensation for the change in load is distributed across the basin (Fig. 3.13). In addition, tilting of the basin with isostatic rebound brings fluvial profiles on the alluvial plain toward grade with a consequent decrease in sedimentation rate and river-power facies in the distal basin (⑦, Fig. 3.14). As rivers approach grade, a greater percentage of sediment from the orogen is transported across the alluvial plain to the coast, enhancing progradation. Therefore, a relative fall in sea level is likely to cause fluvial incision of the coastal zone only when the basin margin topography is steep and/or sediment flux to the coast is low.

Sedimentation at the end of the 6-12 My sequence is characterized by lower river-power facies and rapid progradation. As erosion and rebound decrease with time, sedimentation rates reflect the decrease in sediment supply from the orogen and rivers approaching grade on the alluvial plain. The erosional surface proximal to the orogen and the 'condensed' alluvial section in the distal basin form much of the sequence

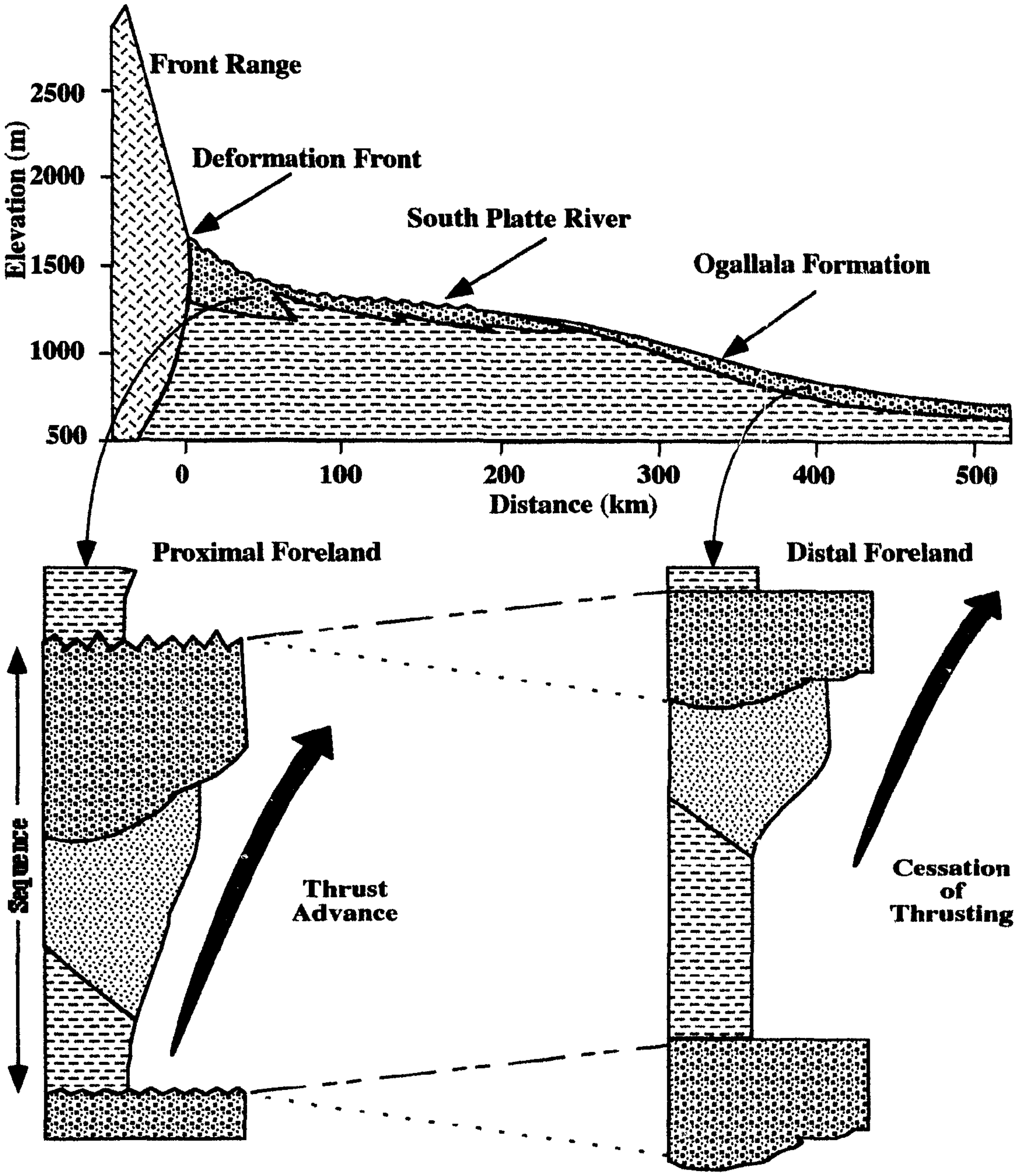

Figure 3.16. This figure shows the conceptual 'two-phase stratigraphic model for foreland sequences' as applied by Heller *et al* (1988) to the Ogallala Fm. They propose that while coarsening upwards cycles proximal to the orogen form during periods of orgenic tectonism (lower left), coarsening upwards cycles in the distal basin form during periods in waning orogenic tectonism (lower right). Coarse clastics in the distal basin come from exhumation of the orogen and reworking of coarse clastics deposited adjacent to the orogen during the last phase of orogenic tectonism. Modified after Heller *et al* (1988).

boundary. These results are consistent with the conceptual model of Heller *et al.* (1988) and numerical model results of Flemings and Jordan (1990).

MT4 Evolution Between 12 and 15 My

With the onset of tectonic convergence at 12 My, isostatic compensation of the growing orogen causes subsidence in the basin (⑧, Fig. 3.14). In the subaerial portion of the basin, low river-power facies retrograde with the reduction in surface slope. Decreasing slopes on the alluvial plain adjacent to increasing slopes on the orogen focus the change in river slope near the deformation front. The result is an increase in river disequilibrium and sedimentation rate proximal to the orogen. This result is consistent with those of Flemings and Jordan (1990), because both results are primarily dependent on the change in surface slope. It is also consistent with model results of Paola *et al.* (1992), who show that increased rates of basin subsidence with constant sediment flux result in retrogradation of the higher energy facies.

In MT4, continued orogen growth and increasing orogen-to-basin sediment flux result in the growth of the alluvial plain and progradation of moderate river-power facies into the basin (⑨, Fig. 3.14). Progradation of higher river-power facies occurs because sediment flux from the orogen dominates over the effects of basin subsidence, consistent with model results of Paola *et al.* (1992). Progradation is enhanced by increasing precipitation rates on the alluvial plain, similar to MT1. The increase in precipitation causes an increase in discharge, thus increasing fluvial carrying capacity; this increase in carrying capacity opposes the effects of decreasing surface slope. However, the rapid convergence of time lines away from the orogen shows that in distal parts of the basin the effects of subsidence and orogen growth on surface slope dominate over the effects of changes in precipitation. Therefore the results of increased tectonic convergence seen in MT4 are similar to those found by Flemings and Jordan (1990).

Sediments deposited adjacent to the peripheral bulge during the quiescent period are uplifted and eroded, as isostatic compensation for the growing orogenic load causes the bulge to migrate toward the orogen (❿, Fig. 3.14). Peripheral bulge uplift is followed by a decrease in elevation and migration away from the orogen with growth of the orogen and alluvial plain, consistent with the findings of Flemings and Jordan (1989). The extent to which erosional surfaces created by peripheral bulge migration are preserved varies significantly along strike (Fig. 3.15). This variation is particularly evident in longitudinal section D-D' (②, Fig. 3.17) which shows how the erosional surface associated with flexural upwarp ends down dip in alluvial sedimentation. Relative sea-level change along the basin axis caused by isostatic compensation for the growing orogenic and sedimentary loads causes retrogradation of alluvial facies and alluvial onlap of the erosional surface (D-D', Fig. 3.17). Erosion of basin margin sediments and alluvial onlap are the last phase in the creation of the sequence boundary encasing the 6-12 My constructive/destructive orogenic cycle. This sequence boundary comprises an unconformity proximal to the orogen overlain by a flooding surface in some areas, either a flooding surface or a shift to deeper-water sedimentation near the basin axis synchronous with erosion of the distal basin margin, and an unconformity on the distal basin margin.

MT5 - Response Times of an Orogen/Foreland Basin System

The response times of an orogen/foreland basin system are estimated using the retro-foreland orogen-to-basin sediment flux $Q_{S(retro)}$ (Fig. 3.18). Convergence velocity is varied 'on/off' as a step function, with 3 My intervals between changes in v_T.

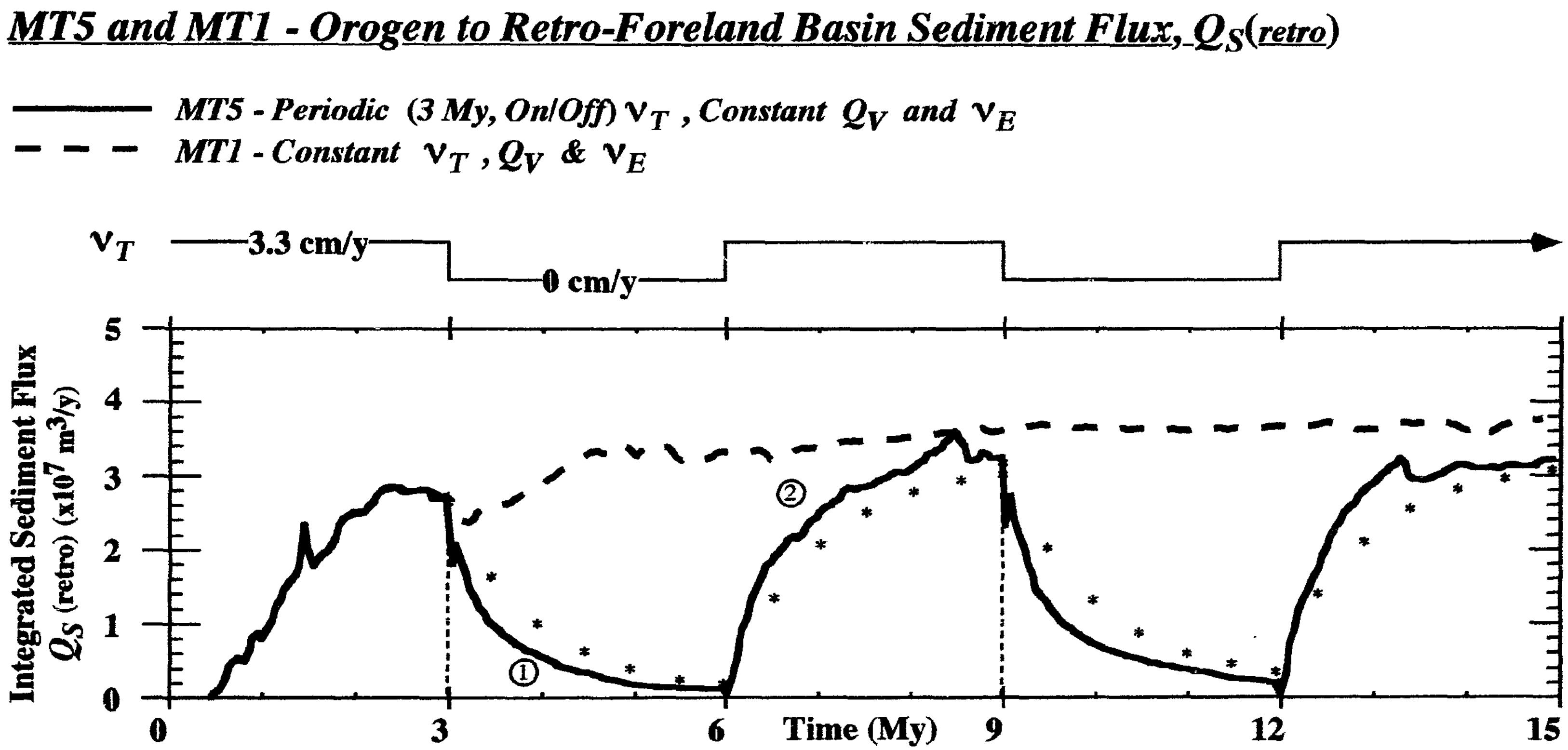

Figure 3.18. The MT5 retro-foreland orogen-to-basin sediment flux ($Q_{S(retro)}$) characterizes the orogen/foreland basin system response to changes between constructive and destructive orogen states with changes in v_T. MT1 characterizes the response of a system with constant v_T, Q_V and v_E. Asterisks show an exponential curve with a 0.5 My response time.

MT5, MT5a and MT5b, like MT1, use a parallel convergent-margin initial condition so that $Q_S(retro)$ integrated along the entire retro-wedge can be used to characterize the response of the system to changes in v_T.

A comparison of MT5 with MT1 illustrates the effect of a step function variation in v_T on $Q_S(retro)$ (Fig. 3.18). During the initial period of tectonic convergence, $Q_S(retro)$, MT5 and MT1 are effectively the same. In MT5, the change from tectonic convergence to quiescence at 3 My and 9 My causes $Q_S(retro)$ to decrease in an exponential manner from one equilibrium toward a new equilibrium approaching zero until tectonic convergence resumes at 6 My and 12 My, respectively (①, Fig. 3.18). The decrease in $Q_S(retro)$ is a consequence of decreasing orogen elevation, precipitation and denudation rates with time, as discussed for model MT4 between 9 My and 12 My. The character of the decrease in $Q_S(retro)$ in MT5 implies that the orogen/foreland basin system evolves at a rate proportional to the disequilibrium between actual and graded fluvial profiles, because fluvial erosion is the dominant mechanism of erosion in MT5. The exponential character of the decrease suggests the relationship between the disequilibrium and the rate of change is approximately linear; therefore,

$$\frac{dQ_S(retro)}{dt} \approx \frac{-1}{\tau}\left(Q_S(retro) - Q_S(equilibrium)\right) \qquad \text{(Eq. 3.1)}$$

where τ is the response time and $Q_S(equilibrium)$ is the integrated sediment flux from the retro-wedge when all rivers maintain a graded dynamic equilibrium. Kooi and Beaumont (submitted) have shown that in a fluvial transport model identical to the one used here, the graded condition is equivalent to that of a river carrying at capacity. The response time, τ, is the time required to reduce the initial disequilibrium by a factor of $1/e$. Kooi and Beaumont (submitted) also show that τ for each uniform segment, Δl, of any river is

$$\tau_{\Delta l} = \frac{\Delta l \times l_f}{K_f q_r} \qquad \text{(Eq. 3.2)}$$

where l_f is the erosional length scale, K_f is the fluvial transport coefficient and q_r is the local discharge.

Therefore two main factors influence τ, 1) the disequilibrium in fluvial profile introduced by the change in orogen topography with the step function in V_T (tectonics), and 2) the separate interaction among orographic precipitation (ergo q_r), topography and tectonics. Two model experiments are required to separate these effects into their respective tectonic (τ_T) and climatic (τ_C) model response times. Model MT5 gives a composite or mixed response time (Fig. 3.18), while in MT5a precipitation is constant after 3 My so that the measured response time is solely a measure of the tectonic response. Separation of τ_C which requires a model where a tectonic response to a change in climate is minimized, is discussed in Chapter 5.

Comparison of models with orographically controlled precipitation and uniform precipitation illustrates the difference a change in precipitation with time has on the response of Q_S(retro) to a change in tectonics (MT5, MT5a, Fig. 3.19). In models MT5 and MT5a at 3 My there is an instantaneous decrease in V_T to 0 cm/y causing a change from constructive to destructive orogen state. In model MT5a the constant precipitation rate causes the total retro-wedge fluvial discharge to remain relatively constant. Q_S(retro) shows an exponential decrease as elevation and surface slopes decrease with erosion of the orogen (Fig. 3.20). The tectonic response time, τ_T, is ~700 ky. In contrast, the Q_S(retro) for MT5 initially decreases more rapidly than MT5a (Fig. 3.19). This difference occurs because in MT5 the decrease in Q_S(retro) caused by decreasing surface slopes is compounded by the reduction fluvial discharge as precipitation rate decreases with

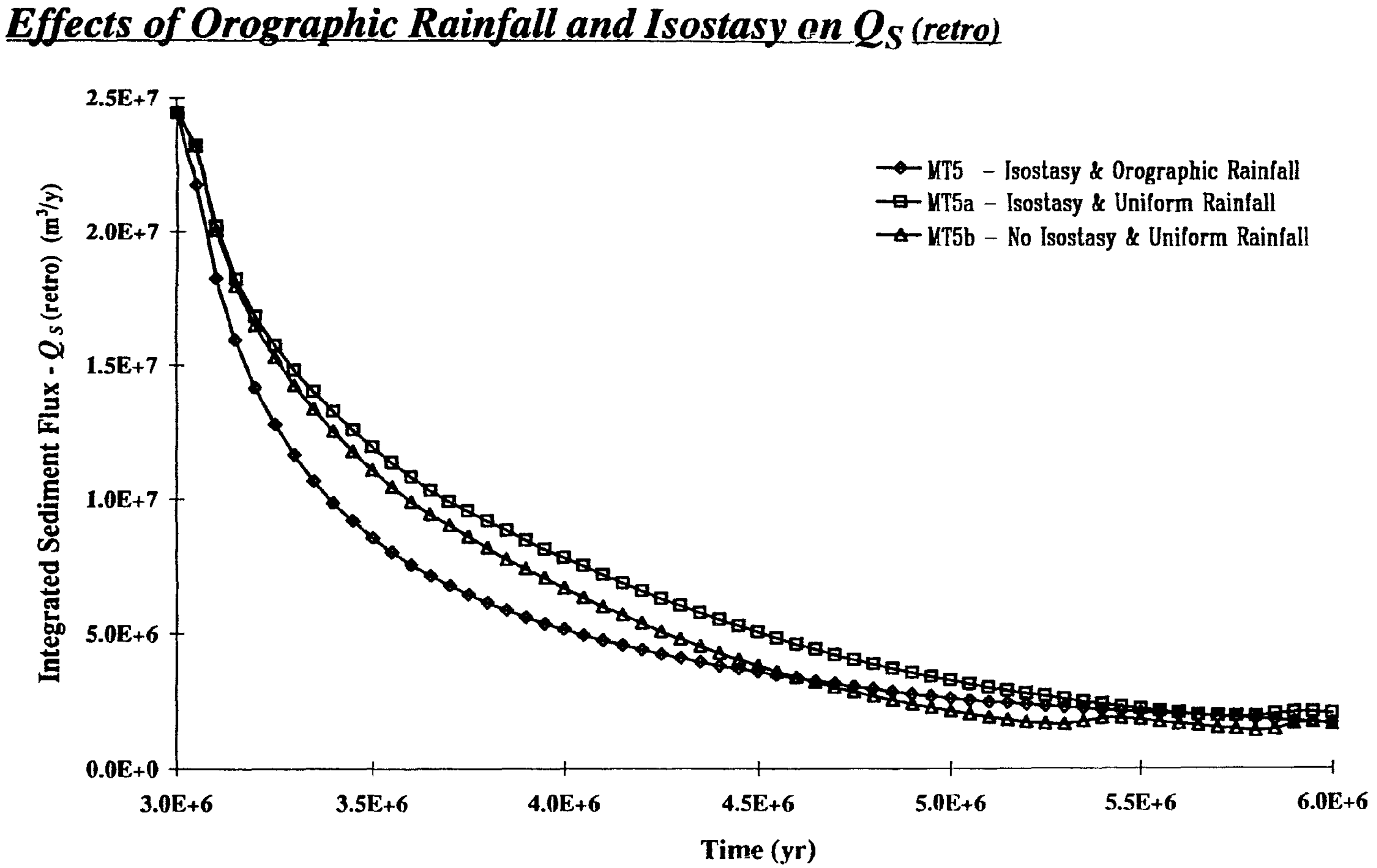

Figure 3.19 Comparison of orogen-to-basin sediment flux between models with isostasy and orographically controlled rainfall (MT5), isostasy and uniform rainfall (MT5a), and no isostasy and uniform rainfall (MT5b).

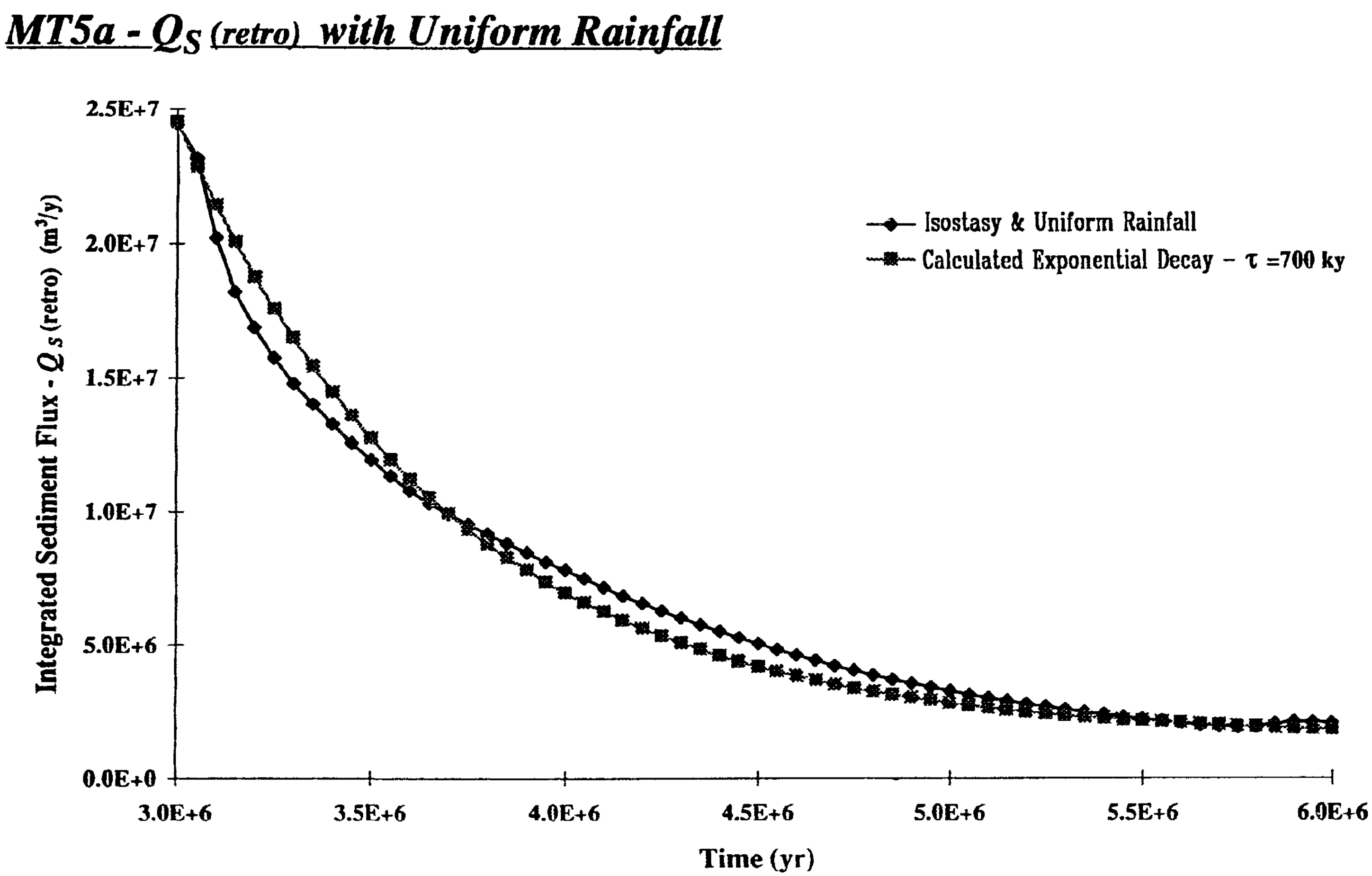

Figure 3.20 Comparison of orogen-to-basin sediment flux under conditions of uniform rainfall to a calculated exponential decline with a response time of 700ky.

MT6 at 15 My, Enlarged Retro-Foreland Basin - Periodic v_T, Constant Q_V and v_E

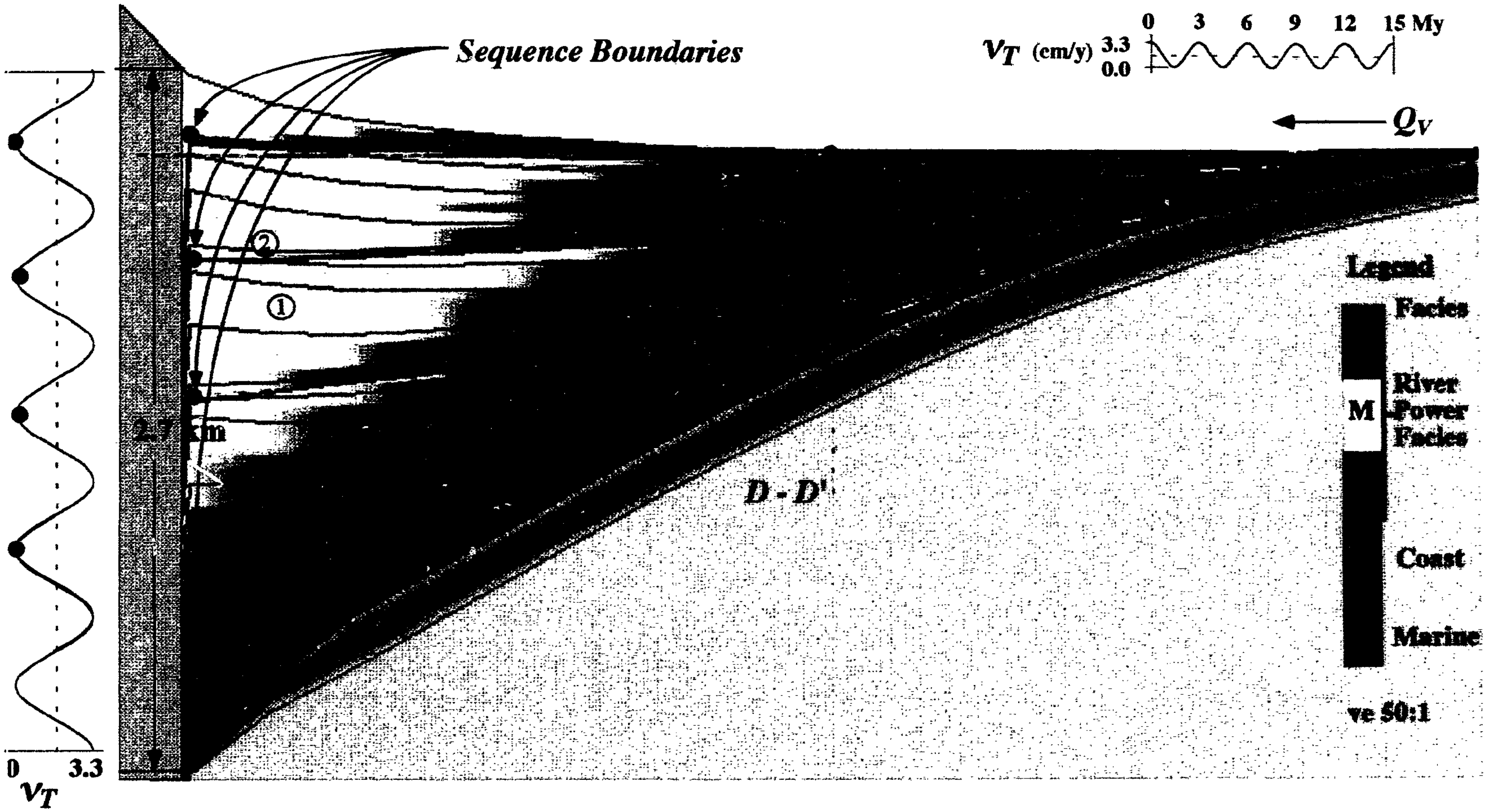

Figure 3.23. Stacked sequences of MT5 retro-foreland basin along A-A' (Fig. 3.20) with sedimentary facies (colour) and time-line (black) geometry. Sequence boundaries comprise erosional surfaces proximal to the orogen, low sedimentation rates and flooding surfaces in the medial basin, and erosional surfaces adjacent to the peripheral bulge. Sequence boundaries are coeval with times of minimum v_T.

MT7 at 15 My - Periodic v_T, Constant Q_V and v_E

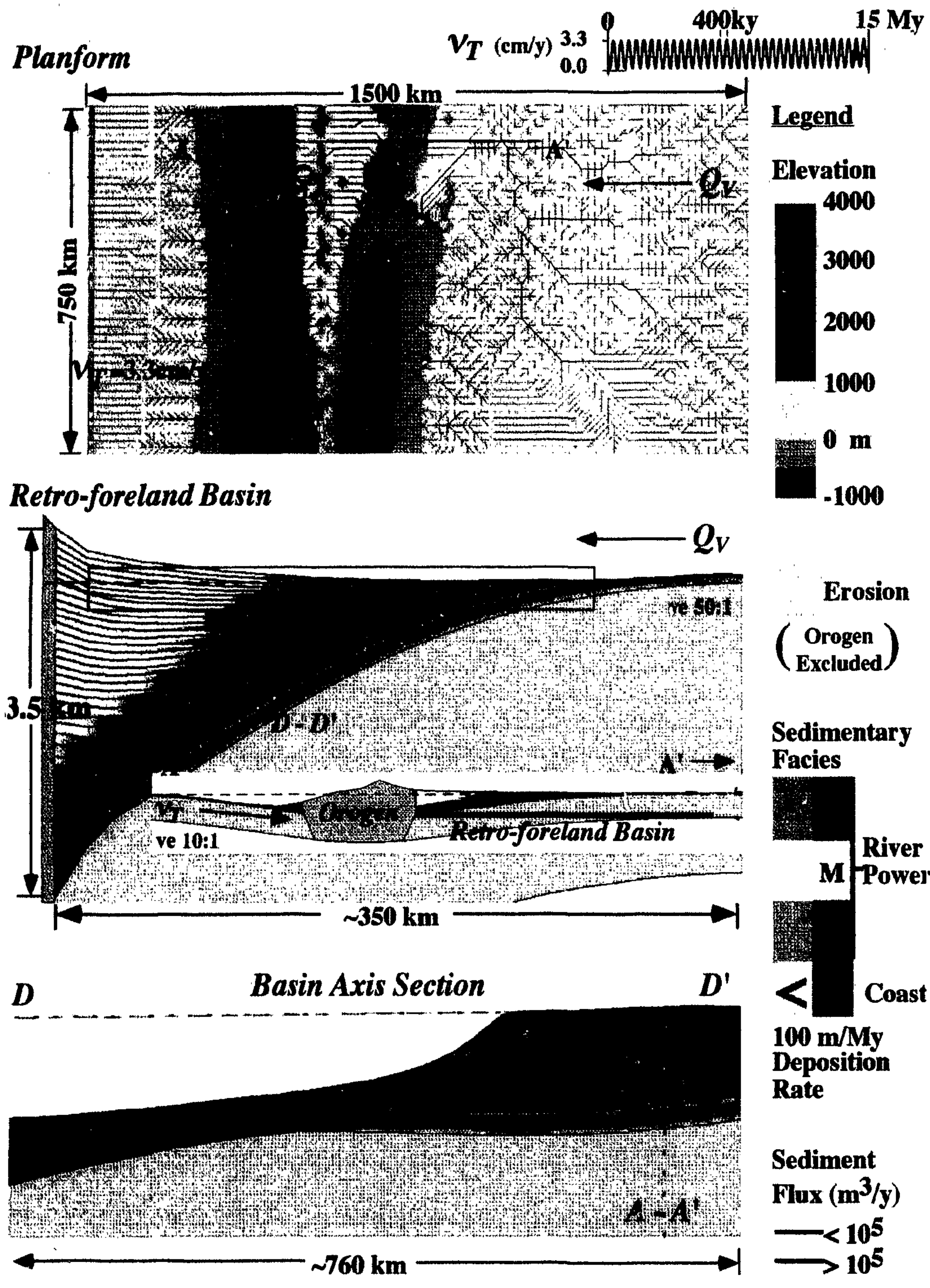

Figure 3.27. MT7 shows in planform, transverse sections (regional and retro-foreland basin) and longitudinal section (D-D'), the development of an orogen/foreland basin system with 400 ky periodicity in orogen tectonics. MT7, unlike MT6, is characterized by parasequences, instead of stacked lower order sequences (see area in box enlarged, Fig. 3.28).

unreasonable when compared with small, modern orogens like the Southern Alps, Irian Jaya/Papua New Guinea, or Taiwan (Schwab, 1976; Dahlen and Suppe, 1988). Further, sedimentation rates in the basin are on the order of 1 mm/y or less, while surface slopes on the orogen, on the alluvial plain, along the subaerial basin axis and in the marine environment are comparable with similar slopes in nature. The difference in response times is caused by the difference in choice of K_f. Kooi and Beaumont use a lower K_f which make their model rivers less efficient at eroding and transporting material away from the orogen.

3.3.2 Effect of Orogen/Foreland Basin Response Time on Stratigraphy

Model results for MT6 and MT7 use a sinusoidal fluctuation in v_T and show how the stratigraphic response of a retro-foreland basin differs when the period of fluctuation (3 My) is much greater than response times τ_T and τ_C, and when the period of fluctuation (400 ky) is of the same order as the response times. A period of 3 My is used for reasons previously discussed; a 400 ky period is used because it is on the order of the shorter climatic response time (τ_C). Furthermore the results discussed below can be compared with the effects of 400 ky periodicity in climate fluctuations and eustasy in subsequent chapters.

MT6 - 3 My Sinusoidal Tectonic Periodicity

Figure 3.22 shows the effect of a 3 My sinusoidal fluctuation in v_T on retro-foreland basin development after 15 My in planform, transverse and axial sections. The retro-foreland basin shows stacked low-order sequences, characterized by marine sedimentation that becomes progressively alluvial (①, Figs. 3.22, 3.23); therefore, the energy of the depositional environments increases upward in each sequence. In general, surface elevation. The difference also indicates that the composite response is largely governed by climate change initially, and that the climate response time (τ_C) is shorter than the tectonic response time. The best fit of an exponential curve to Q_S(retro) has a response time, τ_S, of ~500 ky (①, ②, Fig. 3.18), 200 ky shorter than τ_T. The composite response of Q_S(retro) does not show an exponential decrease (Fig. 3.18) because when discharge varies with time the change in Q_S with time becomes non-linear (Eqs. 3.1, 3.2).

Response time is also affected by isostasy (Kooi and Beaumont, submitted). Isostasy increases the response time by counteracting the effects of erosion on surface relief. Kooi and Beaumont (submitted) note that τ scales by a factor of $1/(1-\varphi)$, where φ is the constant of proportionality for local isostatic compensation (i.e., φ is the ratio of the density of eroded material, ρc, to mantle density, ρm). If the model used local isostatic compensation instead of flexural compensation this factor should have a value of ~4.71, given φ = 2.6 kg/m3/3.3 kg/m3 (Table 2.1). Models with and without flexural isostatic compensation are used to illustrate the effect of isostasy on response time; MT5b is the same as MT5a except it does not include isostasy. In MT5b, between 3 and 6 My, Q_S(retro) decreases exponentially similar to MT5a; however τ in MT5b is ~600 ky, ~100 ky shorter than the model with isostasy (Figs. 3.20, 3.21). Therefore, isostasy increases the response time in MT5a relative to MT5b by a factor of ~1.17. This factor is much less than 4.71 (local compensation) indicating flexural isostasy in these models has a minor effect on response time relative to the effect a model with local isostatic compensation would have.

The response times of ~700 ky and ~600 ky in MT5a and MT5b respectively are short in comparison with the response times of Kooi and Beaumont (submitted). In the MT5 suite of models, erosion rates are on the order of 1 mm/yr, which is not

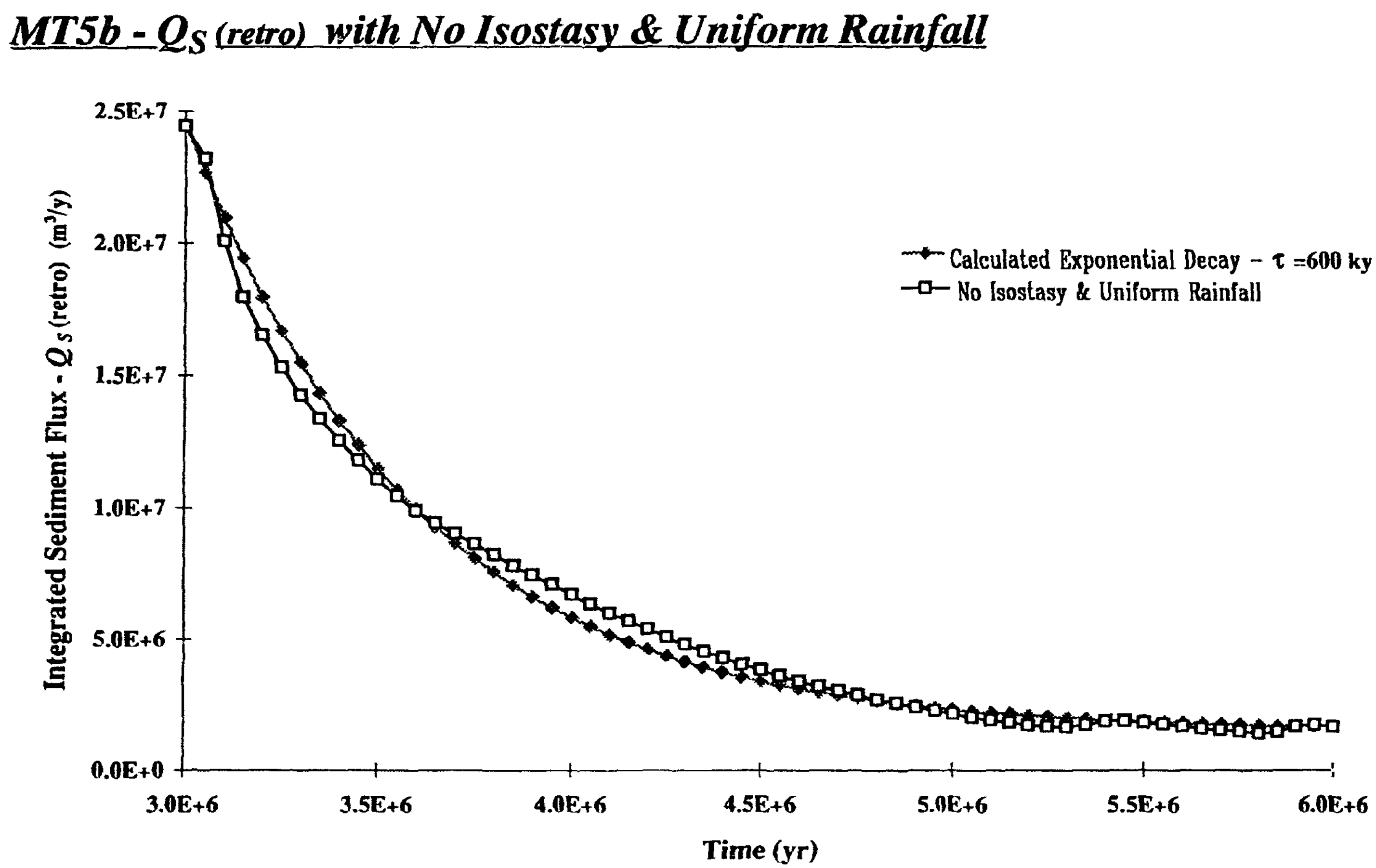

Figure 3.21 Comparison of orogen-to-basin sediment flux under conditions of no isostasy and uniform rainfall to a calculated exponential decline with a response time of 600ky.

unreasonable when compared with small, modern orogens like the Southern Alps, Irian Jaya/Papua New Guinea, or Taiwan (Schwab, 1976; Dahlen and Suppe, 1988). Further, sedimentation rates in the basin are on the order of 1 mm/y or less, while surface slopes on the orogen, on the alluvial plain, along the subaerial basin axis and in the marine environment are comparable with similar slopes in nature. The difference in response times is caused by the difference in choice of K_f. Kooi and Beaumont use a lower K_f which make their model rivers less efficient at eroding and transporting material away from the orogen.

3.3.2 Effect of Orogen/Foreland Basin Response Time on Stratigraphy

Model results for MT6 and MT7 use a sinusoidal fluctuation in v_T and show how the stratigraphic response of a retro-foreland basin differs when the period of fluctuation (3 My) is much greater than response times τ_T and τ_C, and when the period of fluctuation (400 ky) is of the same order as the response times. A period of 3 My is used for reasons previously discussed; a 400 ky period is used because it is on the order of the shorter climatic response time (τ_C). Furthermore the results discussed below can be compared with the effects of 400 ky periodicity in climate fluctuations and eustasy in subsequent chapters.

MT6 - 3 My Sinusoidal Tectonic Periodicity

Figure 3.22 shows the effect of a 3 My sinusoidal fluctuation in v_T on retro-foreland basin development after 15 My in planform, transverse and axial sections. The retro-foreland basin shows stacked low-order sequences, characterized by marine sedimentation that becomes progressively alluvial (①, Figs. 3.22, 3.23); therefore, the energy of the depositional environments increases upward in each sequence. In general,

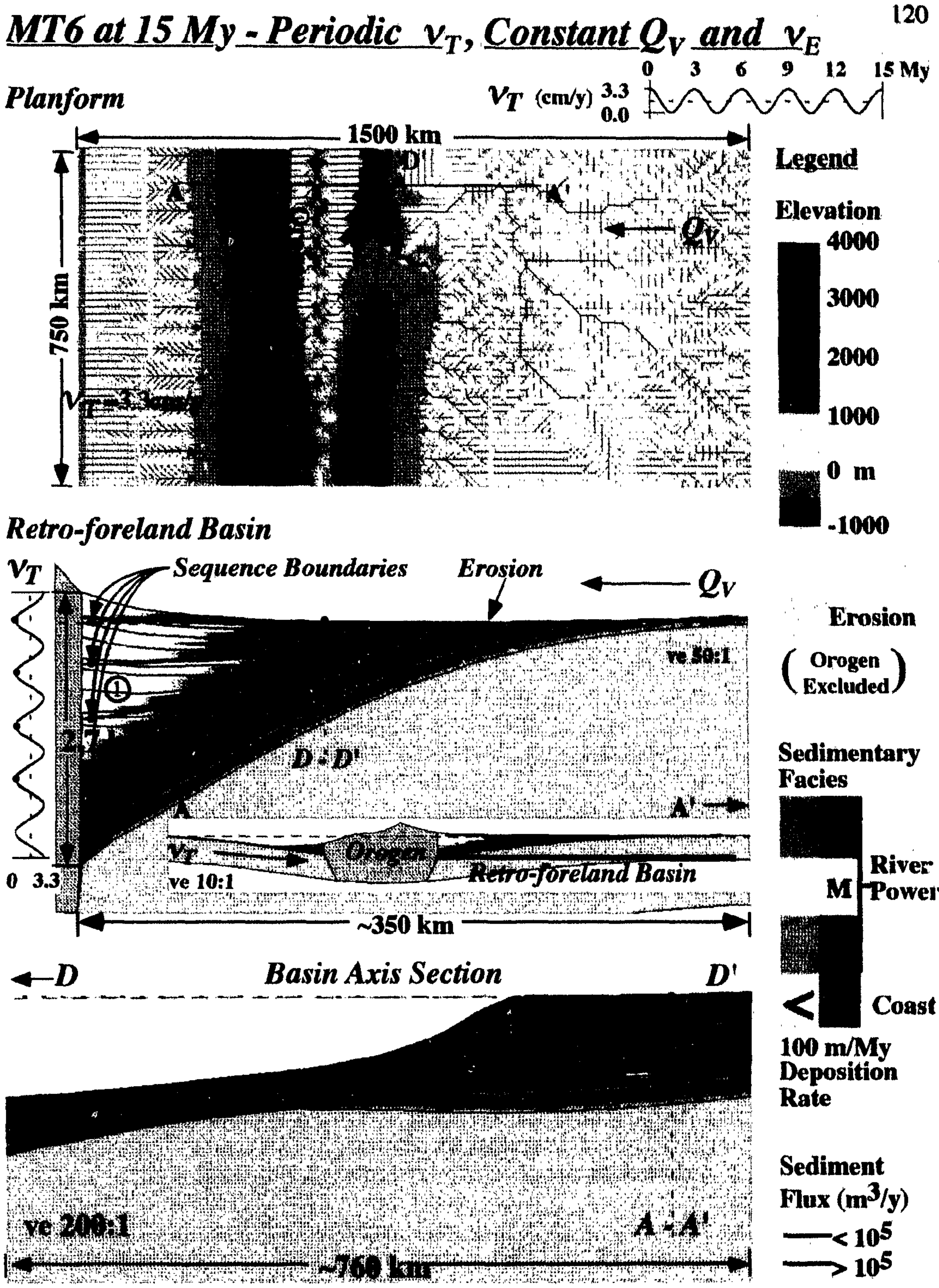

Figure 3.22. MT6 is shown in planform, transverse section (regional A-A' and retro-foreland basin) and longitudinal section (D-D') at 15 My. MT6 is characterized by stacked sequences. Sequence boundaries are in phase (coeval) with times of minimum v_T (dots).

each sequence is dominated by more alluvial sediment as the basin fills. Sequence boundaries comprise unconformities near the orogen, disconformities near the basin axis, and unconformities along the distal basin margin, all of which may be immediately overlain by a flooding surface. These sequences are similar to the sedimentary cycles created by the step function fluctuations in v_T (MT4, Figs. 3.13-3.15, 3.17).

The two-phase sequence boundaries and maximum progradation in MT6 are in phase with times of tectonic quiescence (② and ③, Fig. 3.23). This correlation is consistent with Kooi and Beaumont (submitted), who note that when the period of tectonic change is very long relative to the response time of the system, the times of maximum and minimum sediment yield are almost in phase with periods of maximum and minimum tectonic uplift, respectively; that is, the response of the system is in phase with the forcing function. In addition, stratigraphic markers of tectonic periodicity in the present model such as erosion proximal to the orogen, the change between moderate and low river-power facies, and coastal facies are in phase with this periodicity across the entire basin. This correlation indicates that the effects of accelerating and decelerating orogen growth are experienced synchronously across the basin.

A natural example of stacked sequences is observed in the Alberta Foreland Basin (Fig. 3.24) (Leckie and Smith, 1992; Stockmal *et al.*, 1992). While these Alberta sequences occur on time scales three to five times longer than those in MT6, the fundamental principles are interpreted to be the same. In general, the facies in each sequence progress from marine to non-marine, sequences become progressively alluvial with basin filling, and sequence boundaries are unconformities and/or coeval flooding surfaces (Leckie and Smith, 1992; Stockmal *et al.*, 1992). Episodic growth of the Cordillera is suggested as the primary mechanism responsible for the development of

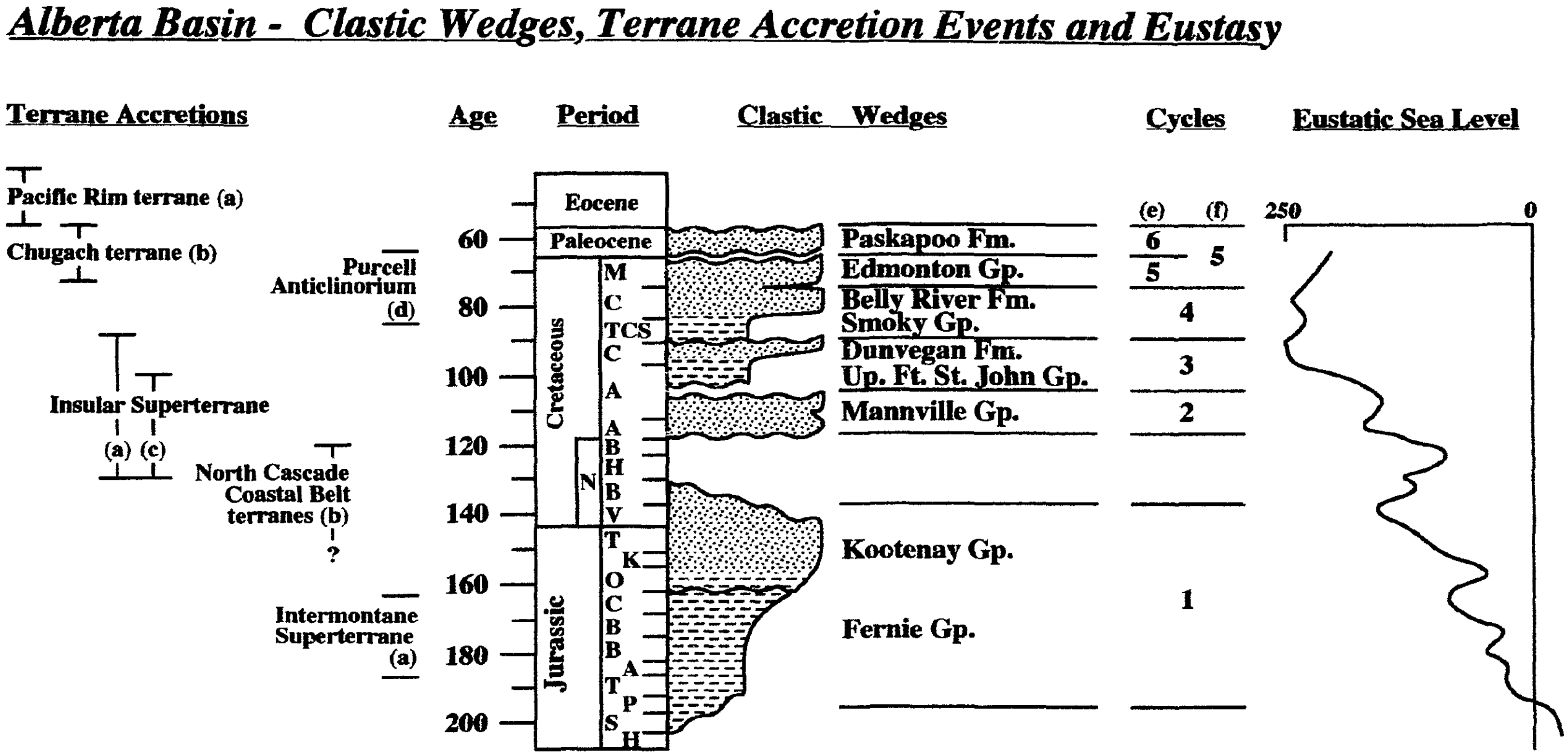

Figure 3.24. Modified after Stockmal *et al* (1992, e), this figure identifies six "first order" clastic wedges (cycles) of the Alberta Foreland Basin as a function of time. Leckie and Smith (1992) (f) are in agreement with Stockmal *et al* (1992) (e), except Leckie and Smith place the Paskapoo Fm and Edmonton Gp in a single cycle. The sea-level curve is from Haq *et al* (1987); "times of accretion of allochthonous terranes taken from: (a) Galbrielse and Yorath (1989); (b) Monger *et al* (in press); and (c) Thorkelson and Smith (1989)" (Stockmal *et al*, 1992); timing of the Purcell Anticlinorium development is from Price (1981); and in the time scale "absolute ages and Jurassic and Cretaceous age names, abbreviated to single letters, from DNAG timescale: Palmer, 1983" (Stockmal *et al*, 1992).

these sequences (Fig. 3.24) (Fermor and Moffat, 1992; Leckie and Smith, 1992; Stockmal *et al.*, 1992). Stockmal *et al.* (1992) note that the timing of accretionary 'docking' events coincides with sequence (cycle) development. They hypothesize that "tectonic loading of the edge of the North American continent by cordilleran over-thrust sheets, causing flexural subsidence of the Alberta basin, should be related in some manner to terrane accretion events and/or plate boundary dynamics." In MT6 episodic orogen growth is caused by periodic changes in convergence velocity. These changes have the same effect as spatial changes in pro-lithospheric thickness (i.e., micro-continents) because the rate of material accretion to the model orogen, per unit length along strike, is caused by both accretion as the product of convergence velocity and pro-lithospheric thickness, and accretion caused by orogen growth (Sec. 2.2.2).

Cycle 2 in the Middle Cretaceous (Barremian-Aptian) is caused by a transgressive/regressive cycle (Leckie and Smith, 1992). Conglomerates and other alluvial fan deposits at the base of the sequence reflect sedimentation associated with a period of tectonic quiescence (A, Fig. 3.25; Leckie and Smith, 1992), similar to the conceptual model of Heller *et al.* (1988) . Transgression of the Boreal and Moosebar seas proceeded from the north with progressive but intermittent flooding of the foreland basin (B and C, Fig. 3.25). This transgression has superimposed upon it higher frequency transgressive/regressive cycles that may be caused by eustasy (Leckie and Smith, 1992). The higher-order cycles are characterized by shoreward-stepping progradational/ retrogradational cycles. Timing of the low-order transgression overlaps with accretion of the North Cascade, Coastal Belt and Insular Superterrane (Stockmal *et al.*, 1992). Following the incursion of the Moosebar Sea, a thick clastic wedge prograded northward across the foreland basin forming extensive flood plain deposits including stacked

Alberta Foreland Basin, Cycle 2 (Barremian to Aptian)

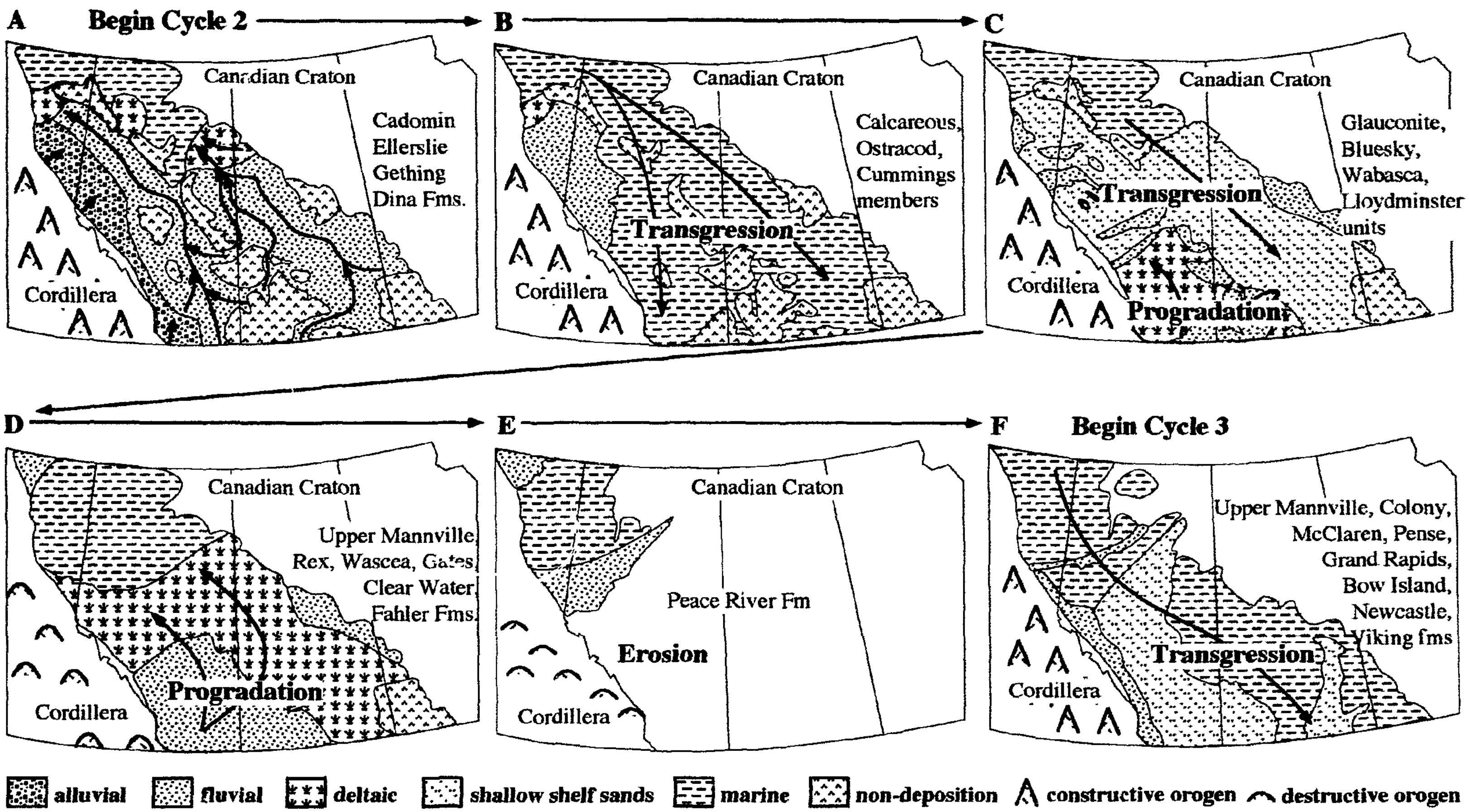

Figure 3.25. Modified after Leckie and Smith (1992), this figure shows paleographic maps for Cycle 2. Maps A to F decrease in age from Barremian to Aptian, and show the change in paleography that may be associated with the change from constructive (B - C) to destructive (D - E) orogen states.

shoreline sandstones and conglomerates (D, Fig. 3.25). Higher-order progradational/ retrogradational cycles are superimposed on the lower-order regression (Leckie and Smith, 1992). Whether the regression is related to an increased sediment supply from the orogen, a eustatic sea-level fall, or a relative sea-level fall caused by net exhumation of the orogen remains unresolved. The transition from Cycle 2 to Cycle 3 is characterized by an erosional hiatus (E, Fig. 3.25) and/or abrupt facies changes caused by rapid Cycle 3 transgression (F, Fig. 3.25). Fermor and Moffat (1992) suggest that the unconformity, where observed in the present day Foothills, may represent a reduction in tectonic activity. Model MT6 results suggest that isostatic rebound associated with a change to a destructive orogen state is one mechanism for creating the erosional surface and abrupt facies changes which characterize the Cycle 2-Cycle 3 boundary.

Cycle 3, similar to Cycle 2, is thought by Plint *et al.* (1993) to be related to a tectonic episode in Cordilleran growth (Fig. 3.26). They suggest that the westerly thickening mudstone-dominated coastal-plain wedges of Cycle 3 may have been deposited during load-induced tilting of a formerly near-horizontal strandplain (Fig. 3.26). Thick shale successions conformably overlying the coastal plain wedges correspond to periods of increased tectonism and basin subsidence. By contrast, the extensive progradation of shoreface sandstones is associated with reduced rates of both basin subsidence (Fig. 3.26) (Plint *et al.*, 1993) and, probably, orogen growth.

MT7 - 400 ky Tectonic Periodicity

Model MT7 has the same parameter values as MT6, except that the period of fluctuation in v_T is 400 ky. Figure 3.27 shows MT7 results at 15 My in planform, transverse and axial sections. Time lines are at 400 ky intervals, coeval with times of

Alberta Basin - Dunvegan Formation and Smoky Group, Cycle 3

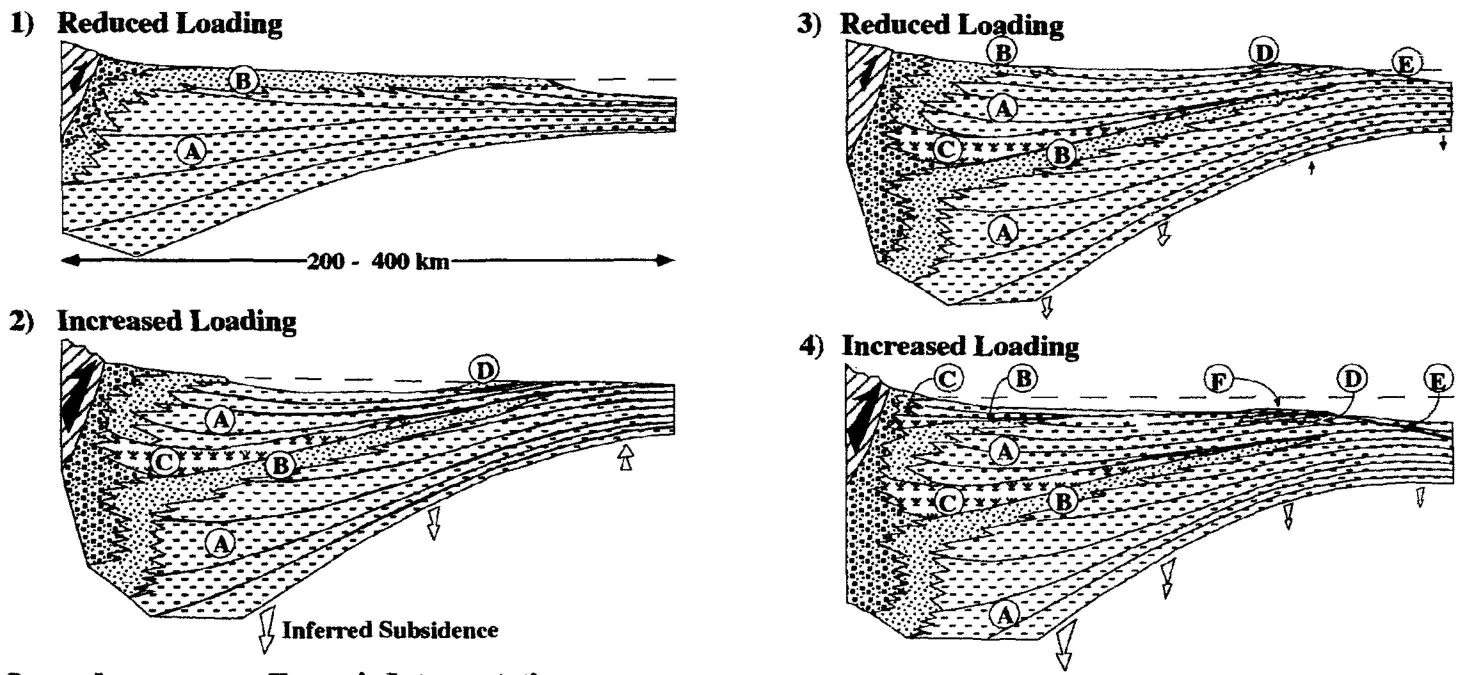

Legend

- alluvial clastics
- shoreface sands
- coastal plain mud
- marine mud
- oolitic ironstone
- orogen

Tectonic Interpretation

- (A) Increased loading, rapid subsidence; mudstone dominates
- (B) Reduced loading, slow subsidence; rapid progradation
- (C) Increased loading, backtilting; coastal plain aggrades before transgression
- (D) Continued rapid loading; subaerial erosion over rising forebulge
- (E) Reduced loading, forebulge subsidence, trangressive shoreface erosion
- (F) Increased loading, backtilting; new forebulge not yet significant

Rock Examples

- (A) Shaftesbury, Kaskapau, Muskiki
- (B) Dunvegan, Cardium, Marshybank
- (C) Musreau - Cardium, Unit G - Marshybank
- (D) Doe Creek & Pouce Coupe Sandstones
- (E) Cardium E5, E7 & sub-Bad Heart surfaces
- (F) Bad Heart

Figure 3.26. Modified after Plint (1993), this figure schematically shows the possible relationships between tectonism, flexural isostatic compensation, facies distribution, and erosional surfaces in Cycle 3. Circled letters in each diagram indicate a geological example and associated tectonic interpretation.

maximum v_T. Figure 3.28 shows an enlarged portion of A-A' (Fig. 3.27) with time lines at 50 ky intervals.

The effects of changes in the rate of tectonics are of limited extent, but evident throughout the basin. Truncation of time lines adjacent to the orogen indicates that regrading of fluvial systems when the orogen is in a destructive phase results in erosion of strata (①, Fig. 3.28), consistent with model results MT4 and MT6. In the central and distal basin, time lines have a cyclical pattern of a rapid increase in sedimentation rate after a v_T maximum, followed by a gradual decrease in sedimentation rate through the next v_T minimum until the next v_T maximum. Divergence of time lines toward the orogen and retrogradation of low river-power facies occur mainly with decreasing v_T (②, Fig. 3.28). The shift to more uniformly spaced time lines and progradation of moderate river-power facies occurs predominantly in association with increasing v_T (③, Fig. 3.28). These associations, by comparison with MT6, suggest that the MT7 facies distribution lags behind and is not in phase with the periodicity of v_T, consistent with the model results of Kooi and Beaumont (submitted). These authors demonstrate that a lag and decrease in sediment yield is expected because the fluvial incision rate cannot keep pace with the rate of tectonic uplift. In addition, while the stratigraphic characteristics of periodicity in orogenic tectonism (MT4, MT6) are present, they are suppressed. In MT7, for example, erosional surfaces (Fig. 3.28), progradational and retrogradational alluvial facies (Figs. 3.27, 3.28), and basin axis transgressive/regressive cycles (D-D', Fig. 3.27) are all present, similar to MT6, but are of limited extent (Figs. 3.22, 3.23). The length scale of these changes in stratigraphy is related to the period of fluctuation in tectonism, relative to the response time of the model.

MT7 at 15 My, Enlarged Retro-Foreland Basin - Periodic v_T, Constant Q_V and v_E

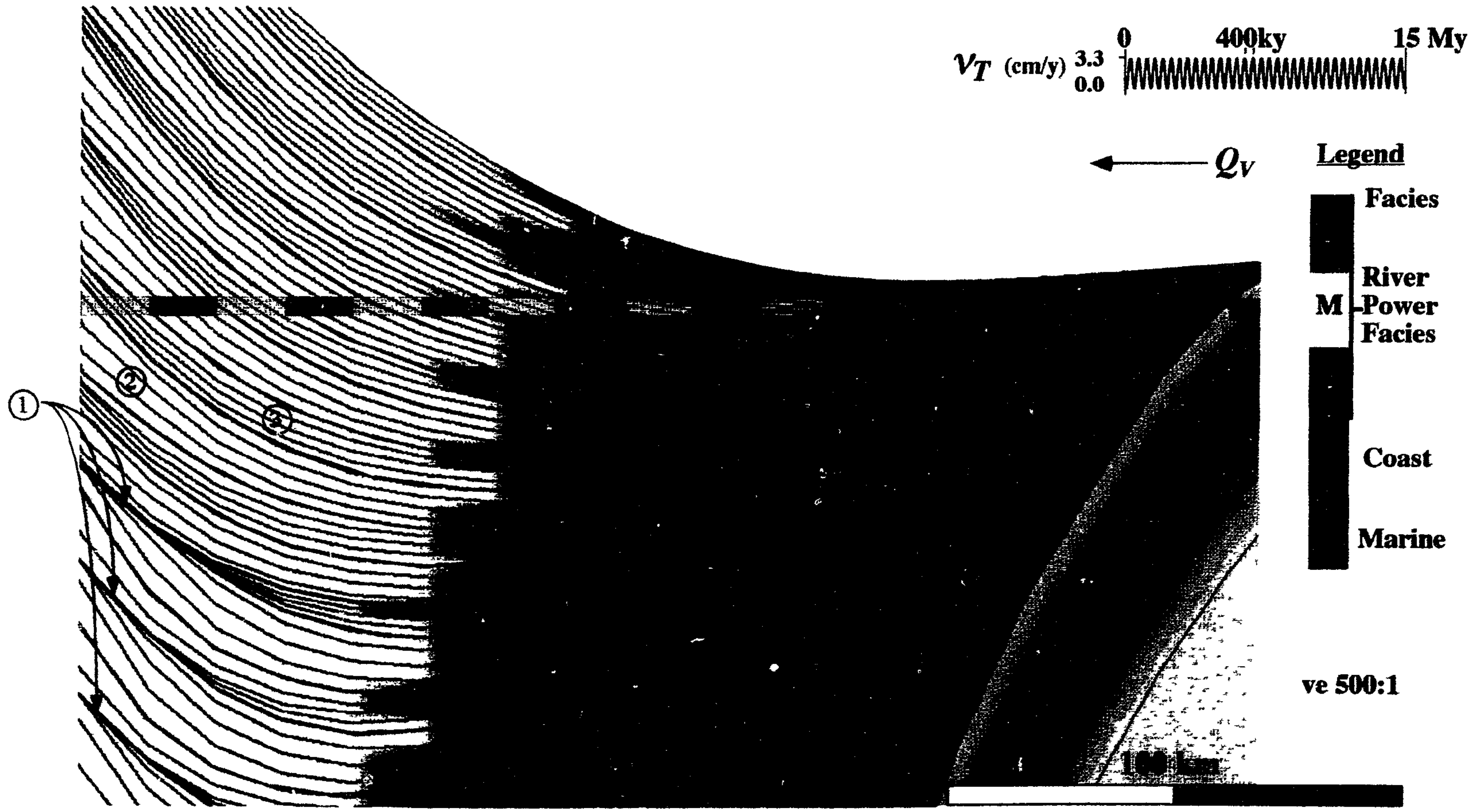

Figure 3.28. Enlargement of MT7 retro-foreland basin (box Fig. 3.27) shows develo‸ment of erosional surfaces and progradational/retrogradational cycles caused by 400 ky periodicity in v_T. Basin facies are in colour; time lines (black) are in **50 ky** intervals. Red lines are coeval with times of maximum v_T, while blue lines are coeval with times of minimum v_T.

When the period of fluctuation is on the order of or less than the minimum response time, the fluvial system is unable to maintain a dynamic equilibrium and basin stratigraphy reflects the change in a transient response of the fluvial system as it regrades toward a new equilibrium. The transient response is in essence a partial or intermediate response to the forcing function, which in MT7 is tectonics. The length scale is reduced because of the inability of the fluvial system to respond completely to the change in tectonics. Changes in stratigraphy are experienced across the entire basin because advective (fluvial) transport is continuous in the subaerial environment, and because fluvial transport controls sediment flux to the coast. As a consequence, in MT7 the extent of erosion adjacent to the orogen, retro and progradation of river-power facies on the alluvial plain, and regressive/transgressive cycles are all reduced by the decrease in tectonic periodicity. The result is that as the erosional surfaces identifying the sequence boundaries become poorly defined while the flooding surfaces remain evident, basin stratigraphy appears to show the development of stacked parasequences, rather than sequences as in MT6. Therefore, as periodicity in v_T (tectonism) changes from much greater to being on the same order of the system response times, local stratigraphic response changes from being evident over longer to shorter length scales, over the entire basin.

3.4 Summary

Model results from MT1 to MT7 demonstrate the influence of a number of factors on the development of foreland-basin stratigraphy, including basin setting, convergent margin geometry, transverse *vs.* longitudinal sediment transport, periodicity in orogenic tectonism, and orogen/foreland basin response time. The findings from the model results are summarized in the following points:

When the period of fluctuation is on the order of or less than the minimum response time, the fluvial system is unable to maintain a dynamic equilibrium and basin stratigraphy reflects the change in a transient response of the fluvial system as it regrades toward a new equilibrium. The transient response is in essence a partial or intermediate response to the forcing function, which in MT7 is tectonics. The length scale is reduced because of the inability of the fluvial system to respond completely to the change in tectonics. Changes in stratigraphy are experienced across the entire basin because advective (fluvial) transport is continuous in the subaerial environment, and because fluvial transport controls sediment flux to the coast. As a consequence, in MT7 the extent of erosion adjacent to the orogen, retro and progradation of river-power facies on the alluvial plain, and regressive/transgressive cycles are all reduced by the decrease in tectonic periodicity. The result is that as the erosional surfaces identifying the sequence boundaries become poorly defined while the flooding surfaces remain evident, basin stratigraphy appears to show the development of stacked parasequences, rather than sequences as in MT6. Therefore, as periodicity in ν_T (tectonism) changes from much greater to being on the same order of the system response times, local stratigraphic response changes from being evident over longer to shorter length scales, over the entire basin.

3.4 Summary

Model results from MT1 to MT7 demonstrate the influence of a number of factors on the development of foreland-basin stratigraphy, including basin setting, convergent margin geometry, transverse *vs.* longitudinal sediment transport, periodicity in orogenic tectonism, and orogen/foreland basin response time. The findings from the model results are summarized in the following points:

- Foreland basin setting can be characterized as either a pro-foreland or retro-foreland basin depending upon the position of the basin relative to the subducting plate (Dickinson, 1974; Johnson and Beaumont, 1995). Model results MT1 and MT2 show that asymmetry in the development of pro- and retro-foreland strata occurs primarily because of the higher rates of entrainment of strata into the orogen in the pro-foreland setting. This result is consistent with the generic effects of "higher thrust velocities" on foreland basin stratigraphy of Flemings and Jordan (1989); they did not identify the tectonic setting of the basin. Models MT1 and MT2 also show asymmetry in rainfall distribution, and therefore erosion rates, between the windward and leeward sides of the orogen. These effects are shown to either enhance or subdue the asymmetry created by the tectonic setting. For example, a windward (wetter) pro-foreland basin has greater orogen-to-basin sediment flux to counter the effect of entrainment on basin filling than a leeward (drier) pro-foreland basin where all other conditions are equal.

- Stratigraphic development of the model foreland basin records landform evolution and sediment transport in response to the interaction of tectonic, surface, climatic and isostatic processes. The effects of tectonics are greater proximal to the orogen, because of the focusing effect of orogen growth on rainfall distribution and the disequilibrium between actual and graded river profiles. Both rainfall and river disequilibrium increase with orogen growth and decrease with orogen wasting. Characteristics of an orogen/foreland basin system response to changes in orogen state are summarized in Table 3.1. These results are consistent with both field observations (*e.g.*, Burbank *et al.*, 1988, Burbank *et al.*, 1992) and the model results of Flemings and Jordan (1989, 1990) and Paola *et al.* (1992).

Change in Tectonic Convergence	Orogen		Alluvial Plain				Peripheral Bulge		
	Growth Rate $\pm$ ve	Q_S	Erosion	Sedimentation Rate Gradient	Sea Level	Facies $\Leftarrow / \Rightarrow$	Sea Level	Facies	Erosion
$v_T \Downarrow$	destructive	$\Downarrow$	Yes	$\Downarrow$	fall	$\Rightarrow$	fall	$\Rightarrow$	Yes
$v_T \Uparrow$	constructive	$\Uparrow$	No	$\Uparrow$ then $\Downarrow$	rise	$\Leftarrow$ then $\Rightarrow$	rise	$\Rightarrow$ then $\Leftarrow$	Yes

Table 3.1. Summary of stratigraphic characteristics reflecting change between constructive and destructive orogen states, with variations in the rate of tectonic convergence v_T. Arrows pointing to the right denote progradation, while arrows pointing the left denote retrogradation. Arrows pointing up indicate an increase and arrows pointing down indicate a decrease.

- Surface processes link the processes of orogen tectonics, isostasy, climate and eustasy to basin stratigraphy. Incorporating orographically controlled precipitation with fluvial transport in the model causes planform variability in precipitation and fluvial transport. It also causes rainfall distribution and drainage networks to evolve with model topography, the latter changing through the interaction of all model processes. Coupling of rainfall distribution with fluvial transport overcomes the problem of spatial and temporal variability in transport coefficients associated with using a purely diffusive approach to modelling surface processes. Models that use only diffusion do not account for temporal changes in precipitation and resultant changes in rates of erosion, sediment transport and deposition associated with orogen growth or wasting. Consequently, such models may initially overestimate the orogen-to-basin sediment flux and transport away from the orogen, progressively underestimate these fluxes as the orogen/foreland basin system grows, and may once again overestimate these fluxes when the orogen becomes extremely large.

- In nature, foreland basin stratigraphy typically preserves the relative effects of both transverse and longitudinal basin filling (*e.g.*, Taiwan, Covey, 1986; Molasse Foreland Basin, Homewood *et al.*, 1986; Ebro Basin, Marzo *et al.*, 1988; Alberta Basin, Leckie, 1989; Himalayan Foreland Basin, Burbank, 1992). Comparison of MT1 and MT3 model results illustrates that along-strike variation in orogenic tectonism is one mechanism which creates competition between transverse and longitudinal sediment transport in foreland basins. The comparison also illustrates the effect of longitudinal sediment transport on foreland basin filling. These two results suggest that sectional models, such as Flemings and Jordan (1989, 1990) and Sinclair *et al.* (1991) probably overestimate the rate of subaerial basin filling by not accounting for transport out of the plane of section. Furthermore, those models with marine basins, such as Peper (1993), probably underestimate the rate of seaway filling because they do not account for the ability of advective transport to allow sediment to bypass the alluvial plain and be deposited in the seaway.

- Model results from MT4 and MT6 show that periodicity in orogen state causes the formation of progradational/retrogradational cycles in basin facies, and that these cycles can be characterized as sequences. Each sequence is composed of a lower succession of sediments related to orogen growth and an upper succession related to orogen wasting. In general, there is an upward increase in alluvial sediment and river-power facies with continuous progradation in each sequence. The relative abundance of alluvial to marine sediment increases in each younger sequence with filling of the basin. Sequence boundaries are composed of an unconformity and/or flooding surface near the orogen, a flooding surface or shift to deep-water sedimentation near the basin axis and an unconformity along the distal basin margin. These results are consistent with the conceptual model of Heller *et al.* (1988) and the numerical model results of Flemings and Jordan (1990).

- The change to a constructive orogen state is characterized by an overall increase in both river-power facies and sedimentation rates proximal to the orogen and a relative rise in sea level in the basin. Sediments deposited on the lower alluvial plain record a decrease in river-power facies and sedimentation rate caused by a decrease in surface slope, and may record transgression of the lower alluvial plain. Coastal deposits adjacent to the peripheral bulge prograde while sediments previously deposited over the peripheral bulge are uplifted and incised. With orogen growth and increased orogen-to-basin sediment flux, the alluvial plain grows and facies prograde into the basin. Isostatic compensation of the growing orogen and alluvial plains causes the peripheral bulge to migrate away from the orogen, accompanied by retrogradation of sedimentary facies adjacent to the bulge. The change to a constructive orogen state is initially characterized by high-energy depositional environments on the margins of the basin and lower-energy depositional environments in its central portion, both in partial support of and in places contrary to Blair and Bilodeau (1988).

- The change to a destructive orogen state is characterized by a reduction in sedimentation rate, with possible erosion and reworking of sediments adjacent to the orogen and a relative fall in sea level. Sedimentation on the lower alluvial plain is characterized by decreasing river-power facies and sedimentation rate, as well as by rapid and extensive transverse and longitudinal progradation. In the models presented, sediment flux to the coast is sufficient to allow the rate of progradation to exceed the rate of sea-level fall, preventing the erosion of the shoreface.
- MT6 model results show that sequence development is in phase with the tectonic forcing when the period of change is much greater than the minimum response time of the system. MT7 model results show that when the period of change is on the order of the minimum response time of the system, stratigraphic changes caused by tectonic periodicity are less extensive and, as a consequence, parasequences rather than sequences are formed. In addition, there is a phase lag between tectonic forcing and stratigraphic changes. It is expected that as the period of tectonic pulses gets much shorter than the minimum response time of the system, the stratigraphic response becomes indistinguishable from an orogen/foreland basin system in a continuous constructive state. The results of MT6 and MT7 are consistent with the conclusions of Kooi and Beaumont (submitted) about system response. The

implication for interpretation of natural orogen/foreland basin systems is that the development of foreland basin stratigraphy may largely depend upon the time scale of tectonic activity in comparison with the response time of the system. This conclusion is consistent with those of Paola *et al.* (1992).

Chapter 4

Effects of Climate on Orogen/Foreland Systems

4.1 Introduction

Climate influences the development of orogen/foreland basin systems by affecting rates of erosion, sediment transport and deposition through variations in factors such as precipitation, temperature and the biosphere. The effect of precipitation on fluvial processes is investigated because these processes are a dominant mechanism of erosion and sediment distribution in most foreland basins (*e.g.*, Alberta Foreland Basin, Leckie and Smith, 1992; Ebro Foreland Basin, Spain, Marzo *et al.*, 1988; Himalaya Foreland Basin, Burbank, 1992; Magdalena Foreland Basin, Smith, 1986; Molasse Foreland Basin, Homewood *et al.*, 1986; North Slope Foreland Basin, Alaska, Bird and Molnaar, 1992). The coupling of climate with fluvial processes is strong in orogen/foreland basin systems because of the focusing effect of orogen topography on rainfall distribution (Barry and Chorley, 1971). Therefore, changes in rainfall distribution directly affect orogen growth rates and the stratigraphic development of foreland basins in a manner similar to changes in tectonics. However, the effects of climate change on foreland basin stratigraphy differ from those of tectonics in periodicity, magnitude, and spatial distribution.

In this study, 'climate' is limited to precipitation and wind, where wind is the prevailing direction and magnitude of vapour flux. Model topography and vapour flux are the principal controls on the temporal and spatial distribution of rainfall. This simplistic definition of climate excludes a wide range of considerations, including form of precipitation, evaporation, and freeze/thaw periodicity; as well as such related factors as glaciation, the groundwater prism and the chemical and mechanical contributions of vegetation. While the potential for much more sophisticated models exists, the 'climate' model used herein provides useful input at a level of sophistication which is complementary to other model processes in the integrated orogen/foreland basin model.

In nature, rainfall varies on time scales of seconds to millions of years and spatial scales of millimeters to thousands of kilometres (Harrison, 1991). For the model experiments, variations in vapour flux, Q_V, over temporal scales of orogenic tectonism (10^5-10^7 years) and spatial scales of the orogen and foreland basin (10^4-10^7 m) are relevant. Temporal variations in Q_V along a model boundary are part of each model's input. There are no feedbacks between Q_V and the effects of climate change; spatial variations in vapour flux ($Q_V(y)$) result from the effect of topography on the rate of precipitation. There is, however, a feedback between the development of topography and Q_V through its effect on fluvial discharge, which influences rates of fluvial erosion, sediment transportation and deposition.

The orographic effect of rainfall distribution as observed in modern orogens such as the central North American Cordillera (Fig. 4.1a) or the southern Andes (Fig. 4.1b) is simulated in the model by making precipitation dependent on Q_V, the upwind depletion of Q_V, and an elevation-dependent extraction efficiency. Precipitation changes downwind from the model boundary in proportion to the change in surface elevation (relative to an elevation of maximum precipitation) and depletion of the vapour flux (Sec. 2.4). As a consequence, orogen/foreland basin systems in the model have a wetter windward side and a drier leeward side, similar to modern orogens, although the decrease in precipitation across the orogen does not necessarily imply that the leeward foreland basins are characterized by 'dry' climatic conditions in an absolute sense. The relative effects of windward and leeward settings on the stratigraphic development of foreland

Orographically Controlled Rainfall Distributions

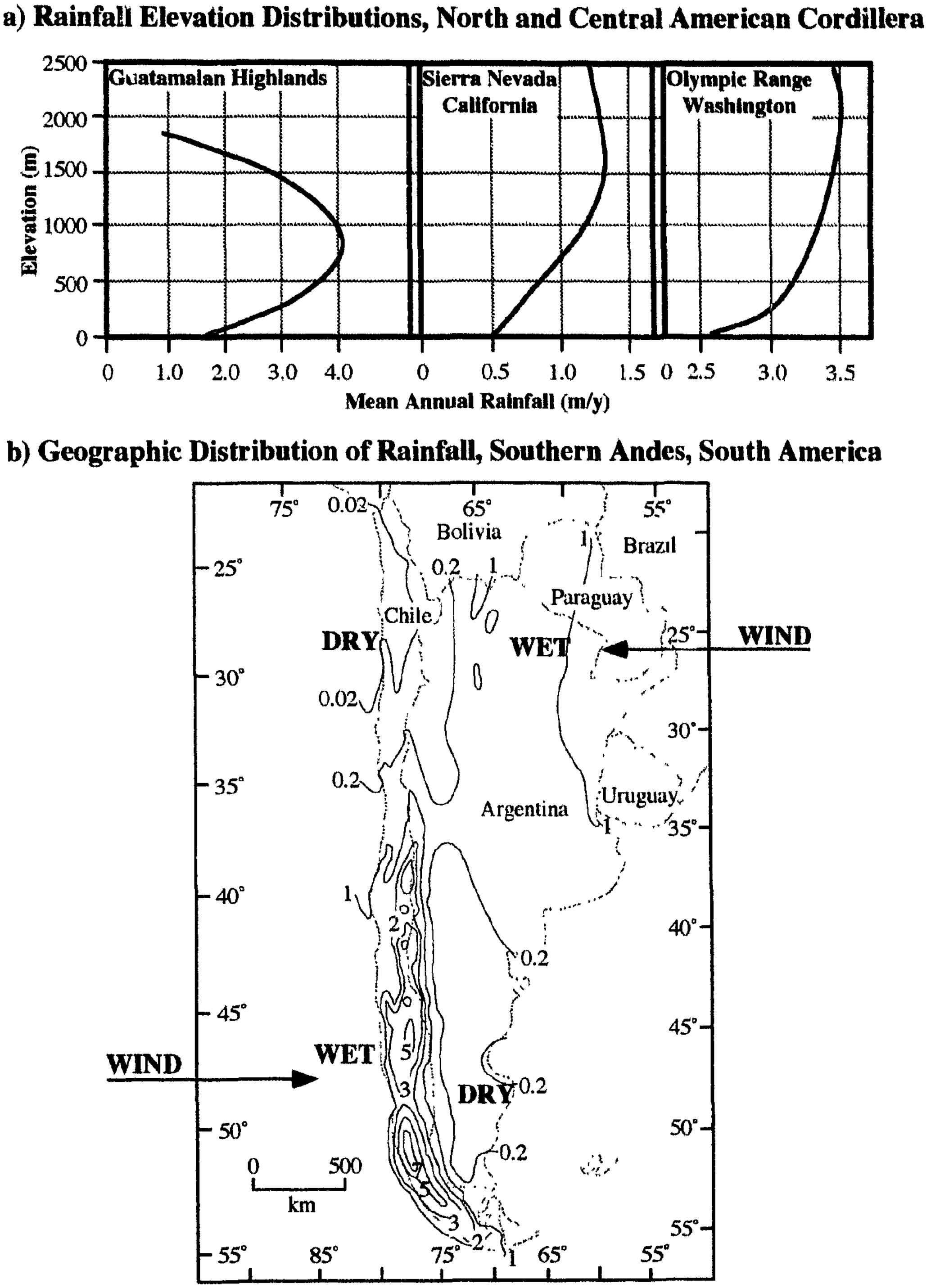

Figure 4.1. Examples of orographically controlled rainfall distribution: a) rainfall variation with elevation along the north and central American Cordillera (after Barry and Chorley, 1971) and b) geographic distribution of rainfall over the southern Andes; contours shows rainfall rates in m/y (after Prohaska, 1976).

basins are examined by comparing sequence development in retro-foreland basins in which the prevailing vapour flux moves in opposite directions while all other parameter values are identical.

In nature, an orogen/foreland basin system may experience a change between wetter and drier climatic conditions due to a change either in climate (*e.g.*, Himalaya, Burbank, 1992) or prevailing wind direction relative to the strike of the orogen. The effects of climate change, from wetter to drier and drier to wetter, are investigated by varying Q_V with time, while all other model parameter values remain constant. Variations in Q_V are chosen to demonstrate the effects of large changes in Q_V that do not cause a change in orogen state. As with the tectonic models, a step function in Q_V is used to estimate the climatic response time (τ_C) of the orogen/foreland basin system and to demonstrate the shorter and longer term stratigraphic response to changes in Q_V that occur over periods approximately equal to or much greater than τ_C. Model results are also presented for orogen/foreland basin systems using a sinusoidal change in Q_V, where the period of fluctuation is on the order of, or much greater than τ_C. These results contrast the stratigraphic character of foreland basins where the orogen/foreland basin system has either sufficient time or insufficient time to maintain a dynamic equilibrium during changes between wetter and drier climatic conditions.

In the model, due to orographic controls on precipitation, changes in climatic conditions affect foreland basin stratigraphy in a manner similar to changes in tectonics. Tectonic changes cause the greatest variations in precipitation over the orogen because precipitation is strongly coupled to surface elevation. This coupling also causes variation in Q_V to have the greatest effect on precipitation over the orogen. As a consequence, the effects of coeval changes in v_T and Q_V can reinforce or counteract each other. Model results are presented that show how changes in climatic conditions can enhance or retard the effects of tectonics on basin stratigraphy.

4.2 Windward vs. Leeward Settings

The contrast between windward and leeward settings on development of low-order foreland basin sequences is shown by comparing results for models with a step function in the rate of tectonic convergence (v_T) and opposite directions of vapour flux (Q_V) relative to v_T. In model MT4, a retro-foreland basin develops in a windward setting (Figs. 3.14-3.16, 3.18). Model MC1 uses the same initial condition and parameter values as model MT4, but the direction of Q_V is reversed so that the retro-foreland basin is in a leeward setting. In addition, the position where the convergent margins collide has been moved downwind to ensure that depletion of Q_V across the windward continent is approximately the same in both MC1 and MT4. MC1 is made similar to MT4 to show how comple e low-order sequences develop in a leeward setting. Model results for MC1 are presented in planform and transverse section, similar to MT4 (Fig. 4.2).

After 15 My the MC1 retro-foreland basin is sediment-starved relative to MT4 (Fig. 4.2). The planform expression of this difference in sediment supply is seen in the relative extent of alluvial plain progradation. In MC1, the alluvial plain of the retro-foreland basin is ~100 km wide between the orogen and the seaway along A-A' (①, Fig. 4.2). By contrast, in MT4 the alluvial plain has extended to ~350 km after 15 My, the retro-foreland basin is entirely alluvial along A-A', and progradation has caused partial filling of the seaway. Further along strike, near B-B' in MT4, the topography of the retro-foreland basin seaway, alluvial plain and orogen are similar in both MC1 and MT4 (②, Fig. 4.2; Fig. 3.16). The increasing difference along strike parallels the change in orogen age and growth. The difference between MC1 and MT4 at 15 My along A-A' reflects

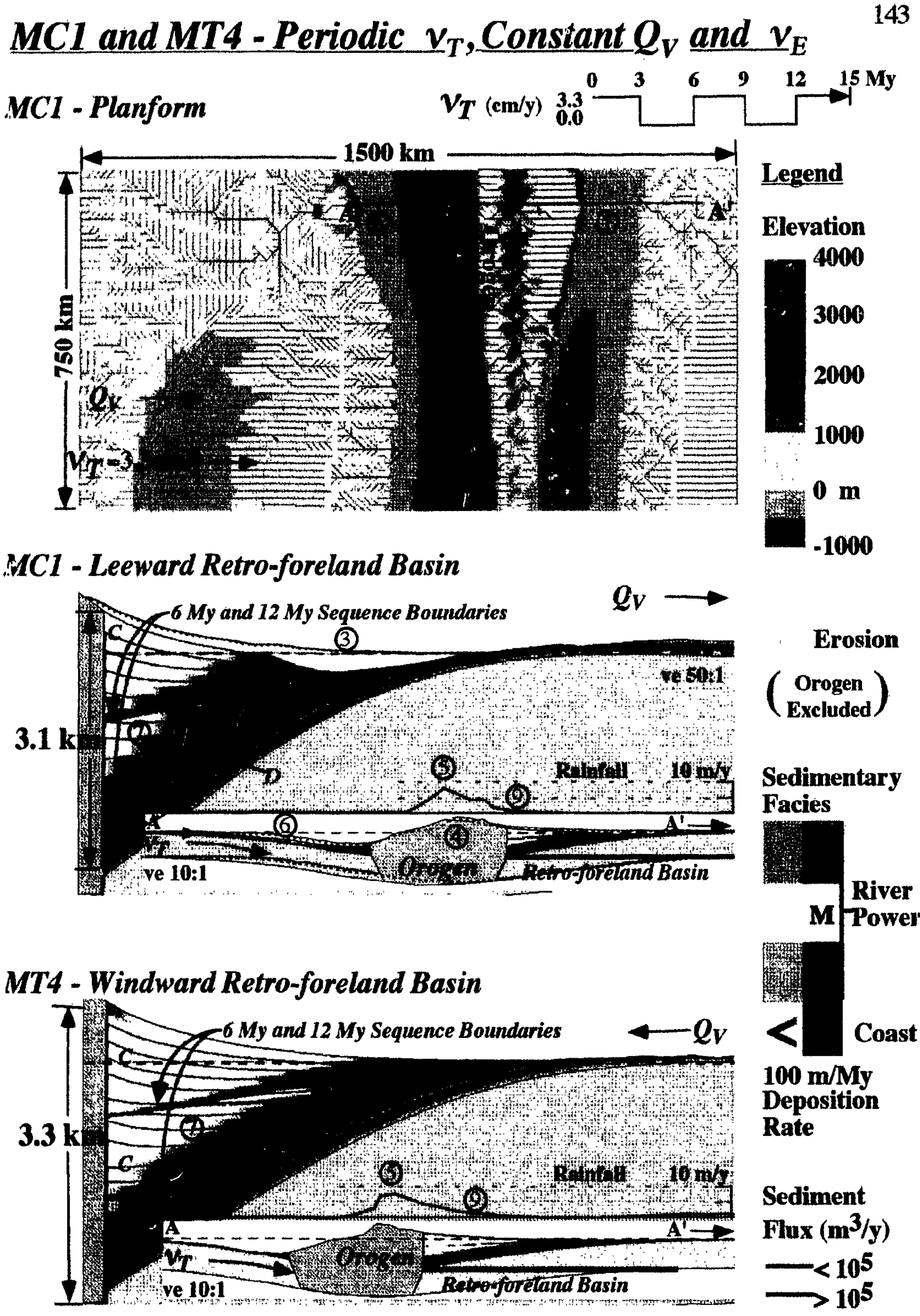

Figure 4.2. MC1 is shown in planform and transverse sections at 15 My. MT4 is shown in transverse sections at 15 My, for comparison. Time lines (black) are at 500 ky intervals. Sequences comprise sediments deposited during constructive (C) and destructive (D) orogen states. Sequence boundaries are highlighted with red dashed lines. The windward MT4 retro-foreland basin has significantly more rainfall (blue lines) than the leeward MC1 retro-foreland basin.

how changes in rainfall distribution affect erosion rates and sediment delivery to retro-foreland basins.

Much of the difference in sediment fill between MC1 and MT4 retro-foreland basins (③, Fig. 4.2) is found in the size of the MC1 orogen and the sediment fill of the MC1 pro-foreland basin. For example, in Figure 4.2 the regional profile along section A-A' of MT4 is shown in dashed lines over the MC1 regional section (④, Fig. 4.2). Although pro-foreland precipitation and therefore denudation rates and sediment flux, are greater in MC1 than in MT4 (⑤, Fig. 4.2), the pro-foreland basin remains marine because the rate of orogen growth is sufficiently fast to re-entrain much of the sediment deposited in the pro-foreland basin into the orogen. The pro-foreland basin in MC1 also differs from MT4 in that it contains sediment that is deposited adjacent to the peripheral bulge and is then advected into the basin (⑥, Fig. 4.2). The difference in sedimentation rate is a result of precipitation and erosion rates on the windward continent. As a consequence, much of the difference between MC1 and MT4 is found in the orogens.

Comparison of MC1 and MT4 retro-foreland strata shows that both contain stacked prograding sequences (Fig. 4.2). Sequence boundaries are similar, comprising proximal and distal erosional surfaces with a medial condensed section. In MC1, however, the sequences are less extensive and contain a greater proportion of marine sediment. While the orogen is in a constructive state, progradation rates are slower in MC1 than in MT4 (⑦, Fig. 4.2). Sedimentation rates over identical time intervals are comparable proximal to the orogen and slower in the basin, as indicated by time lines and basin profiles (③, Fig. 4.2). Further, marine facies distribution in MC1 indicates that seaway width is increasing with time, despite progradation (⑧, Fig. 4.2), reflecting the dominance of relative sea-level rise, caused by isostatic compensation of the growing orogenic and sedimentary loads, over progradational filling of the basin. These

MC2 - Periodic Q_V, Constant v_T and v_E

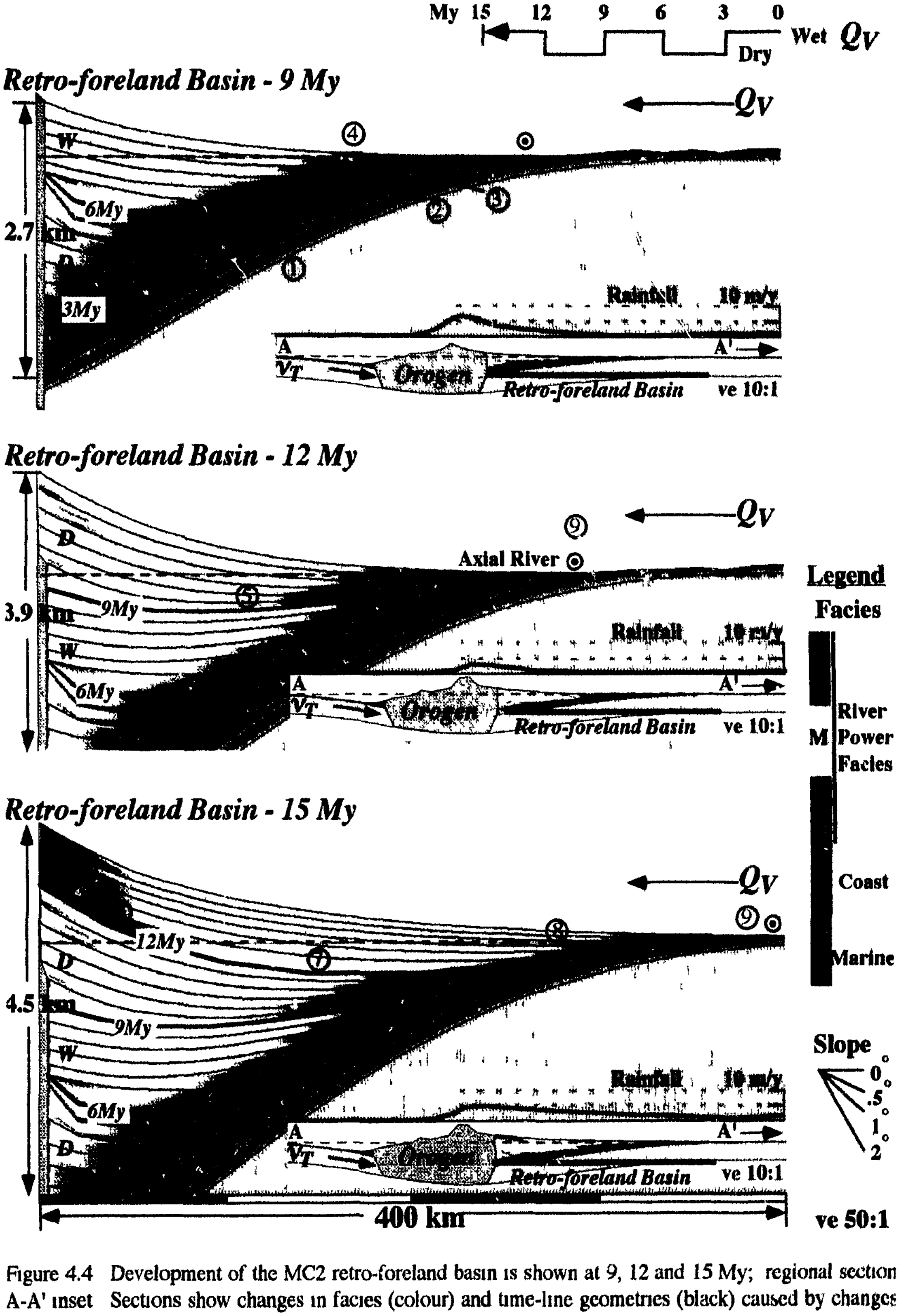

Figure 4.4 Development of the MC2 retro-foreland basin is shown at 9, 12 and 15 My; regional section A-A' inset Sections show changes in facies (colour) and time-line geometries (black) caused by changes between wetter (W) and drier (D) climatic conditions Time lines are at 500 ky intervals.

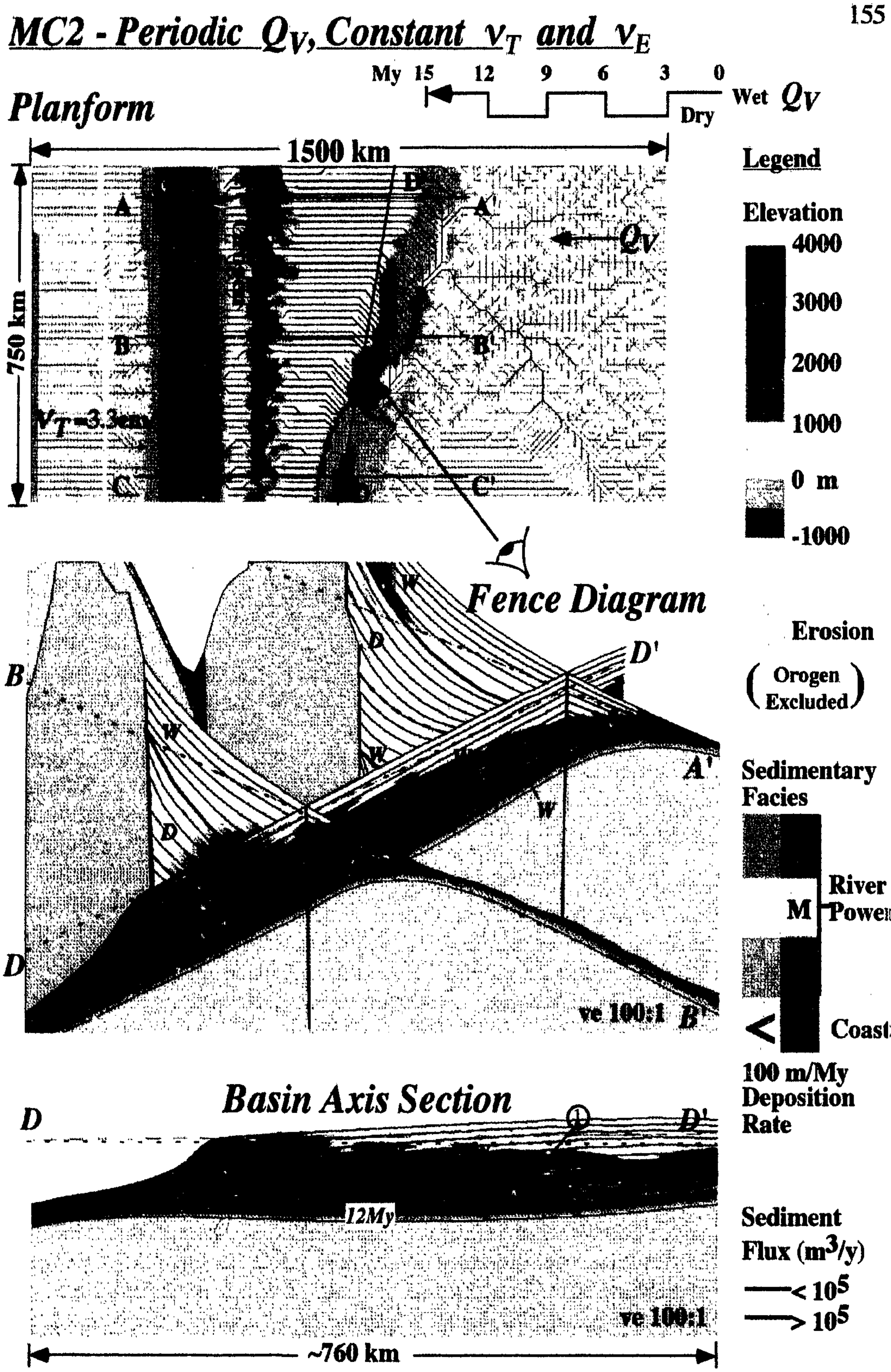

Figure 4.6. MC2 in planform, fence diagram and axial section, at 15 My. This figure shows the spatial relationship of sedimentary facies (colour) and time-line geometries (black) associated with wetter (W) and drier (D) climatic conditions.

4.3 Temporal Variation in Climate

The effect of climate change between wetter and drier conditions on the development of orogen/foreland basin systems is demonstrated by varying the boundary vapour flux (Q_V) of the model with time. Changes in Q_V increase or decrease the model's aridity, thus varying the amount of moisture available for precipitation at any time (Sec. 2.4). In nature, climate is observed to change both cyclically (Gilbert, 1895, cit. Fischer *et al.*, 1990) and episodically (*e.g.*, late Cenozoic global increase in aridity, Crowley and North, 1991). Some of the model results presented use a temporal step function in Q_V to show the system's response to instantaneous changes in climate and to estimate its response time to changes in Q_V. A period of 3 My is used, consistent with climatic periodicity on the order of 1 My as observed in the Tertiary (Crowley and North, 1991), the duration of third order sequences (Allen and Allen, 1990) and the 2 My and 3.4 My periodicity in orbital eccentricity (Fischer *et al.*, 1988). Eccentricity in combination with precession (elliptical progression of the earth's spin axis) is thought to modify earth's climate by causing periodic change in the amount of solar energy received (Fischer *et al.*, 1988). Other model results use a sinusoidal variation in Q_V to demonstrate the effect of system response time on the development of foreland basin stratigraphy. With both step and sinusoid functions, Q_V varies such that if rainfall were uniform across the model, precipitation would change by 0.5 m/y between the wettest and driest climatic conditions.

4.3.1 Wet/Dry Step Function Climate Periodicity

MC2 - Effect of Climate Periodicity on Retro-foreland Basin Stratigraphy

The orogen/foreland basin system in model MC2 experiences wet/dry periodicity in Q_V, while the pro-lithosphere convergence velocity (v_T) and all other parameter values differences between MC1 and MT4 result from lower orogen-to-basin sediment flux in the retro-foreland basin ($Q_S(retro)$), while subsidence rates proximal to the orogen are about the same. The lower $Q_S(retro)$ is a consequence of lower precipitation and erosion rates on the leeward orogen. Rainfall distributions at 15 My reflect this difference (⑤, Fig. 4.2).

The difference in rainfall distribution between MC1 and MT4 is primarily expressed through the effects of a difference in orogen-to-basin sediment flux; however, there is also a significant difference in rainfall across the retro-foreland alluvial plain (⑨, Fig. 4.2). Rainfall on the plain inhibits the effect of decreasing surface slope on fluvial carrying capacity by increasing river discharge. Fluvial systems in the leeward setting are, therefore, less efficient than those in the windward setting at moving sediment away from the orogen. This difference between MC1 and MT4 contributes to slower rates of progradation and steeper surface slopes on the alluvial plain in MC1 (③, Fig. 4.2). Stratigraphically the steeper slopes are expressed as an increase in time line divergence toward the orogen.

In summary, these model results imply that sequences developed in a leeward foreland basin setting (MC1) are characterized by comparable aggradation rates, slower progradation rates and a higher proportion of marine sediments than those in a windward setting (MT4). These differences compare favourably with the interpreted effects of orographically controlled rainfall distributions on the development of the Wopmay and Thelon orogen/foreland basin systems, Northwest Territories, which Hoffman and Grotzinger (1993) suggest characterize the difference between leeward and windward foreland basins. The windward foreland basins are dominated by progradation of "molassoid" facies, while leeward basins are dominated by aggradational "flyschoid" facies.

Hoffman and Grotzinger (1993) further speculate that windward foreland basins should be overfilled and contain a relatively thin section of dominantly fluvial or shallow marine, progradationally stacked sediment, while leeward foreland basins should be underfilled and contain a thick section of dominantly aggradationally stacked deep-water marine sediments. This suggestion is based on the assumption that windward orogens have higher erosion rates which, by implication, cause higher orogen-to-basin sediment flux and slower basin subsidence rates than leeward orogens. Windward foreland basins should, therefore, 'fill and spill' faster than their leeward counterparts.

MC1 and MT4 model results indicate that basin subsidence associated with small orogens is controlled by the growth rate of the entire orogen and not the relative rate of erosion on either the windward or leeward sides of an orogen. Therefore, while windward foreland basins fill and spill faster than leeward basins under equivalent tectonic and climatic conditions, they are not necessarily lacking in the development of significant marine sections. They may, however, record a shorter and perhaps earlier period of marine basin development. In addition, alluvial sediments in a windward basin may extend further from the orogen and be preserved, while sediments in an equivalent leeward basin may have traveled less distance and thus may not be preserved because they were tectonically recycled. This relationship will be true whether the basin is in a pro- or retro-foreland basin setting, although the rate of tectonic recycling will be much higher in the pro-foreland basin setting. In general, while the orogenic load continues to grow, leeward foreland basins record longer periods of system development than windward basins, and sediments are more likely to be preserved if the rate of tectonic recycling is slow. An additional factor not considered here is the relative buoyancy of the subducting pro-lithosphere which will partly determine the isostatic balance of the overall system.

4.3 Temporal Variation in Climate

The effect of climate change between wetter and drier conditions on the development of orogen/foreland basin systems is demonstrated by varying the boundary vapour flux (Q_V) of the model with time. Changes in Q_V increase or decrease the model's aridity, thus varying the amount of moisture available for precipitation at any time (Sec. 2.4). In nature, climate is observed to change both cyclically (Gilbert, 1895, cit. Fischer *et al.*, 1990) and episodically (*e.g.*, late Cenozoic global increase in aridity, Crowley and North, 1991). Some of the model results presented use a temporal step function in Q_V to show the system's response to instantaneous changes in climate and to estimate its response time to changes in Q_V. A period of 3 My is used, consistent with climatic periodicity on the order of 1 My as observed in the Tertiary (Crowley and North, 1991), the duration of third order sequences (Allen and Allen, 1990) and the 2 My and 3.4 My periodicity in orbital eccentricity (Fischer *et al.*, 1988). Eccentricity in combination with precession (elliptical progression of the earth's spin axis) is thought to modify earth's climate by causing periodic change in the amount of solar energy received (Fischer *et al.*, 1988). Other model results use a sinusoidal variation in Q_V to demonstrate the effect of system response time on the development of foreland basin stratigraphy. With both step and sinusoid functions, Q_V varies such that if rainfall were uniform across the model, precipitation would change by 0.5 m/y between the wettest and driest climatic conditions.

4.3.1 Wet/Dry Step Function Climate Periodicity

MC2 - Effect of Climate Periodicity on Retro-foreland Basin Stratigraphy

The orogen/foreland basin system in model MC2 experiences wet/dry periodicity in Q_V, while the pro-lithosphere convergence velocity (v_T) and all other parameter values remain constant, using the same initial conditions and parameter values as MT4. MC2 uses an oblique convergent margin setting to show the effect of changes in rainfall distribution on both longitudinal and transverse fluvial sediment transport. The results are presented at 9, 12 and 15 My in planform (Fig. 4.3), in transverse sections (Figs. 4.4, 4.5), in basin axial section (Fig. 4.6) and in fence diagram (Fig. 4.6). Results at 9 My illustrate retro-foreland basin stratigraphy; at 12 My they show the effects of climate change from wet to dry, and at 15 My the effects of a climate change from dry to wet.

MC2 - Evolution during the first 9 My

During the first 9 My, MC2 has experienced an initial 3 My period of wet climatic conditions followed by a 3 My dry period and another 3 My wet period. In section, the retro-foreland basin develops a prograding sedimentary wedge adjacent to the orogen and a transgressive system adjacent to the peripheral bulge (Fig. 4.4). These facies distributions are generally consistent with foreland basins adjacent to constructive orogens. The regional section A-A' of MC2 (inset, Fig. 4.4) shows the asymmetry in basin filling typical of this setting.

Most of the sediments deposited in the retro-foreland basin during the first 3 My have been entrained into the orogen (Fig. 4.4). However, a retrogradational succession of continentally derived low river-power and coastal facies are present over the earlier position of the peripheral bulge along A-A' (①, Fig. 4.4), indicating that sediment flux from the continent was insufficient to keep pace with the relative rise in sea level caused by isostatic compensation of the growing orogenic and sedimentary load during the first 3 My. The orogen remains in a constructive state throughout changes between wet and dry climatic conditions.

Between 3 My and 6 My, the change to a drier climate is indicated by the decrease in marine sedimentation rates adjacent to the orogen (Fig. 4.4). Adjacent to the

MC2 - Periodic Q_V, Constant v_T and v_E

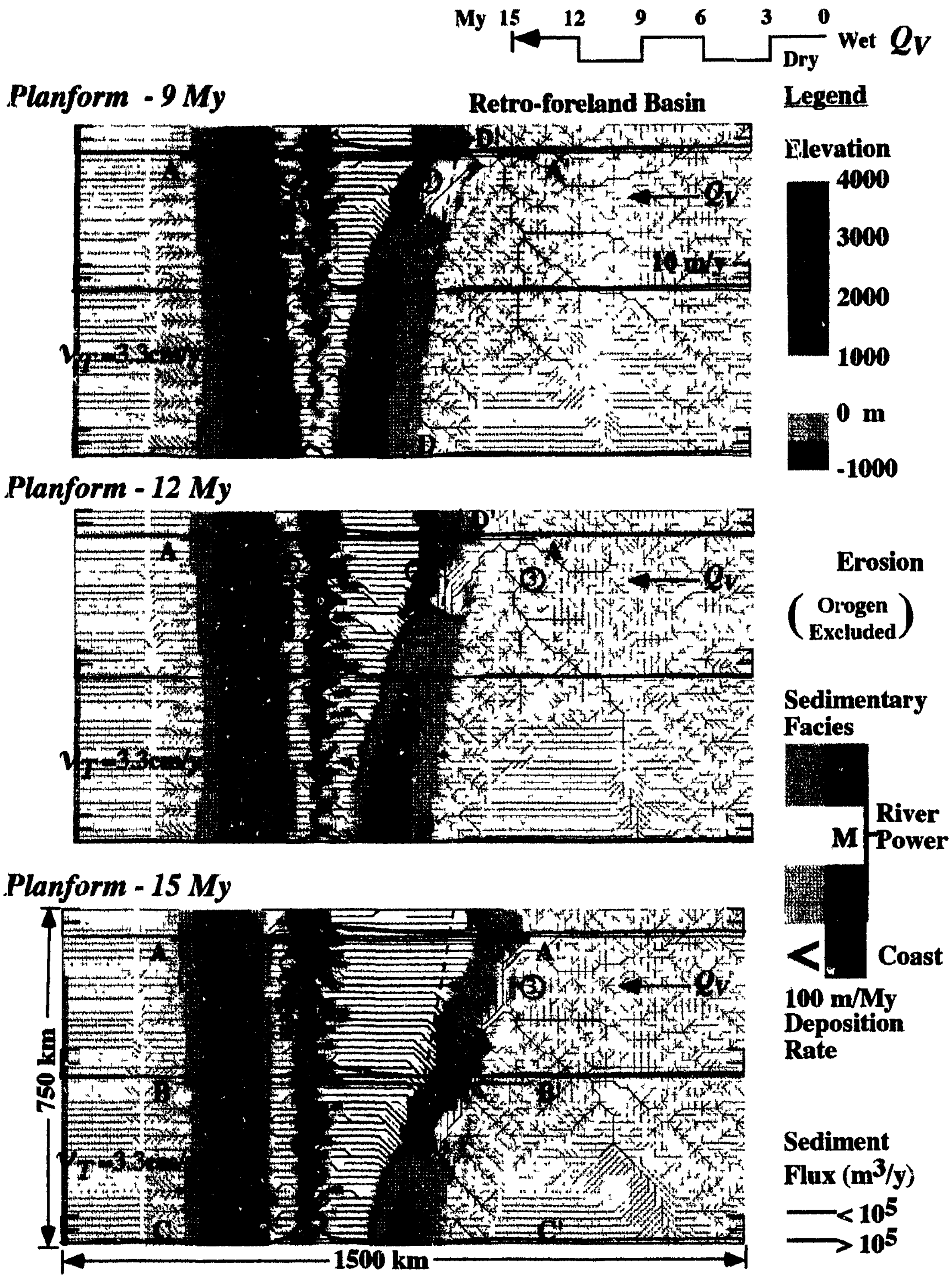

Figure 4.3. Planform surface elevation, facies distribution, subaerial erosion and fluvial drainage network of MC2 at 9, 12 and 15 My. Rainfall distributions are shown over lines of section A-A', B-B' and C-C'. Comparison of 9 and 12 My results show model evolution during an interval of drier climatic conditions, while comparison of 12 and 15 My show model evolution during an interval of wetter climatic conditions.

peripheral bulge, the change in climate is characterized by a decrease in continental sediment flux to the seaway, as observed in the decrease of alluvial sediment volume deposited adjacent to the peripheral bulge (②, Fig. 4.4). In natural foreland basins (*e.g.*, Upper Cretaceous, U.S. Western Interior, Laferriere *et al.*, 1987), the decrease in terrigenous flux is typically associated with an increase in carbonate deposition. This process is not yet incorporated into the model. In MC2, transgression of the peripheral bulge continues, consistent with the relative rise in sea level caused by continued growth of the orogen and alluvial plain. However, the rate of transgression has decreased relative to the previous 3 My, as indicated by its shorter extent. Comparison of the extent of transgression with the extent of progradation indicates that transgression kept pace with progradation and the seaway maintained an approximately constant width. Therefore, while sediment flux to the seaway has decreased with the change in Q_V, it is sufficient to keep pace with the relative rise in sea level described above. When the ratio of relative sea-level rise to sediment flux is constant, the thickness of marine facies deposited remains approximately constant, as seen in MT3 (Fig. 3.11).

When the climate again becomes wet at 6 My, erosion rates increase and the orogen growth rate decreases. These changes cause an increase in the orogen-to-basin sediment flux, coeval with a decrease in the rate of basin subsidence. This combination increases the rate of progradation and filling of the seaway (③, Fig. 4.4), coeval with a change from retrogradation to aggradation of coastal facies adjacent to the peripheral bulge (④, Fig. 4.4). Retrogradation stops because the sediment flux off the continent is sufficient to oppose the effect of the relative rise in sea level caused by isostatic compensation of the growing orogenic and sedimentary loads. The change to aggradation is caused by both an increase in sediment flux from the continent and a decrease in the rate of isostatically forced basin subsidence. The increase in precipitation causes an increase in erosion rates on both the continent and the orogen and thus the increase in sediment flux from the continent and the decrease in basin subsidence rate respectively. By ~8 My the seaway at A-A' has been filled (③, Fig. 4.4) and axial drainage develops in the now alluvial foreland basin, promoting longitudinal progradation (①, Fig. 4.3).

MC2 - Evolution Between 9 My and 12 My

At 9 My, as at 3 My, there is an instantaneous decrease by half in Q_V (Table 3.1), which then remains constant until 12 My. Stratigraphically, this change is preserved at A-A' as a rapid retrogradation toward the orogen of low river-power facies (⑤, Fig. 4.4). This shorter term effect of climate change is followed after less than 1 My by resumed progradation. There is also a higher gradient in sedimentation rates away from the orogen, characterized by increased divergence of time lines toward the orogen (Fig. 4.4).

The transient period of retrogradation is primarily a consequence of the decrease in precipitation that accompanies the instantaneous decrease in Q_V at 9 My, which reduces fluvial discharge (q_f) and thus the carrying capacity of rivers ($q_f e^{qb}$). The attendant reduction in river power causes, in part, the retrogradation of low and moderate river-power facies on the alluvial plain (⑤, Fig. 4.4). On the orogen, the reduction in $q_f e^{qb}$ causes an instantaneous decrease in erosion rates and reduces the orogen-to-basin sediment flux ($Q_{S(retro)}$). While erosion rates and $Q_{S(retro)}$ decrease, the tectonic flux into the orogen ($Q_{T(pro)}$) remains approximately constant. As a consequence, the rates of both orogen growth and basin subsidence increase. Subsidence contributes to the retrogradation of river-power facies by decreasing both the surface slope of the alluvial plain and fluvial transport of sediment away from the orogen. The combination of increased orogen elevation and decreased fluvial discharge, together with the lower slope of the alluvial plain, creates a high gradient in fluvial carrying capacity adjacent to the orogen. The disequilibrium between fluvial sediment flux and transport capacity results in high sedimentation rates that decrease rapidly away from the orogen, as observed in the 9.5 and 10 My time lines (Fig. 4.4).

The transient response to the instantaneous change in precipitation is not localized to the orogen and upper alluvial plain; rather, it extends to the distal alluvial plain and seaway, as evidenced by a small transgression along the basin axis (①, Fig. 4.6). This transgression is a consequence of both the relative rise in sea level with basin subsidence and the decrease in the sediment transport to the coast with increased sedimentation adjacent to the orogen. It is interesting to note that transgression occurs along the basin axis, but does not occur on the alluvial plain along B-B' (①, Fig. 4.5). This preferential transgression along the basin axis reflects lower surface slopes along the axis, and possibly a greater reduction in sediment flux to the coast than along the alluvial plain.

During the 10 to 12 My interval precipitation increases on the orogen and alluvial plain because it is orographically controlled. This increase in precipitation causes an increase in discharge and thus in fluvial carrying capacity, resulting in higher erosion rates on the orogen, an attendant increase in orogen-to-basin sediment flux and increased efficiency of transport away from the orogen. Progradation of coastal facies resumes after approximately 1 My (Fig. 4.4). There is a negative feedback in that the same increases also inhibit both the rate of orogen growth and basin subsidence. The increase in orogen growth rate is also countered by the increasing size of the orogen and constant $Q_T(pro)$. The overall effect of decelerating orogen growth, basin subsidence and fluvial transport is that fluvial profiles evolve toward a dynamic equilibrium, as reflected in model time lines between 10 and 12 My (Fig. 4.4). Although progradation proceeds, sedimentation rates (time-line separation) continue to reflect a more rapid decrease in carrying capacity away from the orogen than were typical with wetter climatic conditions

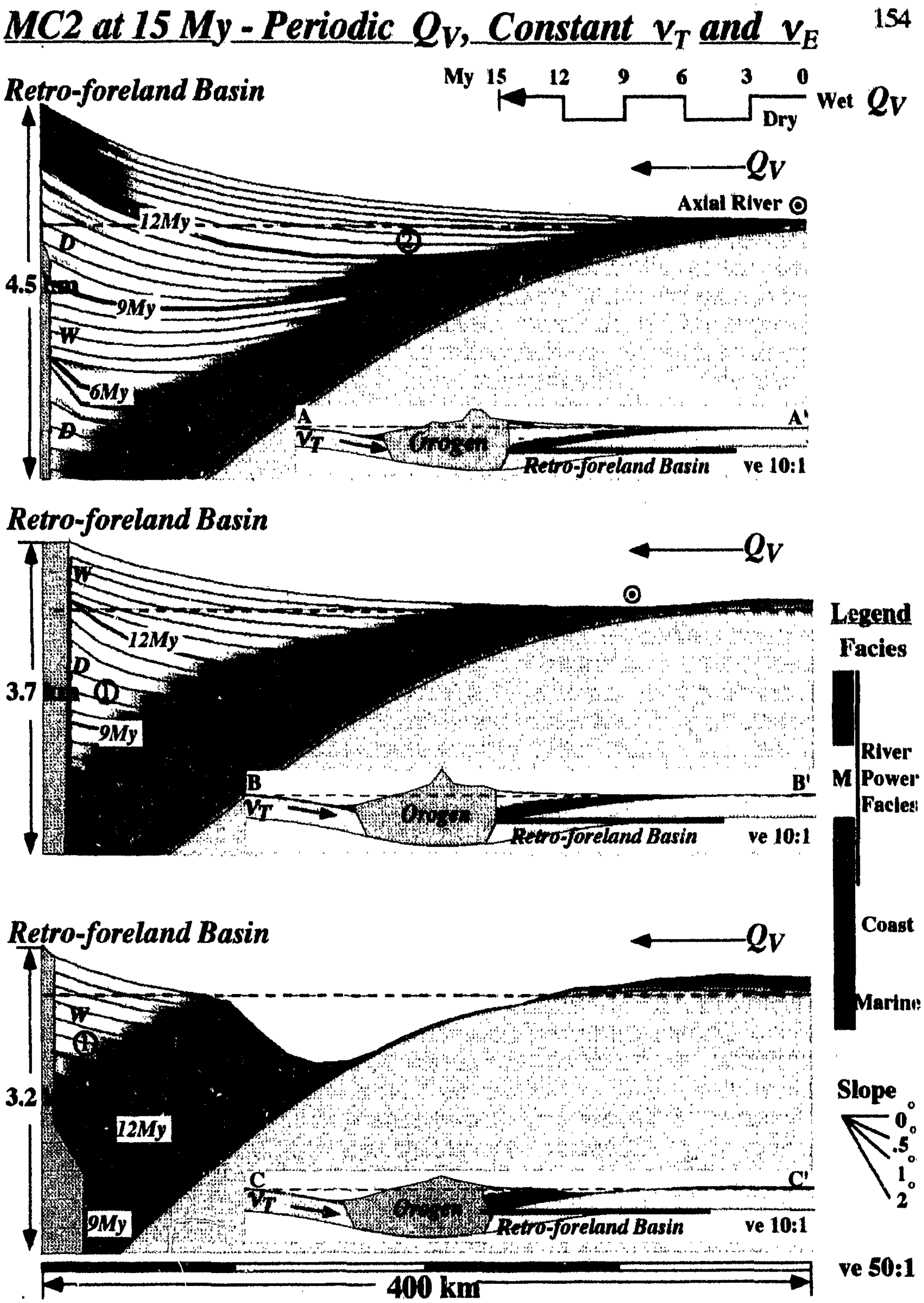

Figure 4.5. MC2 retro-foreland basin at 15 My along sections A-A', B-B' and C-C' (inset). Sections show facies (colour) and changes in time-line geometry (black) along strike. Time lines are at 500 ky intervals. 'W' and 'D' denote sediments deposited during wetter and drier climatic conditions, respectively.

(Fig. 4.4). This gradient in carrying capacity reflects the higher rates of orogen growth and basin subsidence, in combination with less efficient fluvial transport away from the orogen caused by the drier climatic conditions.

In general, the change to drier climate conditions reduces both the rate of erosion on the orogen and the efficiency of sediment transport across the alluvial plain. The result is an increase in sediment thickness adjacent to the orogen which is accommodated partially by isostatic compensation and partially by increased alluvial plain elevation and surface slope. As a consequence, surface sediment distribution at the end of the dry period at 12 My is remarkably similar to the surface sediment distribution at the end of the wet period at 9 My (Fig. 4.3).

MC2 - Evolution Between 12 My and 15 My

The instantaneous increase in Q_V at 12 My causes an increase in precipitation on the orogen and fluvial discharge (q_f) to the basin. Erosion rates increase on the orogen, while tectonic flux ($Q_T(pro)$) remains approximately constant. The result is a decline in the rate of orogen growth and an increase in sediment flux to both the pro-foreland and retro-foreland basins. In the latter case, this causes extensive filling of the seaway (Fig. 4.3). Growth of the alluvial plain causes migration of the peripheral bulge and trunk river away from the orogen. The trunk river of the axial foreland basin captures the trunk river of the continental drainage network (③, Fig. 4.3). This river capture subdivides drainage off the continent and leads to a change in flow direction. There is no significant change in the pro-foreland basin seaway (Fig. 4.3) because the increased sediment flux to the pro-foreland basin is tectonically recycled into the orogen. The orogen's growth is observed as an increase in width and a modest increase in elevation (Fig. 4.3).

In the retro-foreland basin, the increase in precipitation on the orogen with the change in Q_V is expressed as an increase in river-power facies and a decrease in sedimentation rate adjacent to the orogen (⑥, Fig. 4.4). The former reflects the increase in q_f, while the latter reflects both the increase in river carrying capacity ($q_f^{eq^b}$) and the decrease in the basin subsidence rate caused by the decrease in orogen growth rate. Continued basin subsidence and sedimentation adjacent to the orogen immediately after the change in Q_V indicate that the increase in precipitation and erosion rates on the orogen does not cause a change to a destructive orogen state.

Coeval with the decrease in sedimentation rate adjacent to the orogen, sedimentation rates increase in the retro-foreland basin (⑦, Fig. 4.4), beginning with a transient increase for ~1 My after the change in Q_V, and followed by more uniform sedimentation rates. This transient increase in sedimentation rates reflects the regrading of the rivers on the alluvial plains with the increase in $Q_{S(retro)}$ and the increase in precipitation across the plain (Fig. 4.4). The increase in sediment transport results in higher sedimentation rates on the distal alluvial plain and an increase in the rate of progradation (⑧, Fig. 4.4). There is a feedback here in that enhanced sediment transport and sedimentation rates increase the elevation of the alluvial plain, which causes an increase in precipitation (Fig. 4.4). With additional precipitation, q_f and therefore $q_f^{eq^b}$ increase, which opposes the effect of decreasing surface slope on $q_f^{eq^b}$ and, therefore, on sedimentation rates. This feedback makes sedimentation rates progressively more uniform across the alluvial plain (Fig. 4.4). The result is a change in time-line geometries from steeper to shallower profiles adjacent to the orogen (Fig. 4.5) and a change from shallower to modestly steeper profiles in the distal basin (②, Fig. 4.5). There is also an increase in both the rate of transverse (Fig. 4.5) and longitudinal progradation (②, Fig. 4.6) as well as the rate of migration of the peripheral bulge and axial river away from the orogen (⑨, Fig. 4.4). The increase in sedimentation rates and the modest increase in surface slope on the lower alluvial plain enhance migration of the trunk river and peripheral bulge away from the orogen.

Times of rapid axial progradation in MC2 are fundamentally different from MT4, where periods of rapid axial progradation are related to a fall in relative sea level caused by erosional unloading of the lithosphere. In MC2, the rate of progradation increases while relative sea level continues to rise (②, Fig. 4.6) due to the increase in sediment flux to the coast. This increase is observable in the high river-power facies of the lower axial river (Fig. 4.6).

Comparison with Himalayan Foreland Basin

Changes in time-line geometry and trunk river migration shown in MC2 are similar to those observed in the Siwalik Formation of the Himalayan Foreland Basin (Burbank, 1992). Burbank suggests that the more wedge-shaped geometry of the Lower and Middle Siwalik Formation is associated with the growth of the Himalayan-Tibetan orogen (①, Fig. 4.7). This geometry is interpreted to reflect localization of sediment transport away from the orogen due to basin subsidence caused by isostatic compensation of the growing Himalayan orogenic load. However, the mid-Miocene global increase in aridity (Crowley and North, 1991) may have also contributed to the wedge-shaped geometry.

In MC2, the interval of drier climatic conditions between 9 My and 12 My develops a similar time-line geometry because of increased rates of orogen growth and decreased rates of transverse sediment transport away from the orogen. Furthermore, during the initial period of retrogradation, subsidence reduces the slope of the alluvial plain. As a consequence, the distal plain adjacent to the peripheral bulge becomes broad and flat, dipping gently along the basin axis. The result is an increase in the area over which longitudinal drainage may be the dominant fluvial architecture preserved along the basin axis, similar to a suggestion of Burbank (1992) (②, Fig. 4.7).

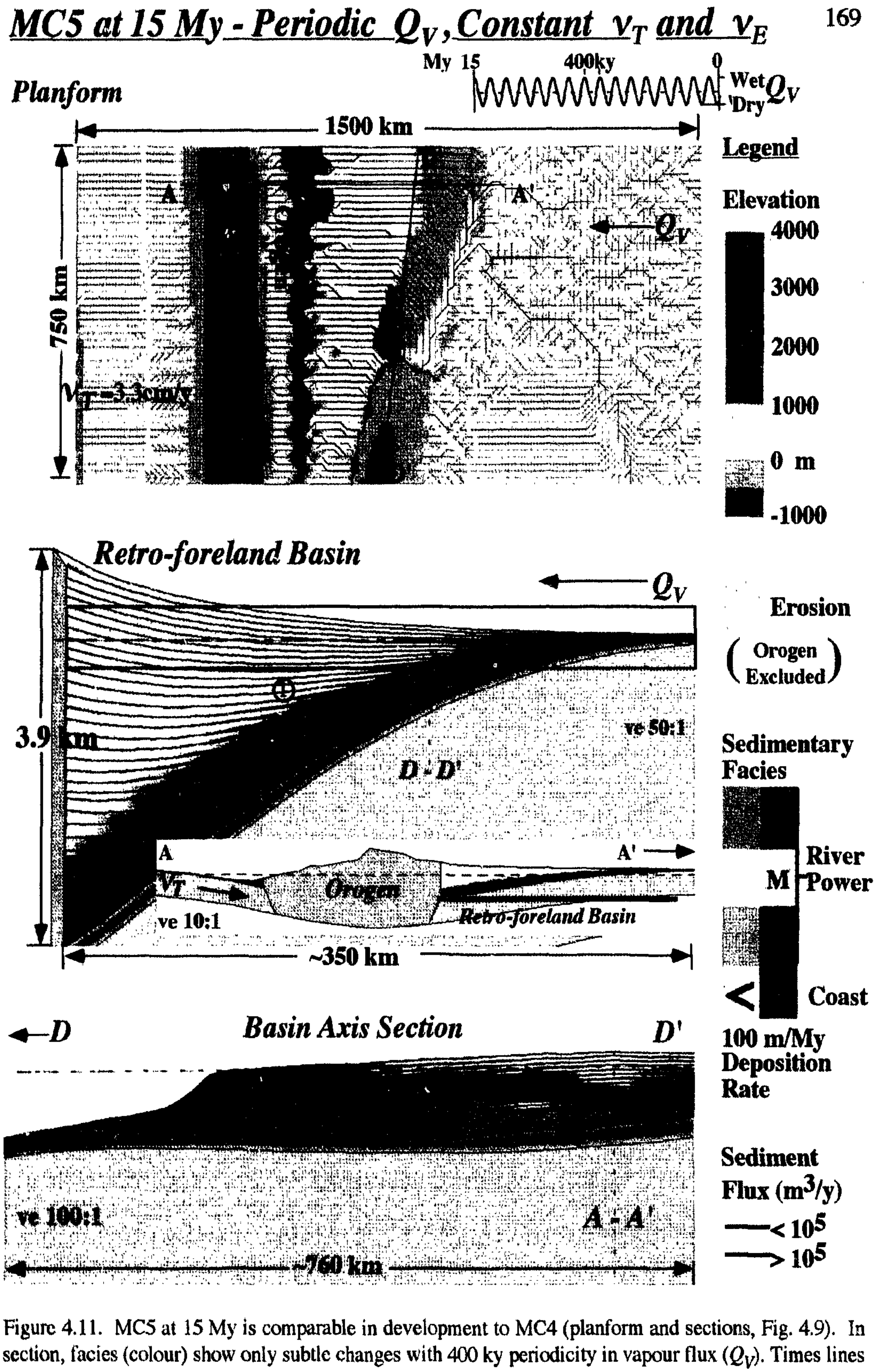

Figure 4.11. MC5 at 15 My is comparable in development to MC4 (planform and sections, Fig. 4.9). In section, facies (colour) show only subtle changes with 400 ky periodicity in vapour flux (Q_V). Times lines are at 400 ky intervals and, therefore, show no change with Q_V. Box outlines the region enlarged in Figure 4.12.

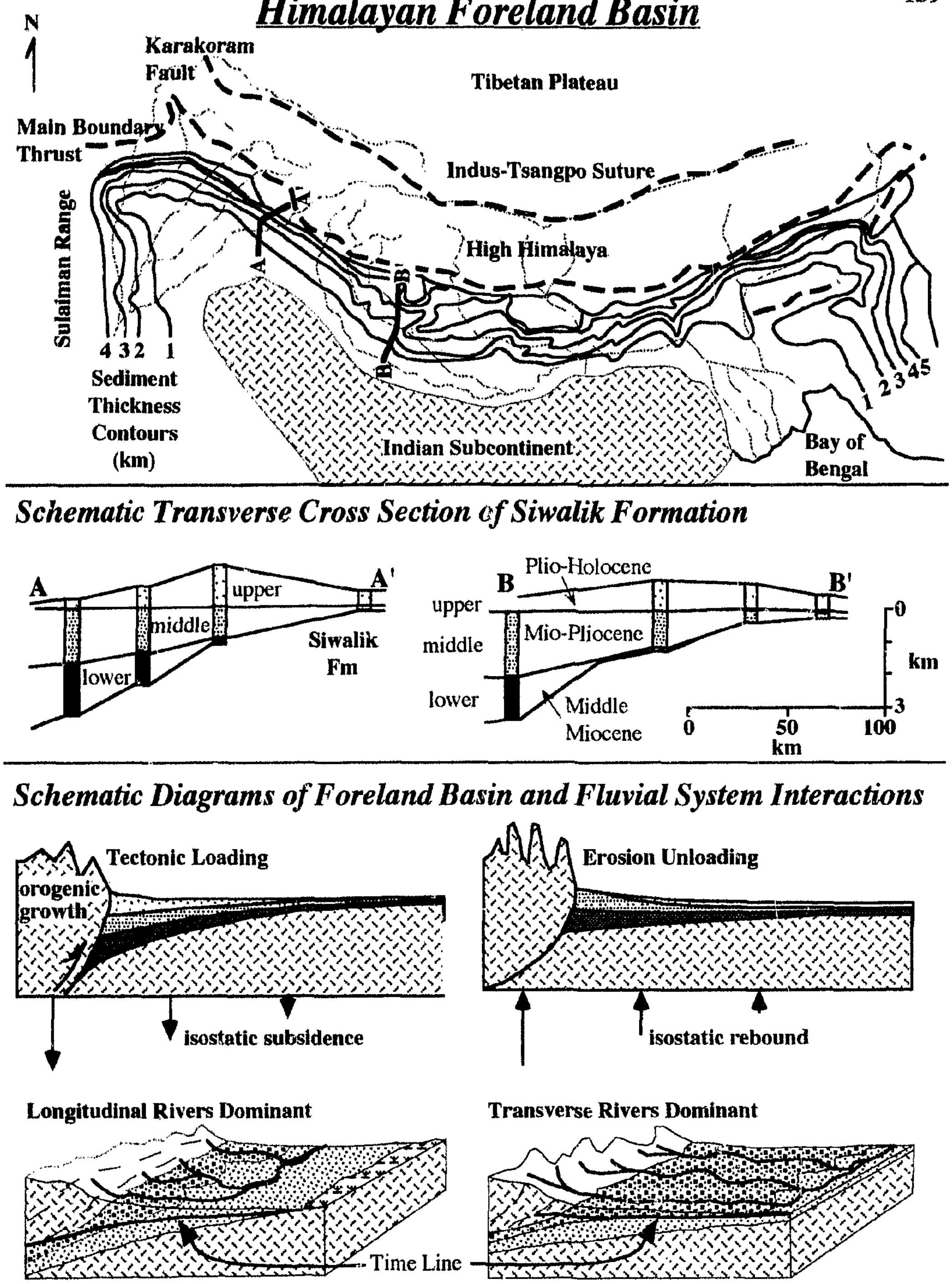

Figure 4.7. Modified after Burbank (1992). Upper panel shows the major drainage and fault patterns of the Himalayan system. Isopachs show the asymmetric wedge of foreland basin strata. Schematic cross sections show the change from Lower and Middle Siwalik stratal thickening toward the orogen, to a more tabular depositional geometry in the Upper Siwaliks. Schemetic diagrams illustrate how this change may be related to modifications in fluvial depositional patterns with the change from tectonic loading to erosional unloading in the orogen.

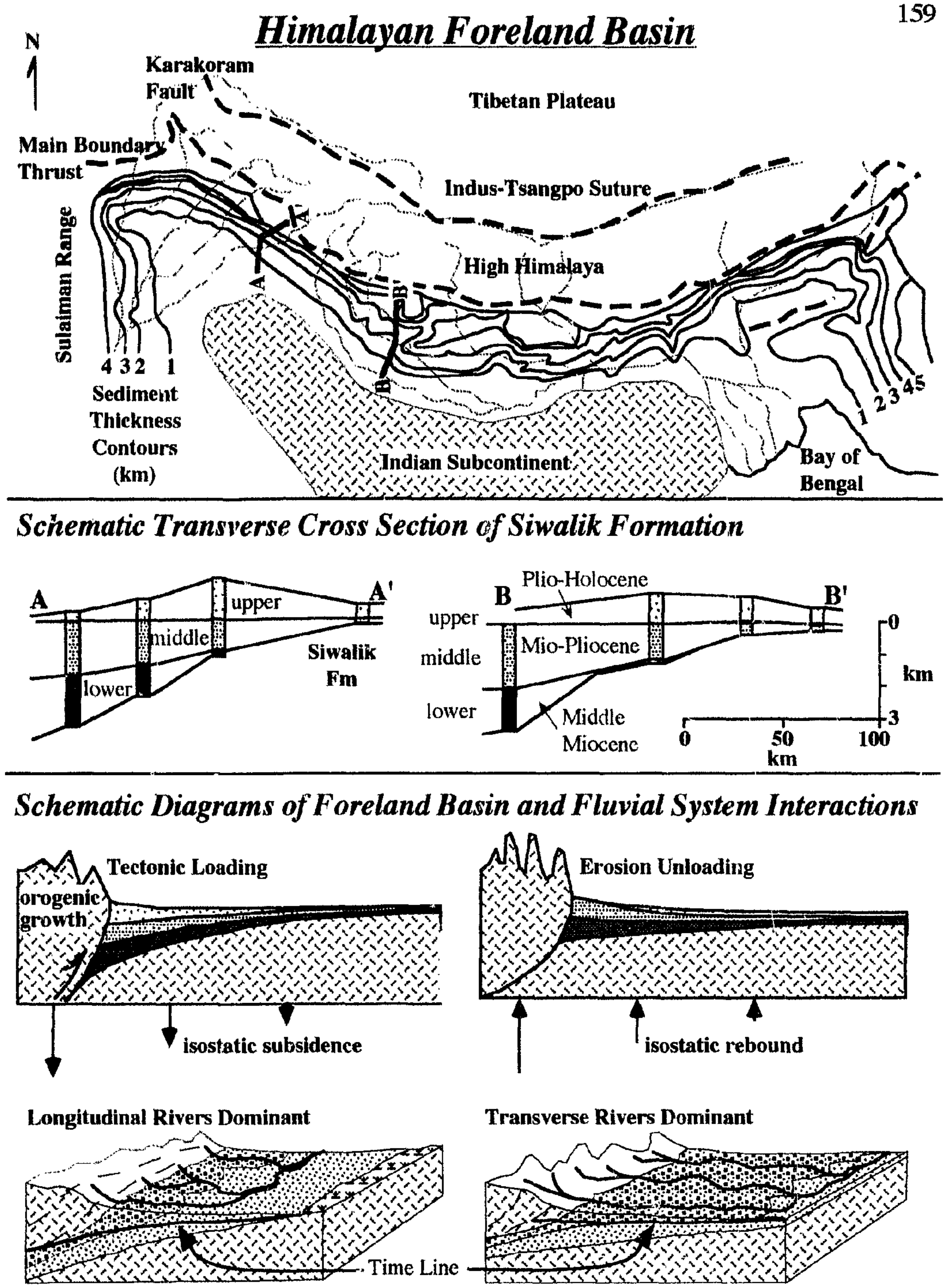

Figure 4.7. Modified after Burbank (1992). Upper panel shows the major drainage and fault patterns of the Himalayan system. Isopachs show the asymmetric wedge of foreland basin strata. Schematic cross sections show the change from Lower and Middle Siwalik stratal thickening toward the orogen, to a more tabular depositional geometry in the Upper Siwaliks. Schemetic diagrams illustrate how this change may be related to modifications in fluvial depositional patterns with the change from tectonic loading to erosional unloading in the orogen.

Burbank interprets the change from a wedge-shaped to a tabular geometry in the Upper Siwalik Formation as progradation of alluvial fans into the foreland basin and the dominance of transverse sediment transport over longitudinal transport (③, Fig. 4.7). He suggests that this change in sediment distribution is caused by the combination of erosional unloading of the orogenic load, an increase in sediment supply to the foreland basin due to flexural rebound, and decreased accommodation space (④, Fig. 4.7). Model MT4 results between 9 My and 12 My show that the evolution from an angular to a more tabular geometry *may* result from a change in orogen state (Fig. 3.15). These results also demonstrate the migration of the axial river by transverse progradation of the alluvial plain (Fig. 3.14). However, model MC2 results between 12 My and 15 My show similar changes (⑨, Fig. 4.4; ③, Fig. 4.5) accomplished solely by a change in climate, with no change in orogen state. The orogen continues to grow throughout the 12-15 My interval and there is an increase, not a net loss, in the load flexing the foreland basin downward during this period.

MC3 - Orogen/Foreland Basin Response Times

In model MC3, the response time of an orogen/foreland basin system to a step function change in Q_V is estimated using the orogen-to-basin sediment flux in the retro-foreland basin ($Q_S(retro)$). Model MC3 uses the same parameter values as MC2. In addition, MC3, like MT5, uses a parallel convergent margin geometry so that an integrated along-strike value of orogen-to-basin sediment flux, $Q_S(retro)$, can be used to characterize the response of the system to changes in Q_V.

In MC3, the instantaneous changes in Q_V cause an immediate increase or decrease in $Q_S(retro)$ (Fig. 4.8). Subsequently, $Q_S(retro)$ returns toward an asymptotic value of $Q_S(retro)$ for MT1. The anomalous character of $Q_S(retro)$ between 3 My and 6 My (①, Fig. 4.8) is caused by deflection of rivers from the retro-foreland basin to the pro-foreland basin with growth of the orogen. This behaviour is not observed after 6 My because drainage networks have become better established in the orogen.

Orogen-to-basin sediment flux, $Q_S(retro)$, increases following an upward step in Q_V as increased precipitation increases river capacity (②, Fig. 4.8). Tectonic flux into the orogen remains approximately constant except for increases related to increased sediment flux to the pro-foreland basin. Therefore, the increase in erosion rates reduces the growth rate of the orogen. The increase in $Q_S(retro)$ is, however, transient, and $Q_S(retro)$ decreases with time as rivers on the orogen and the alluvial plain erode and re-deposit sediments to establish new equilibrium profiles. The decrease in $Q_S(retro)$ is a consequence of increasing alluvial plain elevation, which forces depletion of $Q_V(y)$ approaching the orogen, thereby reducing precipitation and denudation on the orogen. The decrease in $Q_S(retro)$ is opposed by growth of the orogen and the attendant increase in rainfall extraction efficiency. The character of the decrease in $Q_S(retro)$ implies that the fluvial system evolves at a rate proportional to the disequilibrium between the actual and a graded fluvial profile.

Conversely, the instantaneous fall in Q_V (*i.e.*, the change to a drier climate) causes a decrease in $Q_S(retro)$ (③, Fig. 4.8), because of lower vapour flux, thus reducing precipitation and erosion rates on the orogen. Tectonic flux into the orogen remains approximately constant except for decreases caused by decreased sediment flux to the pro-foreland basin ($Q_T(pro)$). With lower rates of material removal from the orogen, the overall rate of orogenic growth is enhanced; that is, a greater portion of $Q_T(pro)$ is stored in the orogen. The result is an increase in orogen elevation and thus in precipitation, which causes an increase in erosion and, therefore, $Q_S(retro)$. The character of the

MC3 and MT1 - Orogen to Retro-foreland Basin Sediment Flux, $Q_{S(retro)}$

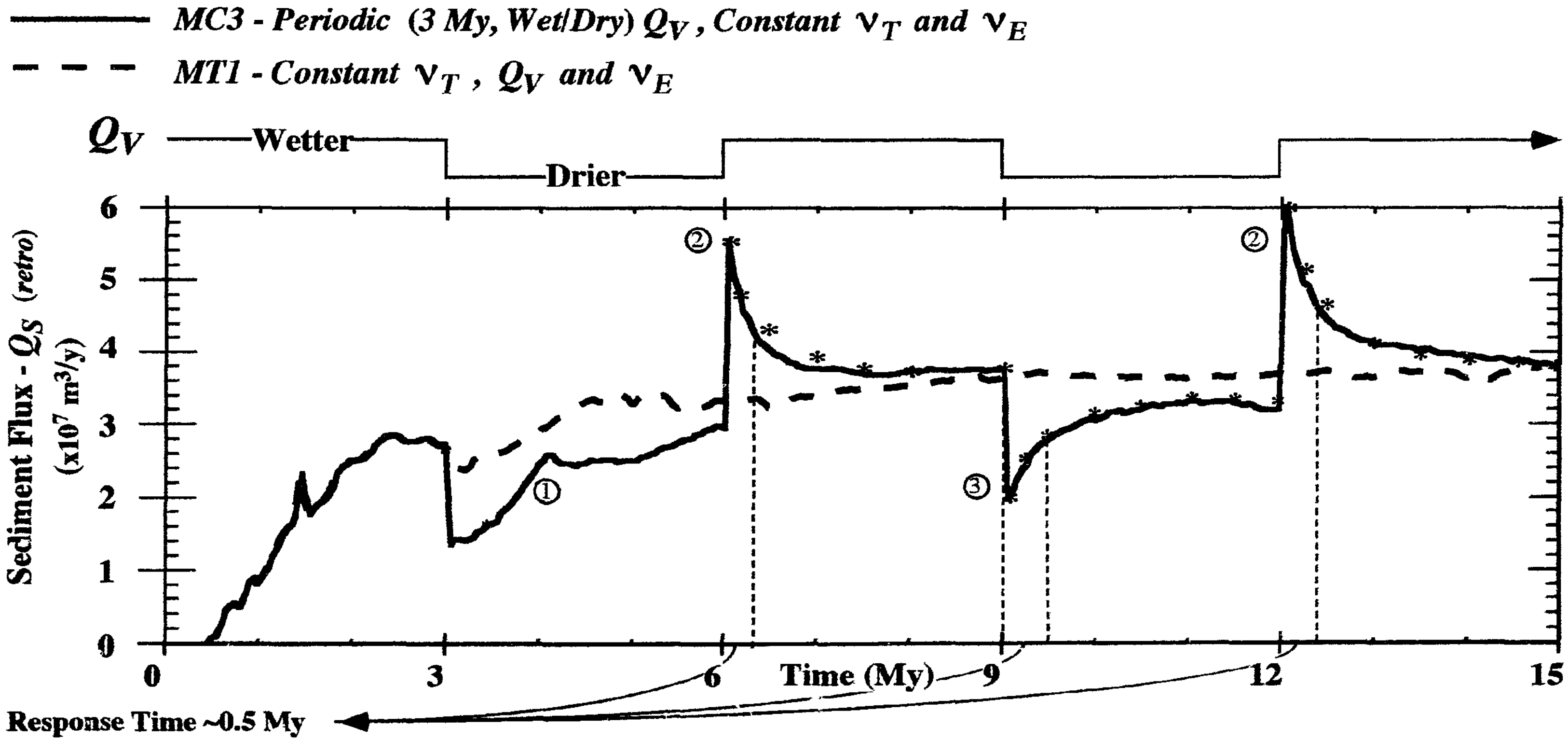

Figure 4.8. The MC3 retro-foreland orogen-to-basin sediment flux ($Q_{S(retro)}$) characterizes the orogen/foreland basin system response to changes in vapour flux (Q_V), *i.e.*, between wetter and drier climatic conditions. MT1 characterizes the response of a system with constant v_T, and Q_V. The estimated reponse time for MC3 assumes that $Q_{S(retro)}$ increases and decreases exponentially with instantaneous changes in Q_V. Asterisks show the calculated exponential response when the response time, τ, is 0.5 My.

increase in $Q_S(retro)$ suggests that the MC3 orogen/foreland basin system evolves at a rate proportional to the rate at which fluvial profiles move toward grade.

The approximately exponential increase or decrease in Q_S(retro) after an instantaneous change in QV suggests that the relationship between the rate of change in QS(retro) and the disequilibrium between the actual and equilibrium profile is approximately linear (Fig. 4.8). The asterisks in Figure 4.8 are an exponential curve calculated according to

$$Q_S(t) = Q_S(equilibrium) + \left(Q_S(initial) - Q_S(equilibrium)\right)e^{-t\tau}$$

where Q_S(initial) is the value of Q_S(retro) just before the instantaneous change in Q_V, Q_S(equilibrium) is the approximate value of Q_S(retro) at the asymptote, and τ is the response time. The difference between this exponential curve and the change in Q_S(retro) is sufficiently small that this composite response, unlike MT5, provides a relatively good measure of one response time; the climatic response time, τ_C ~500 ky. This composite response is a good measure of τ_C both because in MC3 climate is the only process that changes and because the response time for climate change (τ_C ~500 ky) is shorter than for tectonic change (τ_T ~700 ky; MT5a, Fig. 3.20). Furthermore, since tectonics are only modified in a minor way by climate change, there is little evidence of the tectonic response in the composite response. If climate change had a larger effect on tectonics and, for example, caused a change in orogen state, then the composite response would show the effects of both climate and tectonics, similar to MT5.

4.3.2 Periodic Climate Change and Orogen/Basin System Response Time

Model results are used to show the effects of sinusoidal fluctuation in Q_V on retro-foreland basin stratigraphy. In model MC4 the period of fluctuation is much greater than the estimated τ_C above, while in model MC5 it is on the order of τ_C. Orogens in both model results do not change state with variations in Q_V. Models MC4 and MC5 use the same initial conditions and parameter values as MT6 and MT7 respectively, except that Q_V varies while v_T remains constant.

MC4 - 3 My Climatic Periodicity

Figure 4.9 shows the effect of sinusoidal fluctuations in Q_V on retro-foreland basin stratigraphy at 15 My in planform, transverse (A-A') and axial (D-D') sections. The period of fluctuation in Q_V is 3 My, much longer than the estimated climatic response time of the system.

At 15 My the retro-foreland basin seaway is partially filled. Transverse rivers extend across most of the basin, and coalesce in a trunk river which subparallels the peripheral bulge along the basin's distal edge (Fig. 4.9). River-power facies of sediment deposited by the axial trunk river increase as the trunk river discharge increases with collection from tributaries draining the alluvial plain and peripheral bulge. Migration of the peripheral bulge and the axial river with growth of the alluvial plain captures the river draining the continent (①, Fig. 4.9), similar to MC2.

Climate periodicity is recorded in basin strata as a change in the divergence of time lines and as progradation or retrogradation of alluvial facies (Fig. 4.9). The change in time-line convergence reflects variations in the gradient of sedimentation rate (*i.e.*, change in sedimentation rate across the basin) with periodicity in Q_V. Intervals of higher Q_V ('wet' intervals) correspond with more uniform or parallel time line geometry (②, Fig. 4.9), while periods of lower Q_V ('dry' intervals) correspond with convergence of time lines away from the orogen (③, Fig. 4.9). Progradation and retrogradation of river-power facies on the lower alluvial plain also reflect periodicity in Q_V. Wet intervals correspond to greater fluvial sediment transport and, therefore, progradation of moderate river-power facies. Conversely, dry intervals correspond with a decrease in the efficiency of fluvial

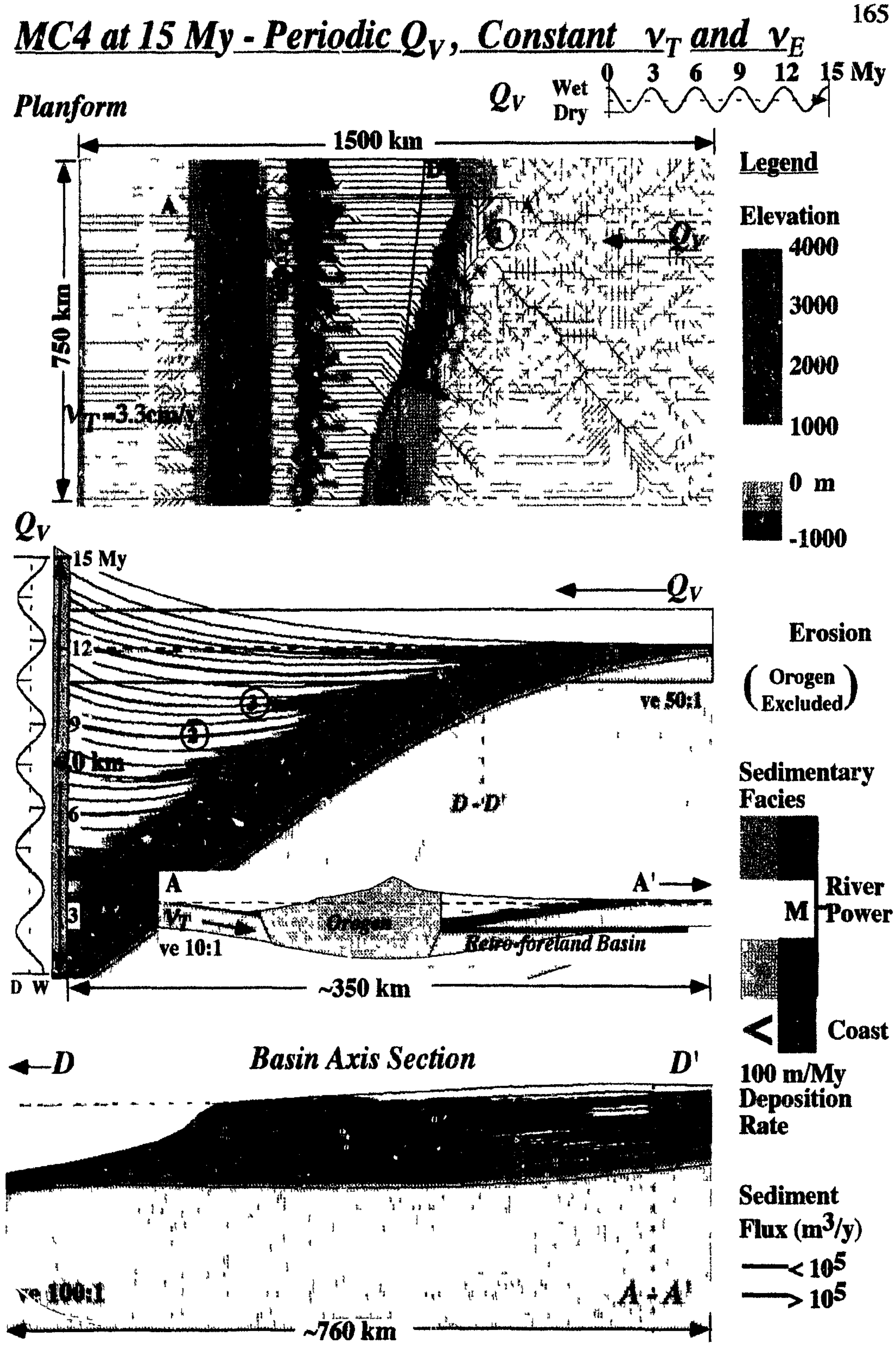

Figure 4.9 MC4 is shown in planform, transverse (regional A-A' and retro-foreland basin) and longitudinal section (D-D'), at 15 My. Time lines are at 0.5 My intervals. Those lines coeval with minimum Q_T are red, while those coeval with maximum Q_T are blue. Box outlines the region enlarged in Figure 4.10.

transport across the alluvial plain, and therefore retrogradation of lower river-power facies.

Changes in the distribution of basin facies and time-line geometry are in phase with changes in Q_V (Fig. 4.9). This relationship is particularly evident in the symmetry of time-line spacing about times of maximum and minimum Q_V (Figs. 4.9, 4.10). This synchronization occurs because the 3 My period of fluctuation in Q_V is much longer than the ~0.5 My climatic response time; thus there is sufficient time for fluvial systems to regrade in response to changes in Q_V. This result is consistent with those of MT6 and with Kooi and Beaumont (submitted). Further expression of there being sufficient time for the fluvial system to respond to changes in Q_V is found along the basin axis where progradation is uninterrupted by changes in Q_V, unlike MC2 (Figs. 4.9, 4.6). In MC4, unlike MC2, the rate of progradation decreases during drier intervals (④, Fig. 4.9), and there is no transgression (①, Fig. 4.6). The transgression in MC2 is a transient effect of the instantaneous change in Q_V. In MC4, the rate of change in Q_V is sufficiently slow that the decreasing sediment flux to the coast through fluvial systems in dynamic equilibrium can keep pace with the rate of change in relative sea-level rise. This comparison does not imply that climate change can only cause transgression as a transient effect of rapid climate change; transgressions might also occur with a fluvial system in dynamic equilibrium if the minimum value of Q_V were lower.

Comparison of the climatic effect on alluvial plain sedimentation (A-A', Fig. 4.9) with that on basin axis sedimentation (D-D'), emphasizes that in the models the effects of climate change on facies distribution and time-line geometry is greatest adjacent to the orogen due to orographic control of precipitation at higher elevations.

MC4 at 15 My, Enlarged Retro-foreland Basin, Periodic Q_V, Constant v_T and v_E

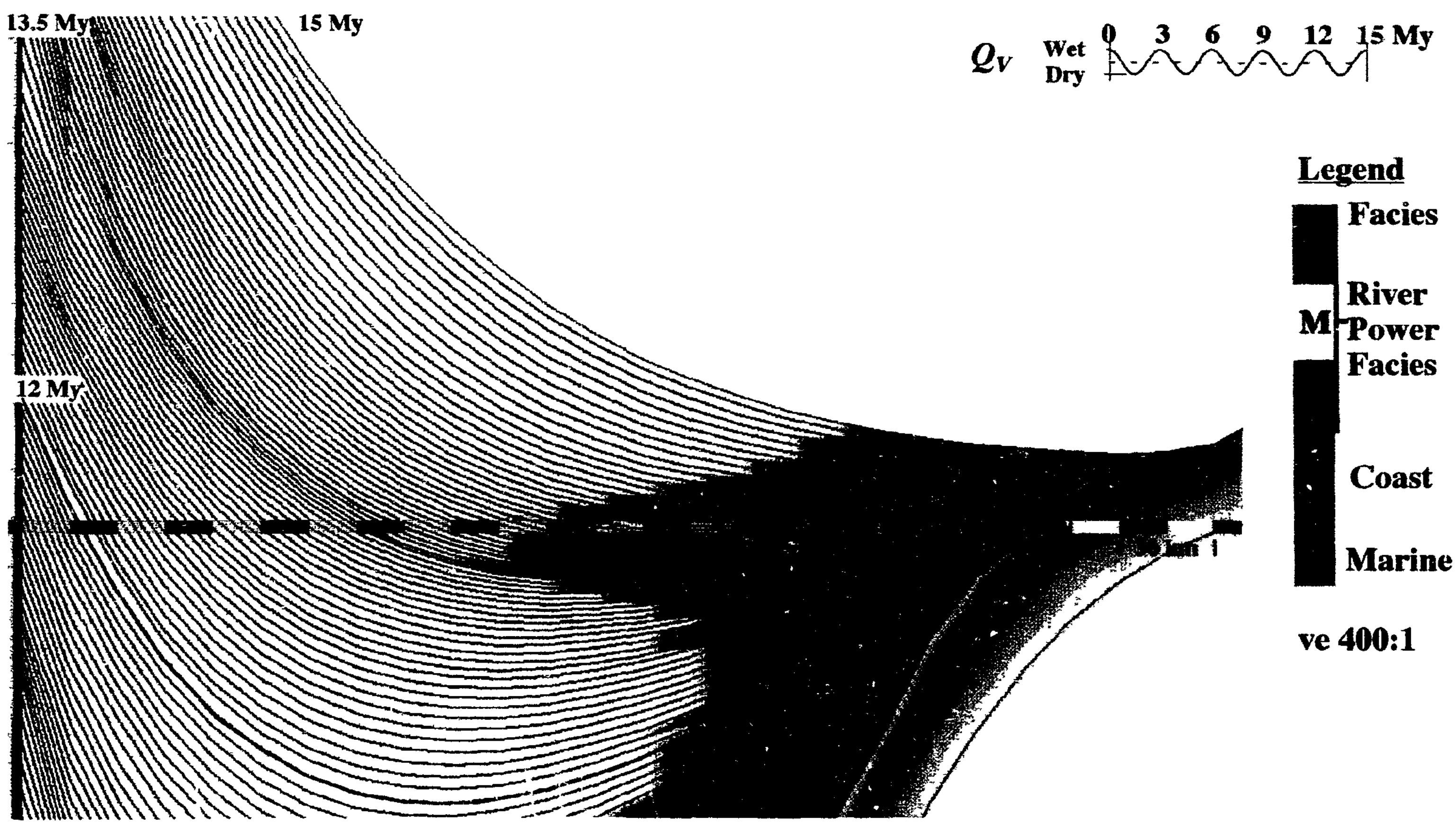

Figure 4.10. The enlarged MC4 retro-foreland basin (box, Fig. 4.9) shows progradation and retrogradation of alluvial facies (colour) and changes in time lines (black) with periodic changes in vapour flux (Q_V). Time lines are at 50 ky intervals. Time lines coeval with minimum Q_V are red, while lines coeval with maximum Q_V are blue.

MC5 - 400 ky Climatic Periodicity

The effect of 400 ky sinusoidal fluctuations in Q_V on retro-foreland basin stratigraphy is shown at 15 My in planform, transverse and axial sections in Figure 4.11. In general, the development of the orogen and retro-foreland basin appears similar to that of MT3 (Figs. 4.11, 3.10). The effects of periodicity in Q_V on model facies are progradation and retrogradation of moderate river-power facies in the distal basin (①, Fig. 4.11; Fig. 4.12). The lateral extent of facies changes in MC5 is less than that observed in either MC2 or MC4 (Figs. 4.4, 4.10). In MC5, the period of fluctuations in Q_V is on the order of the climatic response time of the orogen/foreland basin system (~0.5 My). Fluvial systems on both the orogen and foreland basin therefore lack sufficient time to respond completely to changes in Q_V, limiting the extent of progradation and retrogradation, similar to MT7. In Figure 4.11, time lines are at 400 ky intervals, coeval with times of maximum Q_V, and therefore do not demonstrate the effects of periodic Q_V fluctuation.

Retro-foreland basin stratigraphy of MC5 also preserves the characteristic changes in sedimentation rate (time-line geometry) that result from changes in Q_V (Fig. 4.12), similar to MC2 and MC4. In MC5, however, the rate of change in Q_V is sufficiently fast that its effects are preserved between periods of maximum and minimum Q_V (Fig. 4.12), unlike MC4. Therefore, time lines show an increased convergence away from the orogen subsequent to periods of decreasing Q_V (②, Fig. 4.12) similar to the increase in time-line convergence caused by an instantaneous decrease in Q_V, as in MC2 (Fig. 4.10). Similarly, in MC5, periods of increasing Q_V show time lines that characterize more uniform sedimentation across the basin (③, Fig. 4.12), which corresponds to the change in sedimentation rates caused by an instantaneous increase in Q_V in MC2 (Fig. 4.10). Time-line geometries, therefore, differ from MC4 in that changes

MC5 at 15 My, Enlarged Retro-foreland Basin - Periodic Q_V, Constant n_T and n_E

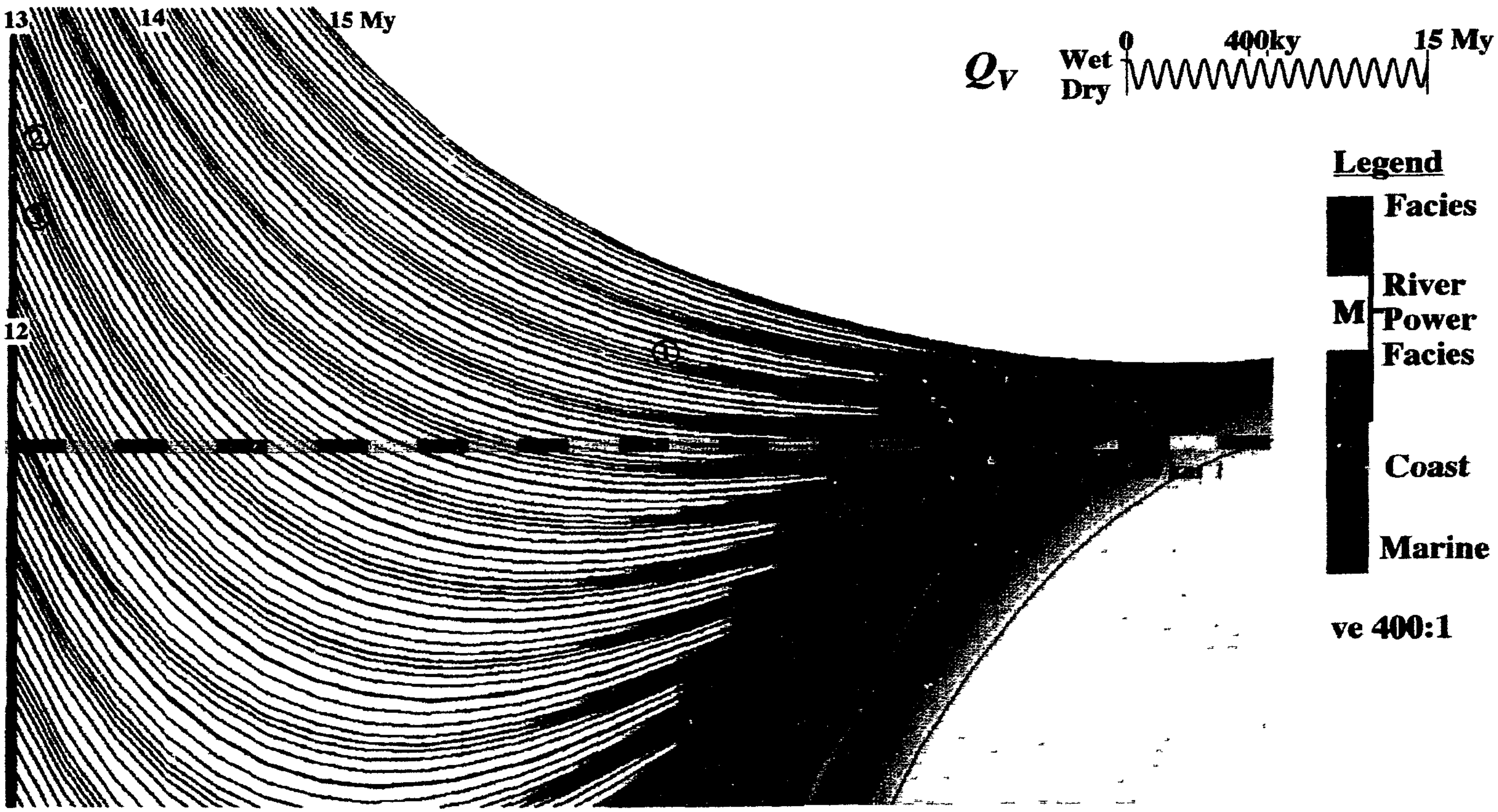

Figure 4.12. In section, the MC5 retro-foreland basin (box, Fig. 4.11) shows progradation and retrogradation of alluvial basin facies (colour), and changes in time-line (black) geometry, with 400 ky periodicity in vapour flux (Q_V). Time lines are at 50 ky intervals. Red lines are coeval with minimum Q_V, while blue lines are coeval with maximum Q_V.

in time-line spacing are asymmetric about periods of maximum and minimum Q_V (Figs. 4.12, 4.10). This asymmetry indicates that regrading of rivers tends to lag behind, out of phase with changes in Q_V. The phase lag is analogous to the MT7 results and the results of Kooi and Beaumont (submitted). These authors find that a phase lag in sediment yield is to be expected when the periodicity of the forcing function (in their case the tectonic uplift rate) is on the order of the climatic response time of the orogen/foreland basin system.

In summary, MC5 results show essential stratigraphic characteristics related to periodicity in Q_V, similar to MC2 and MC4. However, these characteristics are different in extent and timing, reflecting the inability of surface processes to respond in dynamic equilibrium to changes in Q_V when the period of change is on the order of, or less than, the minimum response time of the system. If a similar phase lag occurs in natural systems, then the minimum response time of the fluvial system will be an important consideration when correlating changes in sedimentary fluvial architecture with independent evidence of climate change (e.g., isotope or palynological data). For example, the minimum system response time may provide a reasonable explanation for why sedimentary facies can lag behind other indicators of rapid climate change. Measurements of the lag, while other factors remain constant, may provide a method for estimating the minimum response time of natural systems.

4.4 Coupled Tectonic and Climatic Periodicity

Natural climate change can occur independently of tectonics (for example, glaciation or global warming). It can also change in association with tectonism, as when orogens modify global circulation patterns, leading to changes in weather patterns (*e.g.*, Himalayan monsoons, Crowley and North, 1991). In addition, both tectonics and climate can change over very different time scales.

Model results herein indicate that changes in tectonics and climate both affect development of foreland basin stratigraphy, principally through their effect on fluvial systems in the orogen and across the alluvial plain. For example, models MC2 and MT4, respectively, show that either an increase in vapour flux or a decrease in the rate of tectonic convergence can cause a decrease in the orogen growth rate and an increase in the progradation rate. The opposite is also true (Fig. 4.3). Models MTC1 and MTC2 show the effect on retro-foreland basin stratigraphy when Q_V and v_T reinforce and counteract each other, respectively.

Comparison of MTC1 and MTC2

In MTC1 and MTC2, Q_V and v_T vary with a period of 3 My and have the same parameter values as MC4 and MT6, respectively; the time-averaged Q_V and v_T are the same in both MTC1 and MTC2, and all other parameter values remain constant. In MTC1, maximum Q_V occurs when v_T is at a minimum, while the opposite occurs in MTC2. Model results are shown in planform, transverse and axial sections at 15 My (Figs. 4.13, 4.14, 4.15, 4.16).

The results at 15 My show a partially filled retro-foreland seaway, similar to MT6 (Figs. 3.20, 3.21), with stacked, low-order sequences characterized by increasingly alluvial sedimentation (Figs. 4.13, 4.14, 4.15, 4.16). As in MT6, the sequences are a consequence of the 3 My periodicity in v_T which changes the orogen state. Sequence boundaries comprise an unconformity proximal to the orogen, a laterally correlative decrease in sedimentation rates, a flooding surface in some instances and an unconformity in the continentally-derived sediments adjacent to the peripheral bulge. Although the overall width and thickness of the MTC1 and MTC2 basins are comparable, sequences are better developed in MTC1. These sequences are better developed because the effects of periodicity in Q_V enhance rates of orogen growth, erosion and sediment transport. When v_T is increasing, both orogens change from a destructive to a constructive state. Strata in these intervals are characterized by an increase in the divergence of time lines toward the orogen, a retrogradation of river-power facies in some instances, and subsequent progradation of alluvial facies away from the orogen (Fig. 4.15; ①, Fig. 4.16). The decrease in MTC1, while v_T is increasing, enhances orogen growth rates and retards sediment transport away from the orogen. Associated changes in sediment flux to the seaway and subsidence rates, enhance initial retrogradation, inhibit subsequent progradation and promote development of a deeper seaway. Conversely, increasing Q_V in MTC2 while v_T is increasing has the opposite effect, causing higher rates of erosion in the orogen, thereby inhibiting orogen growth and increasing precipitation across the alluvial plain, thus enhancing transport away from the orogen. These effects prevent retrogradation, enhance progradation, and promote a shallower marine basin. As a consequence, strata created in MTC1 differ from MTC2 in that time-line gradients in alluvial facies are steeper, retrogradation is more extensive, progradation is less extensive and the seaway is deeper (Figs. 4.15; ②, 4.16).

When v_T is decreasing in MTC1 and MTC2, both orogens change from a constructive to a destructive state. Basin stratigraphy in these intervals is characterized by a decrease in sedimentation rates, a decrease in the divergence of time lines toward the orogen, an increase in the rate of progradation and erosion of sediments deposited adjacent to the orogen (Figs. 4.15, 4.16). In MTC1, increasing Q_V enhances the exhumation rate of the orogen, the rate of isostatic rebound, the orogen-to-basin sediment flux ($Q_S(retro)$), and the transport of sediment to the seaway. The opposite is true with decreasing Q_V in MTC2. The result is that rivers regrade toward equilibrium faster in MTC1 than in MTC2. As a consequence, strata in MTC1 differ from MTC2 in that sedimentation rates are slower (③, Figs. 4.15, 4.16), progradation rates are faster and erosional surfaces are more extensive (④, Figs. 4.15, 4.16). The results show that

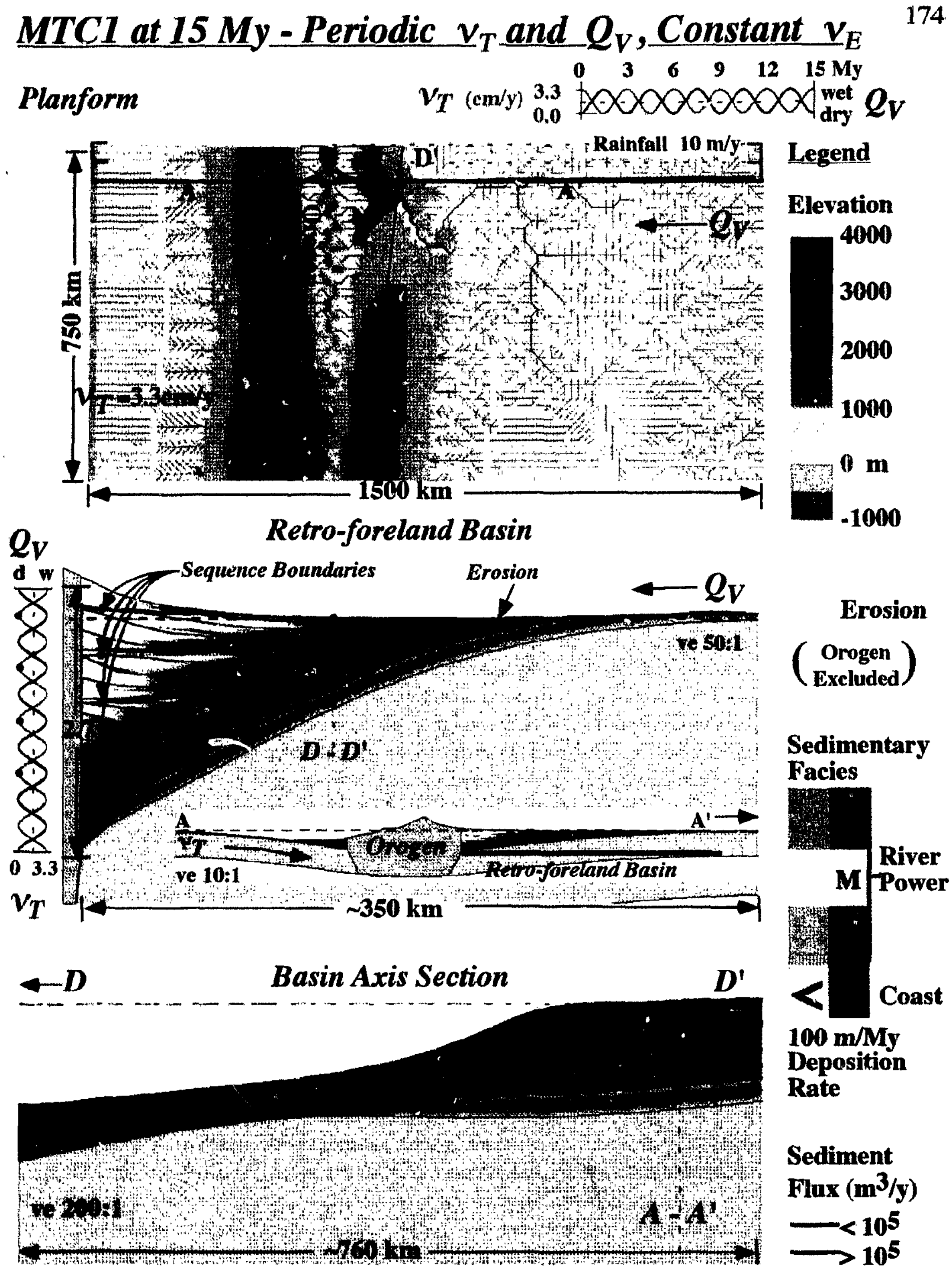

Figure 4.13. MTC1 is shown in planform, transverse and longitudinal sections at 15 My. MTC1 experiences periodic fluctuation in v_T and Q_V. Facies (colour) and time-line geometry (black) characterize stacked sequences. Time lines are at 500 ky intervals. Sequence boundaries are coeval with times of minimum v_T and maximum Q_V (black dots).

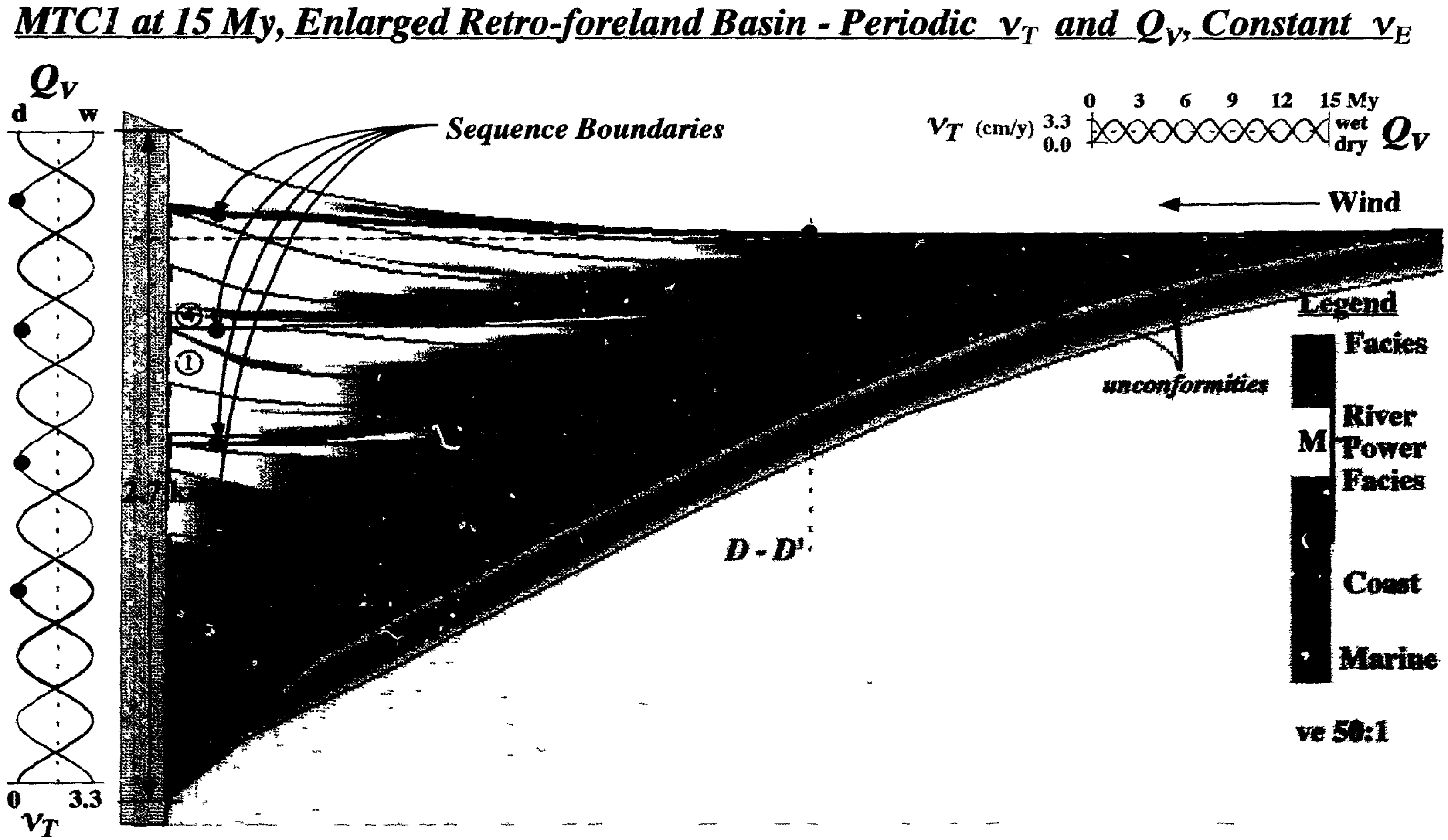

Figure 4 14. In the MTC1 retro-foreland basin, sedimentary facies (colour) and time-line (black) geometry characterize stacked sequences. Sequence boundaries comprise erosional surfaces proximal to the orogen, low sedimentation rates and perhaps flooding surfaces in the medial basin, and erosional surfaces adjacent to the peripheral bulge. Sequence boundaries are coeval with times of minimum v_T and maximum Q_V.

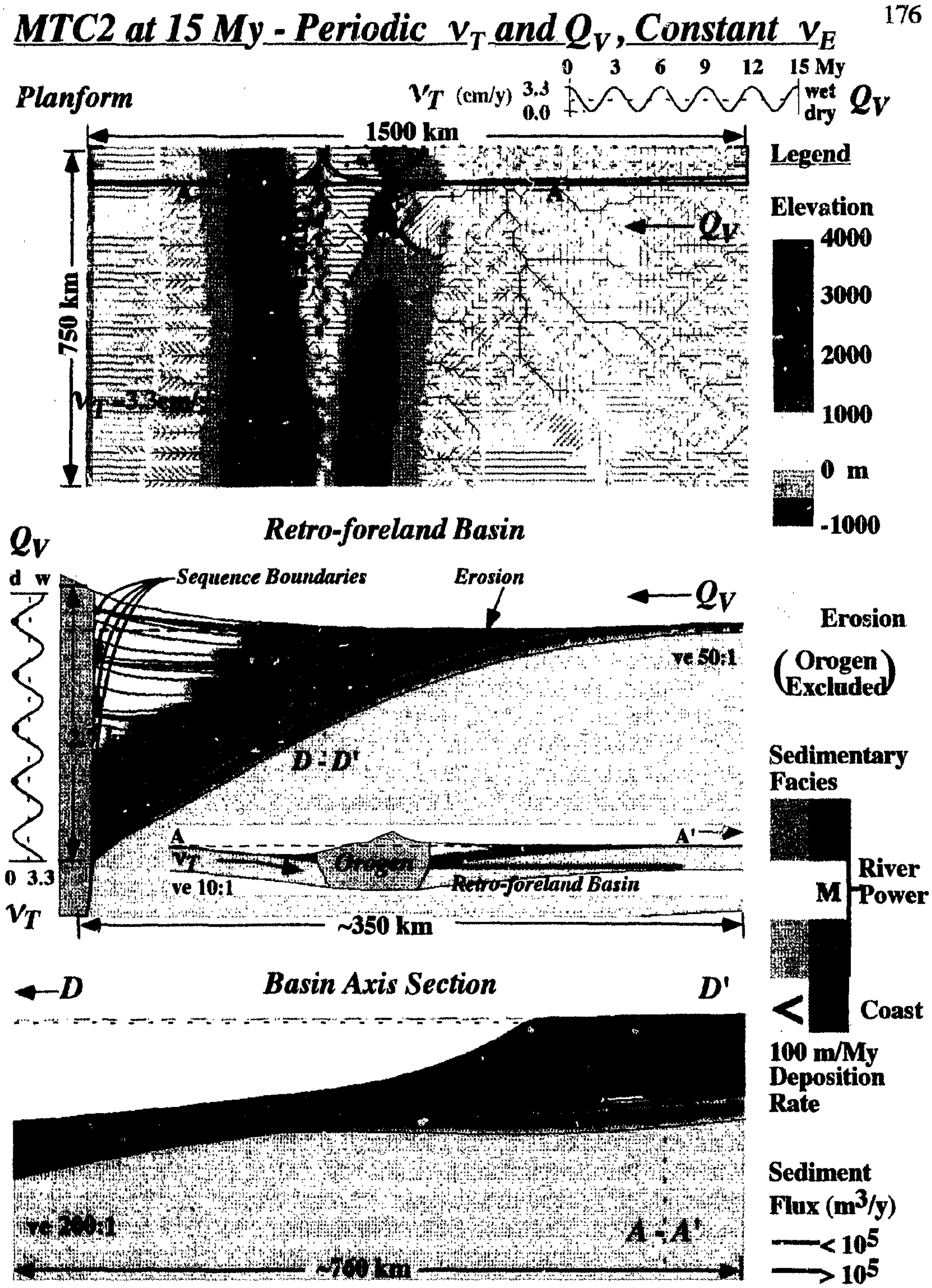

Figure 4.15. MTC2 is shown in planform, transverse and longitudinal sections at 15 My. MTC2 experiences periodic fluctuation in v_T and Q_V. Sedimentary facies (colour) and time-line geometry (black) show poorly developed stacked sequences. Time lines are at 500 ky intervals. Sequence boundaries are coeval with times of minimum v_T and Q_V (black dots in sections).

MTC2 at 15 My, Retro-foreland Basin - Periodic v_T and Q_V, Constant v_E

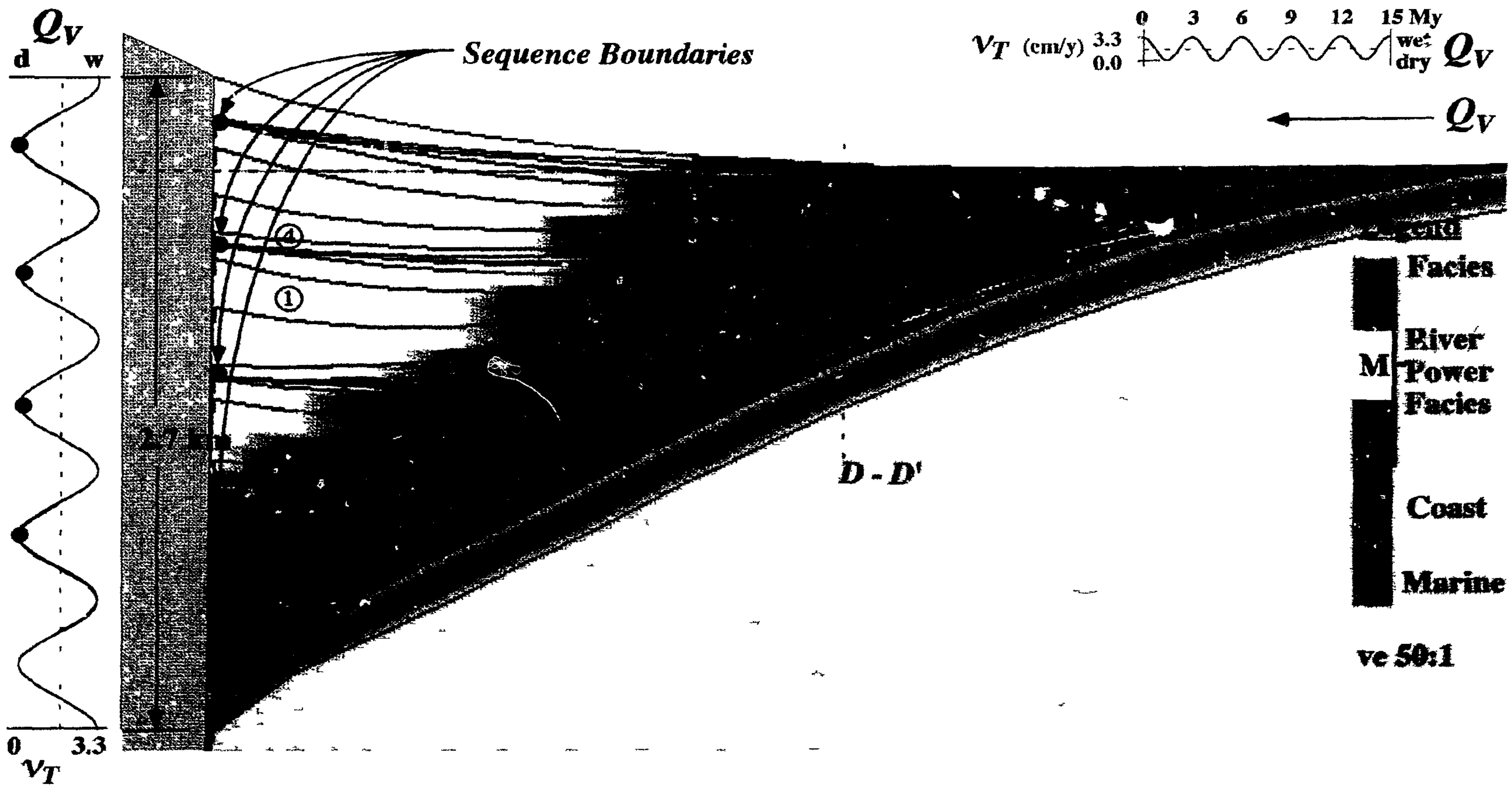

Figure 4 16 In the MTC2 retro-foreland basin, sedimentary facies (colour) and time-line (black) geometry characterize poorly developed stacked sequences Sequence boundaries comprise erosional surfaces proximal to the orogen, low sedimentation rates in the medial basin, and erosional surfaces adjacent to the peripheral bulge Sequence boundaries are coeval with times of minimum v_T and Q_V

sequences and sequence boundaries are better developed in MTC1 than in MTC2 (Figs. 4.15, 4.16). In summary, although both MTC1 and MTC2 are similar in overall geometry, the retro-foreland basin stratigraphy differs significantly in the two models because the effects of periodicity in Q_V reinforce or counteract those of periodicity in v_T (Figs. 4.13, 4.14, 4.15, 4.16).

4.5 Summary

Model results demonstrate the influence of windward and leeward basin setting (MC1, Section 4.2), periodicity in precipitation (MC2, Section 4.3.1), and orogen/foreland basin response (MC3 to MC5, Section 4.3.2) on the development of foreland basin stratigraphy. Results also show that changes in either precipitation or tectonics can reinforce or counteract each other (MTC1, MTC2, Section 4.4). The findings from the model results are summarized in the following points:

- Leeward forelands in the model and nature have less precipitation than their windward counterparts. They typically have lower erosion rates, smaller orogen-to-basin sediment flux and lower transport rates away from the orogen. As a consequence, leeward foreland basins are likely to show a larger gradient in decreasing in sedimentation rates away from the orogen, steeper subaerial surface slopes, and slower basin filling rates away from the orogen than windward foreland basins in an equivalent tectonic setting.
- Characteristics of a model response to changes between wetter and drier climatic conditions are summarized in Table 4.1. These characteristics are more or less evident, depending on the amplitude and rate of vapour flux by comparison with the minimum response time of the system.

Change in Vapour Flux (Q_V)	Orogen		Alluvial Plain				Peripheral Bulge		
	Growth Rate ± ve	Q_S	Erosion	Sea Level	Sedimentation Rate Gradient	Facies $\Leftarrow / \Rightarrow$	Sea Level	Facies	Erosion
$Q_V \Downarrow$	$+\Uparrow$	$\Downarrow$ then $\Uparrow$	No	rise	$\Uparrow$ then $\Downarrow$	$\Leftarrow$ then $\Rightarrow$	rise	$\Rightarrow$ then $\Leftarrow$	Yes
$Q_V \Uparrow$	$+\Downarrow$	$\Uparrow$	No	rise	$\Downarrow$	$\Rightarrow$	rise	$\Rightarrow$	No

Table 4.1. Summary of stratigraphic characteristics reflecting change between wetter and drier climatic conditions, with variations in vapour flux Q_V. The symbol $\Rightarrow$ denotes progradation and $\Leftarrow$ denotes retrogradation, while $\Uparrow$ denotes increase and $\Downarrow$ denotes decrease.

- Cyclic variations in vapour flux between wetter and drier conditions create cyclic retrogradational/progradational sedimentation cycles. However, large variations in precipitation (MC2, Fig. 4.4) can occur without creating regionally extensive erosional or flooding surfaces, and therefore, without creating sequence boundaries. Furthermore, such variations do not necessarily cause a change in orogen state.

- The period of change in vapour flux relative to the minimum response time of the orogen/foreland basin system strongly influences the character of foreland basin stratigraphy. When the period of change in vapour flux is much greater than the minimum response time, the stratigraphic characteristics of climate change (Table 4.1) are evident and in phase with this periodicity. When periodicity in vapour flux is on the order of the minimum response time, changes in facies distribution and chronostratigraphy are subtle and the periodicity of facies change lags behind. The implication for understanding natural/orogen foreland basin systems is that high frequency changes between wetter and drier climatic conditions are likely to be best preserved where fluvial systems change character over short space scales (*e.g.*, alluvial fans, Frostick and Reid, 1989; deltas, de Boer *et al.*, 1991). Furthermore, stratigraphic indicators of climate change may lag behind independent indicators.

- In the model, climate change generally has a greater effect on the upper watershed than on the lower alluvial plain or seaway, due to orographic control of precipitation. The effects of climate change are similar to those of change in tectonics, because both cause change in basin stratigraphy through impacts that preferentially focus on the orogen and higher elevations of the alluvial plain. As a consequence, changes in tectonics and climate can either reinforce or counteract each other, thereby enhancing or retarding their effects on foreland basin stratigraphy.

Chapter 5

Effects of Eustasy on Orogen/Foreland Basin Systems

5.1 Introduction

Sea level marks the transition between subaerial and submarine surface processes; it is characterized either by facies diagnostic of shoreline sedimentation or by the juxtaposition of facies and/or stratal geometries that reflect this transition. Historically, changes in sea level on time scales of less than 10 My have been inferred from the landward or seaward migration of the shoreline (Suess, 1906, cit. Christie-Blick *et al.*, 1990). Shoreline migration occurs because of competition among the rates of relative sea-level change, sediment delivery to the shoreface and sediment removal from the shoreface (Galloway, 1989; Schumm, 1993; Wescott, 1993). Eustasy is one mechanism that can cause a relative change in sea level.

Eustasy is a global relative change in sea level caused by changes in seawater volume or surface relief of the earth. In nature, eustatic changes vary from millimetres to hundreds of metres over time scales of 1 to 10^8 years. Some of the processes believed responsible for global sea-level variations and the related magnitude and duration of these changes are (Revelle *et al.*, 1990):

• Glacial accretion and wastage	10^{-2} to 10^2 m,	10^1 to 10^5 years
• Changes in river, lake and aquifer volumes	10^{-3} to 10^1 m,	10^2 to 10^5 years
• Crustal deformation	10^{-1} to 10^2 m,	10^2 to 10^8 years.

Of particular interest to this research are sea-level variations on the time scales normally associated with tectonics of 10 ky to 10 My and with relative sea-level changes on the order of 1-100 metres.

Eustasy significantly affects foreland basin stratigraphy, principally through changes in fluvial baselevel that result in lateral changes in the distribution of subaerial and submarine environments (Galloway, 1989; Schumm, 1993; Wescott, 1993). The effects of eustasy differ from those of tectonic and climatic processes in that eustasy has a relatively small influence on sediment delivery to the coast (Schumm, 1993).

Progradation and retrogradation result from competition between net sediment flux and the eustatically forced change in coastal volume (Sec. 2.9). In the model, net sediment flux to the coast is primarily determined by the difference between fluvial transport to, and marine transport away from, the coast (Sec. 2.9). Changes in net sediment flux primarily reflect how local changes in subaerial and submarine surface slope affect fluvial and submarine transport. Eustatically forced changes in fluvial sediment flux are a consequence of headward regrading in response to surface slope and baselevel changes. Changes in coastal volume are primarily determined by coastal geometry, the rate of relative sea-level change and the marine depositional surface slope.

Model experiments illustrate the influence of changes in topography and coastal volume on the development of transgressive/regressive cycles. Step function changes in sea level are used to isolate the effects of topography from the effects of net sediment flux. Sinusoidal fluctuations are used to show how competition between net sediment flux and changes in coastal volume affect the rates of progradation and retrogradation. Both step and sinusoidal changes in sea level are varied between ±50 m elevation relative to model datum for periods of 400 ky and 3 My. An absolute sea-level change of 100 m is used, based on the average sea-level fluctuations for periods of less than 10 My in the Tertiary (Haq *et al.*, 1988). The 400 ky period is chosen because it approximates the 400 ky period of eccentricity in Earth orbit (Milankovitch Cycle) associated with global sea-level change. The 3 My period is chosen because it is on the order of magnitude of the 2 My and 3.4 My periodicity in orbital eccentricity (Fischer *et al.*, 1990) and approximates the median period for global sea-level change based on Haq *et al.*'s (1988) coastal onlap chart. These periods are consistent with those used in the tectonic and climate model experiments.

In nature, erosional surfaces can be created by eustatically forced rise or fall in sea level. Erosional surfaces associated with a rise in sea level may be caused, for example, by currents, or by wave-cutting or slumping of lowstand deposits (Christie-Blick *et al.*, 1990). Erosional surfaces created by a fall in relative sea level are caused by fluvial incision of highstand shorelines. The latter type of surface has been defined as *a* Type-1 erosional surface by Van Wagoner *et al.* (1988) and Posamentier *et al.* (1988).

Type-1 surfaces form when the rate of relative sea-level fall is greater than the rate of basin subsidence at the shoreline, giving rise to incision with baselevel lowering. Schumm (1993) adds that Type-1 surfaces may form under these conditions only if the shelf slope is steeper than the alluvial plain slope. Furthermore, Schumm (1993) observes that while an increase in slope at the shoreline and a relative sea-level fall are necessary conditions for the creation of Type-1 surfaces, they do not ensure the formation of such a surface because neither the effects of sediment delivery to and away from the coast nor those of river regrading by changes in sinuosity have been considered. Therefore, the formation of a Type-1 surface requires that the effects of sea-level fall be greater than those of both sediment delivery to the coast and of regrading. These conditions are likely to occur with rapid changes in sea level.

The model results show the development of Type-1 surfaces. One model experiment, using an instantaneous change in sea level, is designed to show in detail the development of a Type-1 surface. Model experiments with sinusoidal changes in sea level illustrate how competition between net sediment flux and the change in coastal volume affect the development of Type-1 surfaces. This model and others also show how erosional surfaces can be created by both a relative rise and fall in sea level.

Both climate and tectonics have significant effects on net sediment flux and relative sea-level change. Changes in climate and tectonics modify the fluvial sediment flux through regrading of the upper fluvial system. Relative sea level is modified through isostatic compensation by changing the distribution of orogenic and sedimentary loads. Eustatic fluctuations in sea level act either to reinforce or counteract the effects of tectonics or climate. Several model experiments show how eustasy reinforces or counteracts these effects of periodic changes in climate and tectonics.

5.2 Eustasy-Dominated Stratigraphic Sequences

When eustatically forced changes in coastal volume are much greater than the change in net sediment flux, the extent of transgression and regression is effectively determined by the coastal topography and the amplitude of sea-level change. In nature, however, the extent of transgression and regression is not exclusively determined by these factors because there is usually sediment flux to the coast that changes with regrading of the fluvial system in response to changes in baselevel. Sediment flux also continues to change as fluvial systems respond to the continued interaction of tectonic, climatic and isostatic processes. Models in which eustatic sea-level changes take the form of a step function are used to illustrate the limiting case where these changes totally dominate the concurrent sedimentary response Transgressions and regressions are created by an alternating instantaneous rise and fall in sea level separated by periods of constant sea level ($v_E = 0$). Model ME1 illustrates how the character of stratigraphic sequences caused by step eustatic changes evolves during the progressive filling of a

ME2 at 10.605 My - Periodic ν_E, Constant Q_V & ν_T

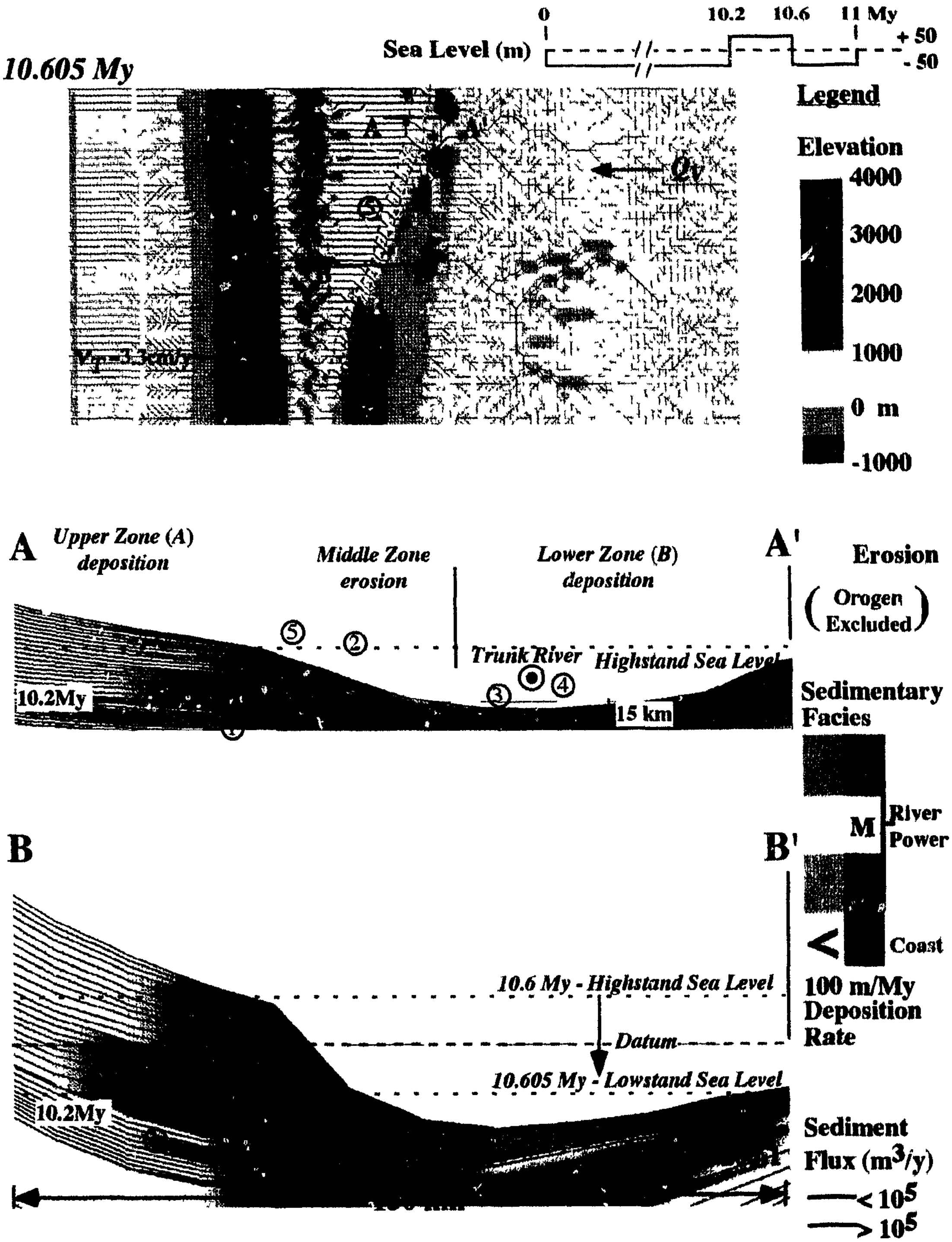

Figure 5.5. ME2 is shown in planform and section at 10.605 My, immediately after the fall in sea level. Sections A-A' and B-B' show how the highstand adjacent to the alluvial plain varies along strike. Facies are in colour; time lines (black) are at 20 ky intervals.

retro-foreland basin. Model ME2 provides a detailed example of how a single sequence and a Type-1 erosional surface are created.

ME1 - Orogen/Foreland Development

Model ME1 illustrates how the effect of eustasy changes as the alluvial plain surface slope progressively evolves during foreland basin development. Sea level alternately rises and falls between ±50 m elevation at 400 ky intervals, but otherwise remains constant. Initial conditions and all other parameter values are the same as for MT3, except that the continental plates have an initial slope of 1/10000 toward the ocean, as discussed in MT4. ME1 after 15 My is shown in planform, fence diagram and sections (Figs. 5.1, 5.2).

In planform, the ME1 orogen elevation, extent of basin filling and facies distributions are comparable to those of MT3 (Figs. 3.9, 5.1). Axial progradation appears somewhat more extensive in ME1 because sea level is at –50 m elevation. Furthermore, sediment flux from the craton also contributes to axial progradation, as evidenced by the higher river-power facies deposited along the axial river in ME1.

In section, the general character of ME1 facies shows growth of the alluvial plain, reduction in river-power facies adjacent to the coast and tapering-out of marine facies with filling of the basin (Fig. 5.2). These results are similar to the facies distribution in MT3 where v_E, v_T and Q_V are all constant (Fig. 3.10). Facies distributions in ME1 differ from those in MT3 because eustasy creates transgressive/regressive cycles along the

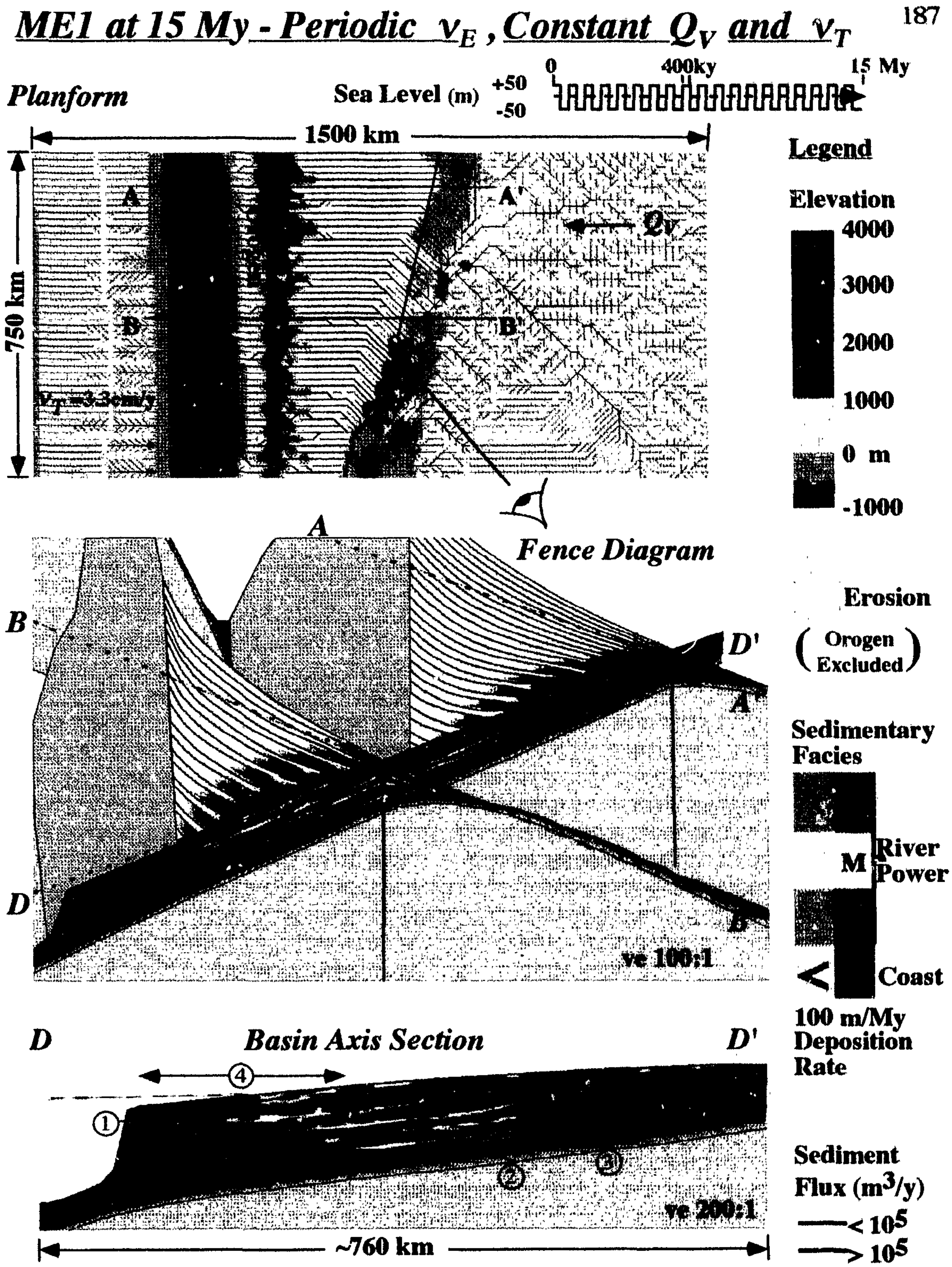

Figure 5.1. ME1 retro-foreland basin in planform, fence diagram and axial section at 15 My. ME1 shows the change in extent of retrogradation and progradation (facies in colour) with filling of the retro-foreland basin. Time lines (black) are at 400 ky intervals and are synchronous with sea-level change.

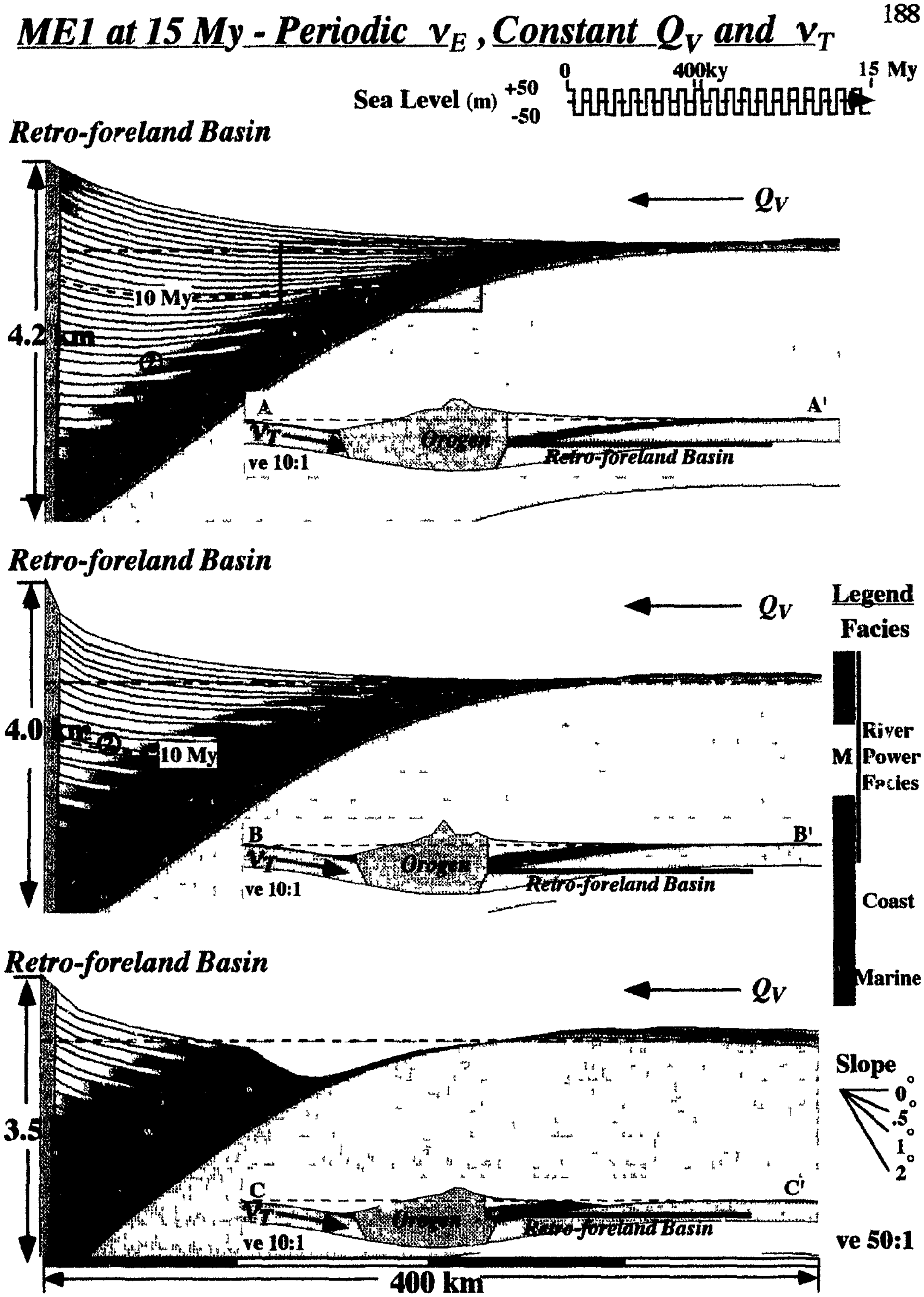

Figure 5.2 ME1 at 15 My in regional and enlarged retro-foreland basin sections. Sections show how the extent of transgressive/regressive cycles changes along strike, and with filling of the basin. Time lines (black) are at 400 ky intervals and synchronous with sea-level change. Box outlines the region enlarged in Figure 5.3.

seaway margins (Fig. 5.2). Time lines shown in Figure 5.2 are at 400 ky intervals, in phase with the 400 ky step function in V_E; each time line marks either a rise or fall in sea level. The boxed area in Figure 5.2 is enlarged in Figure 5.3 to show the effects of instantaneous sea-level change.

In ME1, eustasy forces an instantaneous relative rise in sea level that causes flooding and deposition of coastal and/or marine facies over the lower alluvial plain (①, Figs. 5.2; 5.3). The maximum extent of flooding reflects both eustasy and the relative rise in sea level caused by isostatic compensation for the change in water load. Surface slope and the relative sea-level rise determine the extent of transgression because for an instantaneous change in sea level, there is no sediment flux to compete with the change in coastal volume (Sec. 2.9). As a consequence, these events do not create retrogradational facies at the instant when sea level changes.

Following the eustatic change, there is minor retrograde facies deposition filling the newly created coastal volume followed by progradation. Progradation resumes because net sediment flux to the coast is once again greater than the change in coastal volume created by the isostatically forced rise in relative sea level (②, Fig. 5.2; Fig. 5.3). The increase in sedimentation rates adjacent to the coast and the new disequilibrium between fluvial and marine sediment fluxes is reflected in the change in time-line geometry (②, Fig. 5.3). Sedimentation causes a local increase in the submarine surface slope and a decrease in the subaerial surface slope. The former causes an increase in sediment transport away from the coast; the latter causes an increase in sedimentation rates and regrading of the fluvial system toward the orogen, as observed in the direction of time-line convergence (③, Fig, 5.3). Both act to reduce the sediment flux disequilibrium at the coast, and to establish a new fluvial equilibrium profile. This

ME1 at 15 My, Enlarged Retro-foreland Basin - Periodic v_E, Constant Q_V and v_T

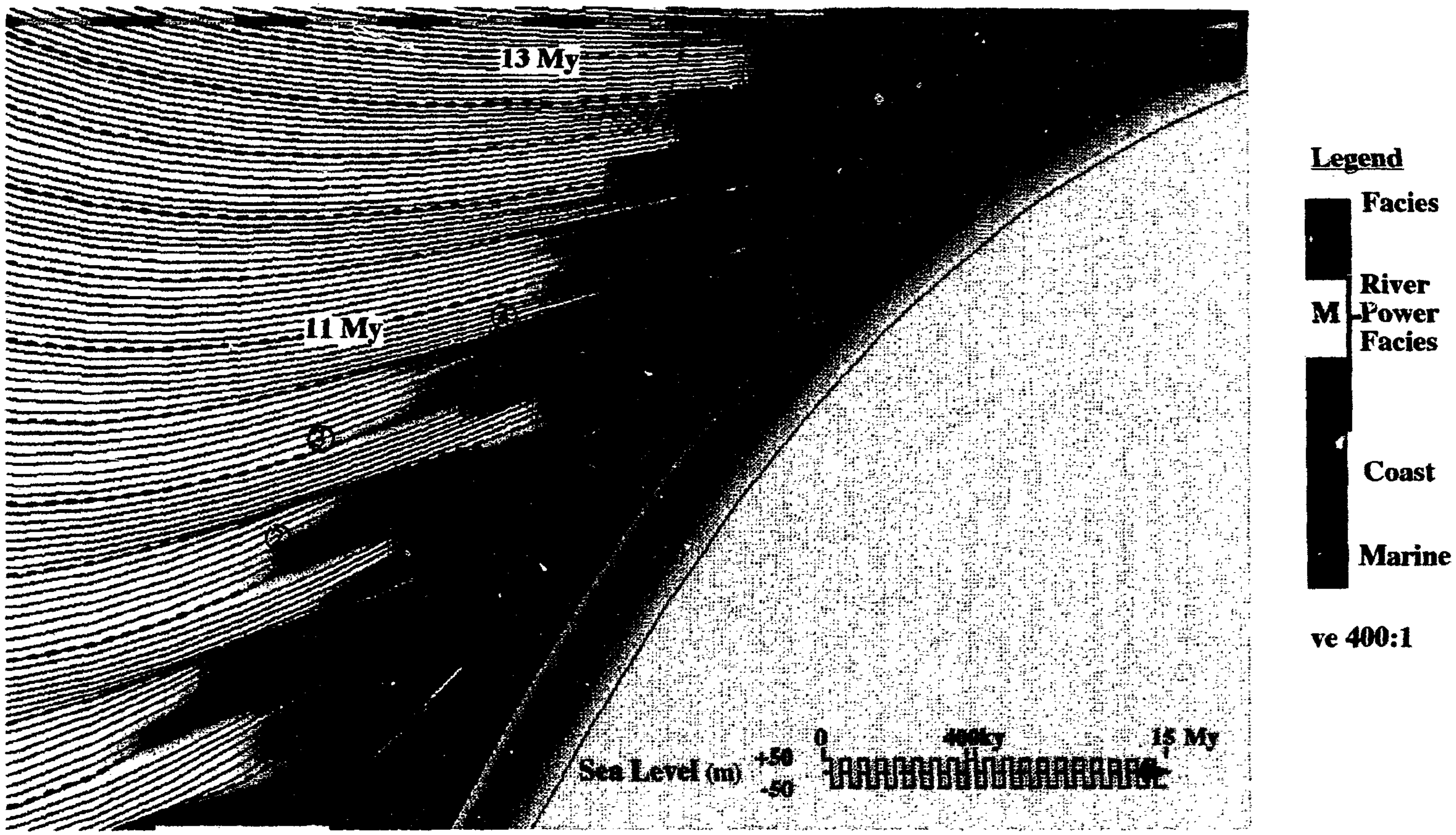

Figure 5.3. Enlarged portion of the ME1 retro-foreland basin (box, Fig. 5.2). Basin facies are in colour and time lines (black) are in 50 ky intervals. Blue dashed lines mark the change to eustatic highstand; red dashed lines mark the change to eustatic lowstand.

profile exhibits uniform sedimentation rates at ~150 ky, after a sea-level rise. The rate of progradation increases with time because the remaining seaway volume decreases with filling of the basin. This decrease results from the increasing alluvial plain elevation and the decreasing effects of isostatically forced relative sea-level rise.

The rise in sea level and establishment of new progradation along the seaway margin also result in erosion of the submerged lowstand seaway margin (①, Fig. 5.1). This erosion is caused by the increase in submarine transport rates accompanying the increase in surface slope across the submerged margin. In nature, the behaviour may be analogous to the effects of ravinement (Swift, 1968), or to erosion of the margin crest by slumping (Galloway, 1989) as previously suggested by Jordan and Flemings (1991). The submarine transport model can only mimic these processes by diffusion.

In the model, the eustatically forced relative sea-level fall causes an instantaneous regression (Figs. 5.2, 5.3) and a change in fluvial baselevel, but no immediate progradation. However, subsequent to the fall, lowstand alluvial facies prograde seaward past the previous lowstand margin and continue to prograde until the next sea-level rise (②, Fig. 5.1). The fall in baselevel causes fluvial erosion of highstand deposits (③, Fig. 5.1; ④, Fig. 5.3). ME1 does not provide good examples of erosional surfaces caused by regression; these erosional surfaces are discussed in more detail in model ME2. A fall in baselevel also results in a decrease in sedimentation rates across the lower alluvial plain, reflecting a decrease in the disequilibrium between actual and graded river profiles.

The extent of both transgression and regression increases as the basin fills and continues until the seaway closes during lowstand (③, Fig. 5.2). These increases reflect the reduction in surface slope of the alluvial plain with basin filling and illustrate how coastal volume varies inversely with subaerial surface slope (Sec. 2.9). As filling of the basin continues, the lateral extent of these cycles decreases as continued aggradation and increasing surface elevation of the alluvial plain prevent transgression during highstand. The latter is enhanced by the decreasing influence of isostatic subsidence on the distal alluvial plain as the basin fills. Decrease in the extent of these cycles shows how coastal volume varies directly with the amplitude of relative sea-level change.

Transgressive/regressive cycles are more extensive along the basin axis than across the basin, because surface slopes are much lower along the axis (Figs. 5.1, 5.2). The Persian Gulf is a modern example of extensive flooding of a foreland basin axis. The gulf is ~250 km wide, ~700 km long and less than 100 m deep. Sediment flux from the Zagros and Taurus mountains has been insufficient to prevent the transgression that resulted from eustatic rise over the last 10 ky. Similarly, extensive flooding along the axis of the North Slope Foreland Basin, Alaska, is thought to have been caused by eustasy (Bird and Molenaar, 1992). Here the +250 km axial transgression of the alluvial Nanushuk Group and deposition of the marine Coleville Group is coeval with the eustatic rise in sea level that peaked in the early Turonian (Fig. 3.13). In the model, transgressive/regressive cycles decrease in extent along the basin axis with time (④, Fig. 5.1) because the axial subaerial slope increases with basin filling. The increase in slope is caused by a reduction in the rate of progradation relative to the increase in alluvial plain elevation (*i.e.*, 'rise' increases faster than 'run'). This difference reflects a decrease in the rate of progradation caused by the increased water depth along strike with growth of the orogenic and sedimentary loads similar to MT3.

ME2 - Sequence Development

Model ME2 shows in detail the effects of an instantaneous sea-level rise and fall on a partially filled foreland basin. Particular attention is paid to the way in which erosional surfaces develop with sea-level fall. Model ME2 differs from ME1 in that sea level is fixed at –50 m elevation for the first 10.2 My, then rises instantaneously to +50 m and remains constant for 400 ky before falling to –50 m and remaining constant for another 400 ky. The tectonic timestep interval is 5 ky in the last 1 My of model ME2 in order to increase temporal resolution. All other initial conditions and parameter values are the same as in ME1.

In ME2, sea level rises at 10.2 My, when the retro-foreland basin axis is partially subaerial, causing a transgression of ~400 km along the basin axis (Fig. 5.4). Figure 5.5 which shows the highstand margin in planform and section immediately after the subsequent instantaneous sea-level fall, is used to illustrate the margin's development. Transgression extends ~100 km onto the alluvial plain (①, Fig. 5.5). The extent of the transgression is determined by the magnitude of the eustatic rise and the slope of the alluvial plain. Net sediment flux has no effect on the extent of the transgression because the change in sea level is instantaneous. The transgression at A-A' is somewhat wider than at B-B' because the surface slope of the alluvial plain becomes shallower with filling of the basin (①, Fig. 5.5). Following the eustatic rise, isostatic compensation for orogenic and sedimentary loads causes a continued rise in relative sea level. Differences in the rates of sediment transport to and away from the coast result in the development of a highstand margin (②, Fig. 5.5) and a condensed section along the basin axis (③, Fig. 5.5). Progradation resumes because the net sediment flux to the coast is greater than the rate of change in coastal volume once the eustatic rise is complete. The rate of

ME2 at 10.2 and 10.205 My

- Periodic v_E, Constant Q_V and v_T

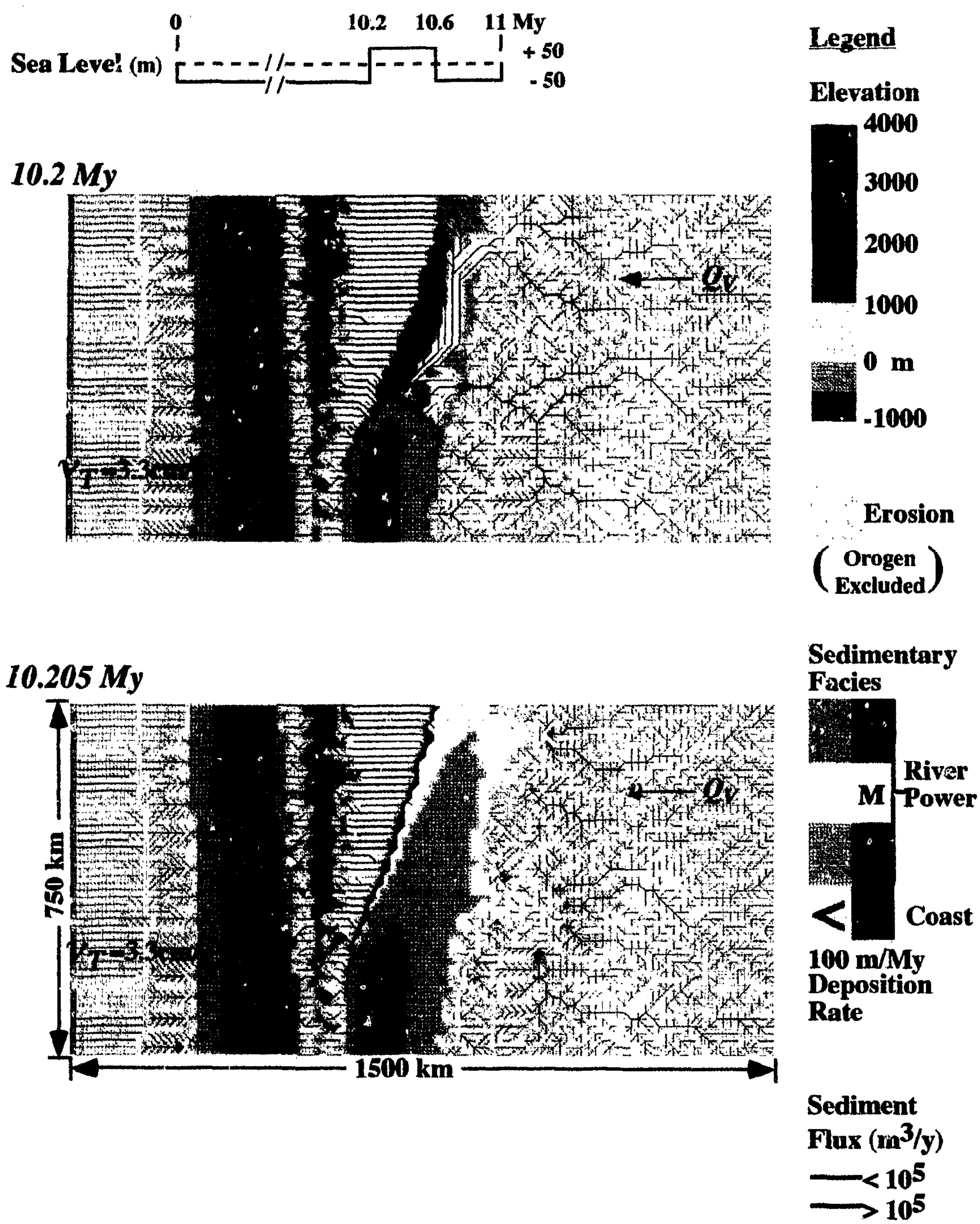

Figure 5.4. Planform of ME2 shows surface elevation (grey), facies distribution (colour), subaerial erosion (pink) and the fluvial drainage network immediately before (10.2 My) and after (10.205 My) sea-level rise. Marine facies (blue) along the basin axis without a fluvial drainage network indicate the flooded region of the retro-foreland basin.

progradation is proportional to the difference between the net sediment flux to the coast and the increase in coastal volume. Progradation rates decrease along strike toward B-B' (②, Fig. 5.5), reflecting a decrease in the difference between net sediment flux and the rate of change in coastal volume. This decrease is caused by a reduction in net sediment flux, which is related to a decrease in orogen-to-basin sediment flux and an increase in sediment transport away from the margin with the steeper submarine surface slopes toward B-B', and by an increase in coastal volume which is caused by higher rates of relative sea-level rise toward B-B' because the seaway is closer to the change in orogenic load.

At 10.6 My, sea level falls from +50 m to –50 m and then remains constant. The instantaneous fall in sea level causes the development of a fluvial drainage network along the basin axis and the deposition of alluvial facies (④, Fig. 5.5). The coastline across the basin axis re-establishes a position close to its location prior to the rise in sea level (Fig. 5.4). These coastline positions differ partly because sea-level highstand causes a reduction in the rate of basin axis sedimentation and partly because isostatic compensation for the growing orogenic and sedimentary load counters the effect of the relative fall in sea level.

The fall in sea level results in erosion and subsequent burial of the highstand seaway margin, thereby creating a narrow unconformity that extends along the basin (Figs. 5.6, 5.7). Erosion of the margin is a consequence of the increase in slope of the fluvial profiles along the exposed highstand margin (⑤, Fig. 5.5) and the rapid rate of sea-level fall, both of which are required for erosion to occur (Schumm, 1993). The increase in slope downstream from the highstand margin causes an increase in the carrying capacity of a river. The instantaneous fall in sea level ensures that progradation

ME2 at 10.7 My - Periodic v_E, Constant Q_V & v_T

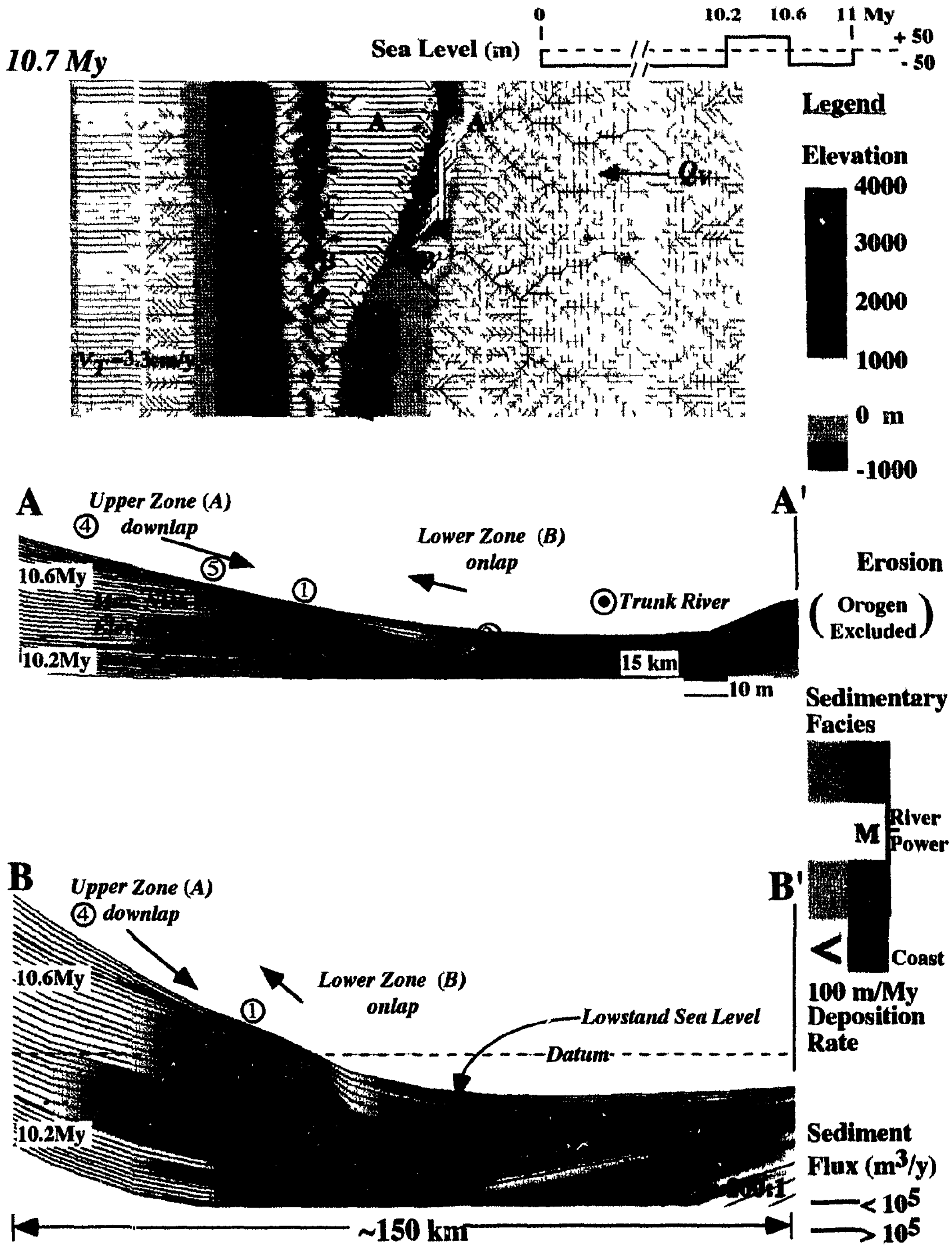

Figure 5.6. ME2 is shown in planform and section at 10.7 My, immediately after the fall in sea level. Sections A-A' and B-B' show how upper zone downlap and lower zone onlap meet, preserving the Type-1 erosional surface. Facies are in colour; time lines (black) are at 20 ky intervals.

ME2 - Periodic ν_E, Constant Q_V and ν_T

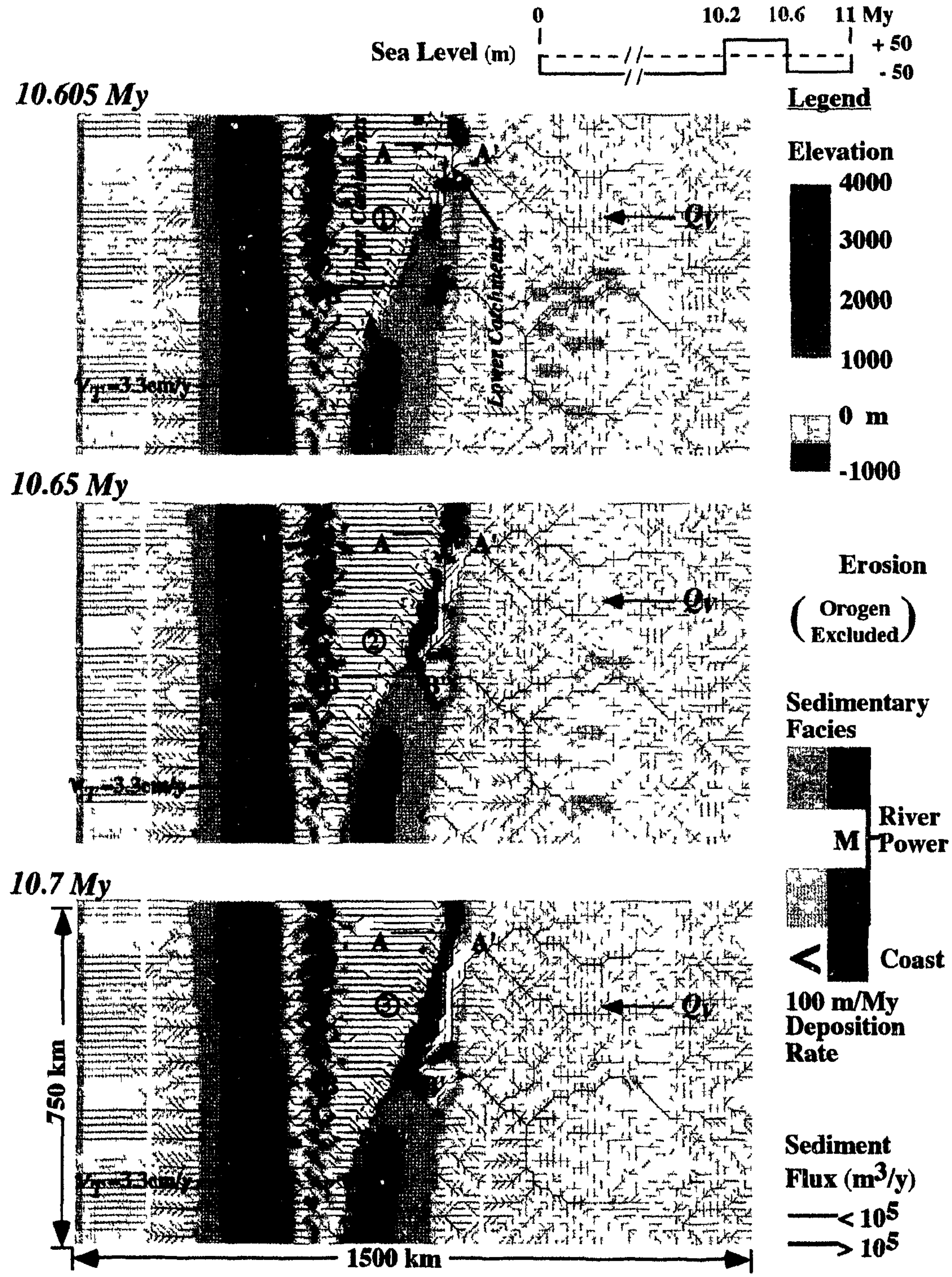

Figure 5.7. Planform evolution of ME2 surface elevation (grey), facies distribution (colour), subaerial erosion (pink) and fluvial drainage network is shown at 10.605, 10.65 and 10.7 My. Dashed areas show changes in the distribution of Type 1 erosional surfaces.

cannot occur during the fall, and therefore there is no aggradational increase in the elevation of the river profile that could prevent erosion (Lane, 1955, cit. Schumm, 1993).

Lane observed that as baselevel shifts horizontally away from the previous shoreline position in the direction of flow, the fluvial profile increases in elevation by aggradation. In the model, fluvial profiles aggrade under similar conditions because the basinward advance of the shoreline by progradation locally extends the river bed at a near horizontal gradient. The local change in river gradient along the extended river bed causes local regrading by sedimentation that propagates headward along the fluvial system, as the system adjusts toward a dynamic equilibrium. Type-1 erosional surfaces typically develop when there is an increase in slope at the shoreline and aggradation of the fluvial profile with regression is insufficient to prevent exposure of this break in slope. Under these conditions, the local increase in gradient causes fluvial incision at the break in slope and thus initiates erosional headward regrading of the fluvial system.

In ME2, the instantaneous fall in sea level causes fluvial incision of the highstand margins, thus creating a Type-1 erosional surface (⑤, Fig. 5.5; ①, Fig. 5.6). Incision of the highstand margin creates a 'nick' point that migrates headward toward the orogen (②, Fig. 5.6). At the base of the highstand margin, a break in slope causes a decrease in carrying capacity and therefore deposition (③, Fig. 5.6). The nick point and break in slope divide each fluvial system into upper, middle and lower zones. The upper and lower zones are characterized by sedimentation and the middle zone by erosion. These results are consistent with the conceptual model of Posamentier and Allen (1993), who suggest that coeval sedimentation occurs both above and below the incised highstand margin.

The upper fluvial zone is characterized by alluvial plain sedimentation (④, Fig. 5.6) and is equivalent to Zone A of Posamentier and Allen (1993). The sedimentation rate in the upper zone is determined by regrading of rivers in response to the orogen-to-basin sediment flux (Q_S), the rate of basin subsidence, and the rate of baselevel change where the nick point is the effective baselevel (⑤, Figs. 5.5, 5.6). The nick-point elevation changes as the rivers in the middle zone erode toward grade by headward incision of both the highstand deposits and the sediments of the upper zone.

The limit of headward incision, which marks the uphill extent of the erosional surface, is determined by basin subsidence and the properties of the fluvial system in the middle zone. This limit is reached when basin subsidence reduces the slope of an incised surface such that sediments of the alluvial plain downlap onto the incised surface (Fig. 5.6). Regrading of the fluvial system in the middle zone is determined by the material properties of the substrate, river discharge and changes in river slope with basin subsidence. The extent of headward incision varies inversely with the basin subsidence rate and the erosional length scales of the substrate, and directly with discharge and relief of the margin. In addition, the rate of erosion is likely to decrease downstream as the disequilibrium between carrying capacity and fluvial sediment flux is reduced by erosion, and carrying capacity either remains constant or decreases with diminishing surface slope. Model ME2 lacks the spatial resolution to display the effects of the along-strike differences in these factors.

The lower fluvial zone is characterized by alluvial sedimentation (③, Fig. 5.6) and is equivalent to Zone B of Posamentier and Allen (1993). In ME2, erosion of the old highstand margin ends when downlap of the upper zone meets onlap from the lower zone. The rate of onlap is determined by regrading of the lower zone adjacent to the highstand margin in response to basin subsidence, incision of the middle zone and changes in the rate of regrading of the trunk river. Factors which influence regrading of the trunk river include: along-strike basin subsidence, changes in baselevel (sea level), changes in carrying capacity with collection of discharge from tributaries, and axial progradation. Both excess carrying capacity and sediment flux from tributaries of the trunk river, including those off the craton, have an indirect effect on the rate of onlap because both affect regrading of the axial river.

In planform, regrading of the fluvial system in each catchment is independent of the adjacent catchment upstream of the nick point. As a consequence, the extent of erosional surfaces may vary significantly along the highstand margin, with varying effects of topography, precipitation and collection on fluvial discharge and transport. In ME2, this variation can be observed as a decrease with time of the along-strike extent of the current erosional surfaces (①, Fig. 5.7). At 10.6 My the erosional surface is essentially uniform in extent along strike. After 50 ky, exposed areas of erosion become separated by intervals where upper and lower fluvial systems have merged (②, Fig. 5.7). After 100 ky, only a few local areas of erosion still exist (③, Fig. 5.7).

In summary, model ME2 results show that when there is a relative fall in sea level, erosion of the highstand margin in each catchment can occur because there is an increase in surface slope at the old highstand margin. Erosion will occur when there is insufficient sediment flux for progradation to cause an aggradational increase in the fluvial profile above the elevation of the highstand margin. Erosion of the highstand margin subdivides the fluvial system into upper, middle and lower systems, in agreement with the conceptual model of Posamentier and Allen (1993). The extent of the Type-1 erosional surface is determined by regrading of the upper fluvial system in response to orogen-to-basin sediment flux, basin subsidence and changes in the nick point elevation; by regrading of the middle fluvial system in response to material properties of the substrate, river discharge and basin subsidence; and by regrading of the lower fluvial system in response to basin subsidence, eustasy and sediment flux delivered to the coast by the trunk river.

5.3 Effect of Eustatic Sea-Level Change on Erosion Rates of the Orogen

Eustasy may affect erosion rates of the orogen through the effect of baselevel change on the regrading of each fluvial system. Model ME3 is an experiment designed to show the effect of fluvial regrading in response to baselevel changes caused by eustasy on the orogen-to-basin sediment flux ($Q_{S(retro)}$). Model ME3 uses a step function in ν_E that causes change in sea-level elevation between ±50 m elevation relative to datum at 3 My intervals. An interval of 3 My is used because it allows abundant time for regrading and facilitates easy comparison with MT1, MT4 and MC3. Model ME3 uses the same initial conditions and parameter values as MT1, MT4 and MC3, except that ν_T and Q_V remain constant while ν_E varies with time. Comparison of ME3 and MT1 shows that in both instances, $Q_{S(retro)}$ increases toward an asymptote and then remains essentially constant (Fig. 5.8). In ME3, $Q_{S(retro)}$ shows no significant change with eustasy; therefore, erosion rates in the orogen are not significantly affected by a regrading of the fluvial systems in response to eustatic changes in baselevel.

5.4 Rate of Sea-Level Change

In the following experiments, eustatically forced sea-level changes are varied sinusoidally in order to examine how the rate of eustatic sea-level change affects the competition between net sediment flux to the coast and the rate of change in coastal

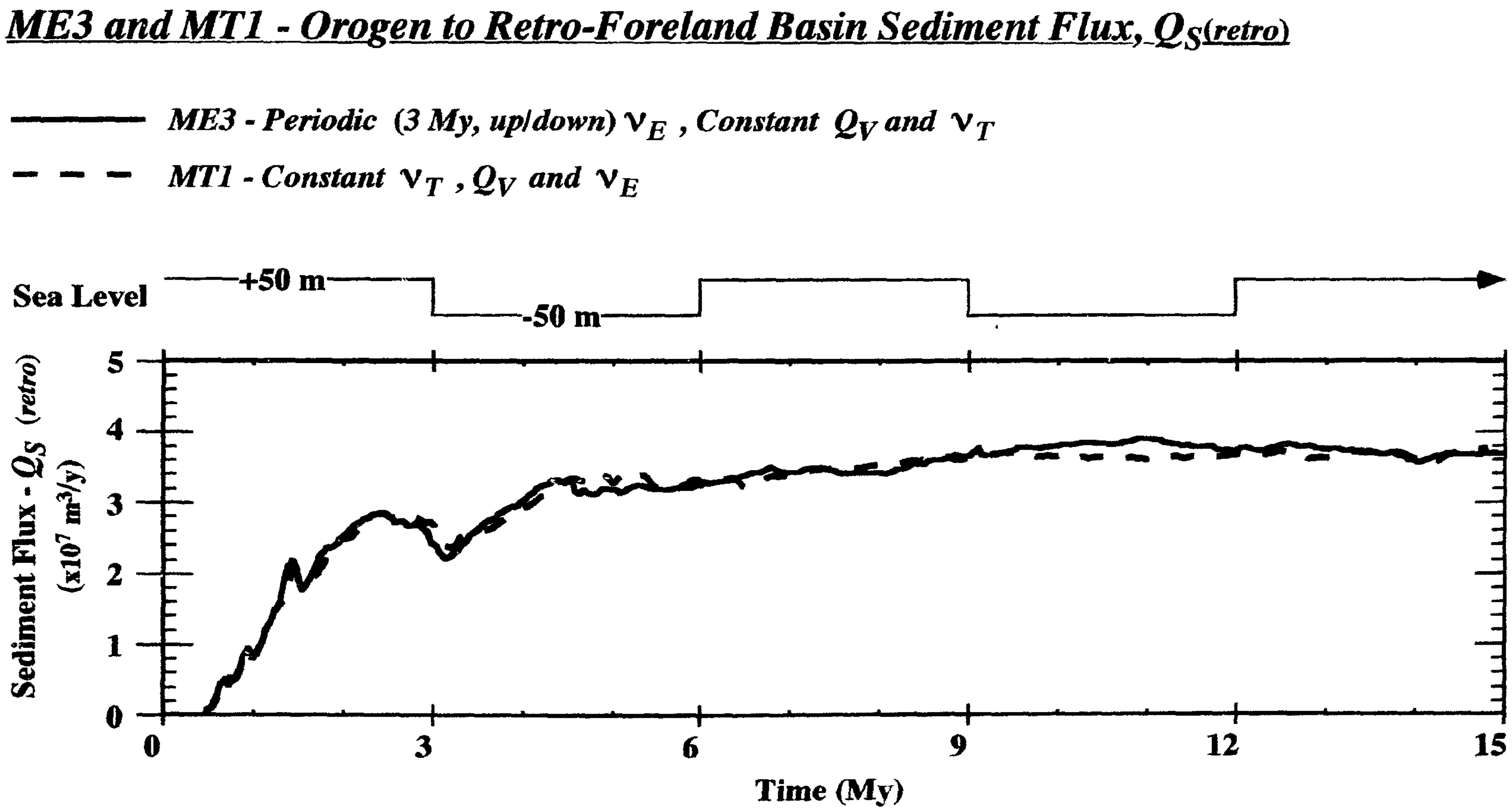

Figure 5.8. Comparison of orogen-to-retro-foreland basin sediment flux ($Q_{S(retro)}$) for MT1 and ME3. The similarity of these curves indicates that eustatic sea-level fluctuations do not have a significant effect on the rate of orogen denudation.

volume. This competition determines the rates of progradation and retrogradation, as well as the timing of changes between progradation, aggradation and retrogradation relative to sea-level highstand and lowstand. In models ME4 and ME5, sea level varies sinusoidally between ±50 m elevation relative to datum. The periods of sea-level change are 400 ky and 3 My, causing the maximum ν_E to differ by approximately one order of magnitude between ME4 and ME5. Both ME4 and ME5 have the same initial conditions and parameter values as ME1, with the exception of ν_E.

ME4 - 400 ky Periodicity in Eustasy

Model ME4 results show the effect of sinusoidal eustatic sea-level fluctuation on the stratigraphy of a wet, windward retro-foreland basin. The period of eustatic sea-level change is 400 ky, and the maximum rate of change is on the order of 1 mm/y. ME4 model results at 15 My are shown in planform, transverse section and axial section (Fig. 5.9).

In planform, model ME4 results show that the extent of orogen growth and sediment filling of the retro-foreland basin are approximately the same as in ME1 after 15 My (Figs. 5.1, 5.9). ME4 basin fill is somewhat more marine than ME1, as indicated by coastal facies along the ME4 basin axis (①, Fig. 5.9). These coastal facies in ME4 are a consequence of sea-level highstand at 15 My.

In section, ME4 shows stacked sequences created by eustasy (A-A', Fig. 5.9; Fig. 5.10). Early in the basin's history the extent of the transgressive/regressive cycles along A-A' is approximately 40 km, increasing to approximately 160 km by ~8 My (A-A', Fig. 5.9). This maximum cycle width is coeval with the change to alluvial sedimentation across the entire basin during sea-level lowstand. The change in cycle extent prior to

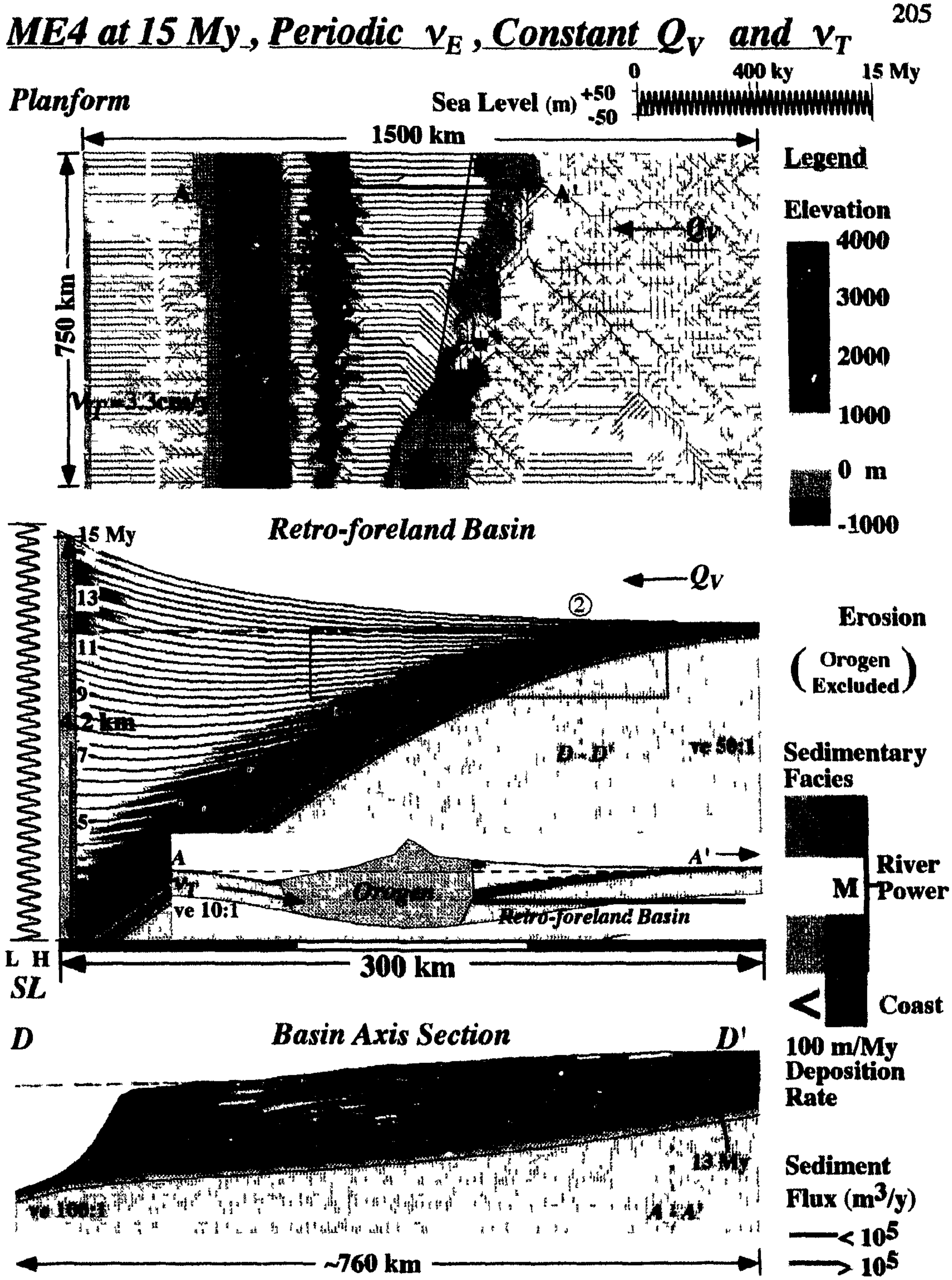

Figure 5 9 ME4 is shown in planform, transverse (A-A' & retro-foreland basin) and longitudinal section (D-D') at 15 My. Time lines are at 400 ky intervals (black lines) and are coeval with the maximum rate of sea-level rise The box outlines the enlarged area in Figure 5 10

ME4 at 15 My, Enlarged Retro-Foreland Basin - Periodic ν_E, Constant Q_V and ν_T

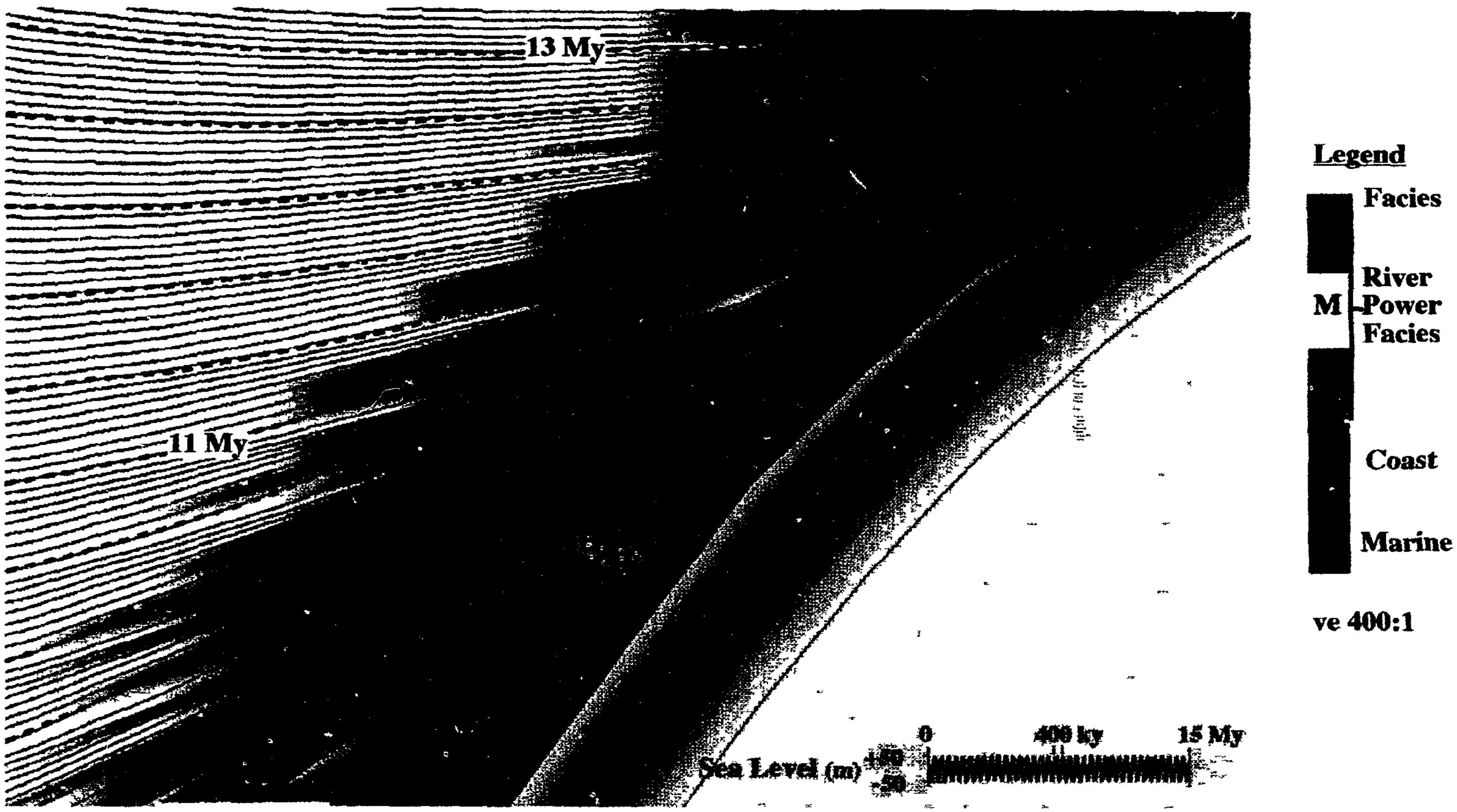

Figure 5.10 Enlarged portion of the ME4 retro-foreland basin (box, Fig. 5.9) Basin facies are in colour and time lines (black) are in 50 ky intervals Blue dashed lines mark sedimentation coeval with eustatic sea-level highstand.

reaching maximum cycle width is a consequence of the decrease in the slope of the alluvial plain as the basin fills, while the amplitude of sea-level variation remains constant, similar to ME1. The decrease in cycle extent, after reaching the maximum cycle width, is a consequence of the increasing alluvial plain elevation associated with filling of the basin and the constant amplitude of sea-level variation. By ~13 My transgression of the seaway no longer causes retrogradation of marine or coastal facies to proceed as far 'inland' (②, Fig. 5.9).

The uppermost transgressive/regressive cycles along A-A' (Fig. 5.9) are enlarged in Figure 5.10. Rising sea level is marked by rapid marine transgression, flooding surfaces and a condensed section in the marine basin (Fig. 5.9; ①, Fig. 5.10). Sedimentation rates increase with a sea-level rise because of the associated change in sediment transport rates to and from the coast (Fig. 5.10). Sediment flux to the coast increases with transgression because landward migration of the coastline reduces the area over which upstream alluvial sedimentation can occur. Sediment transport away from the coast decreases with flooding because of the shallow surface slopes of the flooded alluvial plain. The net increase in sediment flux has minimal influence on the extent of retrogradation because the maximum extent of retrogradation is coeval with the end of sea-level rise (②, Fig. 5.10). Progradation lags slightly behind the change to eustatic fall because the initial rate of fall is less than the rate of relative rise caused by isostasy. In ME4, similar to ME1 and ME2, the dominant factors controlling the extent of retrogradation are the magnitude of sea-level change and the surface slope. This may not be the case if fluvial sediment flux were larger.

Falling sea level in ME4 causes progradation of alluvial facies and the creation of Type-1 surfaces (③, Fig. 5.10). As sea level begins to fall, sediment flux to the basin margin initially keeps pace with the rate of sea-level fall; the result is progradation without erosion of the highstand deposits (④, Fig. 5.10). This situation is an example of how progradation causes a rise in elevation of the river profile (Lane, 1955, cit. Schumm, 1993), thereby preventing erosion of the highstand margin (Schumm, 1993). The situation arises because net sediment flux to the coast is sufficient for progradation to proceed without erosion of the margin (Fig. 5.11). The rate of eustatic sea-level fall continues to increase, while net sediment flux to the coast remains approximately constant. As a consequence, shoreface progradation cannot keep pace with sea-level fall, resulting in subaerial exposure and fluvial incision of the abandoned shoreface, creating a Type-1 erosional surface. In ME4, these Type-1 surfaces are indicated by the convergence of time lines ~100 ky after highstand (③, Fig. 5.10) and are approximately synchronous with the maximum rate of sea-level fall (Fig. 5.10).

ME4 and ME2 results indicate that Type-1 surfaces developed under these model conditions may be poor sequence boundaries because they are asynchronous with sea-level change, discontinuous in extent, and have asynchronous correlative conformities between adjacent catchments. As such, the sequences they bound are poorly constrained. The sequence boundaries can be better identified by the rapid basinward shift in fluvial facies that occurs with the reduction in the rate of relative sea-level rise or fall. This identification, however, depends on distinguishing the rapid basinward shift in facies associated with a eustatic fall from the progradation associated with a eustatic rise.

In contrast, flooding surfaces and their laterally equivalent condensed sections create well-defined regional parasequence boundaries in ME4 and ME2, which appear to be better regional markers than the sequence boundaries. The flooding surfaces are well-defined because the orogen is in a constructive state and eustasy augments the relative

Progradation Without Erosion

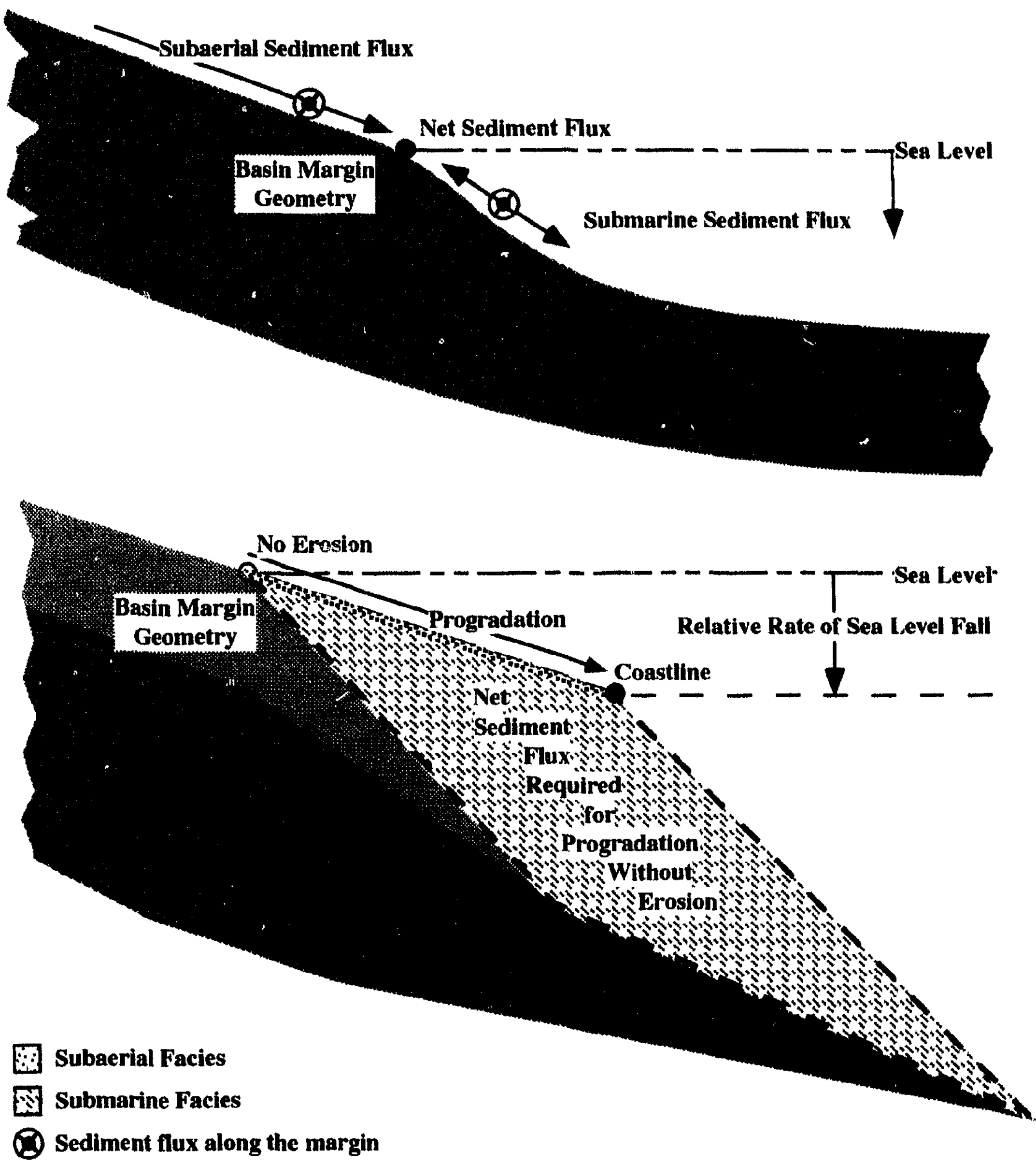

Figure 5.11 Progradation with a relative fall in sea level will proceed without erosion when the net sediment flux to the coast extends the river profile without creating an increase in carrying capacity through discharge or surface slope. The minimum net sediment flux required is determined by the geometry of the basin margin, the depositional submarine surface slope, and the rate of relative sea-level fall.

rise in sea level caused by tectonically forced basin subsidence. However, if the orogen was in a destructive state, then isostatic rebound caused by denudation of the orogen would oppose the eustatic rise and inhibit the development of aerially extensive flooding surfaces. These conditions would favour the development of Type-1 erosional surfaces by enhancing the rate of relative sea-level fall.

ME5 - 3 My Periodicity in Eustasy

Parameter values in ME5 are the same as ME4, except that the period of eustatic change is 3 My instead of 400 ky. This increase in period (or reduction in frequency) while maintaining a constant amplitude of sea-level change causes a reduction in the acceleration, deceleration and maximum velocity of sea-level change.

In planform, the orogen and retro-foreland basin in ME5 are developed to approximately an equivalent degree as ME4 (Figs. 5.9, 5.12). ME5 shows a more uniform change in alluvial facies distribution, having moderate to low power facies where the rivers change direction to flow along the basin axis (Fig. 5.12). In addition, the coastal facies in ME5 are less extensive than in ME4 (Figs. 5.9, 5.12). Both of these features indicate that the rivers are better able to keep pace with the lower frequency of sea-level change in ME5 than in ME4.

In section, ME5 shows stacked retrogradational/progradational cycles caused by fluctuation in sea level (Fig. 5.12). The cycles in ME5 differ from those in ME4 (Fig. 5.9) because of the lower frequency of sea-level change. Transgressive successions in ME5 show that retrogradation of alluvial facies ends ~350 ky prior to sea-level highstand (①, Fig. 5.13). Transgression is limited by the competition between net sediment flux to the coast and the rate of change in coastal volume. Aggradation occurs because the net

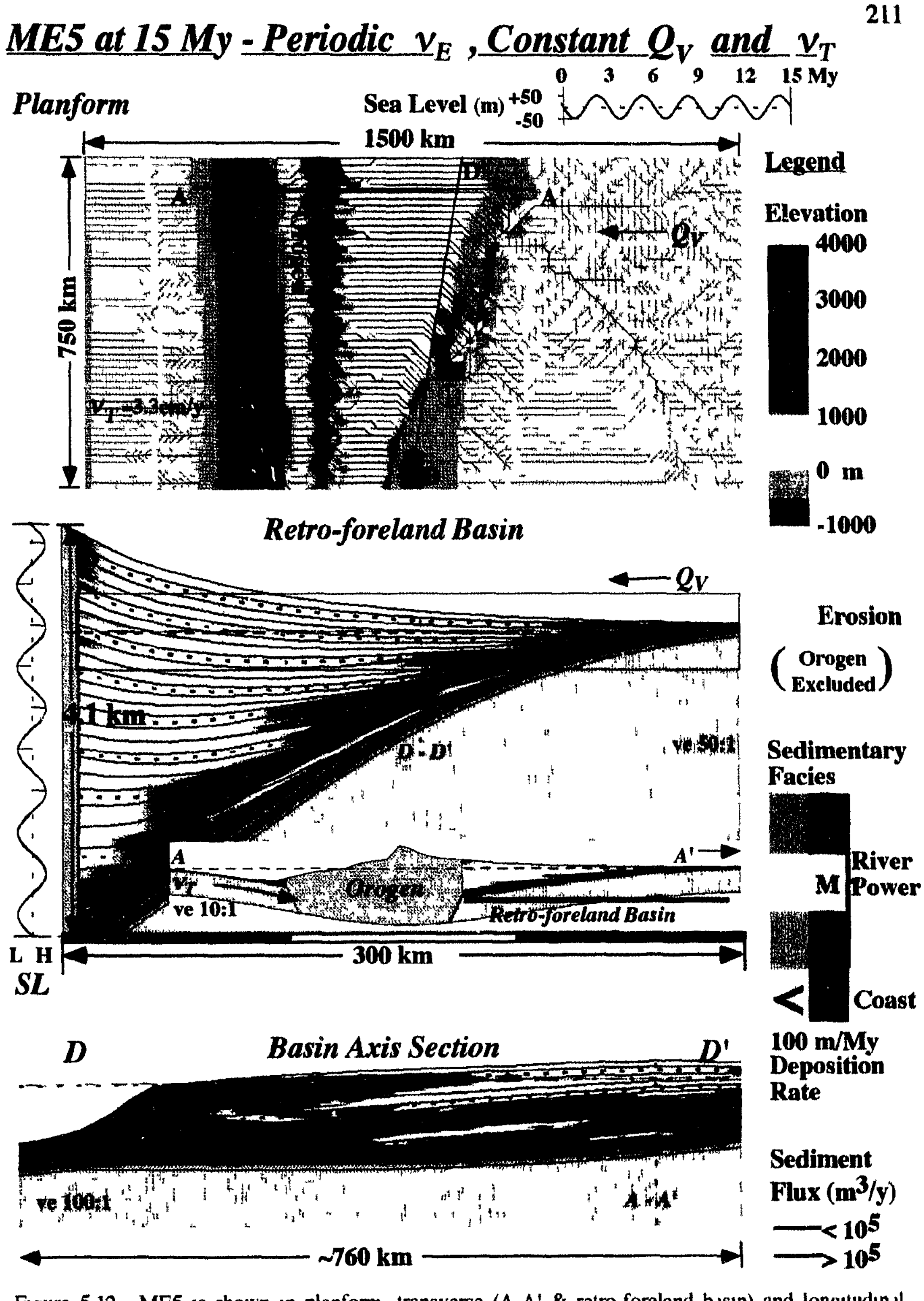

Figure 5 12. ME5 is shown in planform, transverse (A-A' & retro-foreland basin) and longitudinal section (D-D') at 15 My. Blue dashed lines mark sedimentation coeval with eustatic sea-level highstand Red dashed lines mark sedimentation coeval with eustatic sea-level lowstand The box A-A' outlines the region enlarged in Figure 5.13.

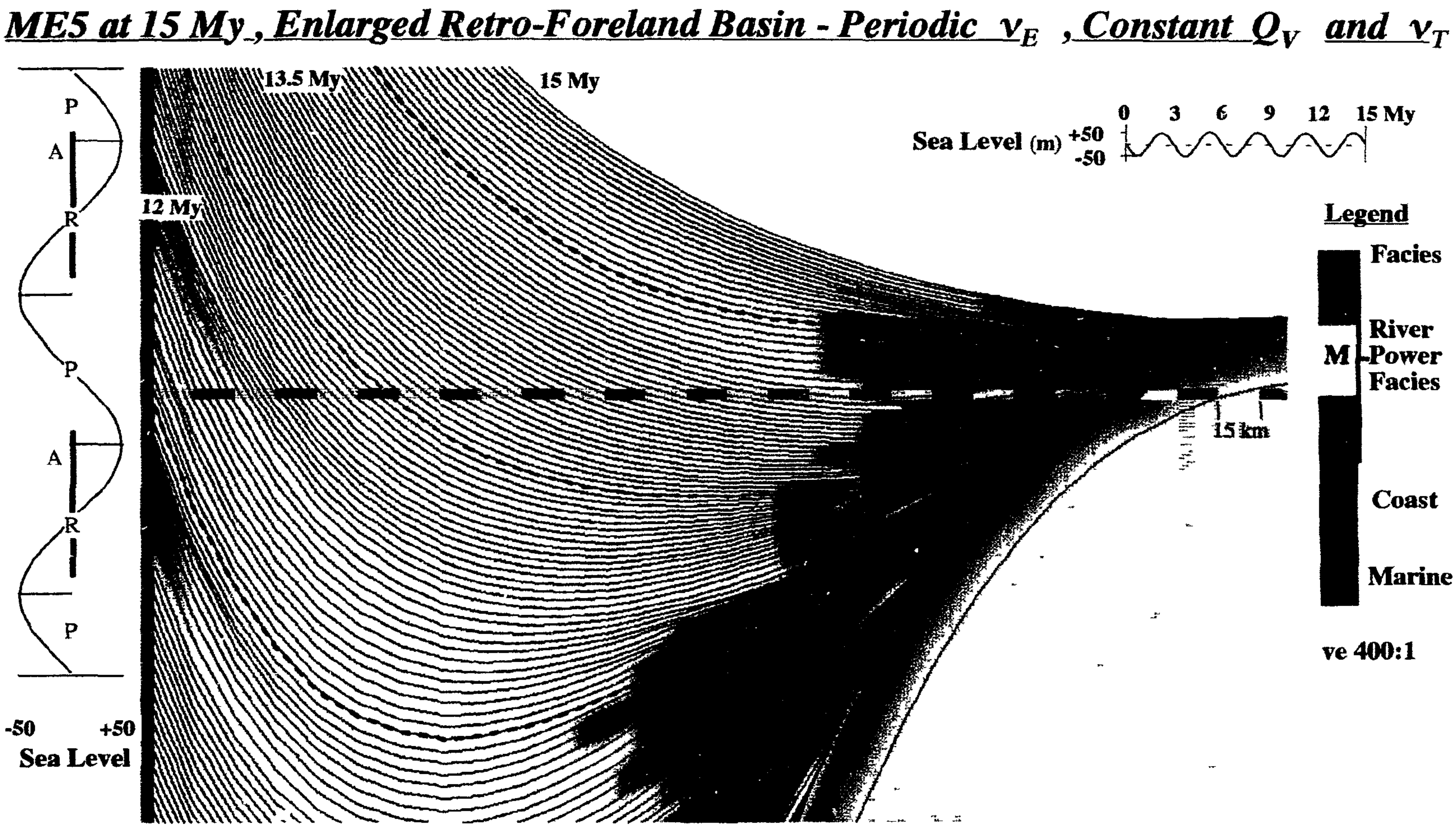

Figure 5.13. Enlarged ME5 retro-foreland basin (box, Fig. 5.12). Basin facies are in colour and time lines (black) are in 50 ky intervals. Blue lines mark eustatic sea-level highstand, and red lines mark eustatic sea-level lowstand. Sea-level curve shows timing of progradation (yellow), aggradation (green) and retrogradation (blue)

sediment flux is approximately equal to the rate of change in coastal volume, within the resolution limits of the model. The shoreline position is subsequently maintained and coastal facies aggrade until progradation begins shortly after sea-level highstand, similar to ME4. However with eustatic fall, progradation in ME5 proceeds without erosion of the shoreface, whereas erosion does occur in ME4 (③, Fig. 5.10; ②, Fig. 5.13) illustrating that in ME5, the net sediment flux to the coast is always sufficient for the rate of progradation to prevent erosion.

ME5 and ME4 are similar in that sea-level variation has no apparent effect on sedimentation close to the orogen (Figs. 5.9, 5.12). Orogen-to-basin sediment flux and alluvial sedimentation rates are approximately the same in ME5 and ME4, as indicated by time-line separation and the extent of basin filling (Figs. 5.9-5.13). In ME5, the effect of baselevel changes on the fluvial system immediately adjacent to the seaway are less evident than in ME4, as reflected in the relatively uniform sedimentation rates upstream from the seaway (②, Figs. 5.10; ①, Fig. 5.13). Both ME1 and ME4 exhibit increases in sedimentation rate adjacent to the coast caused by headward regrading of the fluvial system with faster changes in sea level (Figs. 5.3, 5.10). Net sediment flux at the coast is not measured directly, however, this difference in sedimentation rate is expected to create a minor increase in sediment flux to the coast in ME5 relative to ME4. ME5 and ME4 also differ in that marine surface slopes are somewhat steeper in ME5 (dashed line - ②, Figs. 5.10, 5.13), and this difference is expected to create an increase in sediment flux away from the coast. Overall, net sediment flux at the coast is approximately the same in ME5 and ME4 primarily because orogen-to-basin sediment flux is approximately the same, but also because changes in baselevel are thought to have relatively minor and competing effects on net sediment flux. Therefore, the stratigraphic

MCE2 at 15 My - Periodic v_E and Q_V, Constant v_T

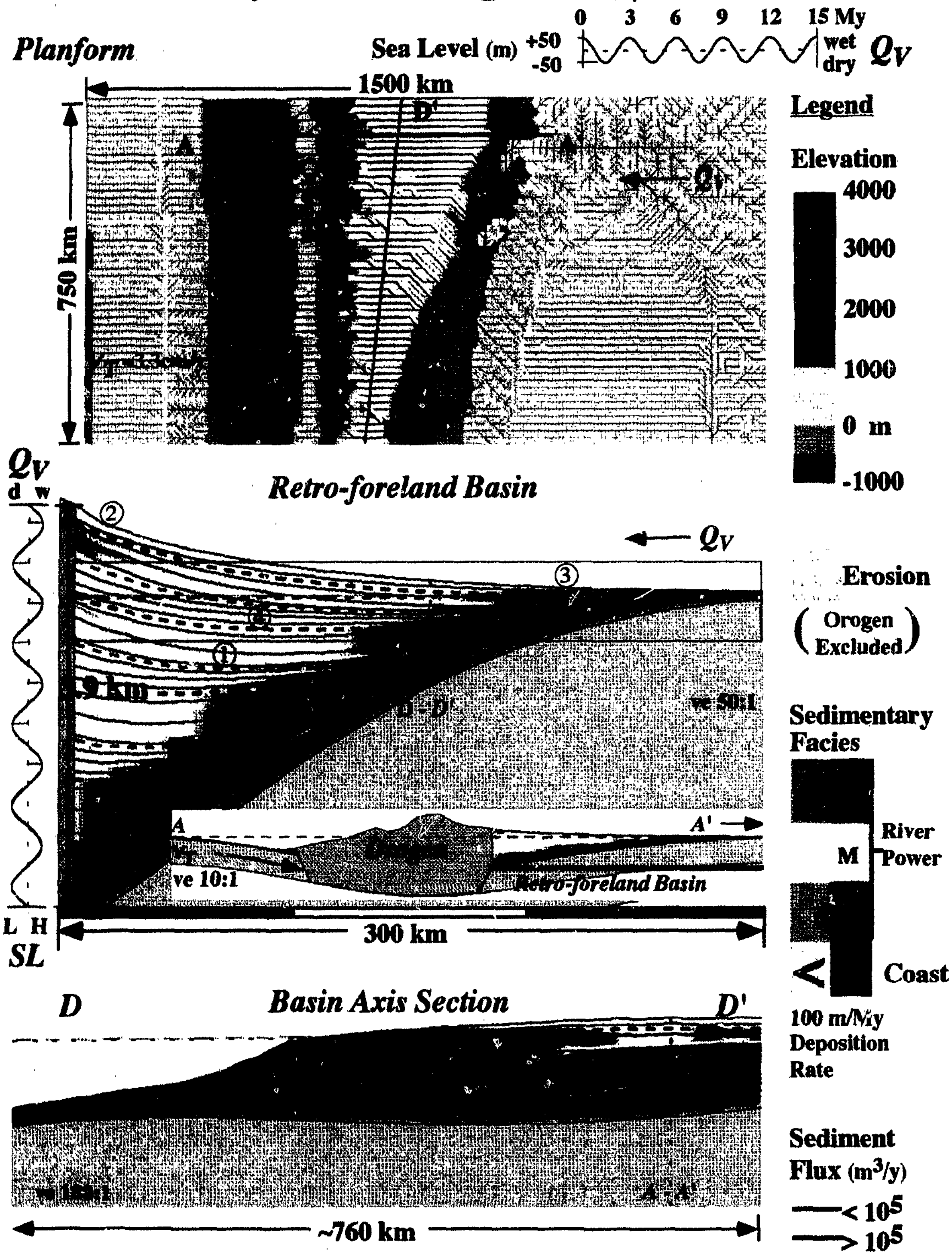

Figure 5.16 MCE2 is shown in planform, transverse (A-A' and retro-foreland basin) and longitudinal section (D-D') at 15 My. Red dashed lines mark sedimentation coeval with sea-level lowstand and dry climatic conditions. Blue dashed lines mark sedimentation coeval with sea-level highstand and wet climatic conditions. The box outlines the region enlarged in Figure 5.17.

MCE2 at 15 My, Enlarged Retro-Foreland Basin - Periodic v_E and Q_V, Constant v_T

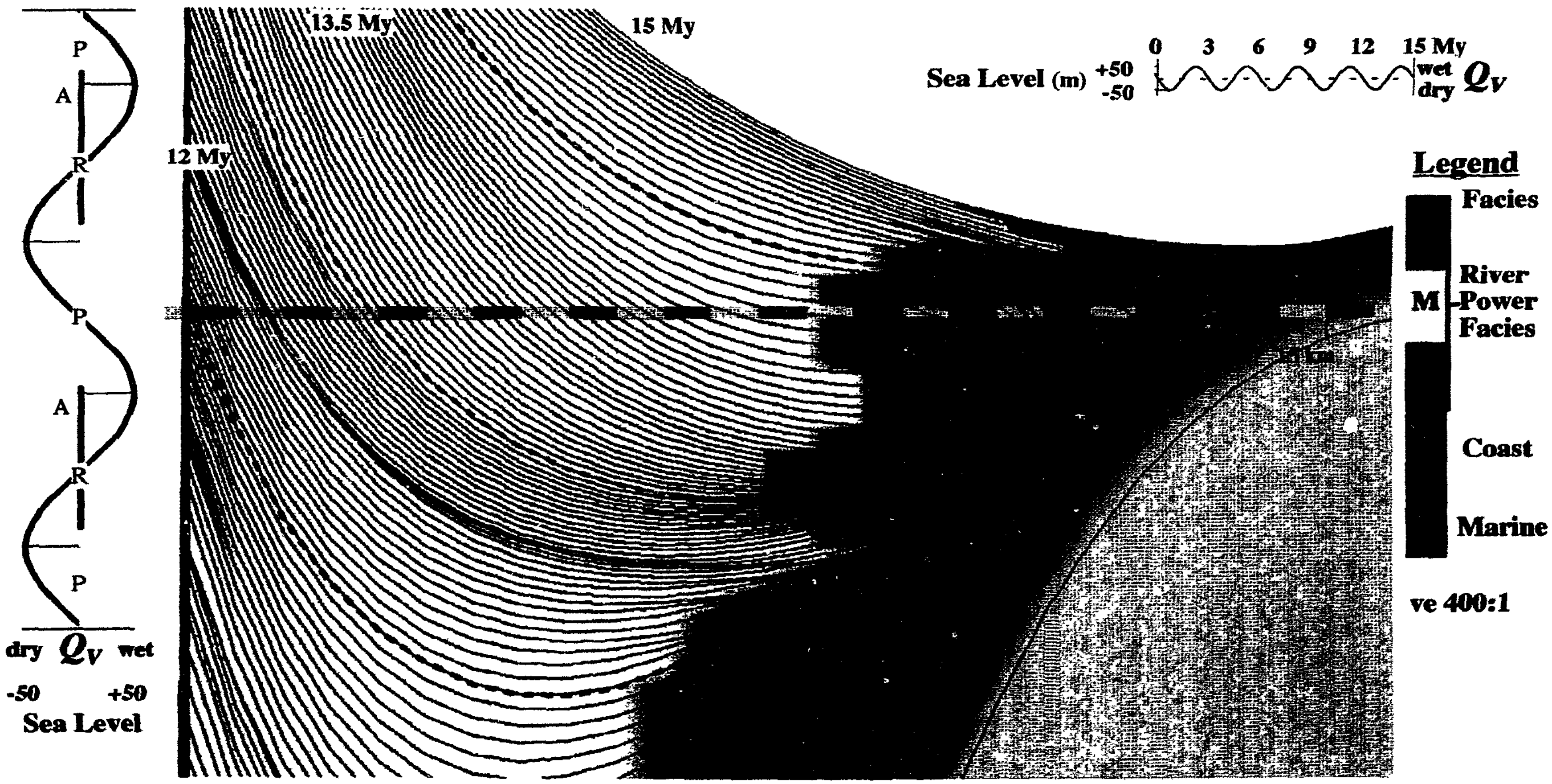

Figure 5.17. Enlarged MCE2 retro-foreland basin (box, Fig. 5.16). Basin facies are in colour and time lines (black) are in 50 ky intervals. Blue dashed lines mark sedimentation coeval with eustatic sea-level highstand and wet climatic conditions. Red dashed lines mark sedimentation coeval with eustatic sea-level lowstand and dry climatic conditions. Sea-level and vapour flux curves show timing of progradation (yellow), aggradation (green) and retrogradation (blue).

differences between ME5 and ME4 are dominantly caused by the slower rate of change in coastal volume with the lower frequency of sea-level change.

5.5 Eustasy Combined with Periodicity in Climate Change or Tectonics

Model results show the effects of eustatic sea-level change in combination with either fluctuations between wet and dry climatic conditions or variations in the rate of orogenic tectonism. Sea level varies sinusoidally between ±50 m elevation relative to model datum with a 3 My period, similar to model ME5. The initial condition and all other model parameter values except Q_V and v_T are the same as ME5. In models with a periodic change in climate, Q_V varies such that if precipitation rates were uniform across the model, they would vary between 0.5 m/y and 1.0 m/y, comparable to MC4. Models with a change in the rate of tectonism have a sinusoidal variation in v_T between 0 and 3.3 cm/y, like MT6.

5.5.1 Combined Effects of Periodicity in Eustatic Sea-Level and Climate Change

Model results MCE1 and MCE2 show how eustatic changes either reinforce or counteract the effects of changes between wetter and drier climatic conditions.

MCE1 - Eustatic Reinforcement of the Effects of Climate Change

In model MCE1, eustasy is the same as in ME5, while variations in Q_V cause changes between wetter and drier climatic conditions using the same parameter values as in MC4. Climatic conditions are wetter when the sea level is low and drier when it is high. The change to a drier climate reinforces the effects of eustatic rise in sea level, in that both promote retrogradation. Similarly, a change to a wetter climate reinforces the effects of a eustatic fall in sea level, since both promote progradation. Model results of

MCE1 are shown in Figure 5.14 in planform, transverse and axial sections, with an enlarged section of the upper retro-foreland basin shown in Figure 5.15.

In MCE1, periods of drier climate and relative rise in sea level produce retrogradation of basin facies together with a modest increase relative to ME5 in time-line divergence toward the orogen (Figs. 5.12, 5.14). The time-line geometry in MCE1 is consistent with the effects of a change to a drier climate in MC4. Sedimentation rates increase adjacent to the orogen because as precipitation and denudation rates decrease, the attendant increase in orogen growth and basin subsidence rates causes an increase in the disequilibrium between the existing and graded river profiles (Figs. 4.10, 5.14). As well, the decrease in rainfall across the alluvial plain reduces the carrying capacity of rivers, causing a decrease in sediment flux to the coast, thereby reducing resistance to transgression and enhancing the rate of retrogradation. In addition, the increased rate of basin subsidence caused by the increased orogen growth rate and localization of sedimentation adjacent to the orogen enhances the effects of eustasy. This increase in the rate of relative sea-level rise promotes retrogradation by increasing the rate of change in coastal volume. Comparison of MCE1 with ME5 shows that the relative reduction in sediment flux to the coast and increase in coastal volume cause the extent of transgression to increase and retrogradation to continue almost until sea-level highstand (Fig. 5.13; ①, Fig. 5.15). Although the latter is difficult to determine for certain because of model resolution, it is inferred from the shorter duration of aggradation. If the retrogradation does occur almost until sea-level highstand then the decrease in net sediment flux with decreased precipitation rates leads to a decrease in the degree to which the change from retrogradation to aggradation is out of phase with sea-level highstand.

MCE1 at 15 My - Periodic v_E and Q_V, Constant v_T

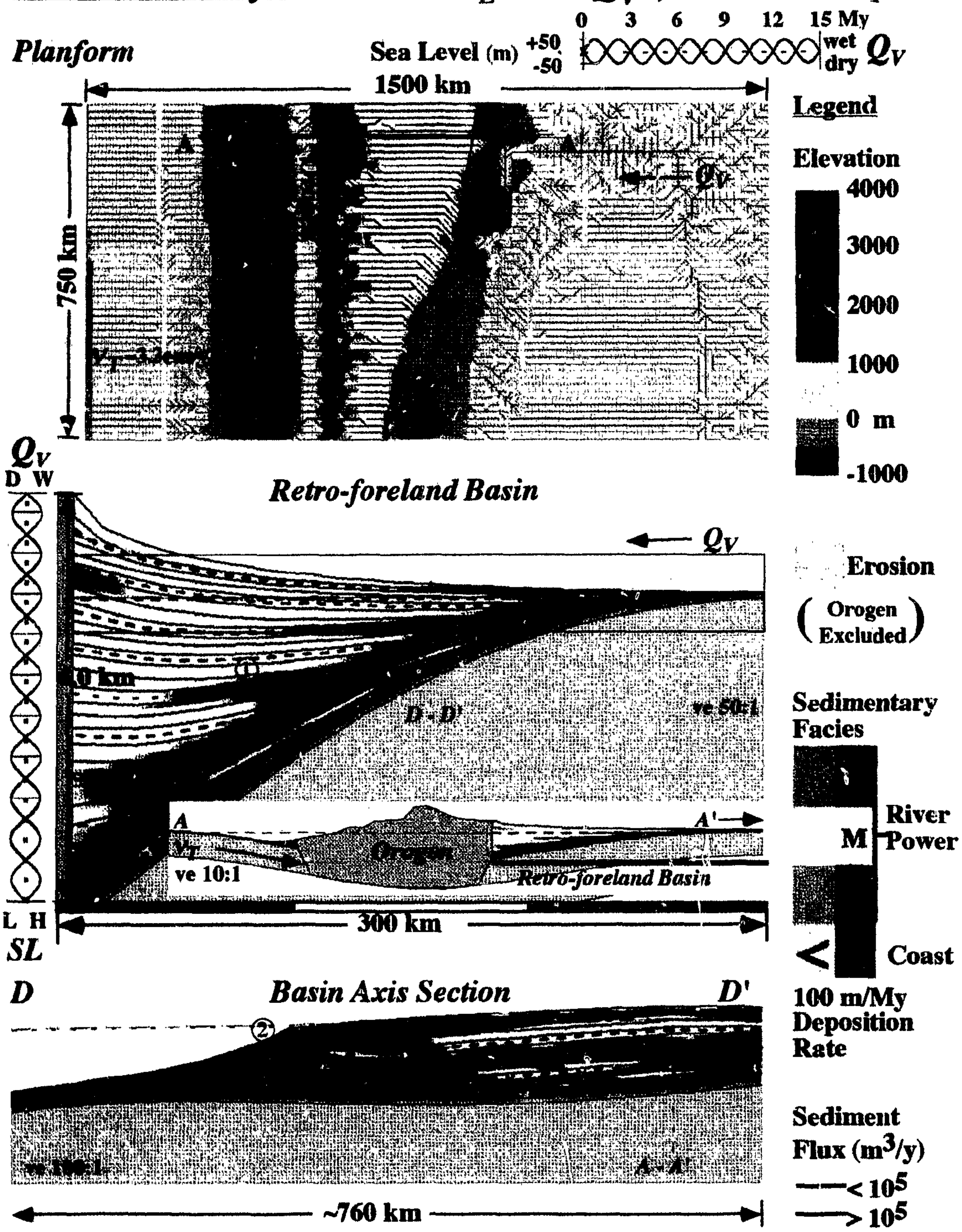

Figure 5.14. MCE1 is shown in planform, transverse (A-A' and retro-foreland basin) and longitudinal sections (D-D') at 15 My. Blue dashed lines mark sedimentation coeval with eustatic sea-level highstand and dry climatic conditions. Red dashed lines mark sedimentation coeval with sea-level lowstand and wet climatic conditions. The box outlines the region enlarged in Figure 5.15. On A-A', the profile of the ME5 orogen is shown as the dotted line inside the MCE1 orogen.

MCE1 at 15 My, Enlarged Retro-Foreland Basin - Periodic v_E and Q_V, Constant v_T

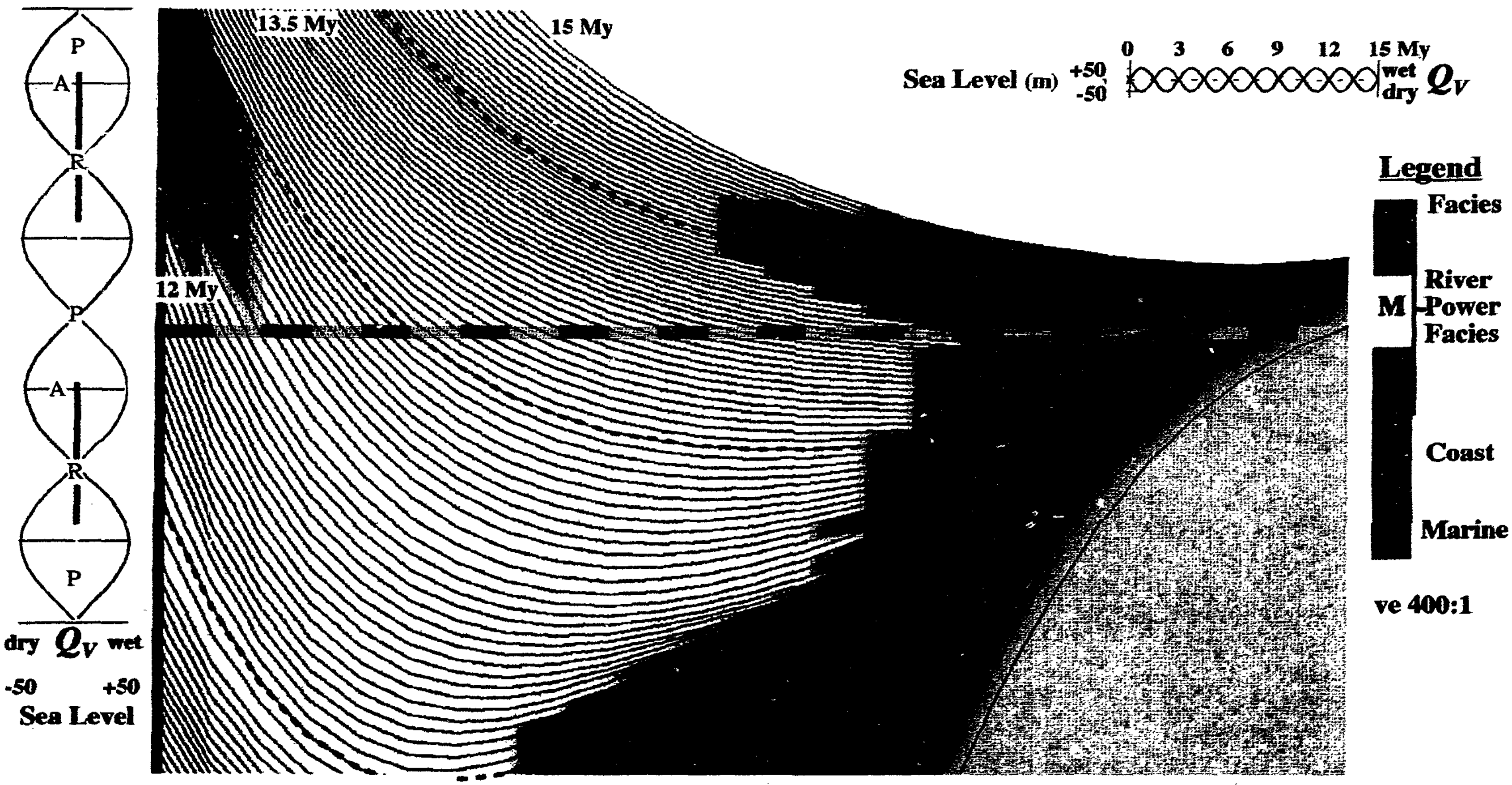

Figure 5.15. Enlarged MCE1 retro-foreland basin (box, Fig. 5.14). Basin facies are in colour and time lines (black) are in 50 ky intervals. Blue lines mark sedimentation coeval with eustatic sea-level highstand and dry climatic conditions. Red lines mark sedimentation coeval with eustatic sea-level lowstand and wet climatic conditions. Sea-level and vapour flux curves show timing of progradation (yellow), aggradation (green) and retrogradation (blue).

Comparison of time-line geometries in MCE1 with MC4 shows that the gradient in sedimentation rate away from the orogen is lower in MCE1; that is, sedimentation rates are more uniform across the alluvial plain (Figs. 5.12, 5.14). Eustasy in MCE1 causes this change in gradient through a rise in baselevel, which promotes disequilibrium between existing and graded profiles of the lower alluvial plain and results in greater sedimentation rates. These increased sedimentation rates counteract the effects of the change to a drier climate.

In MCE1, periods of wetter climate, coeval with a eustatic fall, enhance the rate of progradation by increasing the sediment flux to the coast. The latter occurs because the increased precipitation on the orogen produces higher erosion rates and orogen-to-basin sediment flux, while additional precipitation on the alluvial plain increases fluvial carrying capacity to the seaway. In MCE1, these changes are evidenced by a more uniform (tabular) time-line geometry with the increase in precipitation rate (①, Fig. 5.14), similar to MC4. Figure 5.15 shows the increase in progradation rate caused by the increase in net sediment flux. In MCE1, the sediment flux to the coast is sufficiently large that the rate of eustatic sea-level fall does not exceed the rate of shoreface progradation; thus no Type-1 erosional surfaces are created (Fig. 5.14, Fig. 5.15). In addition, the increase in net sediment flux causes a phase-lag between the change from progradation to retrogradation and sea-level lowstand (②, Fig. 5.14), the higher net sediment flux opposing the initially low rates of eustatic rise.

MCE2 - Eustatic Opposition to the Effects of Climate Change

In MCE2, eustatic sea-level variation and fluctuation in Q_V are the same as in MCE1 except that climate becomes drier while sea level is falling and wetter while sea level is rising, the exact opposite of MCE1. The associations of drier climates with falling sea level and wetter climates with rising sea level in MCE2 are closer to the associations found in nature between cooler and drier climates, and warmer and wetter climates (Wanless and Shepard, 1936; Kershaw and Nanson, 1993) than the opposite association between climate and sea level in MCE1. The MCE2 results below, therefore, are expected to be more typical of what might be expected in nature, than those in MCE1. In MCE2, climate and sea-level change have opposing effects on the development of foreland basin stratigraphy: a change to a drier climate promotes retrogradation; a eustatic fall in sea level promotes progradation. Conversely, a wetter climate promotes progradation, while a rise in sea level promotes retrogradation. Figure 5.16 shows model results of MCE2 in planform, transverse and axial sections. An enlargement of the upper retro-foreland basin is shown in Figure 5.17.

In section, MCE2 shows stacked transgressive/regressive sequences similar to those in MCE1 and ME5 (Figs. 5.12, 5.14, 5.16). Changes in river power across the alluvial plain, accompanied by river regrading caused by changes in precipitation rate and eustasy, are observed in river-power facies and time-line geometry. Periods of wetter climate and a eustatic rise are characterized by retrogradation and subsequent aggradation of alluvial facies. Time-line geometries are either uniform or slightly divergent toward the basin in the upper sequences (Fig. 5.16). A wetter climate increases orogen-to-basin sediment flux, enhances the fluvial transport of sediment across the alluvial plain and increases sediment flux to the seaway, thereby promoting progradation.

Eustasy, however, counteracts progradation by increasing coastal volume. In MCE2, these changes are seen in the increased sedimentation rates immediately adjacent to the orogen and in the approximately uniform sedimentation rates across the basin (①, Fig. 5.16). The effects of increased precipitation are observed in the progression of high river-power facies away from the orogen (②, Fig. 5.16). The combined effects of increasing precipitation and eustasy are observed in the retrogradation and subsequent aggradation of alluvial facies. The extent of retrogradation reflects the competition between the increase in sediment flux to the coast with increased precipitation and the increase in coastal volume with relative sea-level rise (Figs. 5.16, 5.17). Retrogradation is characteristic of the initial dominance of eustasy (①, Fig. 5.17), while the change to aggradation prior to sea-level highstand (②, Fig. 5.17) indicates when retrogradation is limited by net sediment flux. Comparison of MCE2 and ME5 shows that the change to aggradation occurs earlier in MCE2 and that aggradation occurs at higher rates (Figs. 5.15, 5.17). Therefore, the increases in net sediment flux caused by increased precipitation rates cause an increase in the degree to which the change from retrogradation to aggradation is out of phase with sea-level highstand. These differences are a consequence of the larger sediment flux to the coast in MCE2 that results from higher precipitation rates.

The change to a drier climate with a coincident fall in eustatic sea level causes retrogradation of facies proximal to the orogen (③, Fig. 5.16), progradation of facies in the distal basin (④, Fig. 5.16) and an increase in the convergence of time lines away from the orogen (⑤, Fig. 5.16). The time-line geometry is consistent with the effects of this change in climate. The decreased precipitation on the orogen reduces the denudation rate, thereby promoting the rate of orogen growth, the rate of basin subsidence and the disequilibrium between actual and graded river profiles adjacent to the orogen. Sedimentation rates and river-power facies decline across the alluvial plain because the decreased precipitation causes a decrease in fluvial carrying capacity away from the orogen (Figs. 5.16, 5.17). As a consequence, sediment flux to the seaway decreases. This decrease occurs sufficiently slowly that the net sediment flux to the coast is greater than the rate of change in coastal volume caused by the relative eustatic sea-level fall; therefore, no Type-1 erosional surfaces are created (Figs. 5.16, 5.17). Furthermore, the decreases in net sediment flux caused by decreased precipitation rates result in a decrease in the degree to which the change from progradation to retrogradation is out of phase with sea-level lowstand.

5.5.2 Combined Effects of Periodicity in Eustasy and Orogen State

Model results MTE1 and MTE2 demonstrate how eustasy can reinforce or counteract the effects of rate changes in tectonics.

MTE1 - Eustatic Reinforcement of the Effects of Tectonics

In MTE1, eustasy is a sinusoidal variation in sea level between ±50m elevation relative to datum with a 3 My period, the same as ME5; v_T varies between 0 and 3.3 cm/y, the same as MT6. Initial conditions and all other parameter values in MTE1 are the same as ME5 and MT6. As a consequence, in MTE1 sea level falls while the orogen changes from a constructive to a destructive state and rises while the orogen changes from a destructive to a constructive state. The sea-level rise and the change to a constructive orogen state reinforce each other in that both promote retrogradation. Conversely, the fall in sea level and the change to a destructive orogen state reinforce each other in that both promote progradation. MTE1 model results are shown in planform, transverse and axial section (Fig. 5.18); an enlargement of the upper retro-foreland basin is also presented (Fig. 5.19).

Planform comparison of MTE1 and ME5 shows that the orogen in MTE1 is lower in elevation and less extensive along strike (Figs. 5.12, 5.18). In addition, the alluvial plain of the retro-foreland basin in MTE1 is smaller and the seaway is larger. These differences arise primarily because MTE1 has experienced significantly less tectonic convergence than ME5. Planform comparison of MTE1 and MT6 shows that the orogens are of comparable elevation and extent (grey scale, Figs. 5.18, 3.20), while the retro-foreland basin seaway of MTE1 is more extensive. The difference in seaway extent is caused by the influence of eustasy on sediment transport in the basin.

In section, MTE1 shows stacked transgressive/regressive sequences similar to those in MT6 (Figs. 5.18, 3.20). The sedimentary wedge in MTE1, when compared with MT6, is thicker adjacent to the orogen, less extensive in the dip direction, and more extensive along strike. In addition, the upper sequences in MTE1 are dominated by marine sedimentation (①, Fig. 5.18), unlike the equivalent sequences in MT6. The synchronous eustatic rise and increase in tectonics are responsible for the increased volume of marine sediments in MTE1. Eustasy enhances the relative sea-level rise caused by isostatic compensation for the increasing orogenic loads. Therefore, the rate of increase in coastal volume is greater in MTE1 than in MT6, while the net sediment flux to the coast is approximately the same in both models; as a consequence, transgressions are more extensive in MTE1 (Figs. 5.18, 5.19, 3.21). The regional extent of retrogradation reflects the competition between net sediment flux and rate of change in coastal volume, because retrogradation stops before eustatic highstand is reached (Figs. 5.18, 5.19). The sedimentary wedge is thicker adjacent to the orogen in MTE1

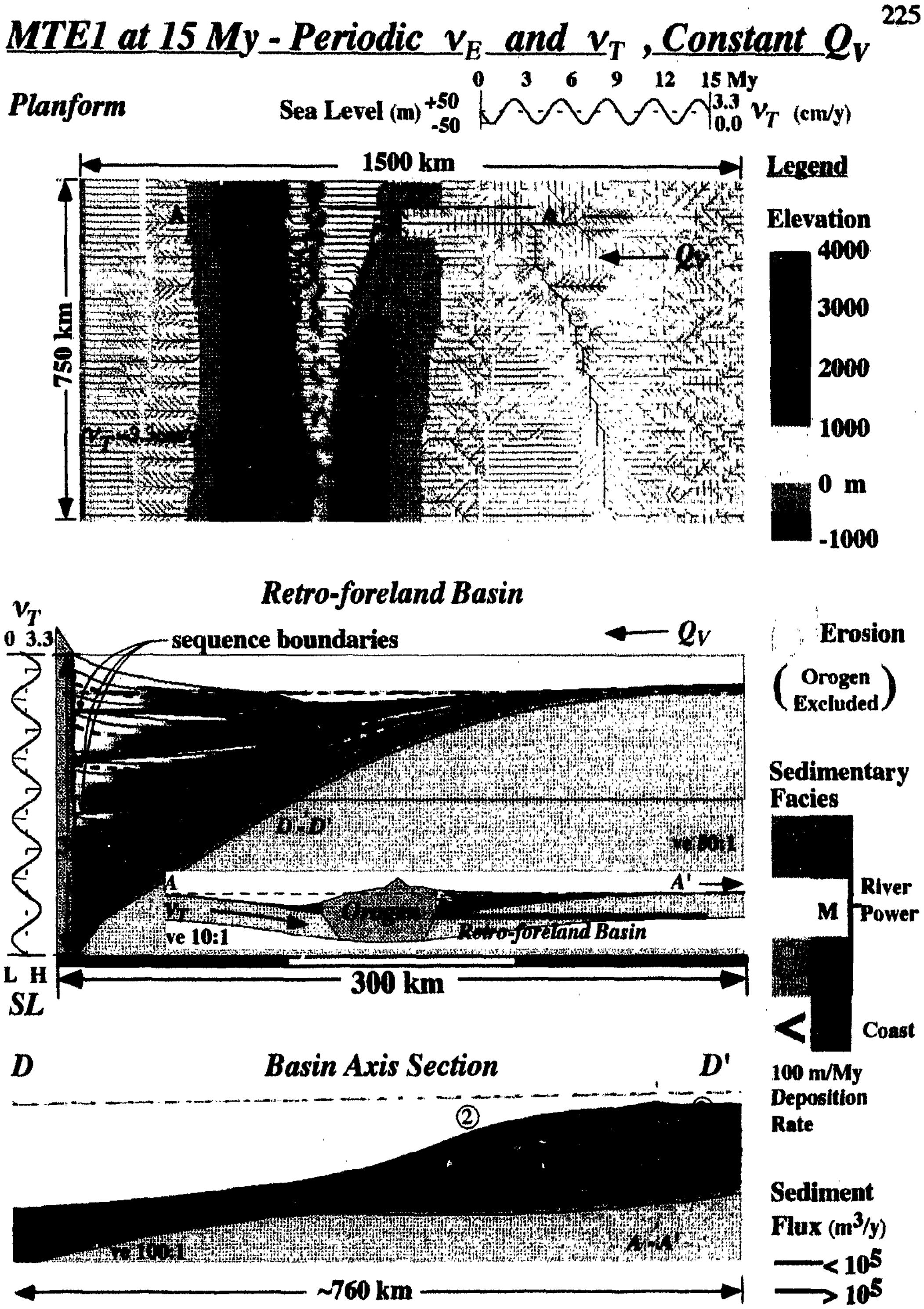

Figure 5.18. MTE1 is shown in planform, transverse section (A-A' and retro-foreland basin) and longitudinal section (D-D') at 15 My. Basin facies (colour) and time-line geometry (black) characterize stacked sequences dominated by marine sedimentation. Blue dashed lines mark sedimentation coeval with eustatic sea-level highstand and maximum v_T. Red dashed lines mark sedimentation coeval with lowstand and minimum v_T. The box outlines the region enlarged in Figure 5.19

MTE1 at 15 My, Enlarged Retro-Foreland Basin - Periodic v_E and v_T, Constant Q_V

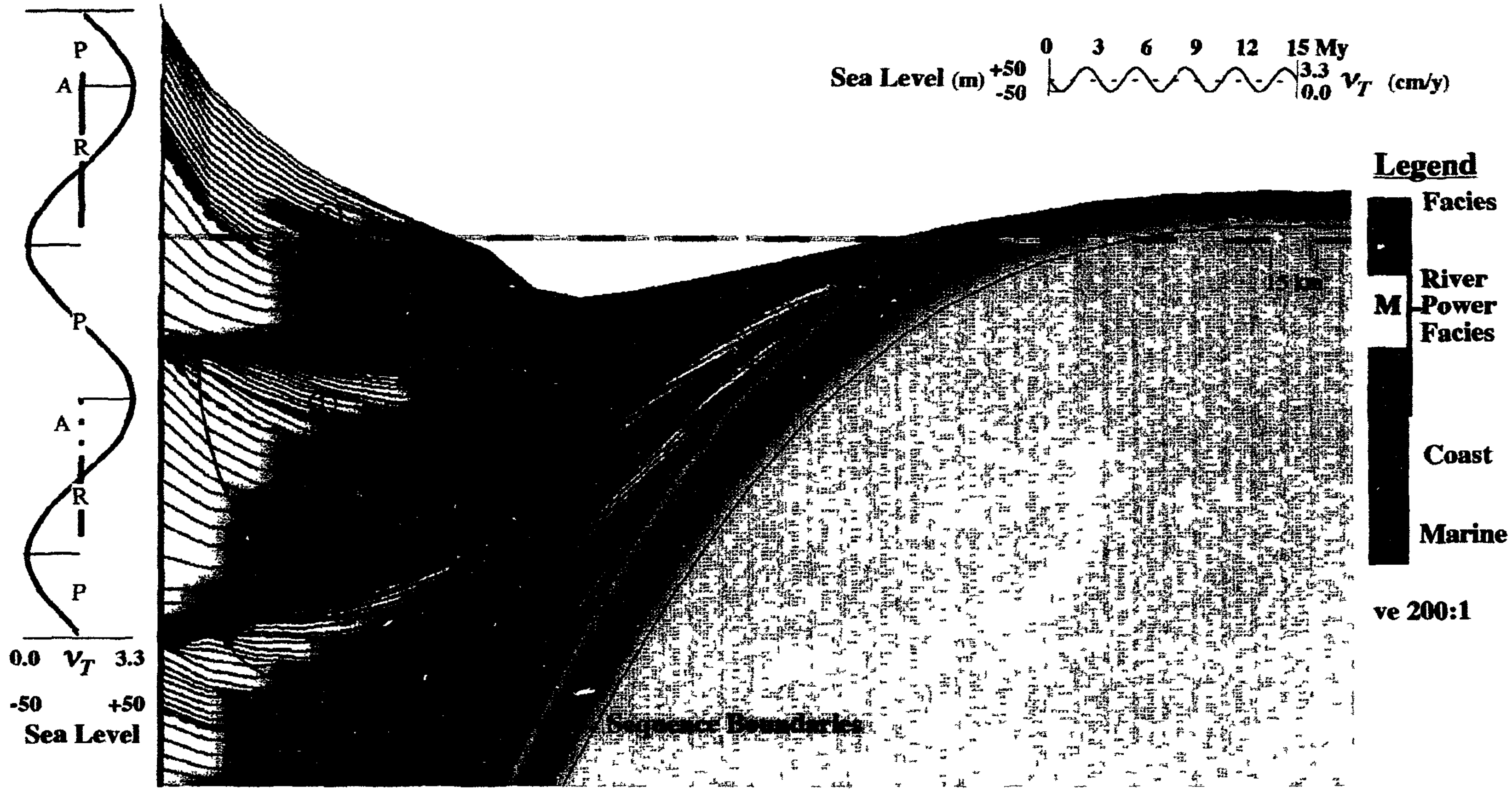

Figure 5 19. Enlarged MTE1 retro-foreland basin (box, Fig 5 18). Basin facies are in colour and time lines (black) are in 50 ky intervals. Blue dashed lines mark sedimentation coeval with eustatic sea-level highstand and maximum v_T. Red dashed lines mark sedimentation coeval with sea-level lowstand and minimum v_T Sea-level and convergence velocity curves show timing of progradation (yellow), aggradation (green) and retrogradation (blue)

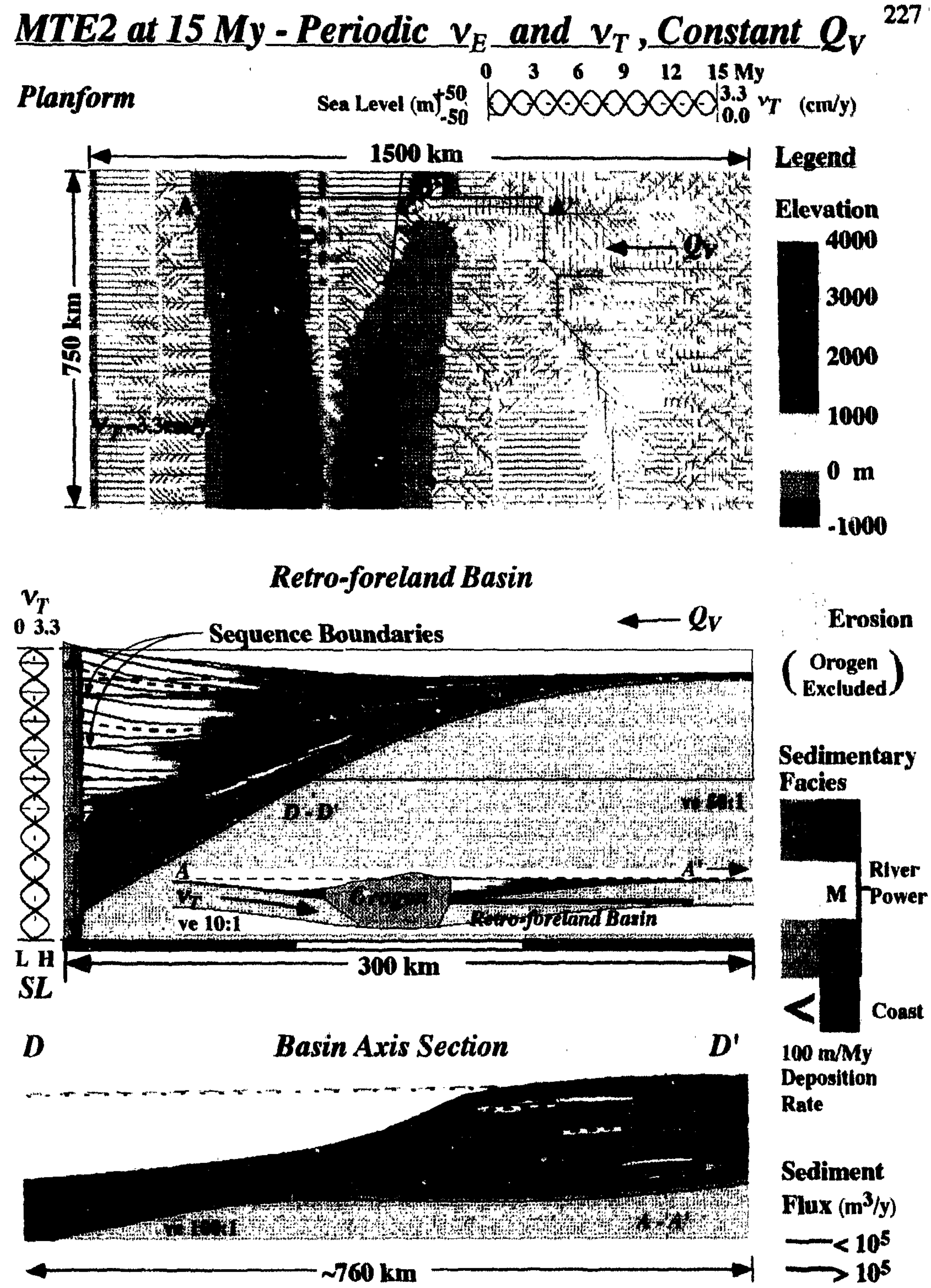

Figure 5.20. MTE2 is shown in planform, transverse (A-A', retro-foreland basin) and longitudinal section (D-D') at 15 My. Sedimentary facies (colour) and time line geometry (black) show stacked sequences. Blue dashed lines mark sedimentation coeval with eustatic sea-level highstand and minimum v_T. Red dashed lines mark sedimentation coeval with sea-level lowstand and maximum v_T. The boxed area is enlarged in Figure 5.21.

than in MT6 because enhanced transgressions during eustatic rise localize deposition proximal to the orogen in MTE1 relative to MT6. The extent of transgression enhances sedimentation adjacent to the orogen because submarine transport is less efficient than subaerial transport away from the orogen. Furthermore, the isostatically forced rate of increase in coastal volume enhances the degree to which the change from retrogradation is out of phase with sea-level highstand.

The eustatic fall in sea level and synchronous decrease in tectonics are responsible for the increased extent of alluvial plain progradation associated with destructive orogen states in MTE1 relative to MT6 (Figs. 5.18, 5.19, 3.21). Eustasy enhances the relative rate of sea-level fall that is caused by isostatic rebound associated with exhumation of the orogen. While the net sediment flux decreases with time, it remains sufficient for progradation to proceed without subaerial exposure and erosion of the shoreface (Fig. 5.18; ①, Fig. 5.19). The result is that alluvial sedimentation is more extensive in MTE1 than in MT6 and no Type-1 erosional surfaces are created. While marine erosion of the lowstand margin deposits does occur with relative sea-level rise and transgression along the basin axis (②, Figs. 5.18, 5.19), these are not Type-1 erosional surfaces. In MTE1, surface slopes along the submerged basin axis (③, Fig. 5.19) are very shallow relative to the submerged lowstand margin (②, Fig. 5.18). As a consequence, the rate of sediment delivery to the margin is less than the rate of sediment removal, resulting in erosion of the margin with transgression. The change from progradation to retrogradation is approximately in phase with sea-level lowstand because both sediment flux from the orogen to the coast and subsidence rates at this time are low.

MTE2 at 15 My, Enlarged Retro-Foreland Basin - Periodic v_E and v_T, Constant Q_V

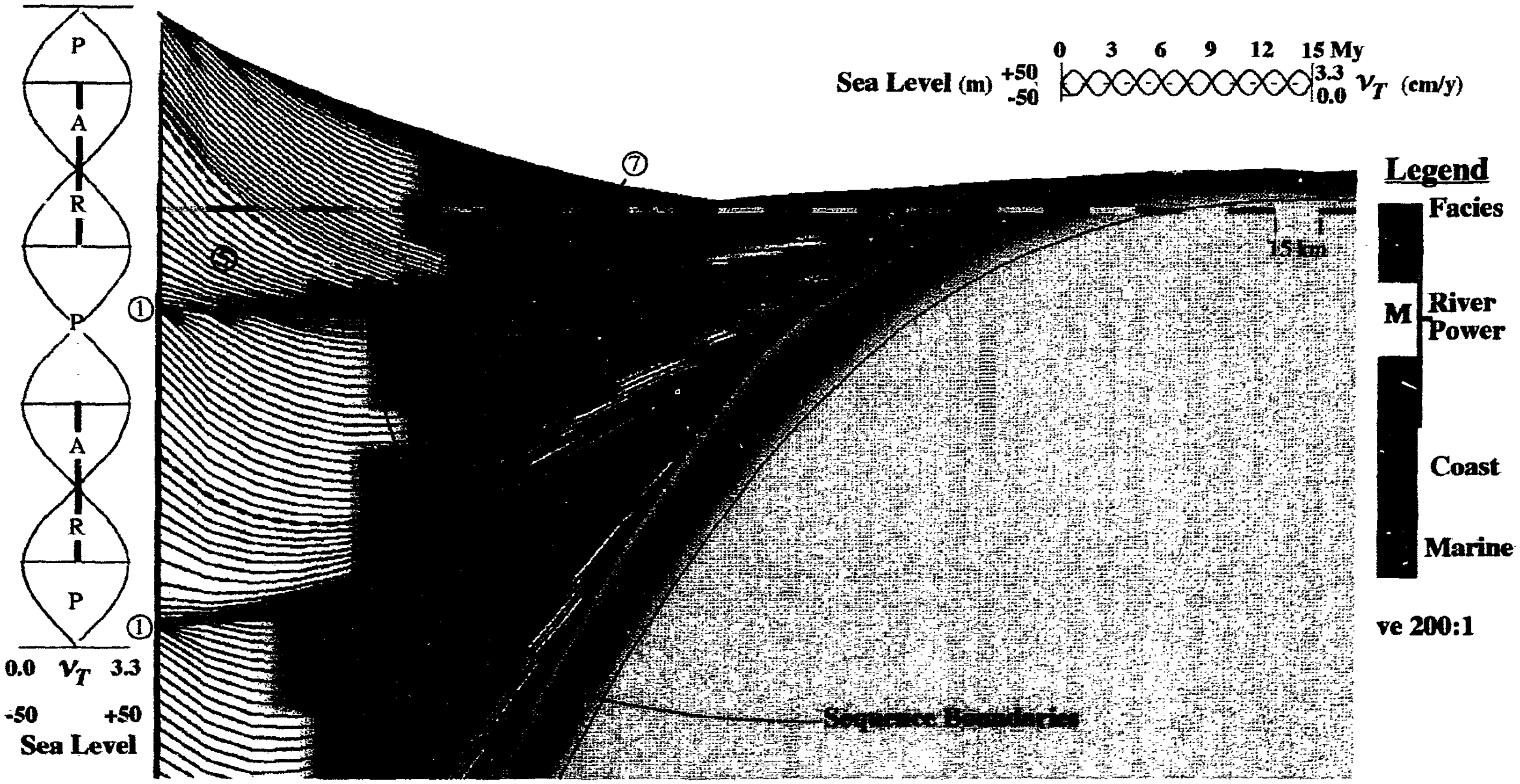

Figure 5.21. In the MTE2 retro-foreland basin (see box, Fig. 5.20) sequences contain progradational, retrogradational and aggradational facies (colour) separated by sequence boundaries composed of erosional surfaces and the rapid transition from marine to alluvial facies in the medial basin. Time lines (black) are at intervals of 50 ky. Blue dashed lines mark sedimentation coeval with eustatic sea-level highstand and minimum v_T. Red dashed lines mark sedimentation coeval with sea-level lowstand and maximum v_T. Sea-level and convergence velocity curves show timing of progradation (yellow), aggradation (green) and retrogradation (blue).

MTE2 - Eustatic Opposition to the Effects of Tectonics

Model MTE2 is similar to MTE1 in that both models have the same amplitude and period of fluctuation in both eustasy and tectonics. MTE2 differs, however, in that sea level falls while the orogen is changing from a destructive to a constructive state and rises while the orogen is changing from a constructive to a destructive state. The change to a constructive orogen state and synchronous eustatic fall in sea level have opposing effects on foreland basin stratigraphy; the former promotes retrogradation, while the latter promotes progradation. Conversely, a change to a destructive orogen state promotes progradation while a coeval rise in sea level promotes retrogradation. Model MTE2 results are shown in planform, transverse and axial sections in Figure 5.20, with an enlargement of the upper retro-foreland basin in Figure 5.21.

The MTE2 orogen at 15 My has just changed from a destructive to a constructive state. As a consequence, the orogen elevation in MTE2 is much lower than in ME5 or MT6 at 15 My (Figs. 5.12, 5.20, 3.20). In planform, however, the length of the orogen along strike in MTE2 is similar to the orogen in MT6 (Figs. 5.20, 3.20), indicating that the MTE2 orogen has developed to an extent similar to MT6 prior to the change in orogen state. In section, the sedimentary wedge adjacent to the orogen in MTE2 is thinner and shows more filling along the basin axis than MTE1 and MT6 (Figs. 5.20, 5.18, 3.20).

The retro-foreland basin of MTE2 contains stacked regressive/transgressive sequences, unlike the transgressive/regressive sequences shown in ME5 and MT6 (Figs. 5.12, 5.20, 3.20). Each sequence is characterized by progradation of alluvial sediments above the sequence boundary followed by retrogradation and aggradation that develop a thick wedge of marine sediments (Figs. 5.20, 5.21). Sequence boundaries in

MTE2 are all associated with maximum rates of sea-level fall, whereas in MTE1 and MT6 erosional surfaces sequence boundaries correspond to sea-level lowstand and minimum tectonics (Figs. 5.19, 3.21).

In MTE2, sequence boundaries consist of an erosional surface proximal to the orogen (①, Fig. 5.21), a rapid transition from marine to alluvial sedimentation in the medial basin (*i.e.*, the inverse of a flooding surface) (②, Fig. 5.21) and erosion of alluvial sediments adjacent to the peripheral bulge (③, Fig. 5.21). Creation of the erosional surface proximal to the orogen is synchronous with sea-level highstand. Filling of the marine basin occurs in part while tectonism is increasing and eustatic sea level is falling (④, Fig. 5.21). With increasing tectonism, isostatic compensation for the growing orogenic load initially reduces the surface slope on the alluvial plain, brings rivers toward grade and causes exhumation of sediments deposited adjacent to the peripheral bulge (③, Fig. 5.21). As the rate of tectonics increases to a maximum and sea level falls to a minimum, rivers on the upper alluvial plain regrade by deposition (⑤, Fig. 5.21), while rivers on the lower alluvial plain are either approaching grade, non-depositional or eroding (⑥, Fig. 5.21). As the rate of tectonics begins to decrease and sea level begins to rise, the area of alluvial sedimentation enlarges, preserving the sequence boundary (Fig. 5.21). Progradation is rapid during this period because sediment flux to the basin is high while the rate of basin subsidence is decreasing. The orogen-to-basin sediment flux remains relatively high as the rate of tectonics decreases; the orogen moves toward steady state and sea level rises. The result is progradation countered by rising sea level (Figs. 5.20, 5.21). Flooding of the basin axis and retrogradation of alluvial facies occur as sea level rises and tectonism continues to decrease (⑦, Fig. 5.21). While retrogradation continues adjacent to the craton, the maximum extent of retrogradation is reached early in the cycle adjacent to the alluvial plain. Retrogradation shifts to aggradation before sea level reaches highstand on the alluvial plain, illustrating the competition between the net sediment flux to the coast and the increase in coastal volume (⑧, Fig. 5.21).

Overall, sequences in MTE2 are dominated by the effect of eustasy over tectonics in the lower alluvial plain and along the basin axis. In these results, progradation/ retrogradation cycles are reversed with respect to the order expected when eustasy is not a factor (MT4 to MT6). These cycles illustrate the effect eustasy could have on the two-phase sequence if eustasy is not in phase with tectonism or if the change in net sediment flux to the seaway is insufficient to dominate over the effects of eustasy.

5.6 Summary

Model results demonstrate the influence of eustatic sea-level change on basin stratigraphy (ME1), sequence development (ME2) and orogen state (ME3). ME4 and ME5 model results show how the rate of eustatic sea-level change affects sequence development. Models MCE1, MCE2, MTE1 and MTE2 show how eustatic change reinforces or counteracts the effects of changes in climate or tectonics. While these results cannot be regarded as a complete sensitivity analysis, some basic characteristics are evident. In summary:

- The effects of eustasy are fundamentally different from those of either climate or tectonics in that eustasy creates sequences through its significant effect on fluvial baselevel.
- Sequences created by eustatic change in sea level are characterized by retrogradation, aggradation and progradation of alluvial facies, with sequence

boundaries composed of flooding surfaces and condensed sections. The extent of transgression and regression depends upon the sediment flux to the coast, topography, and the rate and magnitude of sea-level change. Depending upon its magnitude, the sediment flux can enhance, negate or overwhelm the combined effects of topography and sea-level change.

- Progradation, aggradation and retrogradation are shown to be controlled by competition among the rates of sediment transport to and away from the coast and the rate of change in coastal volume; the latter is controlled by the rate of relative sea-level change and topography. These results are consistent with the conceptual models of Galloway (1989), Schumm (1993) and Wescott (1993).
- Erosion of highstand margins and creation of Type-1 surfaces only occur in model results when there is an increase in slope across the highstand margin and net sediment flux to the coast is not sufficient for progradation to cause a rise in river profile elevation above this margin. These results are consistent with the conceptual models of Posamentier and Vail (1988), Posamentier *et al.* (1988), Schumm (1993) and Wescott (1993). Type-1 erosional surfaces are often discontinuous because the extent of these erosional surfaces is dependent upon the rates of fluvial regrading above, within and below the incised highstand margin. This variability depends largely upon how topography and precipitation affect discharge, and therefore carrying capacity, within each catchment. If present, the erosional surfaces are likely to be associated with the maximum rates of relative sea-level fall.
- Model results MCE1 and MCE2 show how eustasy can reinforce or counteract the effects of wet/dry climate cycles. A change to wetter climatic conditions

synchronous with a fall in sea level reinforces regression by increasing the net sediment flux to the coast while the rate of change in coastal volume decreases. Similarly, a change to a drier climate synchronous with a rise in sea level reinforces transgression by decreasing net sediment flux while the rate of change in coastal volume increases. Conversely, a wetter climate synchronous with a rise in sea level causes an increase in net sediment flux which favors regression; but it also causes an increase in the rate of change in coastal volume, which favors transgression. Alternatively, the change to a drier climate with a fall in sea level causes a decrease in net sediment flux, favoring transgression, while the decrease in the rate of change of coastal volume favors regression.

- Model results MTE1 and MTE2 show how eustasy can reinforce or counter the effects of changes in tectonism through its effect on coastal volume, and thus affect how competition between net sediment flux to the coast and the rate of change of coastal volume controls the rates of progradation, aggradation and retrogradation. Model MTE2 illustrates how a eustatically controlled rate of change in coastal volume can dominate over changes in net coastal sediment flux caused by tectonics and result in progradation/retrogradation cycles which are not consistent with the 'two-phase sequence' of Heller *et al.* (1988).

Chapter 6

Summary and Discussion

This chapter summarizes the main results of the modelling and presents as a basis for discussion comparisons of the primary processes (tectonics, climate and eustasy), their broad scale implications, limitations of the present models and some suggestions for improvements and additional applications.

6.1 Model Components and their Interactions

The principal strengths of the integrated orogen/foreland basin system model developed in this research are the two-sided orogenic belt, the incorporation of advective (fluvial) transport in surface processes, the introduction of orographically controlled precipitation and the inclusion of the effects of planform variations for all processes. In addition, the model processes work in an interconnected, dynamic manner to form a system. Some aspects of the model components warrant additional elaboration and discussion.

Tectonic Processes

The tectonic model is a kinematic representation of the dynamics of a doubly-vergent non-cohesive critical wedge orogen. It has two primary physical properties, the basal and internal coefficients of friction. The geometry is based on plane-strain analytical calculations (Dahlen, 1984) and their extension in numerical models with basal subduction boundary conditions and denudation (Willett *et al.*, 1993; Beaumont and Quinlan, 1994).

For the model results presented, the internal (ϕ) and basal (ϕ_b) coefficients of friction remain constant and therefore the critical taper of the orogenic pro- and retro-wedges changes only with variations in the slope of the basal decollement (β). These results do not consider how changes in the ratio of ϕ to ϕ_b may affect orogen geometry and thus basin stratigraphy. However, such variation in this ratio could be justified as a means of exploring the effects, for example, of hydrostatic pressure or decollement strength on orogen geometry and basin stratigraphy (Dahlen, 1984; Willett, 1992).

In the model results presented $\phi >> \phi_b$. As ϕ approaches ϕ_b wedge taper increases (Dahlen, 1984), minimum and maximum wedge tapers converge toward a common value (Dahlen, 1984), and frontal accretion shifts toward underplating (Willett, 1992); the latter two are characteristics of critical-wedges that are not addressed by the tectonic model used herein. If ϕ were allowed to approach ϕ_b , for example, in a continuously growing orogen/foreland basin system similar to MT1, the orogen would decrease in width and increase in surface slope relative to MT1 (Figs. 3.2 and 3.3) provided equal amounts of material were accreted to either orogen. The associated increase in vertical orogen growth rate would be opposed by an increase in erosion and basin subsidence rates. Erosion rates would increase because of the orographic control on precipitation while basin subsidence rates proximal to the orogen would increase because the orogenic load is less distributed than in MT1. The stratigraphic effects of a smaller ratio of ϕ to ϕ_b would be an increase in fluvial sedimentation rates as a consequence of the increases in sediment flux from the orogen and in subsidence rate of the fluvial profile adjacent to the orogen. In addition, the smaller ratio will cause either an increase in the thickness of marine strata and a decrease in the rate of progradation, or vice versa, depending upon whether or not the change in coastal volume dominates over the change in net sediment flux, or vice versa. In the former case, the distribution of facies in a model with a lower ϕ to ϕ_b ratio at any moment in time may look similar to the facies distribution in MT1 at an earlier moment, only with thicker strata.

In the model results and the discussion above, ϕ and ϕ_b remain constant with time. However, if ϕ or ϕ_b vary with time the orogen/foreland basin system may record changes in subsidence rate that are related more to changes in the form of orogen growth than to changes in the forces causing orogen growth.

The discussion also assumes the orogen is uniform along strike. The main limitation in extending the model to a planform wedge-shaped orogen is the assumption that the wedge can be treated locally as a plane-strain cross section. In the absence of a fully three-dimensional theory, the model uses a strike-length scale on which the orogen behaves coherently under denudation. This scale is justified physically as a measure of the strike-length scale of thrust sheets. It governs the interplay between roughening and smoothing processes within the model orogen and, by extension, the mass transfer between the orogen and the foreland basins. As such, this length scale is an important parameter, yet the sensitivity of the model results to this parameter has not been fully discussed, except to identify that changes in the length scale (l_s) have little effect on model results when ls is greater than five cells (75 km) long; the number of cells is likely to be more important than the absolute length, but this issue has not yet been addressed. Perhaps more important is the great variation in length scales of thrust sheets both among and within orogens such that no single scale can represent natural behaviour. Relating this length scale to the local thickness of the tectonic wedge might offer an improvement, but ultimately, three-dimensional tectonic models must be investigated (*e.g.*, Braun, 1994; Braun and Beaumont, submitted). These models will provide a dynamical framework for three-dimensional kinematic models to be incorporated in the current model.

The tectonic process model is very simple; however, it meets the primary requirements for the current simulations. These requirements are that it, 1) reproduce the large-scale geometry of small orogens and 2) reasonably approximate the mass balance and material flux through an asymmetric orogen formed above a mantle subduction zone. The material flux is derived mainly from the convergent pro-lithosphere, whereas entrainment or accretion into the orogen on the retro side is a more passive consequence of orogen growth. Entrained material is partitioned between orogen growth and loss by denudation. Although the entrainment is in part kinematic, specified initially by $v_T \times d$ (Fig. 2.5), its evolution is dynamic in that it addresses tectonic recycling. The model can simulate constructive, steady and destructive orogen states to at least the first order because mass partitioning is dynamic.

Surface Processes

The surface processes model describes the erosion, transportation and subsequent deposition of material caused by a combination of hillslope, fluvial and submarine processes. It contains the minimum number of processes that can represent the denudation and incision of an orogen, the fluvial transport of sediment to the neighbouring foreland basins and the dispersal of clastic sediments in epeiric seas. The approach is designed to achieve a balance between the time and spatial scales at which each of the component processes operates in the overall model. Little would be gained, for example, by detailed modelling of small catchments if these are below the model's numerical resolution; diffusion acts as a proxy for these processes. Inclusion of a fluvial component, a drainage network and a coupling to an orographic precipitation model represents only a first step in the joining of climate, surface processes and tectonic models; this extreme simplification of complex natural processes must be borne in mind when assessing the model results. The model is designed to give a parametric representation of material fluxes under the control of the most basic physical process models.

Material transport by surface processes in nature is highly variable and often 'event dominated,' whereas in the model, diffusive and advective processes are continuous. Therefore, parameter values were chosen such that averaged transport is approximately equivalent to that observed in nature over the time (1000 yr) and space (15 km) scales resolved by the model, and are not necessarily based on physical principles. This approach makes it difficult to calibrate directly model parameters using field observations. Although such calibration is possible for small catchments on short time scales, the long-term large-scale problem remains unresolved.

The present application differs from earlier models in that the model is not sectional and, therefore, sediment is transported in more than one direction. Diffusivities vary according to the material properties of the substrate and between subaerial and marine environments. Further, the diffusivities in the subaerial environment are smaller than in previous models because diffusion is not used as a proxy for fluvial transport in the coupled advective/diffusive surface processes model. Kooi and Beaumont (1994) use the same surface processes model to investigate the relative effects of diffusion and advection on escarpment morphology and retreat rate. They show that when the efficiency of diffusive transport dominates over fluvial transport, model escarpments are characterized by smooth, low gradient, convexo-concave surface morphology. Conversely, when the efficiency of fluvial transport dominates over diffusive transport, escarpment morphology is characterized by steep gradients and rapid changes in surface slopes. In the model results presented herein, parameter values have been chosen such that advective (fluvial) processes play a greater role than diffusive processes, and as a result the orogen surface is characterized by steep gradients and rapid changes in surface slope.

If, however, diffusive processes were made more efficient than advective processes, then transport would become more slope-dependent and less discharge dependent because diffusive transport is both fundamentally slope-dependent and because this process transports material in all downslope directions; fluvial processes only transport material down the path of steepest descent. The effect on the orogen in a model similar to MT1, with comparable rates of orogen-to-basin sediment flux, would be a decrease both in the surface slopes and the rate of change in surface slopes. On the alluvial plain, surface slopes may be higher or lower depending on the efficiency of diffusive transport relative to advective transport. In models where the rate of orogen growth varies along strike, such as MT3, a change to diffusion-dominated transport would cause an increase in along-strike transport on the alluvial plain proximal to the orogen, because of the multidirectional character of diffusive transport relative to the unidirectional character of fluvial transport. The overall effect on basin stratigraphy would be more uniform sedimentation rates and facies distribution along strike. Basin strata may show a decrease in the rate of seaway filling and an increase in marine facies thickness, however this result depends on the efficiency of diffusive transport relative to advective transport. The rate of transport along the basin axis would be significantly reduced both because axial surface slopes are typically very shallow and because diffusive transport lacks the properties which allow fluvial transport to provide a unidirectional corridor for sediment collection, bypass and distribution to the sea.

In advective transport the cumulative effects of fluvial suspended and bedload transport are represented as transport along a network of one-dimensional rivers. Each river is like a corridor draining the surface topography via the paths of steepest descent, but hillsides and river channels are not distinguished. The carrying capacity of a river (river power) is considered to be proportional to the product of local discharge and slope. Discharge is determined by the collection of rainfall over the upstream watershed, and assumes that water is conserved and neither stored nor lost. Rainfall distribution is determined by the climate model. Fluvial sediment entrainment is treated as a first-order reaction to account for the fact that in nature rivers cannot adjust instantaneously to match local changes in carrying capacity. This view is consistent with the concept that a river must do work on the landscape in order to entrain material. Erosion rate is determined by the product of the local disequilibrium between carrying capacity and sediment flux with a rate constant that characterizes the 'detachability' of material from the consolidated or unconsolidated river bed. Similarly, the deposition rate is determined by the product of local disequilibrium between carrying capacity and sediment flux and a depositional rate constant. The depositional rate constant is chosen such that rivers do not exceed their maximum capacity to transport material.

In the model results, erosional and depositional length scales remain constant. While the parameter values used provide a reasonable approximation of fluvial transport rates, it is expected that these values could vary and produce stratal geometries which are grossly similar. For example, a twofold decrease in the erosional length scale would increase the erosion rate and thus sediment supply to the basin. In a model like MT3, assuming there was no change in orogen state, such a decrease in erosional length scale would cause a decrease in alluvial plain sedimentation and an increase in both transverse and axial progradation. These differences reflect the reduction in the overall relief of the orogen-to-seaway fluvial profile caused by increased erosion of the orogen and associated decrease in the rate of basin subsidence. Depending on the erosion rate and material flux into the orogen this increase could cause a change in orogen state. In contrast a twofold increase in the erosional length scale would reduce the sediment supply to the basin and increase the rates of orogen growth and basin subsidence. These increases may or may not be significant depending on the tectonic flux into the orogen relative to the sediment flux out of the orogen. In a model like MT3, such an increase in length scale would cause a perceptible increase in orogen growth and basin subsidence. Stratigraphically, the increase in basin subsidence and decrease in sediment supply would cause sedimentation rates to decrease more rapidly away from the orogen, progradation rates to decrease, and marine facies to increase in thickness. Sedimentation rates on the alluvial plain may increase immediately adjacent to the orogen because of the increased rate of basin subsidence.

The incorporation of a 'fluvial' advective transport mechanism in subaerial transport makes the present model significantly different from previous foreland basin models which are limited to diffusion only. Using the present approach, erosion and sedimentation rates are determined by local downstream variability in surface slope, material properties of the riverbed and changes in discharge, in combination with the integrated effects of variation in these factors over the upstream watershed. For example, in a river carrying at capacity, a local increase in discharge creates an increase in carrying capacity and therefore potential to erode. This erosive potential is 'carried' downstream until either erosion or a decrease in river slope re-establishes the equilibrium between carrying capacity and sediment flux. While the advective model differs from the diffusive model with respect to erosion, it is similar to the diffusive model in that deposition is dependent on slope, because overcapacity can only be created by a local reduction in river slope. This effect of slope can be countered by capture of a river that is under capacity or by an increase in discharge as a result of precipitation.

Climate Processes

Although the climate model considers only precipitation and prevailing wind, it provides a parametric approximation of how precipitation varies across mountainous regions. In nature, upward deflection and decompression of moist air as it approaches and crosses a mountain belt causes an increase in precipitation on the windward slopes and may create a rain shadow on the leeward slopes (Barry and Chorley, 1971; Barros and Lettenmair, 1994). In the model, precipitation rates increase with the height of the orogen, creating wetter windward and drier leeward mountain slopes until the source (the vapour flux) is depleted. The climate model only considered examples where model 'winds' are perpendicular to orogen strike; such models give the greatest orographic contrasts. However, in many orogens (*e.g.*, Caucasus, Lydolph, 1977), the prevailing winds are parallel to strike. There is therefore a need to investigate a further class of models in which the obliquity of the prevailing wind can be varied.

The orogen/foreland basin model incorporates orographically controlled precipitation because it provides a first-order approximation of the natural spatial scaling of fluvial erosion, sediment transport and sedimentation rates. As discussed, the drainage system and scaling of the discharge through catchment size is the primary control on these fluvial surface processes. Orographic distribution of precipitation is the next most important control to surface slope on the way orogen-to-basin sediment fluxes evolve with increasing orogen elevation and relief. The orographic rainfall model controls how rainfall varies using a combination of surface elevation, vapour flux and extraction efficiency.

In the model results presented, the extraction efficiency is constant. Changes in this parameter value would alter both the intensity and symmetry of precipitation across the orogen/foreland basin system. For example, an increase in extraction efficiency causes an increase in precipitation rates on the windward orogen slope and alluvial plain while precipitation rates on the leeward slope and alluvial plain decrease. Increases in extraction efficiency would result in an increase in erosion rates, orogen-to-basin sediment flux, and efficiency of sediment transport across the alluvial plain on the windward side of the orogen. Conversely, on the leeward side of the orogen, this increase in extraction efficiency would cause a decrease in erosion and sediment transport. The effects of an increase in extraction efficiency on stratigraphic development of the windward foreland are an increase in the progradation rate, an increase in the aerial distribution of higher river-power facies and more uniform sedimentation rates across the alluvial plain. Preliminary experimentation with extraction efficiency indicates that the rates of precipitation, erosion, sedimentation and progradation scale approximately linearly with changes in extraction efficiency.

This simple model has not been calibrated against natural systems and, therefore, may over or underestimate the orographic control of precipitation on the alluvial plain (Sec. 2.4). Barros and Lettenmair (1994) review the fundamental controls on orographic rainfall, issues associated with modelling this type of rainfall, and the problems with calibrating such models. With regard to calibration, they discuss problems such as empirical data collection, model vs. real time scales, and 2D vs. 3D calibration. Further consideration of the principles, models, and problems they discuss may provide a more physical basis for the parameterization of longer-term (>105 yr) orographically controlled rainfall, and greater detail on how precipitation on the windward alluvial plain affects alluvial plain geometry and facies distribution.

Masek *et al.* (1994) have recently created a more physically based model for orographically controlled precipitation. In their model, rainfall is determined by the difference between saturated and actual vapour pressures for air parcels in a vertically stratified air mass that experiences no change in horizontal velocity while crossing surface topography. Each air parcel experiences a forced adiabatic ascent or descent in accordance with the velocity of the air mass and surface topography. Vapour pressures in each parcel vary with temperature and depletion of the parcel's specific volume of water. Temperature is determined by the parcel's elevation relative to a fixed lapse rate (variation in temperature with elevation). Changes in vapour pressure and therefore precipitation rate vary directly with surface elevation, similar to the orographic rainfall model used herein.

Masek *et al.*'s model differs from the model used in that the precipitation rate varies exponentially with elevation because saturation vapour-pressure varies exponentially with temperature. Their model would therefore produce a more focused rainfall distribution given similar topography and initial vapour flux; or their model would predict lower precipitation rates on the alluvial plain if maximum rainfall rates were identical and over the same location in both models. Masek *et al.*'s model is a purer orographic precipitation model, but does not necessarily produce a more accurate prediction of precipitation across the alluvial plain. As noted by Barros and Lettenmaier

(1994), "The strong observed dependence of precipitation rates on such factors as cyclonic or frontal convergence, mesoscale convergence associated with mountain-valley winds, atmospheric instability, and humidity content suggests that pure orographic rainfall is unlikely to occur." Understanding the controls of precipitation rates over the windward alluvial plain adjacent to a mountain front requires further research on orographic precipitation. However, it may be more important to include other climate influenced processes, such as weathering and ice-controlled processes, in any improved model rather than to 'develop' a better model of orographic rainfall.

In the present models, climate change is accomplished by a temporal change in vapour flux along the windward boundary of the model. In general, an increase in vapour flux causes an increase in precipitation rates and results in an increase in sediment yield from the orogen. However, natural behaviour may differ significantly under specific conditions. Fournier (1949, cit. Langbein and Schumm, 1958) showed that the precipitation-to-sediment yield relationship is parabolic. A change from drier to wetter conditions can create an increase in sediment yield when climate conditions prior to the change are moderately wet; this is the case with the present model. However, a change from wetter to drier can cause a similar increase when the conditions prior to climate change are moderately dry. Langbein and Schumm (1958) examine the relationship between sediment yield and precipitation in arid and semi-arid environments, and show that sediment yield increases with a change to wetter conditions in arid environments, but decreases with wetter conditions in semi-arid environments. Furthermore, these authors show that vegetation (desert shrub, grasslands, forests) in semi-arid environments may be a principal control on sediment yield, such that yield varies directly with discharge and inversely with the mass density of vegetation.

Vegetation density is shown to increase approximately linearly with precipitation. Wilson (1973) compares Langbein and Schumm's (1958) sediment yield relationship with new data and concludes that it is approximately correct for continental semi-arid climates but unlikely to be correct for other climate regimes.

The implication of the Langbein and Schumm (1958) results for foreland basins in semi-arid climates is that changes in vegetation may counteract or dominate over the effects of discharge on alluvial plain development. For example, an increase in vegetation may prevent erosion and enhance sedimentation by trapping or binding sediment, thereby countering the increase in sediment transport rates away from the orogen that would be expected with an increase in fluvial discharge. In cases where vegetation dominates over the effects of discharge, changes in time-line geometry may be more uniform during drier climatic conditions and more divergent during wetter conditions, depending on how climate change affects the tectonics. Net sediment transport to the coast would also be affected, and could cause transgressions with wetter climates and regressions with drier ones. Jerzykiewicz and Sweet (1988) observe this relationship in the Belly River Formation, Alberta Foreland Basin.

The orogen/foreland basin model does not include the effects of vegetation; therefore changes in sediment yield with precipitation can only approximate the effects of changes between wet and wetter humid environments, dry and drier arid environments, and arid and humid environments, in accord with Langbien and Schumm (1958). Ultimately, the question of how vegetation affects stratigraphic development of the basin should be considered. Such an investigation could start by varying subaerial diffusivities and erosional and depositional length scales with precipitation in a parabolic fashion akin to Fournier (1949, cit. Langbein and Schumm, 1958).

6.2 Tectonic Rates and Settings

Certain general conclusions can be drawn from the model results concerning the relationships between the sedimentary record and the tectonics of the model orogen. These relationships must be assessed to determine whether they are valid in natural systems.

Sedimentary Filling of the Foreland Basin

In the model, the characteristic stratigraphic pattern of retro-foreland basin filling under constant orogen growth and stable climate, and without eustatic changes, is a conformable succession of marine, coastal and alluvial facies that increasingly onlap the craton (MT1, Fig. 3.4). As filling progresses, time-line geometries show the decreasing influence of isostasy on fluvial and marine deposition in the progradation of the alluvial plain and migration of the seaway away from the orogen. Fluvial sedimentation rates decrease away from the orogen primarily because the disequilibrium between actual and dynamic-equilibrium profiles decreases as subsidence, caused by isostatic compensation for changes in the orogenic load, decreases away from the orogen. In addition, the continually increasing progradation rate illustrates the dominance of net sediment flux over the decreasing rate of change in coastal volume; the latter decreasing rate is caused by the decrease in isostatically forced relative sea-level rise with increasing distance from the orogen. These model results are consistent with those of sectional models (Flemings and Jordan, 1989, 1990; Sinclair *et al.*, 1991; Paola *et al.*, 1992) and with observations from natural foreland basins (*e.g.*, Himalaya Foreland Basin, Burbank *et al.*, 1988).

The continual increase in progradation rate is a consistent feature of basins where orogen-to-basin sediment flux exceeds the increase in submarine accommodation space.

The rates of progradation will, however, vary directly with the efficiency of sediment transport to the coast and inversely with the efficiency of transport away from the coast. For example, orogen/foreland basin systems with high precipitation rates over the alluvial plain and therefore more efficient fluvial transport to the coast are expected to have higher rates of progradation than those with lower precipitation rates. In a model similar to MT1, an increase in transport efficiency would cause a decrease in fluvial sedimentation rates and an increase in progradation rates with the increase in sediment flux to the seaway. Progradation rates would be modestly enhanced by a decrease in the rate of relative sea-level rise caused by a greater distribution of sediment load away from the orogen relative to MT1. Stratigraphically, these changes would be reflected in more tabular lines in fluvial deposits, a decrease in the thickness of the marine facies, and an increase in the rate of seaway infilling. In a model similar to MT3, collection of the increased sediment flux in an axial trunk river system and a decrease in the rate of relative sea-level rise would combine to dramatically increase the rate of axial progradation.

While it is almost inevitable that a change in the rate of offshore transport will cause a change in the rate of progradation, the magnitude and orientation of the change is difficult to predict for two reasons. First, the change in efficiency of offshore transport with basin filling is unknown. Second, changes in offshore transport cause changes in net sediment flux and the rate of change in coastal volume which have competing effects on progradation. For example, if offshore transport increased with basin filling in the model, then the net sediment flux to the coast would increase. However, the rate of change in coastal volume would also increase, provided basin bathymetry was uniform, because submarine surface slopes would become steeper. Progradation rates would, therefore, increase only if the net sediment flux at the coast increased faster than the rate of change in coastal volume.

In the model, the cross-sectional area of a filled foreland basin is fundamentally determined by surface topography prior to orogen growth; the density, magnitude and distribution of the orogenic and sedimentary loads; the rheological properties of the plate that control flexural isostatic compensation; and the interaction of surface and climatic processes that control the shape of the upper surface of the sedimentary basin. Along-strike variation in the cross-sectional area of the foreland basin can be caused by non-uniformity in any of the above factors.

For example, in the model it is possible to introduce topographic depressions in the lithosphere. Such depressions could be similar, for example, to intra-cratonic basins such as the Illinois, Michigan or Williston. Whether proximal to the orogen or the peripheral bulge, these sub-basins would be expected to act as depocentres and locally retard the rate of progradation by increasing submarine accommodation. In addition, isostatic compensation of sediment deposited in the depocentres would expand radially the influence of these sub-basins on sediment transport. As a consequence these basins might deflect and capture fluvial sediment flux that would otherwise have been deposited along the foreland basin axis. An interesting feature of tectonically inactive sub-basins in a foreland basin setting is that their depocentre is likely to shift toward the orogen during periods of orogenic growth and away from the orogen during exhumation; the change in depocentre position would reflect the change in dip of lithosphere with isostatic loading. As such, these sub-basins and the strata within them may act as good indicators (dip meters) of changes in load on the lithosphere.

Similarly, along-strike variation in foreland basin filling could also be caused by lateral heterogeneities in the lithosphere. The model assumes the lithosphere is homogeneous and currently does not have the capability to explore the effects of such heterogeneities. However, Waschbusch and Royden (1992), using a 2D model, show how heterogeneity in the rheology of the lithosphere could have a significant effect on the rates of basin subsidence and peripheral-bulge migration by focusing the flexural effects of isostatic compensation about points of weakness in the lithosphere. If similar flexural behaviour of the lithosphere was incorporated into the current model, it is expected that the fundamental stratigraphic response of an orogen/foreland basin system to tectonism, climate change and eustasy would be basically the same as presently shown. The distribution of facies, however, would vary significantly along strike as subaerial and submarine transport mechanisms responded to the different rates of basin subsidence and changes in baselevel. The most dramatic changes in facies distribution would be expected along the basin axis and adjacent to the peripheral bulge where fluvial systems are most sensitive to changes in baselevel.

Another mechanism affecting foreland basin filling not accounted for in the model is sublithospheric loading caused by mantle convection (Mitrovica *et al.*, 1989; Gurnis, 1992). Both Mitrovica *et al.* (1989) and Gurnis (1992) propose that the hypothetical effects of mantle convection on retro-foreland basin subsidence could explain basin widths which are much greater than can easily be explained by flexural isostatic compensation alone. It is expected that if a kinematic model for the effects of mantle convection were incorporated in the composite orogen/foreland basin model, that retro-foreland basin stratigraphy in a model with uniform convergence along strike would develop in a manner similar to MT1. The stratigraphic section adjacent to the orogen would differ in that progradation rates would be slower and the marine facies would be thicker as a consequence of the increased rates of basin subsidence. The peripheral bulge associated with flexural compensation of the orogenic load would create an intrabasinal high that would subdivide the basin into foreland and 'back-bulge' sub-basins. The peripheral bulge may or may not be emergent depending on the rates of convection-driven subsidence relative to orogenic surface-load driven uplift. Because the foreland basin adjacent to the peripheral bulge and the back-bulge basin would be broad and shallow, the sedimentary environments and facies distribution in these parts of the basin would be very sensitive to the effects of both eustasy and changes in sediment flux from the craton.

Pro- vs. Retro-foreland Basin Settings

Asymmetry in the development of pro- and retro-foreland stratigraphy is caused by the intrinsically higher rates of tectonic convergence between the orogen and basin in the pro-foreland basin setting. Pro-foreland basins are dominated by advance of the deformation front and entrainment of basin strata into the orogen. Therefore, model pro-foreland basins tend to be more starved of clastic sediments, more dominated by marine sedimentation and higher in rates of tectonic recycling than their retro-foreland counterparts. The Taiwan foreland basin is a modern example of a small, active pro-foreland basin that exhibits these characteristics (Covey, 1986). Similarly, Flemings and Jordan (1989) demonstrated that foreland basins adjacent to orogens with higher thrust velocities are sediment-starved relative to those with lower thrust velocities. In contrast, retro-foreland basins with less entrainment of strata into the orogen contain a more complete stratigraphic record of orogen/foreland basin development.

While these relationships are fundamental and are expected to apply in natural pro- and retro-foreland basins, characteristics unique to each basin may create the opposite results. For example, thrust velocities in orogenic retro-forelands could be enhanced by low 'basal' coefficients of friction; such situations could occur where the decollements propagate through salt beds, or through shale with abnormally high (over-pressured) hydrostatic pressure. Conditions like these would enhance the rate of orogen advance, material entrainment and tectonic recycling. Alternatively, pro-foreland basins experience a decrease in these rates at the end of each tectonic cycle as convergence between pro- and retro-plates decreases. The result is that pro-foreland basin development becomes similar to retro-foreland basin development. The similarities in nature between inactive preserved pro- and retro-foreland basins, may be due in part to the preferential preservation of pro-foreland strata associated with the final stages of orogen/foreland basin development.

Model results also show that asymmetry in the development of pro- and retro-foreland basin stratigraphy may also be affected by how erosion and sediment transport rates vary across an orogen/foreland basin system with orographically controlled changes in precipitation. Wet windward conditions over the pro-foreland enhance symmetrical development of pro- and retro-foreland basins by increasing sediment transport to the pro-foreland basin; conversely, a leeward pro-foreland basin setting tends to enhance asymmetry. These effects of orographically controlled precipitation on orogen symmetry may be further enhanced by asymmetric growth of an orogen (Willett *et al.*, 1993). Asymmetry in orogen growth caused by the juxtaposition of minimum taper pro-wedge and maximum taper retro-wedge (Willett *et al.*, 1993) creates a much larger catchment area in the pro-foreland than the retro-foreland, assuming the drainage divide is coincident with the tectonic transition between pro- and retro-wedges. If the pro-foreland was windward, the difference in catchment area in combination with orographically controlled precipitation would increase pro-foreland erosion rates and sediment flux to the seaway and decrease pro-wedge accretion rate, relative to a symmetrically growing orogen. The result would be greater symmetry between the pro- and retro-foreland basins, than in an equivalent system with symmetric orogen growth.

Changes in Orogen State and Two-Phase Sequences

Model results (Sec. 3.4) support the interpretation that low-order sequences can develop in foreland basin settings as a consequence of the change between constructive and destructive orogen states (*e.g.*, Middle Cretaceous, Cycle 2, Alberta Basin, Leckie and Smith, 1992). Such sequences are composed of strata that reflect sedimentation patterns associated with alternate constructive and destructive orogen states and correspond to the two-phase sequences of Heller *et al.* (1988). Change to a constructive state initiates the sequence, causing retrogradation possibly followed by progradation. Change to a destructive state completes the sequence with a change to rapid progradation and possible exhumation of sediments deposited adjacent to the orogen. With the change back to a constructive state, strata adjacent to the peripheral bulge may be eroded. The sequence boundary comprises the erosional surface adjacent to the orogen, condensed time lines and the erosional surface caused by uplift of the peripheral bulge. The sequence boundary adjacent to the orogen is typically a sequence boundary/flooding surface and does not show a basinward shift in facies, while the sequence boundary adjacent to the peripheral bulge does show a basinward shift in facies. The results of the present model and those of Flemings and Jordan (1990) and Peper (1993) all contain facies patterns and stratal geometries that support the two-phase sequence of Heller *et al.* (1988).

Constructive Orogens and Retrogradational/Progradational Cycles

Cycles of progradation and retrogradation in the model correlate with the initiation or acceleration of constructive orogenesis. As material flux into the orogen increases, the orogen grows, flexing the lithosphere, and the basins subside. Concurrent increases in orogen elevation generally increase orographic precipitation on the orogen, causing increases in both the denudation rate and the fluvial mass fluxes into the basins. Basin subsidence reduces the slope of the alluvial plain, which reduces local precipitation and therefore increases fluvial disequilibrium adjacent to the orogen. High-discharge, high-energy rivers transport sediment onto the plain and equilibrium is restored by rapid deposition of high-power facies adjacent to the orogen. This behaviour reinforces the long-held conceptual interpretation (Playfair, 1802, *cit.*, Blair and Bilodeau, 1988) that high-energy facies proximal to the orogen are indicators of renewed (and, in the model, accelerating) tectonic activity in the orogen. The present model and other models (*e.g.*, Paola *et al.*, 1992; Kooi and Beaumont, submitted) suggest that the timing and distribution of these facies reflect both the period of the tectonic episode and the ability of the orogen/foreland basin system to respond to tectonic changes (*i.e.*, response time). Rapid facies changes characterize the transient response of the fluvial system to a tectonic pulse as it adjusts toward a new dynamic equilibrium, while more gradual changes reflect change in a dynamic equilibrium. As discussed later, climate changes may induce a similar response.

Enhanced river discharge and carrying capacity may extend across the lower alluvial plain to the coast. If the coast is within the foreland basin, flexural subsidence causes transgression. The extent of transgression across the alluvial plain and along the basin axis is determined by the surface slopes in these two directions and by the competition between sediment delivery to the coast and the flexurally induced rate of relative sea-level change. When the latter dominates, low river-power facies on the lower alluvial plain are replaced by coastal and marine deposits during transgression. This behaviour agrees with geological interpretations; for example, where the change in facies from shoreface sands to coastal and marine mud in the Dunvegan Formation and Smoky Group (Cycle 3) of the Alberta Basin is associated with an increase in Cordilleran tectonics (Plint *et al.*, 1993). Blair and Bilodeau (1988) had previously suggested that such changes from higher-energy alluvial deposition to lower-energy alluvial or marine deposition indicate increased tectonism.

The model results indicate why changes to both higher-energy and lower-energy facies can correlate with accelerating or renewed tectonics; the former is the proximal, the latter the distal response on the alluvial plain.

On the peripheral bulge, the effect of increased orogen tectonics is uplift and migration toward the orogen, causing fluvial incision of the craton and overlying sediments. These changes induce a fall in baselevel and an increase in surface slope, which in turn leads to progradation of subaerial facies away from the craton and fluvial incision of uplifted sediment. Therefore, regression adjacent to the bulge is synchronous with transgression of the alluvial plain with renewed tectonics. Other foreland basin models (*e.g.*, Jordan and Flemings, 1991) produce similar results. In the model, major rivers crossing the bulge are antecedent in character; thus, sediment transport from cratonic catchments beyond the peripheral bulge are largely unaffected by its uplift. In nature, the deflection of such rivers could significantly change the distribution of both coastal and fluvial facies adjacent to the bulge by either enhancing or reducing fluvial discharge and sediment supply.

In orogen/foreland basin systems, unless the increase in tectonic growth rate continues unchecked and/or tectonic accretion rates remain very high, fluvial systems will re-equilibrate with time and a higher orogen-to-basin sediment flux will force a change from retrogradation back to progradation. While this change at the coast is determined by the competition between sediment supply and the rate of tectonically induced relative sea-level rise, the timing of the change is determined by the response time of the system relative to the period of tectonic change. Retrogradation is maximized when the response time is infinitely large relative to the period of change; i.e., an instantaneous sustained change in orogen tectonics. Conversely, it is minimized when the response time is infinitely small relative to the period of change. In the latter case retrogradation may not be recognizably preserved in the stratigraphic record, regardless of the magnitude of change in tectonic convergence or intensity of climate change. A model with a step function in tectonic convergence having an infinitely short period relative to the tectonic response time will produce a stratigraphic response that is indistinguishable from a model with continuous tectonic convergence at half the rate.

Destructive Orogens, Progradation and the Sequence Boundary

As noted earlier, a change to a destructive orogen state causes an increase in the rate of progradation and creates facies, condensed sections and erosional surfaces which comprise the majority of the sequence boundary. Net reduction of orogen mass reduces the surface elevation of the orogen while increasing the surface slope of the alluvial plain during flexural rebound. Sediments are eroded from the upper alluvial plain near the orogen and redistributed into the basin. Heller *et al.* (1988) suggest that this reworking of higher-energy fluvial deposits is a possible mechanism for the redistribution of coarser clastics across large regions of the foreland. Model results show the advance of the higher river-power facies into the basin (MT4, Fig. 3.15; MT6, Fig. 3.20), supporting this suggestion. This advance illustrates that increasing surface slope initially dominates over the effects of decreasing precipitation on river power. In nature, it is expected that the increase in catchment area with the development of a more mature landscape will also counteract the effects of decreasing precipitation on river power.

A more detailed examination of how the competition between increasing surface slope and decreasing discharge affects erosion rates and fluvial transport capabilities in the model requires higher spatial resolution than the present model provides. In general however, a model similar to MT4 with higher spatial resolution could be expected to show the development of a more highly ordered drainage network. If such a model was allowed to evolve and remain tectonically inactive, then progressively larger drainage basins would expand through headward incision in both the dip and strike directions. Development of one catchment area at the cost of another would result from the dominance of headward incision in one catchment over the adjacent catchment. The along-strike expansion of catchments would cause an increase in separation distance between those rivers which are the major source of sediment supply to the basin. This should result in low relief, long wavelength, along-strike variation in surface relief and river-power facies. It is also expected that drainage area development would become progressively more sensitive to spatial variations in precipitation. The catchments with higher precipitation rates would grow at the expense of catchments with lower precipitation rates. The sensitivity of the model to precipitation rates would then raise the question of whether a model for orographically controlled precipitation should be used because in nature as orogen topography decreases, the importance of 'forced' adiabatic air mass ascent on precipitation decreases while the effects of other controls increase in importance; e.g., thermal instability.

Isostatic rebound also enhances progradation rates away from the orogen and along the basin axis. Tilting of the basin increases river gradients so that they approach or exceed grade. Fluvially transported sediment bypasses the alluvial plain and is delivered to the coast, where regression occurs because relative sea level is falling. The combined effect of flexural tilting and uplift therefore promotes progradation. Later in the destructive phase, when orogen elevation is reduced, both the orogen-to-basin sediment flux and rate of progradation decline. In the model, these declines are minor by comparison with the overall progradational pattern. As a natural example, Plint *et al.* (1993) suggest that the rapid progradation of shoreface sands in the Dunvegan, Cardium and Marshybank formations may be associated with reduced loading in the Cordillera.

In model experiments, erosion of an abandoned shoreface is not observed with the isostatically induced relative fall in sea level. Whether the relative rate of sea-level fall is fast enough to cause erosion of the coastal zone depends on the changes in the net sediment flux to the coast. Erosion occurs when there is an increase in slope at the shoreface and progradation does not cause a sufficient aggradational increase in the fluvial profile elevation.

The rate of progradation is determined by the competition between the effects of net sediment flux to the coast and the rate of relative sea-level fall. Because the rates of both the isostatically driven relative sea-level fall and the sediment supply to the coast are fundamentally related to the rate of erosion of the orogen, it is the conditions controlling the efficiency of sediment delivery to and away from the coast that determine if erosion will occur. When surface slopes are low, small changes in environmental factors may be sufficient to cause changes between conditions which prevent or enhance the development of Type-1 erosional surfaces. For example, in nature changes in precipitation rates on the alluvial plain related to changes in orographic controls of precipitation could significantly increase or decrease the ability of a fluvial system to deliver sediment to the coast. Alternatively, changes in bathymetry or prevailing wind direction could change current patterns and significantly enhance or reduce the efficiency of sediment transport away from the coast. Furthermore, such changes are likely to affect littoral transport and thus either enhance or retard the effects of offshore transport. The effects of littoral transport may be particularly important where sediment transport to the coast varies significantly between adjacent fluvial systems. Model experiments investigating development of Type-1 surfaces have not been conducted. However, it is expected that if either marine diffusivity were doubled, or the orographic extraction efficiency were halved, Type-1 surfaces would form with isostatically induced relative sea-level fall.

A new cycle and stratigraphic sequence begins with renewed orogen tectonics, return to a constructive orogen state, deposition of higher-energy alluvial facies adjacent to the orogen and flooding of the alluvial plain. The underlying sequence boundary is composed of erosional surfaces created by exhumation of sedimentary facies adjacent to the orogen; non-depositional or condensed sections of the lower alluvial plain; and condensed sections of the marine basin. The juxtaposition of alluvial and marine facies caused by flooding of the basin is also a characteristic feature of this sequence boundary.

6.3 Climate Setting and Rates of Vapour Flux

Rates of precipitation are also a primary concern in the modelling of orogen/ foreland basin systems due to the manner in which rainfall distributions change with growth of the orogen. Orographically controlled precipitation in the climate model provides a first-order approximation of how rainfall distributions may change across orogen/foreland basin systems as they evolve over long time scales. In addition, variations in the vapour flux along the upwind boundary can be used to investigate how changes in precipitation rates caused by climate change may affect the development of orogen/foreland basin systems.

Climate Oscillation and Retrogradational/Progradational Cycles

Some aspects of the model response to climate change are similar to those induced by tectonic variability. This similarity occurs because the two effects are coupled; orographic precipitation is partly determined by orogen topography (elevation) and denudation of the orogen is determined by the capacity of the model climate. Consequently, while certain aspects of the following discussion appear similar to their tectonic equivalents, they are not necessarily the same as, nor repetitions of, tectonic effects.

Model results show that the change to a drier climate creates a retrogradation/ progradation cycle. Retrogradation is initiated by a decrease in rainfall on the orogen that results in decreases in erosion rates, in orogen-to-basin sediment flux and in the river-power facies on the alluvial plain. There may also be a decrease in precipitation on the upper alluvial plain that inhibits the transport of sediment away from the orogen and decreases river power, as observed in basin facies. The decrease in precipitation also enhances sedimentation adjacent to the orogen, thereby increasing the slope of the alluvial plain. The consequent increase in slope of the alluvial plain is the system feedback by which it tries to attain grade. Chronostratigraphically, the change in sedimentation rates is expressed as an increase in time-line divergence toward the orogen. A decrease in the sediment flux to the coast enhances the possibility that transgression will occur as the orogen grows under reduced denudation. Attendant changes in orogen and sedimentary loads cause uplift and migration of the peripheral bulge toward the orogen, resulting in subaerial exposure and fluvial incision of strata on the bulge and progradation of facies adjacent to it. The rate of progradation may be influenced by decreased precipitation rates on the craton.

Orographic control on precipitation counteracts the effects of a change to a drier climate. Concurrent with the change to a drier climate with lower precipitation rates and decreased erosion rates are increases in orogen elevation, orographic precipitation, denudation rate and fluvial material flux into the basins. As the climate change ends, the system establishes a new equilibrium; retrogradation will return to progradation when the net sediment supply to the seaway exceeds the isostatically induced relative rise in sea level. When growth of the alluvial plain and progradation resume, migration of the peripheral bulge away from the orogen results in transgression of the craton and overlying sediments.

In contrast, change to a wetter climate increases precipitation and initiates progradation, because orogen erosion and orogen-to-basin sediment transport rates increase. The orographic effect extends to the model's alluvial plain, further enhancing river power and sediment transport rates, decreasing surface slope and sedimentation rates adjacent to the orogen while increasing sediment flux to the seaway. The increase in sediment flux reaching the coast opposes any relative rise in sea level and, as shown by the model results, causes progradation. In fact, relative sea level may fall if the orogen changes to a destructive state because of the climate change. Progradation is also enhanced by a reduction in the rate of isostatically induced relative sea-level rise with a decrease in orogen growth. The sedimentary expression of these changes is a decrease in sedimentation rates adjacent to the orogen and an increase on the distal alluvial plain, observed as a shift to a 'tabular' time-line geometry. The increase in river-power facies across the alluvial plain is expressed as the basinward advance of high and moderate river-power facies with progradation.

Windward and Leeward Settings

Model and natural orogen/foreland basin systems show both symmetry and asymmetry in precipitation rates across the orogen. In the model, asymmetry develops with growth of the orogen. In the incipient orogen, rainfall distributions, erosion rates and orogen-to-basin sediment flux are relatively symmetric. With continued orogen growth and increasing elevation, windward precipitation rates increase, while the attendant decrease in vapour flux reduces precipitation rates on the leeward side of the orogen, creating a rain shadow. This asymmetry in precipitation creates asymmetry in erosion rates and in the orogen-to-basin sediment flux across the system. Therefore, leeward basins are typically sediment-starved relative to windward foreland basins in an equivalent setting. In addition, leeward basins have lower precipitation rates on their alluvial plains. In the windward setting, higher precipitation rates across the alluvial plain increase the fluvial discharge of rivers, countering the effects of decreased surface slopes, and thereby increasing the net efficiency of sediment transport away from the orogen. The result is shallower surface slopes on the windward alluvial plain than on its leeward counterpart at a comparable stage of development.

In the model precipitation on the alluvial plain is shown to vary directly with increasing and decreasing surface elevation as part of the orographic effect on precipitation. As previously discussed, orographic precipitation is complicated and model results may under or overestimate how precipitation varies with changes in alluvial plain elevation. Precipitation on the plain has the effect of increasing fluvial carrying capacity and thereby decreasing sedimentation rate and surface slope. Therefore, it is expected that in a model similar to MT3 where fluvial discharge remains approximately constant across the alluvial plain, there would be steeper surface slopes and greater storage of sediment adjacent to the orogen. Stratigraphically, basin facies would show a reduction in the rate of progradation, a decrease in the aerial extent of river-power facies along any time surface, and an increase in the thickness of marine facies. The latter would be consistent with the increase in sediment storage adjacent to the orogen and would foster an increase in basin subsidence, a decrease in sediment transport to the coast, and a decrease in the rate of progradation and seaway infilling.

Climate vs. Tectonic Periodicity

Model results indicate that the effect of a climate change is greatest on the orogen, because topography focuses orographic precipitation. Climate change either enhances or retards erosion rates on the orogen while simultaneously either enhancing or inhibiting fluvial transport across the alluvial plain. Table 6.1 summarizes these effects of climate change and compares them with the effects of changes in tectonism. Overall, the effects of changes in climate and tectonics are similar because of the dominant orographic control on precipitation. It follows that model results support the premise that

Tectonics	Orogen		Alluvial Plain					Peripheral Bulge		
Convergence Rate (v_T)	Growth Rate ± ve	Q_S	Erosion	Sedimentation Rate Gradient	Coastal Flux	Sea Level	Facies $\Leftarrow / \Rightarrow$	Sea Level	Facies	Erosion
$v_T \Downarrow$	destructive	$\Downarrow$	Yes	$\Downarrow$	$\Downarrow$	fall	$\Rightarrow$	fall	$\Rightarrow$	Yes ?
$v_T \Downarrow$	$+\Downarrow$	$\downarrow$	No	$\Downarrow$	$\downarrow$	rise	$\Rightarrow$	rise	$\leftarrow$	No
$v_T \Uparrow$	$+\Uparrow$	$\Uparrow$	No	$\Uparrow$ then $\Downarrow$	$\Uparrow$	rise	$\Leftarrow$ then $\Rightarrow$	$\Downarrow\Uparrow$	$\Rightarrow$ then $\Leftarrow$	Yes
Climate	Orogen		Alluvial Plain					Peripheral Bulge		
Vapour Flux (Q_V)	Growth Rate ± ve	Q_S	Erosion	Sedimentation Rate Gradient	Coastal Flux	Sea Level	Facies $\Leftarrow / \Rightarrow$	Sea Level	Facies	Erosion
$Q_V \Uparrow$	destructive	$\Downarrow$	Yes	$\Downarrow$	$\Downarrow$	fall	$\Rightarrow$	fall	$\Rightarrow$	No ?
$Q_V \Uparrow$	$+\Downarrow$	$\Uparrow$	No	$\Downarrow$	$\Uparrow$	rise	$\Rightarrow$	rise	$\leftarrow$	No
$Q_V \Downarrow$	$+\Uparrow$	$\Downarrow\Uparrow$	No	$\Uparrow$ then $\Downarrow$	$\Downarrow\Uparrow$	rise	$\Leftarrow$ then $\Rightarrow$	$\Downarrow\Uparrow$	$\Rightarrow$ then $\Leftarrow$	Yes
Eustasy	Orogen		Distal Alluvial Plain					Peripheral Bulge		
(v_E)	Growth Rate ± ve	Q_S	Erosion	Sedimentation Rate Gradient	Coastal Flux	Sea Level	Facies $\Leftarrow / \Rightarrow$	Sea Level	Facies	Erosion
$v_E \Downarrow$	no change	constant	Yes ?	$\Uparrow$	$\uparrow$	fall	$\Rightarrow$	fall	$\Rightarrow$	Yes ?
$v_E \Uparrow$	no change	constant	Yes ?	$\Uparrow$ then $\Downarrow$	$\downarrow$	rise	$\Leftarrow$ then $\Rightarrow$	rise	$\Leftarrow$ then $\Rightarrow$	Yes ?

Table 6.1. Summary of stratigraphic characteristics reflecting periodic changes in tectonics, climate and eustasy. Compare grey and white cells for effect of a change in process rate. The symbol $\Rightarrow$ denotes progradation and $\Leftarrow$ retrogradation, while $\Uparrow$ indicates increase and $\Downarrow$ decrease. In combination, $\Uparrow\Downarrow$ indicates an increase followed by a decrease. Facies associated with grey cells typically show retrogradational/progradational cycles, while facies associated with the adjacent white cells show enhanced progradation.

changes in climate offer an alternate mechanism to tectonics for creating changes between more 'angular' and 'tabular' stratal geometries.

Model results clearly illustrate that changes in climate can either reinforce or retard the development of stratigraphic signatures generally characteristic of changes in tectonism because of the similarity of the orogen/foreland basin system response to these two processes Distinguishing between stratigraphic changes caused by climate and those caused by tectonics is assisted by the knowledge that climate changes are often cyclic, recurring over periods consistent with orbital rhythms. In contrast, our current understanding suggests that tectonic changes lack an inherently rhythmic forcing mechanism. Therefore, distinguishing between longer-term episodic changes in climate, such as the mid-Miocene global increase in aridity, and changes in tectonics, is fundamentally more difficult.

Model results indicate that the effects of a change to a wetter climate may be distinguishable from a decrease in tectonic mass flux. In the former case, the increase in orogen erosion rate and the attendant decrease in orogen growth rate combine with an increase in fluvial transport efficiency across the alluvial plain. These changes cause a relative increase in the orogen-to-basin sediment flux, a decrease in the rate of basin subsidence and a decrease in the rate of relative sea-level rise, thus promoting a significant increase in progradation rate. Similarly, a decrease in orogen growth rate caused by tectonics is also accompanied by a decrease in the rate of relative sea-level rise and an enhanced progradation rate. However, the tectonic change is not accompanied by an increase in either orogen-to-basin sediment flux or in river-power and transport efficiency across the alluvial plain; in other words, increasing progradation is achieved with no increase, and possibly a decline, in sediment flux from the orogen. As a consequence, changes in climate may cause greater increases in progradation rates than do changes in tectonics (Table 6.1), but this imbalance must be assessed for each case. A signature of climatically forced increase in progradation is the change to more uniform sedimentation rates and therefore a more 'tabular' time-line geometry, as described previously. In addition, facies on the alluvial plain reflect an increase in river power associated with the higher precipitation rates. However, these indicators are not totally diagnostic. What is required is an estimate of the mass balance of the system measured over the response time: the sediment flux from the orogen and on the lower alluvial plain, combined with the chronostratigraphic geometry.

Other indicators, like the position of longitudinal rivers may be useful (Burbank, 1992). However, indicators which depend on basin geometry are unlikely to be precise, because of the ability of both tectonic and climatic forcing to modulate the behaviour of the orogen and basin without causing a change in orogen state. Another promising line of investigation would be to measure response times of orogen/foreland basin systems to climate and tectonic changes. Conjecture based on the present results is that climate response time would be shorter. If so, sediment flux estimates may allow distinction between higher-frequency tectonic and climate forcing.

An alternative is to examine in greater detail the stratigraphic characteristics of the transient response to changes in climate and tectonics. These responses are fundamentally different in that they have opposite effects on the initial change in discharge. For example, comparison of MT5 and MC3 shows that a rapid change to a wetter climate initially increases orogen-to-basin sediment flux, whereas a sudden end of orogen growth causes a steady decline in the same flux. Such differences in natural environments may produce identifiable changes in fluvial architecture or clastic facies distributions adjacent to the orogen. Gradual changes in climate and tectonics that force the system to evolve through a dynamical equilibrium will not produce similar differences and will, therefore, remain cryptic.

The effects of a change to a drier climate and acceleration in orogen growth may also be distinguishable. In the former, rapid decrease in erosion rate, increase in orogen growth and decrease in the efficiency of transport away from the orogen focus sedimentation adjacent to the orogen. The increase in sedimentary and orogenic loads, combined with the decrease in sediment transport to the seaway, may result in transgression. An acceleration in orogen growth is also accompanied by an increase in the rate of isostatically induced relative sea-level rise, potentially causing transgression. However, this acceleration is accompanied by an increase, rather than a decrease, in orogen-to-basin sediment flux. It is not accompanied by a decrease in sediment transport efficiency caused by reduced precipitation. Therefore, the rapid change to a drier climate causes a reduction in the rate of progradation, or a change to retrogradation, with decreases in sediment flux to the seaway. Thus climate change is expected to cause a greater change in the rate of progradation or a change to retrogradation with comparable changes in orogen growth rate. However, climate and tectonic changes both induce increases in orogen growth rate that produce higher gradients in time lines and in river-power facies across the alluvial plain. Distinguishing between the effects of climate and tectonics depends upon identifying the relative effects of fluvial discharge on orogen-to-basin sediment flux and transport efficiency across the alluvial plain.

Comparison of orogen-to-basin sediment flux for orogen/foreland basin systems that experience step function changes in climate and tectonics shows that the transient responses are significantly different. With the change to a drier climate there is an initial decrease in sediment flux followed by an increase toward an asymptote as the fluvial system progresses toward a dynamic equilibrium. With an increase in tectonics, the flux simply increases toward an asymptote. In nature, such differences may have a significant impact on grain size availability and facies distribution on the upper alluvial plain and across the basin. Further study of how grain size distribution relates to river power is required before the relationship between transient response to changes in climate and tectonics can be explored using this model.

6.4 Orogen/Foreland Basin Response Time

Results from the model for periodic tectonic changes show a characteristic system response time. This composite system response is characteristic of the interaction among model processes and will change if a process changes (e.g., models MT5, MT5a, MT5b). Model results show the stratigraphic response of a system to tectonic forcing with time scales much greater than the system response time, is in phase with the forcing and not attenuated. Forcing with a period comparable to the response time gives a stratigraphic signature that is attenuated and lags behind the forcing. Although the effects of tectonic forcing with time scales that are much shorter than the response time were not explored, it is expected that the stratigraphic response would be strongly attenuated and out of phase.

When the sedimentary response to tectonics is treated as a diffusive process, the length scale (Δl) over which a response occurs is related to the time scale of forcing, because diffusive systems have response times $\tau = \Delta l^2 / K_S$ where K_S is the diffusivity (Culling, 1960; Kooi and Beaumont, submitted). This scaling for depositional systems is discussed by Paola *et al.* (1992) who term the response time 'equilibrium time.' They also demonstrate that under some circumstances fluvial sediment transport may be diffusive and that the diffusivity of a river is proportional to discharge. This dependence on discharge renders diffusivity a scale-dependent parameter and undermines the argument that there is a single length-dependent parameter over which fluctuations, for example, in sediment input are 'felt' in the basin (Paola *et al.*, 1992). The length scale over which a change in sediment input will propagate in a given time depends on discharge, and discharge scales approximately with the area of the river catchment under conditions of uniform precipitation rates. In a physical sense, this means that fluctuations in large rivers should propagate from the orogen to the coast in the same time that fluctuations in a river with a discharge one order of magnitude smaller will propagate one tenth the distance. Under these circumstances the response time scale may be more closely related to river discharge than to Δl^2.

The behaviour described above contrasts the present model results with those of Paola *et al.* (1992). The response time in the models discussed here is a system response time that relates to both denudational and depositional components of the orogen/foreland basin system. The response time scales with discharge (q_r), erosion properties of the river bed ($l_f^{erosion}$), depositional properties of the river ($l_f^{deposition}$) and transport properties of the river (K_f). Furthermore, the response of the system does not propagate diffusively from the orogen into the basin. The approximate scale independence of the model response is illustrated by the instantaneous response of QS(retro) to changes in tectonics (MT5) and by the instantaneous stratigraphic response throughout the entire basin in models with both longer (3 My, MT6) and shorter (400 ky, MT7) periods of tectonic forcing.

However, the models with longer and shorter periodicity in tectonic and climatic forcing do contain differences which indicate that the length and time scales of stratigraphic response vary directly with the period of tectonic change and inversely with the response time of the system. For example, in MT7 relative to MT6, erosional surfaces are less extensive, changes in time-line geometry and fluvial facies distribution more subtle, and transgressive/regressive cycles less extensive. Although both models MT6 and MT7 experience an identical change in the magnitude of tectonic convergence rate, the stacked sequences of MT6 appear as stacked parasequences in MT7. This appearance is caused by the horizontal separation between transgressive/regressive cycles and erosional surfaces adjacent to the orogen, providing the impression that each retrogradation/progradation cycle is separated by a flooding surface rather than the correlative conformity of an erosional surface. This means, for example, that if a thrust sheet is advancing in a slip/stick fashion, the stratigraphic record across the entire basin will record each slip/stick event. When the period of change is much longer than the response time, the stratigraphic effects should be well developed both aerially and temporally and the sequences readily identifiable. However, when the period of change is on the order of the response time, the stratigraphic response will be less well developed so that a localized view of basin strata in isolation from its regional and temporal context may be incorrectly interpreted as having been deposited during a tectonically inactive period.

Finally, as mentioned above and as illustrated in models MT5, MT5a and MT5b, the composite response reflects the interaction of all processes, and will therefore change as processes change. In all models, with the exception of MT5a and MT5b, the processes remained constant while their 'activity' level changed with the evolution of the orogen/foreland basin system. In nature, it is likely that both the processes and their activity levels will change, so that the response time will change with the evolution of the system. For example, while orographic precipitation was used in the composite orogen/foreland basin model, precipitation is actually affected by topographic obstacles to air flow in different ways as the processes controlling precipitation change (Barros and Lettenmaier, 1994). With large mountains, forced lifting of air masses provide conditions which are capable of providing 'continuous' precipitation. However, small hills, such as those that may be associated with incipient orogen growth or the last stages of orogen exhumation, create only a modest amount of air mass lifting, and cannot by lifting alone have the same effect on precipitation. High precipitation rates do however occur over areas of low topographic relief. One process for explaining high precipitation rates in low relief areas is referred to as a seeder-feeder mechanism (Bergeron, 1960 *cit.* Barros and Lettenmaier, 1994). In this process, a 'stationary' cap cloud provides the reservoir or 'feed' for high precipitation rates, while 'seed' for precipitation is provided by clouds brought by passing weather systems. In an orogen/foreland basin system evolving from lower to higher relief, or vice versa, the processes controlling precipitation could change, for example, from a seeder-feeder process to a process dominantly controlled by forced air lifting. This change in processes would be expected to alter the climatic response time of the system.

6.5 Eustasy

Eustasy has an important effect on model foreland basin stratigraphy. When surface slopes adjacent to the coastline are low, net sediment flux to the coast may be less than the rate of change in coastal volume caused by eustasy, and the rates of relative sea-level change caused by other processes such as tectonics or isostasy may also be less than the eustatic rate. These factors will also be important in natural settings.

Extent of Eustatically Forced Transgressive/Regressive Cycles

Model results show that in orogen/foreland systems that develop under constant tectonic and climatic conditions, the maximum extent of eustatically forced transgressive /regressive cycles occurs at the time of seaway closure. In the early stages of basin filling, the lateral extent of these cycles is inhibited by the steeper slopes on the alluvial plain and possibly by greater sediment flux to the coast than occurred when the seaway is nearly closed. Furthermore, the degree to which isostasy enhances eustatically forced changes in relative sea level is greater when the shoreline is closer to the orogen in the early stages of basin filling rather than later, because isostatically induced changes in relative sea level decrease away from the orogen. Subsequent to closure of the seaway, transgressive/regressive cycles are less extensive because of increasing surface elevation on the alluvial plain and along the basin axis caused by continued sedimentation. In general, the cycles are more extensive along the basin axis where surface slopes are shallower than on the alluvial plain. Surface slope of the axis is determined by the rates of aggradation of alluvial facies and progradation of the coastline.

While the pattern of progressively more extensive eustatically forced transgressive/regressive cycles followed by progressively less extensive cycles is a fundamental characteristic of foreland basins, the extent of these cycles can be significantly increased or reduced by both changes in the rates of sediment transport to and/or away from the coast, and by isostatically forced changes in relative sea-level rise or fall. For example, in a model similar to ME1 but with more efficient fluvial sediment transport across the alluvial plain, the decrease in subaerial surface slope would increase the extent of eustatically forced cycles prior to seaway closure, closure would occur earlier and more cycles would occur after closure. Alternatively, a decrease in the efficiency of marine transport in a model similar to ME1 could cause an increase in progradation rate and steeper marine surface slopes adjacent to the coast, while alluvial plain slopes would remain relatively unchanged. Eustatically forced cycles would therefore be fewer and increase in extent faster prior to seaway closure, seaway closure would occur sooner, and less cycles would occur after closure. Each cycle at an equivalent time in basin development would be slightly less extensive than in ME1 because of the steeper marine surface slope.

Finally, a change in the flexural rigidity relative to ME1 will change the overall dimension of the basin and the isostatic contribution to eustatically forced sea-level change. As shown by Beaumont (1978) among others, an increase in flexural rigidity increases the width and decreases the amplitude of isostatic compensation; the reverse is true with a decrease in rigidity. While the basic pattern of how transgressive/regressive cycles change in extent with basin filling remains the same, an increase in rigidity relative to ME1 will cause an increase in the extent of these cycles prior to seaway closure, an increase in the rate of seaway closure and an increase in the extent of these cycles after closure. The increase in extent of the cycles would be caused primarily by lower surface slopes on the peripheral bulge. Although progradation rates would be faster because of the decrease in basin subsidence rates, the slope of the alluvial plain would not be significantly different at equivalent stages of basin filling relative to ME1. A decrease in rigidity will have the opposite effect on the extent of transgressive/regressive cycles. The implication is that, where all other conditions are equal, the stratigraphy of foreland basins developing over weaker lithosphere (Stockmal *et al.*, 1986) may be less sensitive to eustasy than to stronger lithosphere.

Net Coastal Sediment Flux and Rate of Relative Sea-Level Change

In model results, the time of maximum transgression or regression occurs between the time when the rate of sea level change is at a maximum and the time when sea level achieves highstand or lowstand, respectively. These results are consistent with conceptual and numerical models of eustatic effects on basin stratigraphy (*e.g.*, Posamentier *et al.*, 1988; Galloway, 1989; Jordan and Flemings, 1991). Both instantaneous and rapid sinusoidal changes in sea level show that the maximum extents of transgression and regression occur in phase with sea-level highstand and lowstand in the limit when changes in coastal volume are much greater than net sediment flux at the coast. Slower sinusoidal changes in relative sea level show the effects of a decreasing rate of change in coastal volume while the net sediment flux remains approximately constant. Aggradation begins prior to, and ends after, sea-level highstand. Sea-level fall occurs without erosion of the highstand shoreface. The maximum extent of progradation occurs after sea-level lowstand. Variation in transgressive/regressive cycles within the near-full foreland basin shows that as the basin fills, subsidence has a progressively decreasing effect on relative sea-level rise; periods of retrogradation decrease while periods of aggradation and progradation increase.

Although the parallel models in which variations in sediment flux to the coast dominate the rate of coastal volume change produced by eustasy have not been investigated, a conceptual prediction of the transgressive/regressive cycles can be made. For example, net sediment flux is most likely to dominate over the effects of eustasy when relative sea level is cycling slowly with respect to variations in sediment flux to the coast caused by change in either climate or tectonics. With a rising sea level, increasing sediment flux to the coast will cause a change from retrogradation to either aggradation or progradation, while decreasing sediment flux will enhance the rate of retrogradation. Conversely, with a fall in sea level, increasing sediment flux would enhance the progradation rate, while decreasing flux would retard the rate of progradation. The periodicity in relative sea-level change. as related to changes in sediment flux, will determine whether eustatically forced transgressive/regressive cycles can be distinguished from climatically forced cycles. The two types of cycles will be distinct when period frequencies are significantly different, with multiple climatically forced transgressive/regressive cycles occurring within a single eustatic cycle. Progradation and retrogradation will be either enhanced or retarded depending on whether sea level is rising or falling. A natural example of stacked climatically forced high frequency transgressive/regressive cycles is interpreted by de Boer *et al.* (1991) to occur in the South Pyrenean, Tremp-Graus Foreland Basin; however in this example the longer-term relative sea-level rise is caused by tectonics rather than eustasy. In the model, if the frequency of climate change approaches that of eustasy, climatically forced transgressive/regressive cycles should still be distinguishable from eustatically forced cycles by identifying the effects of climate change on the upper alluvial plain adjacent to the orogen.

Erosion and Eustasy

Model results show that erosion of the coastal plain can occur with either a rise or fall in sea level. Typically, erosion is associated with rapid changes in sea level when net sediment flux to the coast is much less than the rate of change in coastal volume caused by relative sea-level rise or fall.

Sea-level Fall

In the model, fluvial erosion of the lower coastal plain may occur during a relative fall in sea level; the principal control is the position of the baselevel of the rivers. Baselevel is determined by the competition between the net sediment flux to the coast, the rate of change of coastal volume and the change in slope across the coastline.

Lowering sea level, in the absence of sediment supply, will cause fluvial incision when the offshore slope is greater than the graded slope of the alluvial plain. Erosion will not occur if the offshore slope is less than the slope of the graded river. Incision is prevented when sediment deposited at the coast and the attendant fluvial profile aggradation prevent lowering of the baselevel below the graded profile as it migrates seaward. In this way, the competition between the rate of fluvial progradation at the coast and the rate of coastline advance toward the ocean can result in either fluvial erosion or deposition on the coastal plain, consistent with the observations of Schumm (1993).

If erosion is to occur, fluvial incision of the shoreface can begin at any time between the start and the maximum rate of relative sea-level fall. Erosion occurs early in the cycle for steep offshore slopes. Model results suggest a threefold division of the fluvial catchments into upper, middle and lower zones is in agreement with the conceptual model of Posamentier and Allen (1993). The upper and middle zones are separated by a nick point in the eroded shoreface; the middle and lower zones are separated by the slope break at the base of the incised shoreface. Individual catchments will have their own response characteristics based on discharge, sediment flux, change in effective baselevel elevation and material properties of the substrate. The extent of erosion and the response time will vary to reflect the rates of regrading of the upper, middle and lower fluvial zones. Fluvial incision of the shoreface continues until facies of the upstream alluvial plain downlap the incised surface and meet with onlapping facies of the lowstand fluvial system.

A consequence of catchment-dependent variability of erosion is that the time in the eustatic cycle when erosion begins and ends will also vary along the lower coastal plain. Therefore, some catchments may experience erosion while others do not. The catchment dependence of the response explains why such an erosional surface is diachronous and intermittent, making it a poor sequence boundary indicator.

Sea-Level Rise

In the model, erosion of lowstand margins occurs during a sea-level rise when sediment flux to the submerged margin is less than sediment flux away from the margin. The principal control is the difference in slope between the flooded coastal region and the offshore region that remains marine throughout the eustatic cycle. Sediment transport in both of these regions is diffusive and fluxes are inversely proportional to the slopes. Sediment transport across the flooded region is inhibited by the low slopes inherited from the fluvial regime. When the sediment flux across this region is less than the corresponding flux down the steeper offshore segment, erosion of the submerged alluvial plain occurs. The same principles probably control offshore erosion in the natural environment, although effects such as slumping of a submerged margin, wave action (ravinement) and currents are unlikely to be solely diffusive even when time averaged. A more accurate prediction of the erosion of lowstand margins requires improved marine sediment transport models.

Interaction of Eustatic and Tectonic or Climatic Change

Eustatic effects in the model differ fundamentally from those of climate and tectonics in that their dominant influence on foreland basin stratigraphy occurs through changes in the baselevel of fluvial systems. Eustasy has relatively little effect on large-scale sediment flux, but instead modifies fluxes between the highstand and lowstand coasts. Tectonic and climate change both affect the large-scale sediment flux to the coast through their effects on regrading of fluvial systems and on relative sea level through isostatic compensation for the changing orogenic and sedimentary loads. Model results show that eustasy can act to reinforce or counteract the effects of climate or tectonics on lower alluvial plain sedimentation. Eustatic rise reinforces sedimentation patterns associated with changes to drier climatic conditions and/or an increase in tectonics; conversely, eustatic fall reinforces sedimentation patterns associated with changes to wetter climatic conditions and/or a decrease in tectonics. These reinforcements cause shifts in the timing of the maximum extent of transgression and regression toward being in phase with sea-level highstand and lowstand, respectively. Conversely, eustasy can retard or reverse the effects of tectonic or climate change on lower alluvial plain sedimentation, causing, for example, a reversal of the expected alluvial-to-marine facies succession in a two-phase sequence (MTE2, Figs. 5.20, 5.21). This ability of eustasy to reverse the coastal stratigraphic effects of both tectonic and climate change illustrates how eustatically driven transgressive/regressive cycles can be a dominant control in foreland basin stratigraphy. Transgressive/regressive stratigraphic cycles can carry a high-fidelity record of eustatic forcing when surface slopes are low and rates of sea-level change are rapid, by comparison with fluctuations in sediment flux caused by climate and tectonics. However, if eustatic cycling is faster than the response time of the coastal system, then the same attenuations and phase shifts demonstrated for tectonic and climatic forcing will occur. This 'coastal' response time may be estimated by the change in depocentre deposition rate with changes in relative sea level. Natural examples of the dominance of eustatic cycles are observed in many foreland basins, typically as stacked parasequences that occur at periods approximately associated with the orbital rhythms in eustasy (*e.g.*, Marshy Bank Formation., Upper Cretaceous, Alberta Foreland Basin, Plint, 1991).

In the model, eustatic effects on foreland basin stratigraphy are distinguishable from those of tectonic and climatic change in that changes to the fluvial system caused by eustatically forced transgressive/regressive cycles have relatively minor effects on alluvial plain sedimentation proximal to the orogen and sediment flux to the coast. As a result eustatically forced retrogradational/progradational cycles are more extensive for equivalent rates of relative sea-level change than those caused by tectonics or climate.

In model results, eustasy has a pronounced effect on foreland basin stratigraphy when periods of sea-level fluctuation are on the order of 400 ky. In contrast, tectonic and climate changes with the same period have only minor effects on basin stratigraphy because the period of change is approximately equal to the response time. The implication is the 'coastal' response time of the system must be much shorter than the response time of the system for tectonic or climate changes. If this implication is correct, it follows that periodic eustatic changes may be preserved in basin stratigraphy when equivalent periods in climate or tectonic changes are not. This observation does not imply that processes producing the most rapid sea-level changes will be the best preserved. Ultimately, if the period of eustatic fluctuations is less than or comparable to the coastal response time, then the stratigraphic signature of sea-level change will be attenuated in the same manner that tectonic and climatic signatures are attenuated under analogous circumstances. Further work is required to determine the response time of fluvial systems to eustatically forced baselevel changes before a formal comparison with other response times can be made.

Chapter 7

Conclusions

This research investigates the relative impacts of orogenic tectonism, climate change and eustasy on the development of foreland basin stratigraphy. A planform orogen/foreland basin model has been created and experiments conducted to identify and examine the effects of these processes on stratigraphic development. Comparisons of model results with examples from natural foreland basins demonstrate the general applicability of the model. The model and experiments are not designed to create results for detailed comparison with any particular orogen/foreland basin system, but rather to illustrate some of the fundamental characteristics of orogen/foreland basins and how the effects of the processes on basin stratigraphy are both similar and different. The objective is to assist in the identification of stratigraphic signatures in nature and to link them with causative processes. The effects of tectonic, climatic and eustatic forcing on synthetic orogen/foreland basin systems are summarized in Table 6.1.

7.1 Orogen/Foreland Basin Model

The planform kinematic orogen/foreland basin continues in the spirit of previous numerical foreland basin models and extends or improves upon them by incorporating:

- planform interactions among the first-order orogen/foreland basin processes modelled
- tectonic processes that create a two-sided orogenic belt and respond systematically to the effects of erosion over a range of length scales
- surface processes that include an advective mechanism for fluvial transport
- climate process that controls the orographic distribution of precipitation

- isostatic and eustatic processes that include the effects of water loading

The principal advantages of this model in comparison with previous models (Table 1.1):

- interaction among all model processes enables the system to operate as an integrated process-response system; response times can be estimated for periodic forcing of model processes; and the effects 'feed back' among the processes, thereby influencing the evolution of the orogen and foreland basin
- combination of orographically controlled precipitation and fluvial processes allows spatial and temporal variation in the rates of subaerial erosion, transportation and deposition to evolve with topography and without requiring changes in transport coefficients
- planform projections and vertical sections provide three-dimensional representations of landform evolution and stratigraphic development

The principal disadvantage in comparison with previous models (Table 1.1):

- the model lacks a kinematic process to emulate the effects of subduction dynamics on basin subsidence (e.g., Mitrovica *et al.*, 1989; Gurnis, 1992)
- the model lacks a process for creating individual thrusts (e.g., Zoetemeijer *et al.*, 1992)
- the model lacks a process for emulating the effects of in-plane stress

7.2 Tectonics

Tectonic model results demonstrate how the development of foreland basin stratigraphy is influenced by basin setting, parallel and oblique convergent margin geometry, orographically controlled precipitation, transverse and longitudinal sediment transport, periodicity in tectonics and orogen/foreland basin system response time.

- Pro- and retro-foreland basin settings illustrate how higher rates of accretion of strata into the orogen reduce the rate of foreland basin filling. Rates of accretion are typically higher in the pro-foreland basin setting, creating asymmetry between the rates of pro- and retro-foreland basin filling.
- Longitudinal sediment transport is a fundamental feature of foreland basins. Planform variations in tectonics are one mechanism for creating competition between transverse and longitudinal sediment transport. In general, longitudinal sediment transport reduces the rate of basin filling by diverting sediment along the basin axis. Models that do not include a mechanism for longitudinal transport are likely to overestimate the rates of foreland basin filling.
- Periodic variations in tectonics cause changes in orogen growth rate, and possibly orogen state, that result in the formation of sequences or parasequences in foreland basin stratigraphy. Increased orogen growth rates can cause retrogradational/progradational cycles, while reduced growth rates or orogen wasting enhance progradation (Table 6.1).
- Stratigraphic variations to changes in tectonics reflect the ability of the orogen/foreland basin system to respond. When the period of tectonic change is short relative to the tectonic response time of the system, the stratigraphic indicators of the tectonic change have only a limited range of development.
- Orogen-to-basin sediment flux response to periodic changes in orogen state suggests that the response of the entire system is a composite of the individual process-response systems. An individual process may dominate in the response of the entire system, as for example, the initial dominance of the

climate change in models with a change in orogen state illustrated by models MT5, and MT5a.

7.3 Climate

Climate model results demonstrate how the development of foreland basin stratigraphy is influenced by windward and leeward basin settings, periodic change in climatic conditions and the orogen/foreland basin response time.

- Under a prevailing 'wind' direction, orographically controlled rainfall causes an asymmetric distribution in precipitation and erosion rates across an orogen/foreland basin system. Foreland basins that develop in a windward setting are characterized by faster filling rates, higher alluvial/marine sediment ratios and lower gradients in surface slope and sedimentation rates across the alluvial plain than their leeward counterparts.
- Periodic changes between wetter and drier climatic conditions create retrogradational/progradational cycles in basin stratigraphy.
- Stratigraphic characteristics of changes in climatic conditions depend on the period of change relative to the climatic response time of the basin system. When the period is much longer than the response time, the effects of climate influence basin stratigraphy over greater length scales. When the period is shorter, the stratigraphic response lags behind the change in climate and preserves the response over much shorter length scales.

7.4 Eustasy

Eustatic model results demonstrate how eustasy alone and in competition with net sediment flux to the coast, influences the development of foreland-basin stratigraphy.

- Eustatic processes differ fundamentally from climatic and tectonic processes in that the dominant influence is through changes in relative sea level (Table 6.1). Eustasy has relatively little effect on sediment flux either to or away from the coast.
- The maximum extent of eustatically forced transgressive/regressive cycles is coeval with seaway closure in the model results. In nature, this observation may significantly modified by the effects of local topography and sediment influx to the seaway.
- In each cycle, the maximum extent of transgression and regression falls progressively out of phase with sea-level high and lowstand, and in phase with the maximum rate of sea-level change as the length of the cycle increases.
- Erosional surfaces are typically created along the coast with sea-level rise and fall; both cases require an increase in the shoreface slope. Type-1 erosional surfaces are variable in extent because of variation in the factors that control regrading in the upper, middle and lower zones of each fluvial catchment along the coast. The time of erosion begins between highstand and the maximum rate of sea-level fall, depending upon net sediment flux to the coast, topography, rate of fall, and basin subsidence rate.

7.5 Relative Effects of Tectonics, Climate and Eustasy

The relative effects of periodic variations in tectonic, climatic and eustatic processes on the development of foreland basin stratigraphy are summarized in Table 6.1 (grey tones). Model results demonstrate that tectonic and climatic changes differ significantly from eustatic variation. Both climatic and tectonic changes have significant effects on the orogen growth rate, orogen-to-basin sediment flux and sedimentation rates on the alluvial plain adjacent to the orogen, while eustasy has little influence in these areas and does not by itself cause changes in orogen state. Eustasy creates synchronous transgressions or regressions on either side of the seaway, while tectonics and climate create asynchronous transgressions and regressions. Furthermore, transgressions and regressions caused by eustasy typically are more extensive than those caused by tectonism and climate, because eustasy has a relatively minor effect on sediment flux to the coast while tectonism and climate typically have a significant effect.

Comparison of tectonic and climatic changes shows that decreases in tectonics and increases in precipitation rates, or increases in tectonics and decreases in precipitation rates, have similar effects on foreland basin stratigraphy (Table 6.1). The effects of climate variations differ from those of tectonics in the changes of orogen-to-basin sediment flux and net sediment flux to the coast. These differences in sediment flux are expressed by differences in sedimentation rates and progradation rates. Progradation rates increase significantly with the change to wetter climatic conditions because of the increase in sediment flux caused by the increase in erosion rates that accompanies increased rainfall. Progradation rates increase at a much slower rate with a decrease in tectonics because of the decrease in orogen growth rate. Similarly, both tectonic and climatic change cause transgressive/regressive cycles; however, only climate change causes a decrease in sedimentation rates because of the decrease in erosion rates that accompanies the initial decrease in precipitation rates.

In answer to the fundamental question, the relative effects of tectonic, climatic and eustatic processes have distinguishing characteristics in model foreland basin stratigraphy. However, preservation of these characteristic facies and stratal geometries depends largely upon the period of change in the forcing process and response times of the orogen/foreland basin system.

Bibliography

Ahnert, F., 1970, Functional relationships between denudation, relief, and uplift in large mid-latitude drainage basins, American Journal of Science, v.268, p.243-263

Allen, P.A. and Allen, J.T., 1990, Basin analysis: principles and applications, Oxford, Blackwell, 451pp.

Allen, P.A., Homewood, P. and Williams, G.D., 1986, Foreland basins: an introduction, in Allen, P.A. and Homewood, P., eds., Foreland Basins, International Association of Sedimentologists, Special Publication No.8, Oxford, Blackwell, pp.199-218

Armstrong, A.C., 1980, Soils and slopes in a humid environment, Catena, v.7, pp.327-338

Audley-Charles, M.G., 1986, Timor-Tanimbar Trough: the foreland basin of the evolving Banda orogen, in Allen, P.A. and Homewood, P., eds., Foreland Basins, International Association of Sedimentogists, Special Publication No.8, Oxford, Blackwell, p.91

Bagnold, R.A., 1966, An approach to the sediment transport problem from general physics, Physiographic and Hydraulic Studies of Rivers, U. S. Geological Survey, Professional Paper 422-I

Bally, A.W., 1981, Thoughts on the tectonics of folded belts, Thrust and Nappe Tectonics, Geological Society of London, Special Publication No.9, pp.13-32

Bally, A.W., 1989, Phanerozoic basins of North America, in Bally, A.W. and Palmer, A.R., eds., The Geology of North America--An overview: Boulder, Colorado, Geological Society of America, The Geology of North America, v.A, 50pp.

Bally, A.W. and Snelson, S., 1980, Realms of subsidence, in Miall, A.D., ed., Facts and principles of world petroleum occurrence, Canadian Society of Petroleum Geologists Memoir 6, pp.9-75

Barr, T.D. and Dahlen, F.A., 1989, Brittle frictional mountain building 2. Thermal structure and heat budget, Journal of Geophysical Research, v.94, No.B4, pp.3923-3947

Barr, T.D. and Dahlen, F.A., 1990, Constraints on friction and stress in the Taiwan fold-and-thrust belt from heat flow and geochronology, Geology, v.18, pp.111-115

Barros, A.P. and Lettenmaier, D.P., 1994, Dynamic modeling of orographically induced precipitation, Reviews of Geophysics, v.32, pp.265-284

Barry, R.G. and Chorley, R.J., 1971, Atmosphere, weather and climate, London, Methuen & Co. Ltd., 379pp.

Beaumont C., 1978, The evolution of sedimentary basins on a viscoelastic lithosphere: theory and examples, Geophysical Journal of the Royal Astronomical Society, v.55, pp.471-498

Beaumont, C., 1981, Foreland basins, Geophysical Journal of the Royal Astronomical Society, v.65, pp.291-329

Beaumont, C., Fullsack, P. and Hamilton, J., 1992, Erosional control of active compressional orogens, in McClay, K.R., ed., Thrust Tectonics, London, Chapman and Hall, pp.1-18

Beaumont, C., Fullsack, P. and Hamilton, J, 1994, Styles of crustal deformation caused by subduction of the underlying mantle, Tectonophysics, v.232, pp. 119-132

Beaumont, C. and Quinlan, G., 1994, A geodynamic framework for interpreting crustal-scale seismic-reflectivity patterns in compressional orogens, Geophysical Journal International, v.116, pp.754-783

Beaumont, C., Quinlan, G. and Hamilton, J., 1988, Orogeny and stratigraphy: numerical models of the Paleozoic in the eastern interior of North America, Tectonics, v.7, pp.389-416

Begin, S.B., Meyer, D.F. and Schumm, S.A., 1981, Development of longitudinal profiles of alluvial channels in response to base-level lowering, Earth Surface Processes and Landforms, v.6, pp.49-68

Bhattacharya, J.P. and Walker, R.G., 1992, Deltas, in Walker, R.G. and James, N.P., eds., Facies Models: Response to Sea Level Change, Geological Association of Canada, p.157

Bird, K.J. and Molenaar, C.M., 1992, The North Slope Foreland Basin, Alaska, in Macqueen, R.W. and Leckie, D.A., eds., Foreland Basins and Fold Belts, American Association of Petroleum Geologists, Memoir 55, pp.363-394

Blair, T.C. and Bilodeau, W.L., 1988, Development of tectonic cyclothems in rift, pull-apart, and foreland basins: sedimentary response to episodic tectonism, Geology, v.16, pp.517-520

Braun, J., 1994, Three-dimensional numerical simulations of crustal-scale wrenching using a non-linear failure criterion, Journal of Structural Geology, v.16, No.8, pp.1173-1186

Braun, J. and Beaumont, C., submitted, Three dimensional numerical experiments of strain partitioning at oblique plate boundaries: implications for contrasting tectonic styles in the Southern Coast Ranges, California and Central South Island, New Zealand, Journal of Geophysical Research

Burbank, D.W., 1992, Causes of recent Himalayan uplift deduced from deposited patterns in the Ganges basin, Nature, v.357, pp.680-683

Burbank, D.W., Raynolds, R.G.H., Hobbs, R. and Tahirkheli, R.A.K., 1988, Thrusting and gravel progradation in foreland basins: a test of post-thrusting gravel dispersal, Geology, v.16, pp.1143-1146

Burbank, D.W., Puigdefabregas, C. and Munoz, J.A., 1992, The chronology of the Eocene tectonic and stratigraphic development of the eastern Pyrenean foreland basin, northeast Spain, Geological Society of America Bulletin, v.104, pp.1101-1120

Carson, M.A. and Kirkby, M.J., 1972, Hillslope Form and Processes, London, Cambridge University Press, 475pp.

Chapple, W.M., 1978, Mechanics of thin-skinned fold-and-thrust belts, Geological Society of America Bulletin, v.89, pp.1189-1198

Chase, C.G., 1992, Fluvial landsculpting and the fractal dimension of topography, in Snow, R.S. and Mayer, L., eds., Fractals in Geomorphology, Geomorphology, v.5, pp.39-57

Christie-Blick, N., Mountain, G.S. and Miller, K.G., 1990, Seismic stratigraphic record of sea-level change, Sea-Level Change, Studies in Geophysics, Washington, D.C., National Academy Press, p.116

Cloetingh, S., 1988, Intraplate stresses: a tectonic cause for third-order cycles in apparent sea level? in Lidz, B.H., ed., Sea-Level Changes: An Integrated Approach, Part I, Society of Economic Paleontologists and Mineralogists, Special Publication No.42, p.19

Coleman, S.M. and Watson, K., 1983, Ages estimated from a diffusion equation for scarp degradation, Science, v.221, pp.263-265

Courtney, R.C. and Beaumont, C., 1983, Thermally activated creep and flexure of the oceanic lithosphere, Nature, v.305, pp.201-204

Covey, M., 1986, The evolution of foreland basins to steady state: evidence from the western Taiwan foreland basin, in Allen, P.A. and Homewood, P., eds., Foreland Basins, International Association of Sedimentologists, Special Publication No.8, Oxford, Blackwell, p.77

Crowley, T.J. and North, G.R., 1991, Paleoclimatology, Oxford, Clarendon Press, pp.183-210

Culling, W.E.H., 1960, Analytical theory of erosion, Journal of Geology, v.68, pp.336-344

Culling, W.E.H., 1965, Theory of erosion on soil covered slopes, Journal of Geology, v.73, pp.230-254

Dahlen, F.A., 1984, Noncohesive critical Coulomb wedges: an exact solution, Journal of Geophysical Research, v.89, pp.10125-10133

Dahlen, F.A. and Suppe, J., 1988, Mechanics, growth, and erosion of mountain belts, in Clark, S.P., ed., Processes in Continental Lithospheric Deformation, Geological Society of America, Special Publication No.218, pp.161-178

Dahlen, F.A., Suppe, J. and Davis, D., 1984, Mechanics in fold-and-thrust belts and accretionary wedges: cohesive Coulomb theory, Journal of Geophysical Research, v.89, pp.10087-10101

Davis, D., Suppe, J., and Dahlen, F.A., 1983, Mechanics in fold-and-thrust belts and accretionary wedges, Journal of Geophysical Research, v.88, pp.1153-1172

de Boer, P.L., Pragt, J.S.J. and Oost, A.P., 1991, Vertically persistent sedimentary facies boundaries along growth anticlines and climate-controlled sedimentation in the thrust-sheet-top South Pyrenean Tremp-Graus Foreland Basin, Basin Research, v.3, pp.63-78

DeCelles, P.G. and Burden, E.T., 1992, Non-marine sedimentation in the overfilled part of the Jurassic-Cretaceous Cordilleran foreland basin: Morrison and Cloverly formations, central Wyoming, USA, Basin Research, v.4, pp.291-313

Dickinson, W.R., 1974, Plate tectonics and sedimentation, in Dickinson, W.R., ed., Tectonics and Sedimentation, Society of Economic Paleontologists and Mineralogists, Special Publication No.22, pp.1-27

Fermor, P.R. and Moffat, I.W., 1992, Tectonics and Structure of the Western Canada Foreland Basin, in Macqueen, R.W. and Leckie, D.A., eds., Foreland Basins and Fold Belts, American Association of Petroleum Geologists, Memoir 55, pp.81-106

Fischer, A.G., Silva, I.P. and de Boer, P.L., 1990, Cyclostratigraphy, in Ginsburg, R.N. and Beaudoin, B., eds., Cretaceous Resources, Events and Rhythms, NATO Scientific Affairs Division, The Netherlands, pp.139-172

Flemings, P.B. and Jordan, T.E., 1989, A synthetic stratigraphic model of foreland basin development, Journal of Geophysical Research, v.94, pp.3851-3866

Flemings, P.B. and Jordan, T.E., 1990, Stratigraphic modelling of foreland basins: interpreting thrust deformation and lithosphere rheology, Geology, v.18, pp.430-434

Frostick, L.E. and Reid, I., 1989, Climatic versus tectonic controls of fan sequences: Lessons from the Dead Sea, Israel, London, Journal of the Geological Society, v.146, pp.527-538

Galloway, W.E., 1989, Genetic stratigraphic sequences in basin analysis I: architecture and genesis of flooding-surface bounded depositional units, American Association of Petroleum Geologists Bulletin, v.73, No.2, pp.125-142

Gurnis, M., 1992, Rapid continental subsidence following the initiation and evolution of subduction, Science, v.255, pp.1556-1558

Hanks, T.C., Bucknam, R.C., Lajoie, K.R. and Wallace, R.E., 1984, Modification of wave-cut and faulting-controlled landforms, Journal of Geophysical Research, v.89, pp.5771-5790

Haq,B.U., Hardenbol, J. and Vail, P.R., 1988, Mesozoic and cenozoic chronostratigraphy and eustatic cycles, in Lidz, B.H., ed., Sea-Level Changes: An Integrated Approach, Part II, Society of Economic Paleontologists and Mineralogists, Special Publication No.42, p.71

Harrison, C.G.A., 1991 Long-term eustasy and epeirogeny in continents, Sea-Level Change, Studies in Geophysics, Washington, D.C., National Academy Press, p.141

Heller, P.L., Angevine, C.L., Winslow, N.S., and Paola, C., 1988, Two-phase stratigraphic model of foreland-basin sequences, Geology, v.16, pp.501-504

Heller, P.L., Burns, B.A. and Marzo, M., 1993, Stratigraphic solution sets for constraining the role of sediment supply, subsidence and sea level on transgressions and regressions, Geology, v.21, No.8, pp.747-750

Hoffman, P.F. and Grotzinger, J.P. 1993, Orographic precipitation, erosional unloading, and tectonic style, Geology, v.21, pp.195-198

Homewood, P., Allen, P.A. and Williams, G.D., 1986, Dynamics of the Molasse Basin of Western Switzerland, in Allen, P.A. and Homewood, P., eds., Foreland Basins, International Association of Sedimentologists, Special Publication No.8, Oxford, Blackwell, pp.199-218

Howard, A.D., 1982, Equilibrium and time scales in geomorphology: application to sand-bed alluvial streams, Earth Surface Processes and Landforms, New York, John Wiley & Sons Ltd., v.7, pp.303-325

Jamieson, R.A. and Beaumont, C., 1988, Orogeny and metamorphism: a model for deformation and pressure-temperature-time paths with application to the central and southern Appalachians, Tectonics, v.7, pp.417-445

Jervey, M.T., 1988, Quantitative geological modeling of siliciclastic rock sequences and their seismic expression, in Wilgus, C.K., Hastings, B.S, Posamentier, H., Van Wagoner, J., Ross, C.A. and Kendall, C.G., eds., Sea-Level Changes: An Integrated Approach, Society of Economic Paleontologists and Mineralogists, Special Publication No.42, pp.46-69

Jerzykiewicz, T. and Sweet, A.R., 1988, Sedimentological and palynological evidence of regional climatic changes in the Campanian to Paleocene sediments of the Rocky Mountain Foothills, Canada, Sedimentary Geology, v.59, pp.29-76

Johnson, D.D. and Beaumont, C. (1995), Preliminary results from a planform kinematic model of orogen evolution, surface processes and the development of clastic foreland basin stratigraphy, in Dorobek, S. and Ross, G., eds., Stratigraphic Evolution of Foreland Basins, Society of Economic Paleontologists and Minerologists, Special Publication No.52

Jordan, T.E., 1981, Thrust loads and foreland basin evolution, Cretaceous Western United States, American Association of Petroleum Geologists Bulletin, v.65, pp.2506-2520

Jordan, T.E. and Flemings, P.B., 1991, Large-scale stratigraphic architecture, eustatic variation, and unsteady tectonism: a theoretical evaluation, Journal of Geophysical Research, v.96, pp.6681-6699

Karner, G.D. and Watts, A.B., 1983, Gravity anomalies and flexure of the lithosphere at mountain ranges, Journal of Geophysical Research, v.88, pp.10449-10477

Kenyon, P.M. and Turcotte, D.L., 1985, Morphology of delta prograding by bulk sediment transport, Geological Society of America Bulletin, v.96, pp.1457-1465

Kershaw, A. P. and Nanson G. C., 1993, The last full glacial cycle in the Australian region, Global and Planetary Change, v.7, pp.1-9

Kooi, H. and Beaumont, C. (submitted), Large-scale geomorphology: classical concepts reconciled and integrated with contemporary ideas via a surface processes model, Journal of Geophysical Research

Kooi, H. and Beaumont, C., 1994, Escarpment evolution on high-elevation rifted margins: insights derived from a surface processes model that combines diffusion, advection, and reaction, Journal of Geophysical Research, v.99, No.B6, pp.12191-12209

Kukal, K., 1990, The rate of geological processes, Geological Survey, Prague, Czechoslovakia, 284pp.

Laferriere, A.P., Hattin, D.E. and Archer, A.A., 1987, Effects of climate, tectonics, and sea-level changes on rhythmic bedding patterns in the Niobrara Formation (Upper Cretaceous), U.S. Western Interior, Geology, v.15, pp.233-236

Langbein, W.B. and Schumm, S.A., 1958, Yield of Sediment in Relation to Mean Annual Precipitation, Transactions, American Geophysical Union, v.39, No.6, pp.1076-1084

Leckie, D.A., 1989, Upper Zuni Sequence: middle Cretaceous to lower Tertiary, in Ricketts, B.D., ed., Western Canada Sedimentary Basin, A Case History, Calgary, Canadian Society of Petroleum Geologists, pp.269-281

Leckie, D.A. and Smith, D.G., 1992, Regional setting, evolution, and depositional cycles of the Western Canada foreland basin, in Macqueen, R.W. and Leckie, D.A., eds., Foreland Basins and Fold Belts, American Association of Petroleum Geologists, Memoir 55, pp.9-46

Lundberg, N. and Dorsey, R.J., 1988, Synorogenic sedimentation and subsidence in a Plio-Pleistocene collisional basin, eastern Taiwan, in Kleinspehn, K.L. and Paola, C., eds., New Perspectives in Basin Analysis, New York, Springer-Verlag, pp.265-280

Lydolph, P.E., 1977, The Caucasus, in Climates of the Soviet Union, in Landsberg, H.E., ed., World Survey of Climatology, Amsterdam, Elsevier, v.7, pp.191-219

Mackin, J.H., 1948, Concept of the graded river, Geological Society of America Bulletin, v.59, pp.463-512

Malavieille, J., 1984, Modélisation expérimentale des chevauchements imbriqués: application aux chaînes de montagnes, Bulletin de la Société Géologique de France, v.26, pp.129-138

Maqueen, R.W. and Leckie, D.A., 1992, Foreland Basins and Fold Belts, American Association of Petroleum Geologists, Memoir 55, pp.445-456

Marzo, M., Nijman, W. and Puigdefabregas, C., 1988, Architecture of the Castissent fluvial sheet sandstones, Eocene, South Pyrenees, Spain, Sedimentology, v.35, pp.719-738

Masek, J.G., Isacks, B.L., Gubbels, T.L. and Fielding, E.J., 1994, Erosion and tectonics at the margins of continental plateaus, Journal of Geophysical Research, v.99, No.B7, pp.13941-13956

Maunder, W.J., 1971, Elements of New Zealand's climate, and Climate areas of New Zealand, in Gentilli, J., ed., Climates of Australia and New Zealand, in Landsberg, H.E., ed., World Survey of Climatology, Amsterdam, Elsevier, v.13, pp.229-261

Mitrovica, J.X., Beaumont, C. and Jarvis, G.T., 1989, Tilting of continental interiors by the dynamical effects of subduction, Tectonics, v.8, No.5, pp.1079-1094

Monger, J.W.H., 1989, Overview of Cordilleran Geology, Part I, Basin Framework, in Ricketts, B.D., ed., Western Canada Sedimentary Basin, A Case History, Calgary, Canadian Society of Petroleum Geologists, pp.9-32

Morisawa, M., 1985, Rivers, in Clayton, K.M., ed., Geomorphology Texts 7, London, Longman, 222pp.

Muñoz, J.A., 1992, Evolution of a continental collision belt: ECORS-Pyrenees crustal balanced cross-section, in McClay, K.R., ed.,Thrust Tectonics, London, Chapman and Hall, pp.235-246

Nash, D.B., 1980a, Forms of bluffs degraded for different lengths of time in Emmet Country, Michigan, U.S.A., Earth Surface Processes, v.5, pp.331-345

Nieuwolt, S., 1981, The climates of continental southeast Asia, in Takahashi, K. and Arakawa, H., eds., Climates of Southern and Western Asia, in Landsberg, H.E., ed., World Survey of Climatology, Amsterdam, Elsevier, v.9, pp.1-66

Paola, C., Heller, P.L. and Angevine, C.L., 1992, The large-scale dynamics of grain-size variation in alluvial basins, 1: Theory, Basin Research, v.4, No.2, pp.73-90

Peper, T., 1993, Tectonic control on the sedimentary record in foreland basins, Amsterdam, Vrije Universiteit, 187pp.

Plint, A.G., 1991, High-frequency relative sea-level oscillations in Upper Cretaceous shelf clastics of the Alberta foreland basin: possible evidence for a glacio-eustatic control? in Macdonald, D.I.M., ed., Sedimentation, Tectonics and Eustasy, International Association of Sedimentologists, Special Publication No.12, Oxford, Blackwell, pp.409-428

Plint, A.G., Hart, B.S. and Donaldson, W.S., 1993, Lithospheric flexure as a control on stratal geometry and facies distribution in Upper Cretaceous rocks of the Alberta foreland basin, Basin Research, v.5, pp.69-77

Posamentier, H.W. and Allen, G.P., 1993, Siliciclastic sequence stratigraphic patterns in foreland ramp-type basin, Geology, v.211, pp.455-458

Posamentier, H.W., Jervey, M.T. and Vail, P.R., 1988, Eustatic controls on clastic deposition I--Conceptual framework, in Lidz, B.H., ed., Sea-level Changes: An Integrated Approach, Part II, Society of Economic Paleontologists and Mineralogists, Special Publication No.42, pp.109-124

Posamentier, H.W. and Vail, P.R., 1988, Eustatic controls on clastic deposition II - sequence and systems tract models, in Lidz, B.H., ed., Sea-level Changes: An Integrated Approach, Part II, Society of Economic Paleontologists and Mineralogists, Special Publication No.42, pp.109-124

Price, R.A., 1973, Large scale gravitational flow of supracrustal rocks, southern Canadian Rockies, in DeJong, K.A. and Schoten, R.A., eds., Gravity and Tectonics, New York, John Wiley & Sons Ltd., pp.491-502

Prohaska, F., 1976, The climate of Argentina, Paraguay and Uruguay, in Schwerdtfeger, W., ed., Climates of Central and South America, in Landsberg, H.E., ed., World Survey of Climatology, Amsterdam, Elsevier, v.12, pp.13-72

Quinlan, G.M. and Beaumont, C., 1984, Appalachian thrusting, lithospheric flexure, and the Paleozoic stratigraphy of the Eastern Interior of North America, Canadian Journal of Earth Science, v.21, pp.973-996

Ranalli, G., 1987, Rheology of the earth: deformation and flow processes in geophysics and geodynamics, Boston, Allen and Unwin Inc., 366pp.

Revelle, R.R., 1990, Sea-level change, Studies in Geophysics, Geophysics Study Committee, National Research Council, Washington, D.C., National Academy Press, pp.3-33

Schumm, S.A., 1977, The Fluvial System, New York, John Wiley & Sons Ltd., 338pp.

Schumm, S.A., 1993, River response to baselevel change: implications for sequence stratigraphy, University of Chicago, Journal of Geology, v.101, pp.279-294

Schwab, F.L., 1986, Sedimentary 'signatures' of foreland basin assemblages: real or counterfeit?, in Allen, P.A. and Homewood, P., eds., Foreland Basins, International Association of Sedimentologists, Special Publication No.8, Oxford, Blackwell, p.395

Sinclair, H.D., Coakley, B.J., Allen, P.A. and Watts, A.B., 1991, Simulation of foreland basin stratigraphy using a diffusion-model of mountain belt uplift and erosion - an example from the central Alps, Switzerland, Tectonics, v.10, pp.599-620

Smith, D.G., 1986, Anastomosing river deposits, sedimentation rates and basin subsidence, Magdalena River, Northwestern Columbia, South America, Sedimentary Geology, v.46, pp.177-196

Stockmal, G.S., 1983, Modeling of large-scale accretionary wedge deformation, Journal of Geophysical Research, v.88, pp.8271-8287

Stockmal, G.S., Beaumont, C. and Boutilier, R., 1986, Geodynamic models of convergent margin tectonics: transition from rifted margin to overthrust belt and consequences for foreland-basin development, American Association of Petroleum Geologists Bulletin, v.70, No.2, pp.181-190

Stockmal, G.S., Cant, D.J. and Bell, J.S., 1992, Relationship of the stratigraphy of the Western Canada foreland basin to Cordilleran tectonics: insights from geodynamic models, in Macqueen, R.W. and Leckie, D.A., eds., Foreland Basins and Fold Belts, American Association of Petroleum Geologists, Memoir 55, pp.107-124

Swift, D.J.P., 1968, Coastal erosion and transgressive stratigraphy, Journal of Geology, v. 75, pp. 444-456

Syvitski, J.P.M., Smith, J.N., Calabrese, E.A. and Boudreau, B.P., 1988, Basin sedimentation and growth of prograding deltas, Journal of Geophysical Research, v.93, pp.6895-6908

Thomas, W.A., 1977, Evolution of Appalachian-Ouachita salients and recesses from reentrants and promontories in the continental margin, American Journal of Science, v.277, pp.1233-1278

Turcotte, D.L. and Schubert, G., 1982, Geodynamics: applications of continuum physics to geological problems, New York, John Wiley & Sons Ltd., 450pp.

Vail, P.R., Mitchum, R.M., Jr., Todd, R.G., Widmier, J.M., Thompson, S., III, Sangree, J.B., Bubb, J.N. and Hatlelid, W.G., 1977, Seismic stratigraphy and global changes of sea level, American Association of Petroleum Geologists, Memoir 26, pp.49-212

Van Wagoner, J.C., Posamontier, R.M., Vail, P.R., Sarg, J.F., Loutit, T.S. and Hardenbol, J., 1988, An overview of the fundamentals of sequence stratigraphy and key definitions, in Lidz, B.H., ed., Sea-Level Changes: An Integrated Approach, Part II, Society of Economic Paleontologists and Mineralogists, Special Publication No.42, p.39

Waschbusch, P.J. and Royden, L.H., 1992, Episodicity in foredeep basins, Geology, v.20, pp. 915-918

Wanless, H. R. and Shepard, F. P., 1936, Sea level and climate changes related to late paleozoic cycles, Bulletin of the Geological Society of America, v.47, pp.1177-1206

Watts, I.E.M., 1969, Climates of China and Korea, in Arakawa, H., ed., Climates of Northern and Eastern Asia, in Landsberg, H.E., ed., World Survey of Climatology, Amsterdam, Elsevier, v.8, pp.1-118

Wescott, W.A., 1993, Geomorphic thresholds and complex response of fluvial systems - some implications for sequence stratigraphy, American Association of Petroleum Geologists Bulletin, v.77, No.7, pp.1208-1218

Westbrook, G.K., Ladd, J.W., Buhl, P., Bangs, M. and Tiley, J.G., 1988, Cross section of an accretionary wedge: Barbados Ridge Complex, Geology, v.16, pp.631-635

Willett, S., 1992, Dynamic and kinematic growth and change of a Coulomb wedge, in McClay, K.R., ed., Thrust Tectonics, London, Chapman and Hall, pp.19-31

Willett, S.D., Beaumont, C. and Fullsack, P., 1993, Mechanical model for the tectonics of doubly vergent compressional orogens, Geology, v.21, pp.371-374

Wilson, L., 1973, Variations in mean annual sediment yield as a function of mean annual precipitation, American Journal of Science, v.273, pp.335-349

Zoetemeijer, R., Sassi, W., Roure, F. and Cloetingh, S., 1992, Stratigraphic and kinematic modeling of thrust evolution, northern Apennines, Italy, Geology, v.20, pp.1035-1038